New membranes based on high performance polymers for proton exchange membrane fuel cells PEMFC

Olesia Danyliv

UNIVERSITÉ GRENOBLE ALPES

THÈSE

Pour obtenir le grade de

DOCTEUR DE L'UNIVERSITÉ GRENOBLE ALPES

Spécialité : **Matériaux, Mécanique, Génie Civil, Electrochimie**

Arrêté ministériel : 7 août 2006

Présentée par

Olesia DANYLIV

Thèse dirigée par **Cristina IOJOIU** et
codirigée par **Jean-Yves SANCHEZ**

préparée au sein du **Laboratoire d'Electrochimie et Physico-Chimie des Matériaux et Interfaces (LEPMI)**
dans **l'École Doctorale Ingénierie-matériaux mécanique énergétique environnement procédés production (IMEP-2)**

Nouvelles membranes à squelette haute performance pour les piles à combustible PEMFC

Thèse soutenue publiquement le **24 juin 2015**,
devant le jury composé de :

Mme Christel LABERTY-ROBERT Professeur, Université Pierre et Marie Curie, Paris	Rapporteur
M. Bruno AMEDURI DR1, Institut Charles Gerhardt, Montpellier	Rapporteur
M. Christophe COUTANCEAU Professeur, Université de Poitiers	Examinateur
Mme Sandrine LYONNARD Dr., CEA Grenoble	Examinateur
M. Lionel OGIER Dr., PME ERAS Labo	Invité
M. Jean-Yves SANCHEZ Professeur, INP Grenoble	Co-directeur
Mme Cristina IOJOIU CR, CNRS	Directrice

UNIVERSITÉ GRENOBLE ALPES

DISSERTATION

To obtain the degree of

DOCTOR FROM UNIVERSITY GRENOBLE ALPES

Speciality: **Materials, Mechanics, Civil Engineering, Electrochemistry**

Ministerial decree: 7 August 2006

Presented by

Olesia DANYLIV

Dissertation directed by **Cristina IOJOIU** and
co-directed by **Jean-Yves SANCHEZ**

Prepared in the **Laboratory of Electrochemistry and Physical Chemistry of Materials and Interfaces (LEPMI)**
In the **Doctoral School Engineering materials, Mechanics, Energy, Environment, Procedures, Production (IMEP-2)**

New membranes based on high performance polymers for fuel cells PEMFC

Dissertation defended publicly on **24 June 2015**,
In front of the jury comprising of:

Ms Christel LABERTY-ROBERT Professor, University of Pierre and Marie Curie, Paris	Reviewer
Mr Bruno AMEDURI DR1, Institute Charles Gerhardt, Montpellier	Reviewer
Mr Christophe COUTANCEAU Professor, University of Poitiers	Examiner
Ms Sandrine LYONNARD Dr., CEA Grenoble	Examiner
Mr Lionel OGIER Dr., SME ERAS Labo	Guest
Mr Jean-Yves SANCHEZ Professor, INP Grenoble	Co-director
Ms Cristina IOJOIU CR, CNRS	Director

Abstract

The dissertation presents production of three new monomers, bearing perfluorosulfonic acid chains, and novel ionomers thereafter. Two main families of proton conducting polymers are described here: random poly(arylene ether)s (PAEs) and poly(arylene ether sulfone)s (PAESs), both random and block-copolymers.

Due to complexity of ionic interactions in a system 'product-solvent' and due to the main requirement of high purity for a monomer, much attention is paid to description of a protocol for production and purification of the ionic monomers. A number of polymerization reactions with different commercial non-ionic monomers are reported. Membranes were prepared from the polymers of high molecular weight (> 50 kDa) by casting-evaporation method from their solutions in dimethylacetamide (DMAc). The influence of production temperature is described briefly.

The membranes in salt and protonated forms are extensively characterized in terms of thermo-mechanical properties. The synthesized materials exhibit: i) high transition temperatures, which allows utilization of these polymers at conditions of a fuel cell functioning; ii) phase separation phenomena, which suggests the materials to have morphology with distinct domains for proton conduction. Additionally, small angle scattering (SAS) is performed in order to verify the presence of a highly-organized structure and to understand more the character of the ionomers' bulk morphology.

Proton conductivity measurements show that not all of the synthesized series possess the outstanding performance in terms of this specific property. However, detailed discussion is proposed to reveal the ionomers' difference between each other and to the reference material for the further improvement.

Preface

This doctoral dissertation was realized in October 2011 – March 2015 in the Laboratory of Electrochemistry and Physico-Chemistry of Materials and Interfaces (LEPMI), CNRS, UMR 5279. The current work is a part of a project NMHT with a SME ERAS Labo as a partner and as an employer of myself in terms of a scholarship CIFRE (October 2011 – October 2014).

The originality and the challenge of this work consider the whole cycle of a proton-conducting material production: starting from the synthesis of a simple unit – a monomer, continuing with polymerization and overall estimation of the polymer performance at laboratory scale, and ending with production of the required material of commercial quantity and testing in real conditions. All the steps, except the latest, were performed in LEPMI, the up-scaling was carried out in LEPMI and ERAS Labo. The measurements of small angle X-ray scattering (SAXS) were performed in INAC SPrAM CEA with the help of Arnaud De Geyer and Emilie Dubard under the direction of Dr. Sandrine Lyonnard.

The current work would not be possible without the guidance of Dr. Cristina Iojoiu and Prof. Jean-Yves Sanchez, whom I thank sincerely to. I express my gratitude to Serge Vidal for the sponsorship of my work, and equally to the staff of ERAS Labo, especially to Lionel Ogier and Laurent Palmonari, for cooperation. Thanks to Dr. Sandrine Lyonnard, Arnaud De Geyer, Emilie Dubard and Matthieu Fumagalli the X-ray analysis was performed and helpful discussion was provided. I would like to express my gratitude to the members of the evaluation committee for their time and important corrections that improved the current manuscript.

I thank to all the colleagues and friends I had an opportunity to work with and to share the nice moments of my stay in Grenoble. And finally, the cordial support of my family and best friends during all the period of the PhD thesis helped to overcome all the difficulties and to arrive to this final point of the defense to obtain a degree of the Philosophy Doctor. I express my deep love and thank to my dearest people for this precious contribution.

Contents

List of abbreviations

Abbreviation	Name
AFM	Atomic force microscopy
DMA	Dynamic mechanical analysis
DMFC	Direct methanol fuel cell
DSC	Differential scanning calorimetry
FC	Fuel cell
IEC	Ion exchange capacity
MW	Molecular weight
NMR	Nuclear magnetic resonance
OST	Oxidative stability test
PAE	Poly(arylene ether)
PAEK	Poly(arylene ether ketone)
PAEKS	Poly(arylene ether ketone sulfone)
PAES	Poly(arylene ether sulfone)
PAN	Poly(acrylo nitrile)
PDI	Polydispersity index
PEEK	Poly(ether ether ketone)
PEEKK	Poly(ether ether ketone ketone)
PEK	Poly(ether ketone)
PEMFC	Polymer electrolyte membrane fuel cell
PES	Poly(ether sulfone)
PFSA	Perfluorosulfonic acid
PI	Poly(imide)
PPK	Poly(phenylene ketone)
PPP	Poly(*p*-phenylene)
PS	Poly(styrene)
PSU	Poly(sulfone)
PTFE	Poly(tetrafluoroethylene)
PVDF	Poly(vinylidene fluoride)
RB	Round bottom
RH	Relative humidity
RT	Room temperature
SANS	Small angle neutron scattering
SAS	Small angle scattering
SAXS	Small angle X-ray scattering
SEC	Size exclusion chromatography
SI	Sulfonimide
SPS	Sulfonated poly(styrene)
STEM	Scanning transmission electron microscopy
TEM	Transmission electron microscopy
TGA	Thermogravic analysis
WU	Water uptake

Chemical compounds and solvents

Abbreviation	Name	Chemical formula
ACN	Acetonitrile	C_2H_3N
BP	4,4'-Dihydroxybiphenyl	$C_{15}H_{16}O_2$
Bz	Benzene	C_6H_6
CH	Cyclohexane	C_6H_8
DCM	Dichloromethane	CH_2Cl_2
DEE	Diethyl ether	$C_4H_{10}O$
DFB	Decafluorobiphenyl	$C_{12}F_{10}$
DIEA	N-Ethyldiisopropylamine	$C_8H_{19}N$
DMAc	Dimethylacetamide	C_4H_9NO
DMF	Dimethylformamide	C_3H_7NO
DMSO	Dimethylsulfoxide	C_2H_6SO
DW	Distilled water	H_2O
EA	Ethyl acetate	$C_4H_8O_2$
EtOH	Ethanol	C_2H_6O
FS	4,4'-Difluorodiphenylsulfone	$C_{12}H_8F_2O_2S$
HA	*n*-Hexane	C_6H_{10}
HS	4,4'-Dihydroxydiphenylsulfone	$C_{12}H_{10}O_4S$
IP	Propan-2-ol	C_3H_8O
NMP	Methyl-1-pyrrolidone-2	C_5H_9NO
THF	Tetrahydrofuran	C_4H_8O
TL	Toluene	C_7H_8

Introduction

In the present life of high energy consummation much research is dedicated to production of new devices for power generation from the sources alternative to fossil fuels. This work concerns elaboration of a new material, being a core part of a proton electrolyte membrane fuel cell (PEMFC), – an ionic polymer (an ionomer).

Nowadays, the main requirements of scientific community towards an efficient ionomer for fuel cells are: i) thermo-mechanical stability, ii) invariance in oxidative environment, and iii) high conductivity performance in a range of temperatures 30 – 120 °C (at least) at humidity control of lower, than 90 % (averagely at 50 % RH). All these requirements must be supported in a long-term functioning.

Nafion is considered as a reference proton-conducting material, mainly, due to its conductivity of 5 – 80 mS/cm at 20 – 60 %RH (exact values of conductivity depend on the polymer thickness and variation of block lengths). For the moment the most part of polymers, performing well at complete humidification, could not adjust the high values at reduced water content.

Nafion was explored to acquire its high performance due to: i) presence of superacid perfluorosulfonic acid (PFSA) lateral groups, and ii) organization of polymer chains into well-separated proton-conductive (hydrophilic) and mechanically stable (hydrophobic) domains. However, production of this material comprises dangerous and expensive procedures of manipulation with fluorinated gases, since this ionomer contains a Teflon-type backbone. Moreover, transition temperature of the perfluorinated main chain is lower, than the required temperature of the ionomer functioning in a fuel cell (FC); this property restricts using polymers with Teflon-type backbone as proton conducting membranes.

The current work addresses two main objectives: i) production of a highly conductive material by introducing lateral long PFSA groups, and ii) use of a polyaromatic main chain in order to obtain a cheaper and mechanically more robust material by a non-toxic procedure. Since several decades the research focuses on aromatic polymers modification with different types of sulfonic acid groups. However the limited number of results is reported on introduction of PFSA lateral groups. Generally, sulfonation of polyarylenes is performed by grafting of SO_3H-containing groups to a ready polymer chain. In the current work the synthesis strategy is changed: first, the perfluorosulfonated monomer is produced, and then it is copolymerized to a high molecular weight material. In such a method structures with a better control of

sulfonic group content and arrangement through a polymer chain are obtained. To the best of our knowledge, this is the first time monomers, bearing long PFSA chains, and subsequently ionomers, are presented. A similar idea was provided before by General Electric Company [1], but the authors did not present the same preparation procedure for the materials, as it is reported in the current work. Besides, no further information has been evidenced since then, which gives an opportunity to claim on originality of the structures, presented in this dissertation.

Unfortunately, the most ionomers, described in scientific publications were never tested in real conditions, neither the materials, produced in the current work, were. Thus, materials' in-lab performance is rather compared to that of Nafion 117 either Nafion 112.

The current manuscript is divided into four chapters:

- Chapter 1 gives a detailed overview on ionomers for PEMFC application, produced during the last decades. The critical discussion in terms of their performance, especially at reduced humidity, is given. In the very beginning, Nafion as a nowadays reference membrane is discussed in brief. Further, more attention is paid to polyaromatic materials and on impact of a spacer between the sulfonic group and a polymer backbone on morphology and properties of ionomers. In the end the objectives for the current work are determined.

- Chapter 2 describes procedures of syntheses of monomers and polymers thereafter. Problems, connected to purification of ionic monomers, are presented and ways of resolving them are given. A wide range of poly(ether)s and poly(ether sulfone)s is proposed as well. Unsuccessful polymerization reactions are also presented in order to clarify the mechanisms and conditions for secondary products formation. However, more attention is paid to analysis of chemical structures and molecular weights of successfully synthesized polymers. Additionally, discussion related to a membrane production method is reported.

- Chapter 3 leads to understanding the membranes' performance with the help of in-lab measuring techniques. Materials are investigated in terms of their thermo-mechanical properties, conductivity, water uptake capability and oxidative stability. Morphology of the membranes is studied with the help of small angle scattering (SAS) techniques, and the results are correlated with other properties of the materials.

- Conclusions summarize main outcomes of the work and perspectives forecast the possible ways to continue the research in the current area. The section of characterization techniques precises conditions of measurements, performed during the work. Annexes propose detailed protocols of syntheses of the monomers and the polymers thereafter.

Chapter 1. State of the art

Ionic polymers acquire their main ability of proton conduction due to: i) presence of sulfonic acid groups along a backbone; ii) solvation of water molecules around these ionic sites with further dissociation of the latter. Therefore, concentration of sulfonic groups per unity, or, in other words, ion-exchange capacity (IEC), expressed in equivalents per gram or per volume of a polymer, is an important factor. It will be used further for easier comparison of ionomers between each other. Additionally, water uptake (WU), which is ability of a polymer to absorb and retain water molecules in its structure, plays significant role in its performance, especially at reduced humidity and high temperature. At the same time at high values of relative humidity (RH) ionomers must not submit to excessive swelling, which would result in delamination of the proton-conducting material from the catalyst support in a real cell.

Recently, much attention has been paid to structuration of the proton-conducting materials. It is believed that morphology of well-separated hydrophilic and hydrophobic domains plays the most important role for high ionomer performance. This assumption is revealed from the long-term study on Nafion. Several models of microphase organization were proposed, and they are summarized in *Table 1.1*.

Table 1.1. The most prominent models of Nafion structuration, proposed during the last 35 years

Inventor	Model	Main features	Methods used	Schematic representation
Gierke T.D. *et al.* [2, 3]	Cluster-network	▪ spherical ionic clusters, having structure of inverted micelles; ▪ clusters connected by short channels; ▪ cluster diameter is 3 – 5 nm, channel diameter is 1 nm	Small angle X-ray scattering (SAXS); transmission electron microscopy (TEM); elastic theory	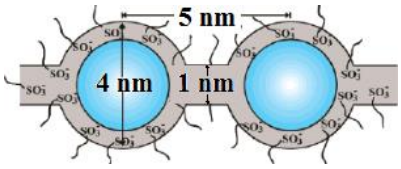 * 1)
Hashimoto T. *et al.* [4, 5]	Core-shell	▪ ionic cluster in a hydrophobic shell; ▪ small angle scattering comes from short-range intraparticle interference; ▪ model applicable to a dry state only; ▪ originally the model was applied to non-fuorinated ionomers [6, 7]	SAXS	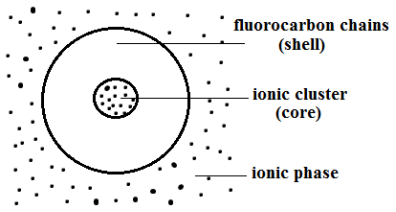 * 2)

Table 1.1. The most prominent models of Nafion structuration, proposed during the last 35 years (continuation)

Inventor	Model	Main features	Methods used	Schematic representation
Haubold H.-D. *et al.* [8]	Sandwich structure	▪ shells made of a polymer and side chains, core is a part for solvent; ▪ arrangement of ionic sites is not precisely determined, could be at interface; ▪ scattering from particles of 1.5 – 4.5 nm	SAXS; theory of random distribution of particles in a homogeneous matrix	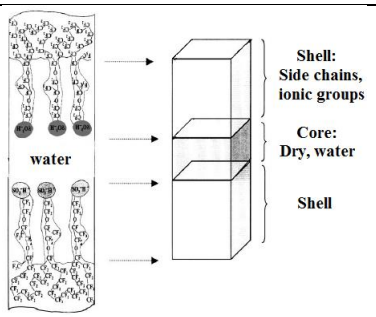 * 3)
Gebel G. *et al.* [9, 10, 11, 12]	Rod-like bundles	▪ at water content of > 50 % water forms continuous phase around elongated bundles of polymer chains, having ionic groups turned outside the hydrophobic bundles; ▪ bundles are randomly orientated at a microscale; ▪ ionomer peak characterizes distance between bundles; ▪ average diameter of a bundle is 1 nm and length 80 nm	SAXS; small angle neutron scattering (SANS)	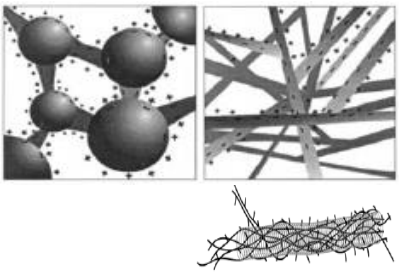 * 4)

* Schemes are reprinted and/or adapted with permission from:

1) Ref. 13. Copyright 2004 American Chemical Society.
2) Ref. 4. Copyright 1981 American Chemical Society.
3) Ref. 8. Copyright 2001 Elsevier.
4) Ref. 9. Copyright 2004 American Chemical Society; and ref. 10. Copyright 2000. Elsevier.

Still the unique conclusion on Nafion structuration is not stipulated. Important points, on which all the researchers appear to be concordant, are:

i) Ionic sulfonate groups aggregate into clusters, which provoke scattering at small angles (approx. $2\theta = 2$ °, which is also called the ionomer peak with $q = 0.15$ Å^{-1}), giving the cluster size of 4 nm. Presence of clustering in other ionomers is an indicator of phase separation at nanoscale. Upon hydration the size of clusters increases, thus scattering vector decreases.

ii) Due to presence of the poly(tetrafluoroethylene) (PTFE) backbone, Nafion is a semi-crystalline material. This property is believed to guide to a better separation between the hydrophilic and hydrophobic domains. The crystallinity depends on the polymer

and / or the membrane elaboration technique, knowing that annealing promotes a higher developed crystalline part [14]. The crystallinity may be detected by X-ray diffraction at $2\theta = 20\ °$ or $q = 1.40\ Å^{-1}$ (approximate values). Since the reply of the amorphous part of a polymer is also situated in the same range, crystallites of bigger size and of higher content may be detected only.

iii) Crystallinity of Nafion creates the second organization, at longer identity period, which appears at very small diffraction angles of $2\theta < 0.07\ °$, which characterizes the ordered species of the size > 125 nm.

All these results were mainly obtained by techniques of SAS. In present times separation and organization of ionic and hydrophobic phases might be observed by electron microscopy as well, which will be shown from the data of other authors. But this is a complementary measurement, since SAS gives more quantitative information on spacing between domains and spots the insight of structure ordering. The idea of ionomer structuration must be applied to other fluorinated or non-fluorinated materials in order to ameliorate the passage of protons and water molecules through the polymer, which is believed to increase the conductivity and water retention at reduced humidity.

It was mentioned that ionomers, containing perfluoroalkane main chain, are characterized by poor thermo-mechanical properties and their production is not an environmentally friendly process. Therefore, polymers with aromatic backbone acquire more attention as a proton-conducting material. Differing by interphenylene bridges in the main chain (where the general name comes from, e.g., poly(arylene ether)s (PAE), poly(arylene ether sulfone)s (PAES) etc.), type of an acid group attached to a polymer backbone (sulfonic, alkylsulfonic, perfluoroalkylsulfonic etc.), method of synthesis and / or functionalization, arrangement of the chemical structure (random, several-block or multiblock copolymer) and by many other factors, it becomes impossible to provide an all-embracing generalization of the existing proton conducting materials. However, in the current chapter it was intended to divide the families of ionomers by the type of sulfonic acid specie being attached to a polymer backbone. For this reason several paragraphs are proposed: i) starting with polymers, where ionic sites are directly attached to a main chain, ii) then discussing about ionomers with aromatic spacers, both a single phenyl and bulky multiring structures, and iii) finishing with long chain connections, including hydrogenated and perfluorinated structures.

1.1. Polyaromatics with sulfonic acid directly attached to a backbone

1.1.1. Synthesis by post-sulfonation

A common way of an ionic group incorporation to a polymer aromatic backbone is its post-sulfonation. Functionalization in such a way may be not complete either inhomogeneous.

Two ways of post-sulfonation have been widely implied to PAES (as cheap, easy in production and modification, and thermo-mechanically attractive materials): i) electrophilic substitution by sulfuric acids, and ii) chemical grafting. The former method results in $-SO_3H$ substitution in the *ortho*-position to activating ether-bridge. Probably, the first research on sulfonation of the commercial PAES UDEL for its application as a proton conductor was reported by Nolte *et al.* [15]. Strength of sulfonating agents was investigated [16]; chlorosulfonic acid together with oleum are found to be too strong agents for some polymers, e.g. for poly(ether ether ketone) (PEEK), leading to a polymer chain scission. Therefore, some polymers must be treated exclusively with mild agents (acetyl sulfate, trimethylsilyl chlorosulfonate [17]), even though the reaction time is much longer and total sulfonation cannot be achieved [18].

Poor stability of a sulfonic group in proximity to an electron-donating specie at acidic aqueous conditions led to elaboration of another method of chemical grafting through metalation (introducing of a metal), occurring in *ortho*-position to a sulfone-bridge. First trials of this method, though, were conducted on poly(phenylene oxide)s, containing no electron-withdrawing species, therefore metalation occurred both at the aromatic ring and at its substituents [19, 20]. Kerres *et al.* [21-25] developed such a method for PAES, additionally implying either chemical (with the help of alkylhalogenides) or physical (acid-base blend) crosslinking to improve mechanical properties of the materials. Further the method of lithiation – sulfination – oxidation was deeply studied by the group of Jannasch to introduce alkylsulfonated substituents in *ortho*-site to the sulfone-bond in a polymer [26]. And recently they produced a monomer and a hydrophilic oligomer in the same way in order to obtain block-copolymers of high performance [27, 28].

1.1.2. Synthesis by condensation of a disulfonated monomer. Random and block-copolymers with SO_3H in ortho-to-ether position

The wide range of polyarylenes was synthesized by a group of McGrath by method of polycondensation with a monomer, already bearing two acid groups, its patented product SDCDPS (*Fig. 1.1 (a)*) [29, 30].

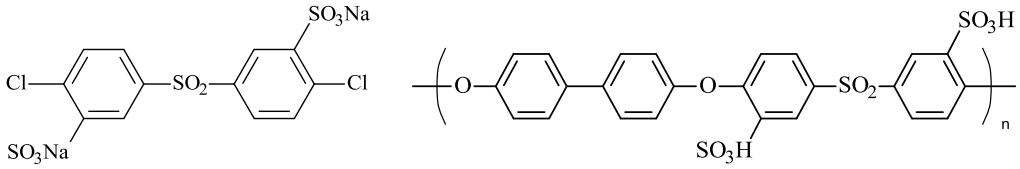

(a) (b)

Figure 1.1. Chemical structures of: a) an ionic monomer SDCDPS, and b) a monomer couple SDCDPS and 4,4′-bisphenol (BPSH)

The first successful synthesis of such an ionic monomer and its further copolymerization with 4,4′-isopropylidenediphenol and 9,9′-bis(4-hydroxyphenyl)fluorene were performed by Ueda *et al.* [31], but the group of McGrath [29] improved production of the monomer, enlarged the range of possible copolymers and studied them in terms of materials for energy conversion.

The series of random copolymers showed the best performance at total humidification for a couple of SDCDPS with 4,4′-bisphenol [29, 32, 33]. It will be further named as BPSH moiety (*Fig. 1.1 (b)*) and statistic polymers thereafter *r*-BPSH. In order to study properties of block-copolymers, the same BPSH moiety was used as a hydrophilic block, but chemical structure of a hydrophobic block was varied, either different perfluorinated spacers were introduced between the two blocks. Most of the materials show good connectivity of the proton-conducting channels that leads to high range of conductivities at both reduced and 100 % humidity (10^{-3} – 10^{-1} S/cm). At the same time, due to a robust and yet interconnected hydrophobic phase the polymers are characterized by sufficiently high mechanical properties together with low degree of in-plane swelling.

Such properties are explained by authors from the point of the well-developed separation of phases and formation of extended and broad ionic domains (in one reference dimensions of ionic domains are estimated by microscopy as 14 – 24 nm for the hydrophilic blocks of 5 – 15 kDa [34], in another reference dimensions of the same species are calculated from SAXS as 21.2 to 36.4 nm [35]).

In order to compare performance of random and block-copolymers, synthesized from the ionic monomer SDCDPS, materials of the similar IEC 1.3 – 1.5 meq/g are studied. Among the series of random polymers *r*-BPSH-40 is chosen, which contains 40 % of sulfonated repeating units BPSH (and 60 % of non-sulfonated BPSH units) and is characterized by IEC 1.5 meq/g. Block-copolymers, in general, are comprised of a hydrophilic block BPSH and a hydrophobic block of different chemical composition. In such a way impact of the hydrophobic part is additionally studied.

Fig. 1.2 proposes two graphs of conductivity dependence: a) on water uptake, and b) on humidity. The first one shows dispersion of the values for the most studied structures, reported in different publications. The names of each series correspond to those, given by authors; for better visualization chemical structures are additionally defined in *Fig. 1.3*. Ideally, parameter lambda (λ) reproduces amount of water molecules per sulfonic acid, however, not all the researchers note such data, hence, water uptake (WU) is used as percentage of polymer swelling in weight. The second graph estimates effectiveness of water retaining by the polymer. On both plots the random copolymer *r*-BPSH-40 is indicated with blue squares. Numbers are for different types of block-copolymers.

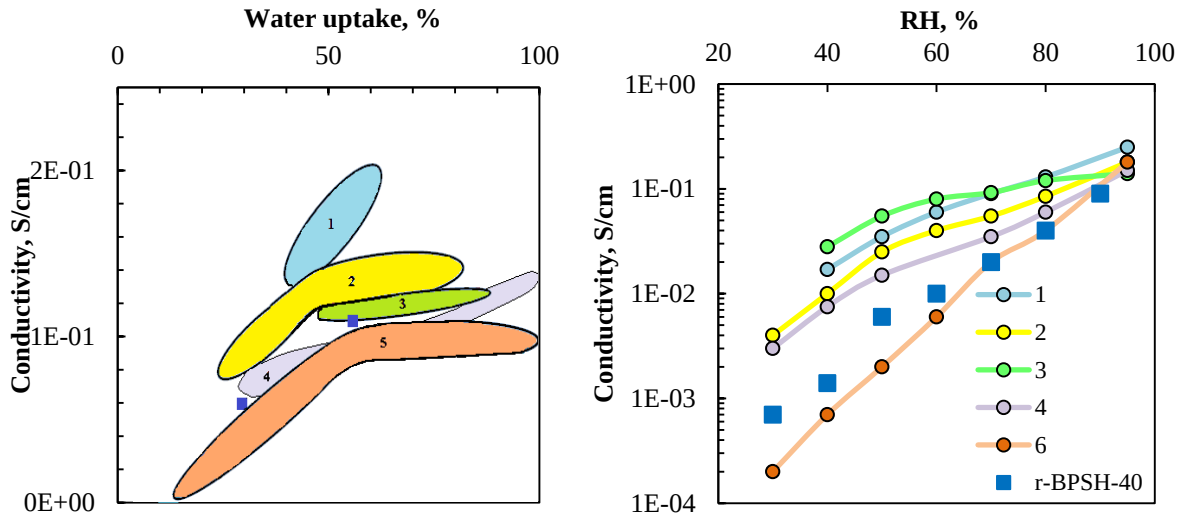

(a) (b)

Figure 1.2. Conductivity data of random and block-copolymers, synthesized from SDCDPS, at: a) total humidification, and b) reduced humidity. For both graphs blue squares are the statistic polymer *r*-BPSH-40, numbers are block-copolymers: 1 – 6FBPS-BPSH [36], 2 – BiSF-BPSH [37-39], 3 – PEEK-BPSH [40], 4 – BPS-BPSH [34, 41-43], 5 – PI-BPSH [44, 45], 6 – PPH-BPSH [46]

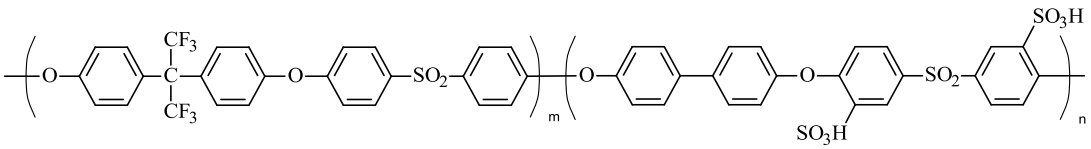

(a)

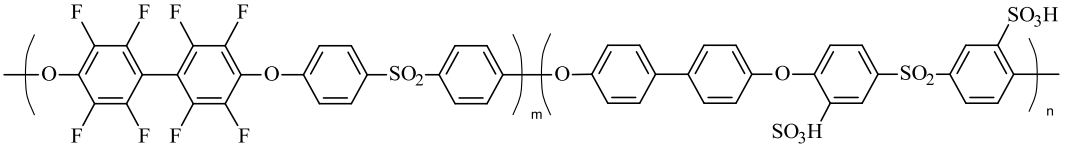

(b)

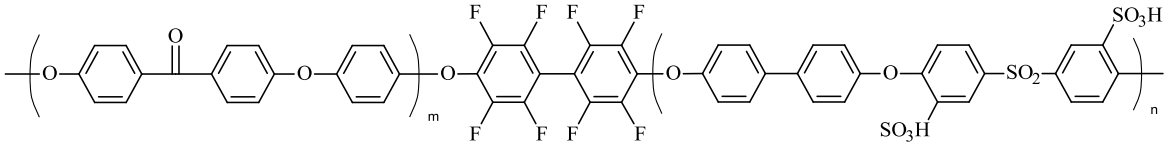

(c)

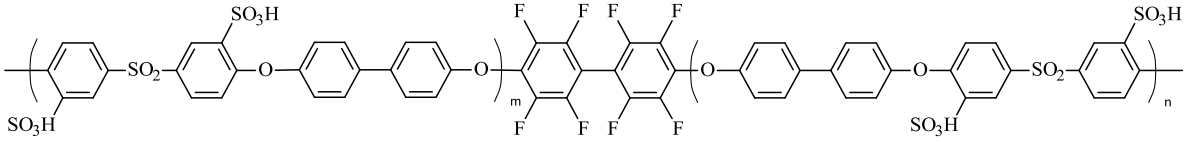

(d)

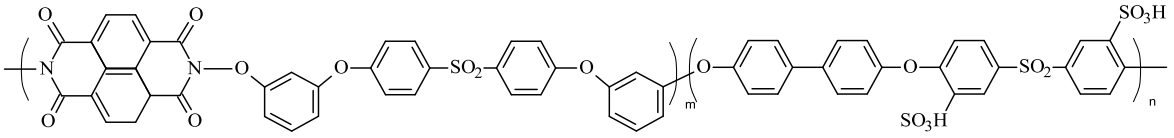

(e)

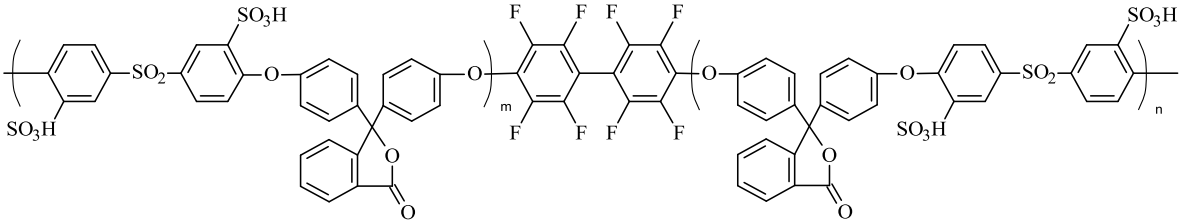

(f)

Figure 1.3. Structures of: a) 6FBPS-BPSH, b) BiSF-BPSH, and c) PEEK-BPSH, d) BPS-BPSH, e) PI-BPSH, f) PPH-BPSH

From both analyses, the block-copolymers 6FBPS-BPSH, BiSF-BPSH and PEEK-BPSH (structures presented in *Fig. 1.3 (a-c)*) show the best conductivities in the whole range of humidity, admitting that at total humidification their conductivities are in the range of 1.2 – $2 \cdot 10^{-1}$ S/cm with the WU of 30 – 60 % only. The block-copolymers, having both PAES hydrophobic and hydrophilic blocks (BPS-BPSH) show comparable conductivities to their

random examples (*r*-BPSH) at complete humidification, but they depend less on water uptake at reduced humidity (the slope, thus, activation energy of the BPS-BPSH is lower, than of its random analog). PI-BPSH, having poly(imide ether sulfone) as a hydrophobic block, and PPH-BPSH, having a bulky phenolphthalein moiety in both blocks, show the lowest conductivity range in dependence on water uptake or relative humidity, respectively. Therefore, we presume that: i) basic groups (such as imide in case of PI-BPSH), and ii) bulky species (both PI-BPSH and PPH-BPSH as examples) negatively influence the ionomer performance. The structures, characterized by the latter parameter, may create highly developed domains that close accessibility of the ionic sites, which are directly attached to the polymer backbone. The same drop in performance was observed for random copolymers, having non-ionic multiphenylene structures, such as fluorene [47].

A comparative study of polymers, containing bulky species was conducted: one sample was sulfonated through the fluorenyl moiety, the other – through the aromatic main chain, and a fluorenyl group stayed unmodified. Hydrolytic test showed better solubility of the latter type of polymers, compared to materials with ionic groups, attached to the fluorenyl specie. Therefore, it evidenced weaker interchain interactions between sulfonic groups, attached directly to a polymer backbone [47]. Additionally, the ionomers, having non-sulfonated bulky moieties (in particular fluorenyl), are characterized by low degree of water fraction in the polymer structure, which results in poorly developed separation between hydrophilic and hydrophobic domains in hydrated state (data from SAXS measurements) [47]. Thereby, negative influence of the bulky structures in a polymer backbone for the materials, having directly attached sulfonic groups to the other, non-bulky aromatic species is evoked; equally, positive influence of the same bulky structures is observed, when the sulfonic sites are bound to these multiphenylene moieties.

The block-copolymers 6FBPS-BPSH from *Fig. 1.3 (a)* (with equal lengths of the both blocks of 15, 10 and 6 kDa) [36] and BiSF-BPSH from *Fig. 1.3 (b)* (with equal block lengths of 15 kDa or hydrophobic to hydrophobic block lengths of 15 to 10 kDa) [37, 39] have highly fluorous hydrophobic blocks that provoke better structuration of their membranes. However, the prominent behavior of the polymer PEEK-BPSH from *Fig. 1.3 (c)* (in particular with equal block lengths of 13 and 17 kDa) [40] is not affected by increased hydrophobicity of one of the blocks, but rather by crystallinity, appearing due to the diphenylketone moiety.

Another important aspect proved by different researches is related to membrane elaboration procedure. McGrath *et al.* proposed two factors, which ameliorate an ionomer performance: i)

a membrane after the solvent evaporation must be annealed at temperature higher, than the T_g of the hydrophobic block (annealing proceeded at 195 °C) [48]; ii) acidification of the membrane is better to be conducted at 100 °C rather than at room temperature [49]. The both corrections to the membrane production procedure increase its conductivity due to the more open hydrophilic morphology, thus, better connectivity of the ionic domains (verified by atom force microscopy (AFM)); additionally, the first modification increases mechanical properties and decreases WU of an ionomer.

The general trends for the block-polyarylenes, synthesized from the SDCDPS, are: i) ionomers with equal lengths of blocks show better structuration: longer the blocks, higher the connectivity of the hydrophobic and hydrophilic domains, leading to formation of a lamellar structure [34]; ii) block-copolymers retain water better than random copolymers at reduced humidity that affirms higher percolation degree at temperatures above 100 °C; iii) due to the block-copolymers' priority of swelling through a membrane plane, rather than in-plane, these materials resist to higher WU level without deterioration of their performance.

Other types of disulfonated monomers have been produced, following the sulfonation method as for SDCDPS. Probably, the full list of structures is presented in a review article of Park *et al.* [17]. The most studied are: disulfonated 4,4′-difluorobenzophenone and disulfonated 4,4′-diaminodiphenylsulfone (*Fig. 1.4*).

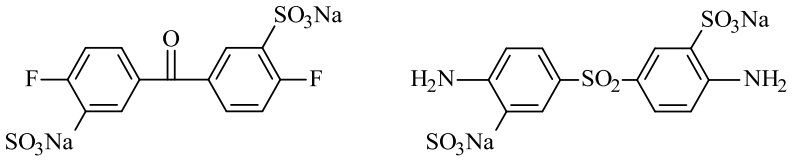

(a) (b)

Figure 1.4. Chemical structures of ionic monomers: a) disulfonated 4,4′-difluorobenzophenone, and b) disulfonated 4,4′-diaminodiphenylsulfone

The disulfonated 4,4′-difluorobenzophenone was polymerized both by nucleophilic substitution or by catalytic homocoupling to produce hydrophilic blocks of poly(arylene ether ketone) (PAEK) [50, 51] or poly(phenylene ketone) (PPK) [52], respectively. The polymers, having linear chains with no bulky moieties, showed high performance at reduced humidity and very tolerant stable gas permeability in a wide range of humidity [52]. Such properties are referred by authors to the rod-like rigid structure of a PPK hydrophilic block. However, when one uses bulky comonomers (naphthalene), again the drop of performance is observed [50].

Disulfonated 4,4′-diaminodiphenylsulfone is a widely used ionic monomer for production of poly(imide)s (PI) [53-58]. The materials show high conductivity at complete hydration and at high degree of sulfonation (IEC > 1.8 meq/g), but their selectivity for direct methanol FC is more promising, than the performance in PEMFC, therefore they are usually produced for DMFC applications.

1.1.3. Ionomers with SO_3H bonded in other than 'ortho-to-ether' position

The polymers, described in the previous section, contain sulfonic acid groups in *ortho*-position to the ether-bridge. As it was mentioned before [21, 26, 59], such a combination is easily cleaved at harsh conditions, leading to degradation of the polymer. Moreover, acidity of the SO_3H is not activated by the ether in the same way as it could be with presence of an electro-withdrawing group in proximity [60]. For this reason several groups worked on elaboration of polymers:

i) having poly(arylene sulfone) backbone with acid groups attached in ortho-position to the sulfone bridge [27, 59, 61, 62]. There are two main ways of their production: either by condensation with thio-compounds (sulfides or thioarylenes) and further oxidation of S-bridges, or by introduction of the sulfonic group to the polymer chain by a common method of lithiation [28];

ii) having sulfonic acid in *meta*-position to the ether bridge [60, 63] by implying the naphthalene-moiety into a polymer backbone.

In the latter case SO_3H is neither activated, nor deactivated by electro-donating group in *meta*-position, hence, the materials of the first type are much more effective in performance. The group of Guiver [60, 63] produced two series of random PAEs: one, having a partially fluorinated backbone (SPAE), and another with highly polar nitrile groups in the main chain (SPAEEN) (*Fig. 1.5*). The both materials were characterized by high conductivity at fully hydrated conditions even at low temperature: $1.5 – 8 \cdot 10^{-2}$ S/cm for the ionomers of IEC 1.0 – 1.9. Interestingly, the polymer series, which contains partially fluorinated hydrophobic part, was characterized by much higher water uptake, than SPAEEN (*Fig. 1.6 (a)*). Presumably, such property is related to interactions between dissociated sulfonic groups and nitriles, which create physical bonding between polymer chains. Due to this phenomenon SPAEEN even of high IEC (1.9 meq/g) does not show important increase in conductivity, compared to SPAE (*Fig. 1.6 (b)*).

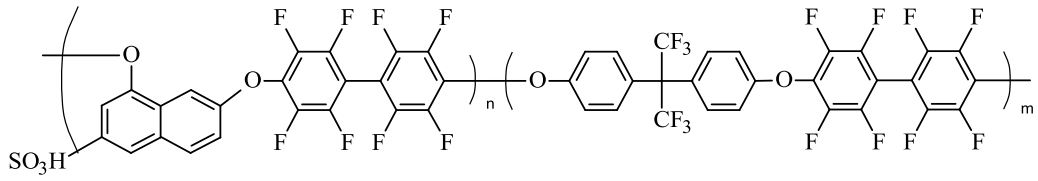

(a)

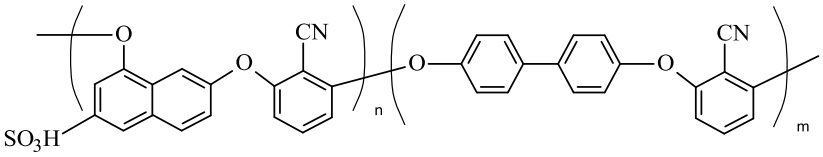

(b)

Figure 1.5. Random copolymers, produced from the ionic monomer 2,8-dihydroxynaphthalene-6-sulfonated sodium salt: a) SPAE and b) SPAEEN

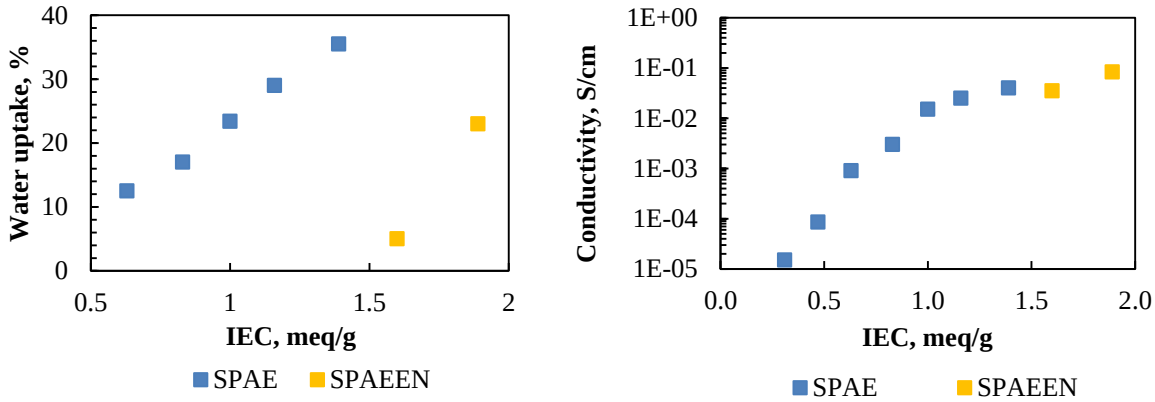

(a) (b)

Figure 1.6. Dependence of water uptake (a) and conductivity (in water at 30 °C) (b) on IEC for SPAE and SPAEEN series

An important observation about naphthalene-containing polymers was evoked by a group of Sakaguchi [64]. Although they explored ionomers, where sulfonic acid groups were directly bound to a polymer chain, rather than to a naphthalene specie, their conclusions about dependence of polymer rigidity and conformation on connecting sites of naphthalene, are valuable. They investigated ionomers, containing one of three types of naphthalene with connecting sites in: i) positions 2 and 7, ii) positions 2 and 6, and iii) positions 1 and 5 (*Fig. 1.7*). The authors claimed that due to the fact that the first two structures are symmetric, they imply to lower rigidity of the polymer backbone, thus higher conductivity of the ionomer, compared to the one, containing a non-symmetric, 1,5-dihyroxynaphthalene. It was also confirmed that a more planar non-ionic bulky structure in a hydrophilic part of an ionomer results in more developed aggregation of ionic clusters, thus in polymers of higher conductivity [65].

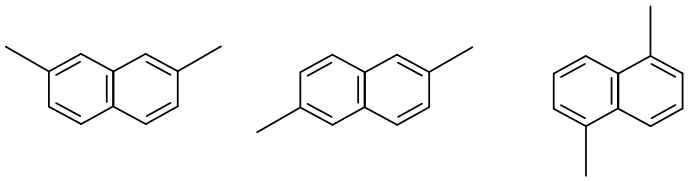

(a) (b) (c)

Figure 1.7. Possible connecting sites of the naphthalene structure: a) in positions 2 and 7, b) in positions 2 and 6, and c) in positions 1 and 5

A new approach on poly(sulfone) synthesis was applied by a group of Kreuer, when they produced a polymer $sPSO_2$-220, containing one sulfonic acid group at each aromatic ring in the structure (*Fig. 1.8*) [59, 61]. The authors achieved extremely high IEC of 4.5 meq/g; the material, obviously, may not be used as a self-standing proton-conducting material because of its water solubility and brittleness. However, the copolymer of reduced IEC (1.3 – 2.3 meq/g) [59] as well as a block-copolymer (1.3 – 1.6 meq/g) with $sPSO_2$-220 hydrophilic block [62] showed outstanding performance, especially at low humidity (16 – 50 % RH) and high temperatures 120-160 °C. For comparison, conductivity of the random copolymer of the IEC 1.3 meq/g is in the range of $3 \cdot 10^{-4} – 3 \cdot 10^{-3}$ S/cm, whereas the block-copolymer of 1.6 meq/g gives the performance of $1.5\text{-}7 \cdot 10^{-2}$ S/cm. Additionally, due to absence of the ether bridges (in case of random copolymers) or to reduced amount of ether linkages in block-copolymers the stability of materials is high.

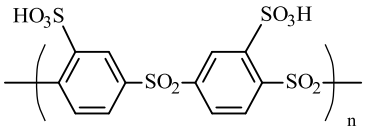

Figure 1.8. Fully sulfonated poly(sulfone) $sPSO_2$-220

A group of Jannasch investigated the common block-copolymers, having barely all the aromatic rings modified with sulfonic acid group in the hydrophilic block by the lithiation-sulfination-oxidation method [27, 28]; their conductivity is 10 times lower, than reported in the previous paragraph. When comparing two ionomers, one must pay attention to the conditions of conductivity measurements: while the group of Kreuer used the in-plane method, Jannasch *et al.* conducted the measurement by a 2-point probe (through plane), which gives lower values. Additionally, the group of Jannasch worked at stable temperature of 80 °C, while changing relative humidity, when another group changed both parameters, so that measurements at 30 % RH were taken at 120 °C and those at 50 % RH – at 150 °C.

The authors also investigated structure-property relation of the SPAS-PAES polymers (illustrated in *Fig. 1.9*) [27], when varying bonding sites of aromatic rings in a polymer backbone: either *meta*-connection, or *para*-linked sequence. It was observed that the material with *meta*-connected phenylenes in a main chain of IEC 1.3 meq/g performs as a polymer with *para*-bridges of IEC 1.8 meq/g. Such phenomenon was explained by higher mobility of the polymers with *meta*-bonded aromatic rings in the backbone.

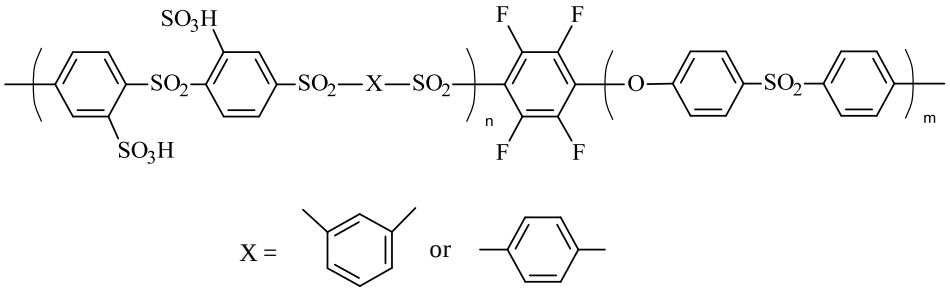

Figure 1.9. General structure of SPAS-PAES with *meta*- or *para*-connected phenylenes [27]

The same effect of the *meta*-connectivity by ether-bridges was observed for the copolymers, having so-called microblocks [66]. These are structures with blocks of multi-(phenylene-ether) species (the most common are 6 and 12 aromatic rings in a microblock). From SAXS measurements they appeared to be highly structured materials with good separation of phases. Higher ordering, bigger interchain distance [67] and higher conductivity in the whole range of humidity and temperature was revealed for the structures with longer and *meta*-connected aromatic segments (in particular, for a 12-ring microblock to a 6-ring). Such an observation again points on the advantage of the hydrophobic part being linear (without bulky structures) and mobile (in terms of inter-aromatic connection).

From the general analysis of the random and block-copolymers, having sulfonic acid groups directly attached to the polymer backbone, one may conclude:

i) block-copolymers are characterized by higher water uptake, than random polymers (data, collected from a number of literature reports, are generalized in *Fig. 1.10*). At low values of IEC degree of swelling for both types of materials may be the same, but starting from a point, where ionic aggregates achieve interconnectivity (so-called percolation threshold) block-copolymers gain more water, than the random. Moreover, the percolation threshold for block-copolymers is lower in IEC that allows obtaining materials of higher conductivity at lower degree of sulfonic acid incorporation.

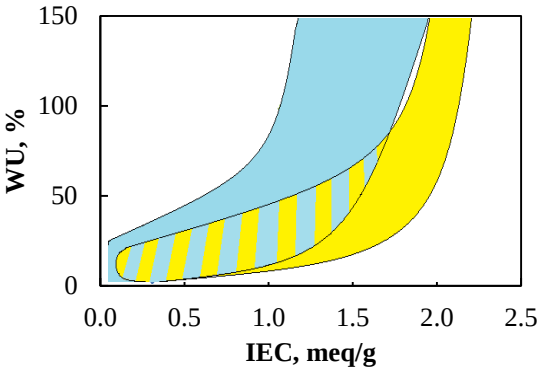

Figure 1.10. Function of water uptake on IEC for: blue area – block-copolymers, yellow area – random copolymers, dashed blue and yellow area – combination of both types of polymers

ii) due to better developed microphase separation in block-copolymers, their bulk morphology may be chemically tuned (*Fig. 1.11*). Varying block lengths, the most favorable in size and orientation hydrophilic domains could be designed.

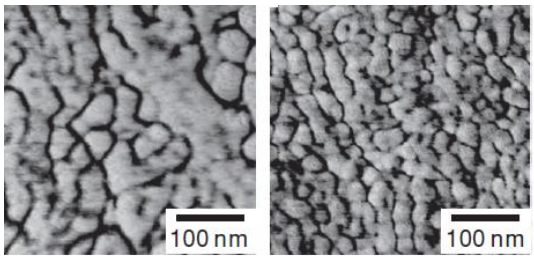

Figure 1.11. AFM images of the microphase separated morphology of the PAES block-copolymers, having hydrophilic to hydrophobic block lengths of: a) 11 kDa / 19 kDa, and b) 11kDa / 14 kDa [28]. Printed and adapted with permission from ref. 28. Copyright 2011 John Wiley and Sons

1.2. Polyaromatics with sulfonic acid on a phenyl spacer

It is known that spacing a protogenic structure from a polymer main chain keeps the hydrophobic environment of the latter, which positively influences material's stability [68] and proton conductivity. Obviously, the easiest way to introduce a phenylsulfonic specie along the chain is with the help of a styrene, bearing either protonated or fluorinated ethylenic part. This is a principle for production of commercial membranes by Ballard and Dais Analytics [18]. The first company releases BAM material, which is a mixture of blocks of non-sulfonated and sulfonated fluorinated polystyrenes; the second corporation produces SSEBS that is a sequence of sulfonated / non-sulfonated polystyrenes, polyethylene and polybutadiene (*Fig. 1.12*). In both cases ionomers are linear and contain sulfonic acid groups at predetermined styrenic parts.

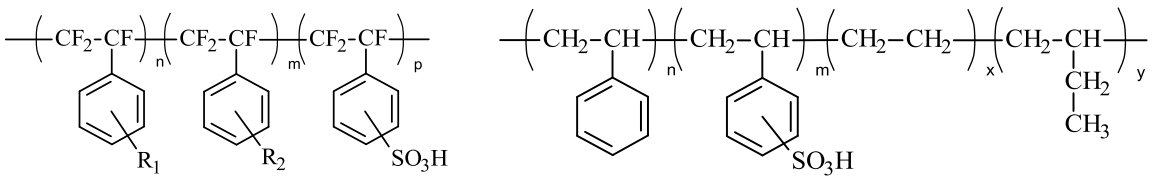

(a) (b)

Figure 1.12. Chemical structures of: a) BAM polymer membrane (Ballard), and b) SSEBS ionomer (Dais Analytics)

To locally increase the ionicity of a polymer, a group of Holdcroft [69-75] proposed and studied in detail the range of poly(styrene)s (PS), poly(acrylo nitrile)s (PAN), poly(vinylidene fluoride)s (PVDF) and poly(chlorotrifluoroethylene-*co*-ethylene) with grafts of sulfonated polystyrene of different length and graft density (*Fig. 1.13*). They concluded that at lower ionic contents these are shorter grafts that lead to higher polymer performance due to formation of large and purer disordered ionic cluster network. However, at high content of sulfonated PS the longer grafts provoke better aggregation of the similar in nature segments and formation of long-range lamellar channels that result in higher proton conductivity [71, 75].

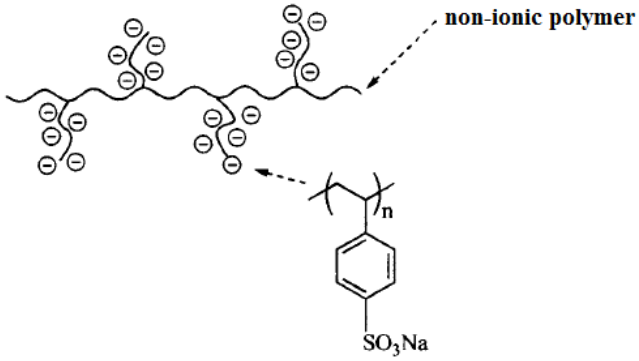

Figure 1.13. Schematic representation of graft polymers, proposed by Holdcroft *et al.* Reprinted and adapted with permission from ref. 70. Copyright 2003, The Electrochemical Society

Due to utilization of fluorinated matrix (the case of the PVDF backbone), the authors could also make important conclusions on influence of crystallinity on the polymer behavior: higher the crystallinity, in general, worse the conductivity of polymers at total either reduced humidity. Such behavior appears because of reduced connectivity between the crystallites, since higher amount of polymer chains participates in crystalline zone formation rather than in the interdigiting between crystallites. Polymers swell more, the ordering stays poor.

Many other groups provided investigations on poly(styrene-*co*-alkylene) [76-81], by varying the amount of PS and sulfonation. In general, the styrene-containing polymers are known to be oxidatively not stable; at low sulfonation degree they are not good conductors and at high

concentration of ionic sites they swell too much. Besides, little information on these polymers is given in terms of their performance at low humidity, which is an important parameter to control. Nowadays more attention is paid to materials with highly controllable organization, therefore styrenic precursors are put aside of investigation.

The group of Guiver developed similar strategy of the polyanionic side chains for PAES, produced by polycondensation, rather than radical polymerization [82]. They introduced a special name to such polymer – a 'comb-shaped' (*Fig. 1.14*). The authors developed several types of structures (PEEK, PEEKK, PES), including random (marked with a prefix '*r*') and block-copolymers (a prefix '*b*' is introduced), bearing lateral poly(phenyl ether) groups with one to four phenylsulfonic acid groups per repeating unit of a lateral chain. For convenience, the polymers will be distinguished by the main backbone, since the grafted lateral chain is the same, it varies only in amount of phenylsulfonic acid groups introduced, thus in IEC.

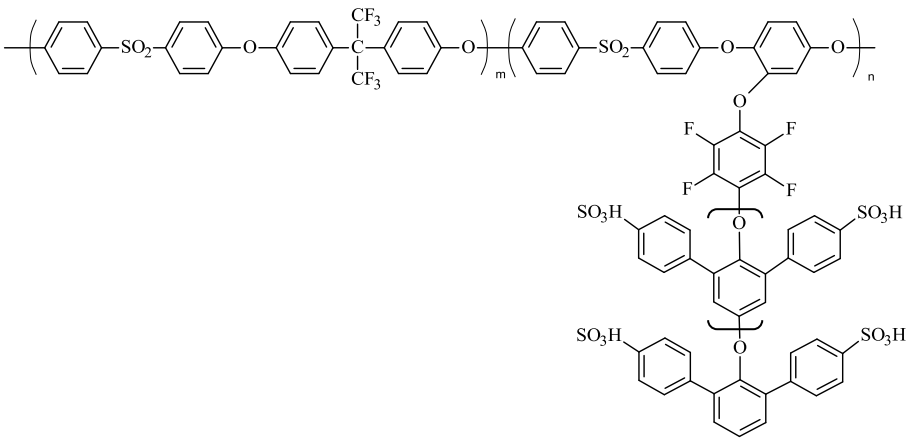

Figure 1.14. Comb-shaped block-copolymer *b*-PES (6F-BPA) with two phenylsulfonic acid groups per repeating unit of a lateral poly(phenylene ether) chain

By analyzing these materials for dependence of IEC, water uptake on conductivity in immersed state and at reduced humidity, one may conclude that PES backbone provokes higher performance, compared to a PEEK or PEEKK main chain (*Fig. 1.15*). In case a polymer main chain contains fluorinated species, such as hexafluoropropyl (marked with suffix 6F-BPA) or octafluorodiphenyl (DFB in suffix), polymer acquires higher hydrophobicity that improves its phase separation and conductivity.

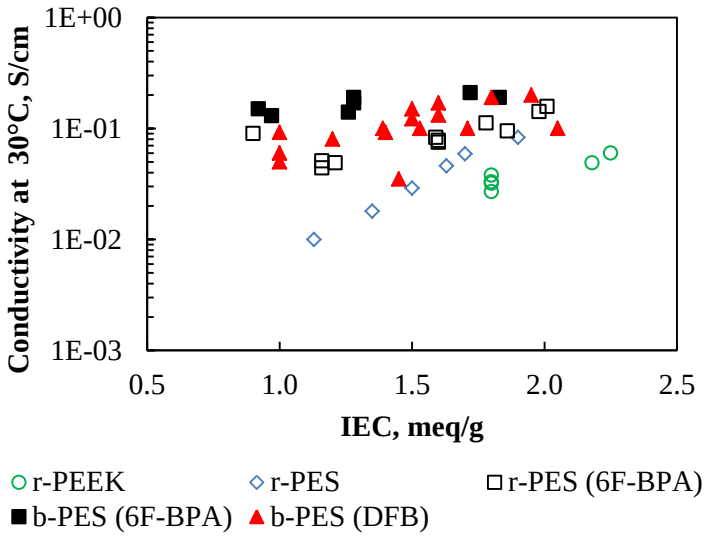

Figure 1.15. Effectiveness of proton conductivity with dependence on IEC for: r-PEEK – sulfonated random polymer with a PEEK backbone [83, 84], r-SPES – random copolymer with a PES main chain [85], r-SPES (6F-BPA) – random copolymer with a PES backbone, containing 6F-BPA moiety [86], b-SPES (6F-BPA) – block-copolymer with a PES main chain, containing 6F-BPA specie [82, 87], b-SPES (DFB) – block-copolymer with a PES main chain, containing DFB comonomer [88, 89]

1.3. Polyaromatics with sulfonic acid on aromatic bulky structures

1.3.1. On a fluorene

Bulky structures in a polymer backbone create a platform for multiple introductions of pendent sulfonic acid moieties. Fluorene (*Fig. 1.16 (a)*), being a commercially available monomer and containing 4 phenyls, has been extensively used for such intentions. The stiffness of the structure due to the strong π-π interaction between the aromatic rings of different polymer chains creates favorable condition for water confinement [90, 91]. Such a property is believed to reason in high proton conductivity at low humidity.

However, early works on random PAES, containing fluorenyl groups (*Fig. 1.16 (b)*), did not show promising performance [68, 90-93]. Surprisingly, sulfonation was performed at two aromatic rings only, at the 2- and 7-positions. Higher sulfonation degree resulted in sulfonation of the main chain.

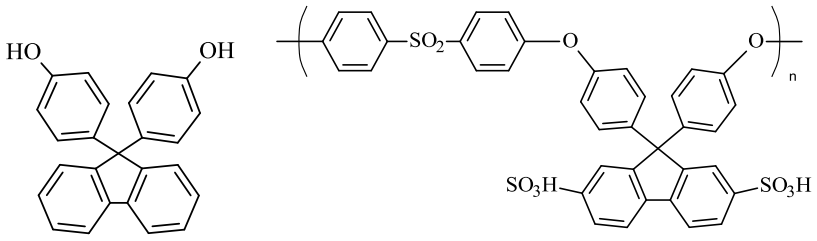

(a) (b)

Figure 1.16. a) Chemical structure of a fluorene; b) first synthesized PAES, containing sulfonated fluorenyl groups

Comparison of random post-sulfonated PAE sequences, carrying fluorene moiety, was performed [93]. Several comonomers, illustrated in *Fig. 1.17*, were studied in order to find a structure with the best performance. On the contrary to the previous results, octafluorodiphenyl specie in the backbone did not contribute to polymer's higher conductivity or reduced water uptake. It was a copolymer of diphenylsulfone and sulfonated fluorene that performed the best. Its conductivity reached that of Nafion at 70 % RH and higher. Based on these results further research on fluorene-containing block-copolymers was mainly conducted with materials, having a hydrophilic block of the sequence sulfonated fluorenyl / diphenylsulfone. On the contrary to the previous research on random copolymers [68, 90, 92, 93], up to four sulfonic acid groups might be introduced to the fluorene specie without any secondary sulfonation of the main chain.

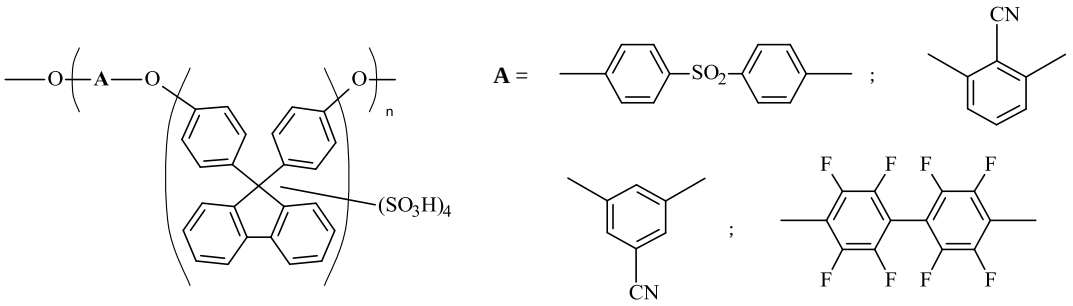

Figure 1.17. Random PAEs with sequences of sulfonated fluorene and: diphenylsulfone, *ortho*-cyanophenyl, *meta*-cyanophenyl or perfluorodiphenyl

Block-copolymers, having a hydrophilic block of the sequence sulfonated fluorenyl / diphenylsulfone and a hydrophobic block of various chemical structures, showed comparable to Nafion performance at reduced humidity down till 40 % RH. *Fig. 1.18* illustrates conductivity of these ionomers; and chemical structures on the right represent variations in hydrophobic block, while hydrophilic part is marked as A.

The plot in *Fig. 1.18* shows two dependences of conductivity on RH for each block-copolymer: one for the ionomer of the lowest IEC, given in literature (filled markers), and another for the material of the highest IEC reported (unfilled markers). Values of IEC are noted in a legend next to each sample. Notably, the ionomers P(Me)AES-A of the minimal IEC show the lowest conductivities, going down till 10^{-5} S/cm at 20 % RH, therefore they are not illustrated in *Fig. 1.18*. Rigid structure of a tetramethylated BPA specie might restrict the most favorable packing of hydrophilic blocks and / or mobility of their ionic sites, which leads to poor performance of the ionomer. Besides, complete sulfonation of P(Me)AES-A ionomers was impossible [94], therefore IEC of these structures is hard to predict in advance. In order to sulfonate P(Me)AES maximal excess of 9 equivalents of chlorosulfonic acid could be used before the degradation of the main chain starts. At such conditions authors achieved the sulfonation degree of 85 % for the block-copolymer of the sequence [12 hydrophobic units]-[8 hydrophilic units] with IEC 2.2 meq/g. On the contrary, only 5 equivalents of $ClSO_3H$ were enough for complete sulfonation of the block-copolymers PAES-A or PNES-A. Hence, these polymers are more preferential for the high-volume production.

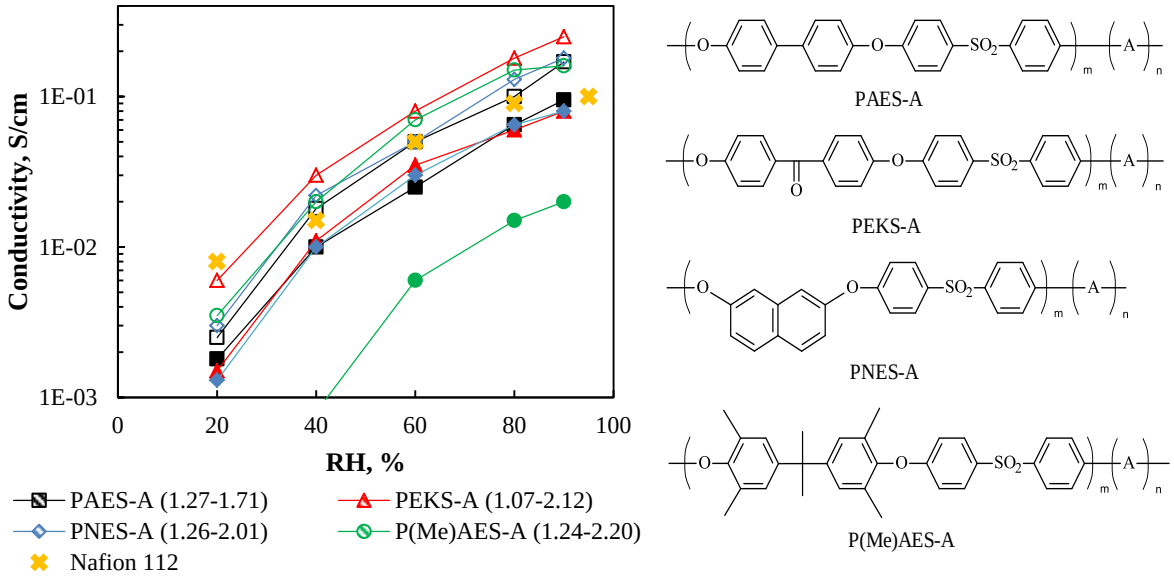

Figure 1.18. Dependence of conductivity on relative humidity, measured at 80 °C, for the block-copolymers, presented on the right. Hydrophilic block A has a constant sequence of sulfonated fluorene / diphenylsulfone, a hydrophobic block varies in chemical structure. Minimal and maximal IECs reported in literature [94-98] are mentioned in parentheses for each block-copolymer

From *Fig. 1.18* it becomes evident that even ionomers, which bear bulky sulfonated fluorenyl structures, require high concentration of sulfonic acid groups to achieve the required proton conductivities. Among the presented materials, it seems as PEKS-A ionomer reaches higher conductivities at lower IEC. From the point of view of chain flexibility, ketone-bridge could

give an additional point for the chain movement, compared to naphthalene or covalent junction in PNES-A and PAES-A structures, respectively.

Although a highly-methylated structure is less interesting in terms of easiness of production, its hydrolytic stability appears to be the most appropriate among the other materials presented. Watanabe *et al.* [68] synthesized a series of polymers of the general formula, shown in *Fig. 1.19*. The authors methylated either *ortho*-to-ether positions in the hydrophobic part (e.g., moiety of diphenylpropane), or *ortho*-to-ether sites in the fluorenyl-specie. It was observed that the former type of methylation is exceptionally effective for inhibition of nucleophilic attack of water on the ionomer. Presumably, in the case of methylation of a linear part of a polymer the structure is stiff indeed. Meanwhile, fluorenyl specie has angled arrangement of its plane to the plane of a polymer chain, therefore it acquires higher free volume, hence poorer stiffness of the main chain.

It is important to notice that methyl-substitution had no effect on oxidative stability of a polymer. On the contrary, presence of electro-withdrawing, highly polar nitrile group in a symmetric *meta*-position to the ether-bridges (*Fig. 1.17*) [93] resulted in polymers resisting to exposure to the Fenton test.

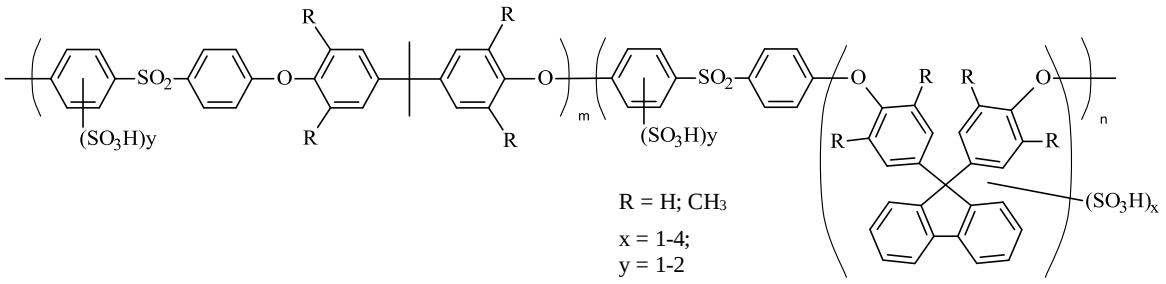

Figure 1.19. Ionomers, bearing methylated species in the main chain [68]

To summarize, one may assure that sulfonated fluorenyl species provoke effective aggregation between adjacent ionic sites, particularly in the sequence of several units. As an example, the ionomers with 4 consecutive hydrophilic units provided with the well-developed phase-separated structure in the form of connected clusters. Double elongation of hydrophilic phase till 8 consecutive units (IEC of the polymer stays in the range 1.0 – 2.0 meq/g) resulted in worm-like morphology with the width of channels 11 nm [97]. As a comparison, the ionomers with sulfonic groups, directly attached to the polymer backbone, could achieve such properties with values of IEC not less than 2.0 meq/g.

1.3.2. On other multiphenylene structures

The idea of synergic increase of ionic density and effective free volume is realized by synthesis of polymer chains with multiphenylene structures, bearing sulfonic acid groups. The way to obtain such highly branched polymers proceeds through multistep substitutions, condensations and couplings. However, due to the non-polar nature of these structures, the final yield is satisfactory and purification of intermediate and final products is not sophisticated. Additionally, sulfonation of such voluminous architectures is also easily achieved by the mild reaction with chlorosulfonic acid in methylene chloride.

From analysis of literature data [99-108] no much difference in performance of random or block-copolymers, containing sulfonated multiphenylated structures, is observed. Such behavior is explained in terms of intimate proximity of sulfonated sites that provoke effective ionic aggregation and formation of well-organized structures.

Two main locations of multiphenylene species may be distinguished: either on a main chain (then a multiphenylene monomer is synthesized and subsequently copolymerized), or at the ends of polymer chains that are grafted to a main backbone (a polymer is 'grown' as a dendromer step-by-step). The first type of polymers will be further called linear (with a prefix *lin*-) and the second type – peripheral (with a prefix *per*-). As an example a reader is referred to *Fig. 1.20*. Also number of sulfonated phenylenes in proximity may be varied; the most common are 6 to 18 sulfonated phenylenes in proximity.

In order to compare poly(arylene ether ketone sulfone)s (PAEKS) with sulfonated multiring structures by both classifications *Fig. 1.21* is presented. It illustrates dependence of conductivity at complete humidification on water uptake for ionomers of different amount of ionic groups in neighborhood. *Fig. 1.21 (a)* presents results for *lin*-PAEKS and *Fig. 1.21 (b)* – for *per*-PAEKS. It might be clearly observed that amount of sulfonated multiphenylene structures does not influence performance of the ionomers. On the contrary, location of the sulfonated multiphenylated structures plays an important role: *per*-PAEKS show approximately twice higher conductivity in water at the same values of WU, than *lin*-PAEKS.

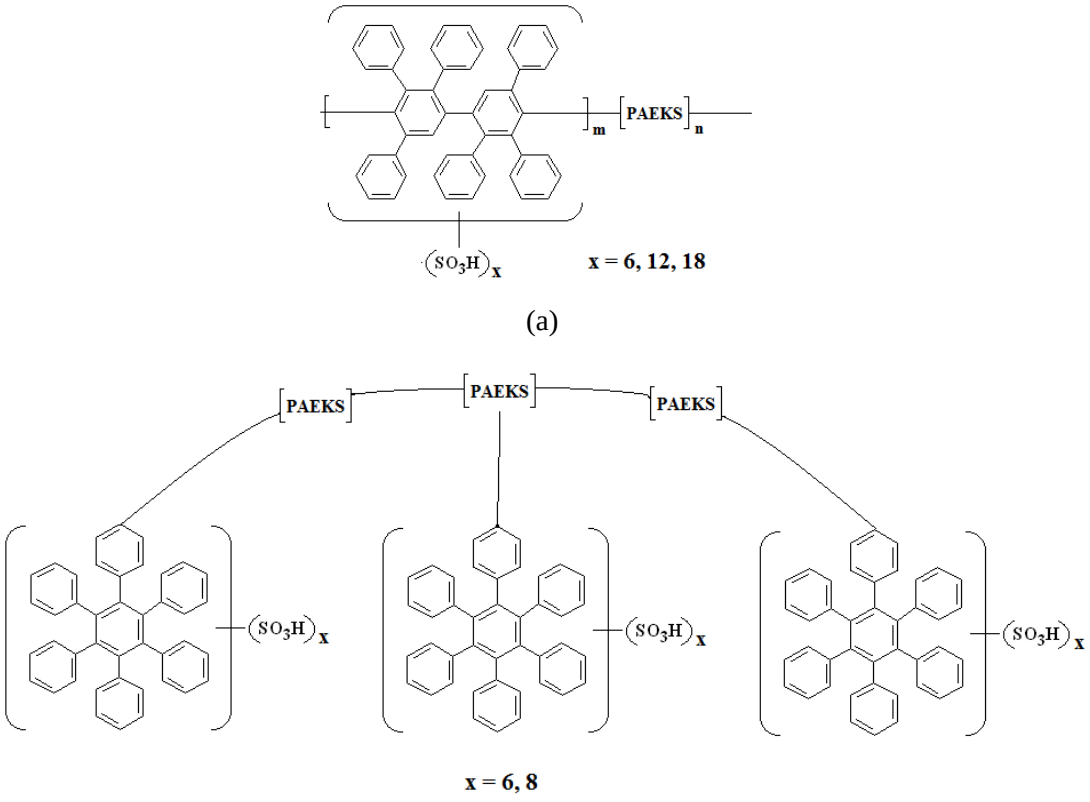

Figure 1.20. Schematic structures of PAEKS, having bulky ionic species: a) through the polymer chain (*lin*-PAEKS), and (b) at a grafted to the main chain polymer spacer (*per*-PAEKS)

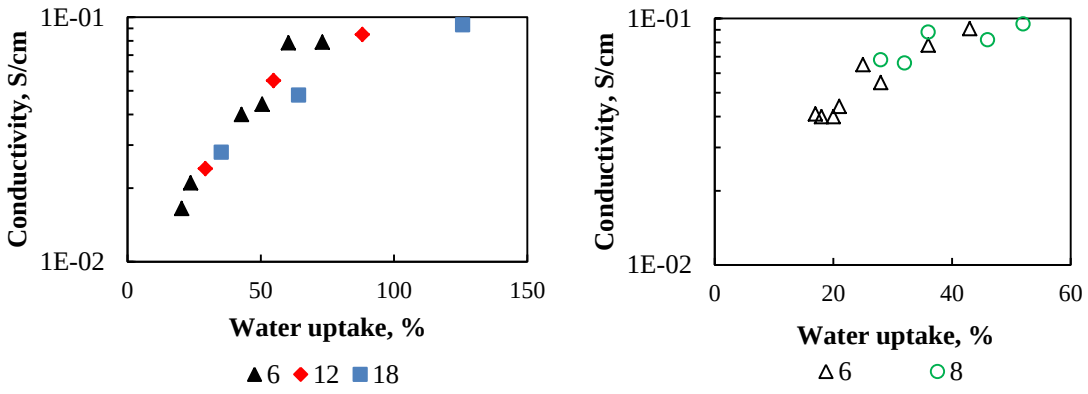

Figure 1.21. Dependence of conductivity on water uptake for: (a) *lin*-PAEKS [103, 104], and (b) *per*-PAEKS [105, 106]. Numbers in legends tell about the amount of sulfonic acid groups in proximity on bulky multiphenylene structures

However, at reduced humidity these are polymers with sulfonic acid groups along the main chain that show higher performance. Such behavior is in good correlation to the bulk morphology of the current ionomers. TEM images (in a dry state) (*Fig. 1.22*) show connected hydrophilic regions for the both types of ionomers: the *lin*-PAEKS has spherical ionic clusters with satisfactory connectivity, the *per*-PAEKS shows a highly regular worm-like structure.

When the former type of polymers is characterized by ionic aggregates of 9 nm, the latter has clusters of size 2 – 3 nm. Due to bigger hydrophilic shells *lin*-PAEKS has an opportunity to retain water molecules better at reduced humidity. However, its cluster connectivity may be worse, than in *per*-PAEKS (for confirmation mathematical evaluations must be performed), therefore *per*-PAEKS outperforms *lin*-PAEKS under complete humidification.

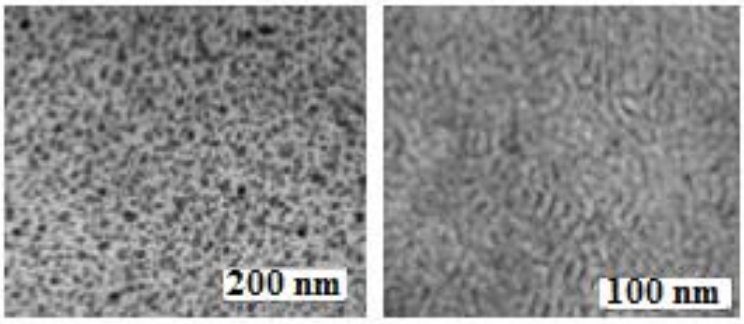

(a) (b)

Figure 1.22. TEM images of: a) the *lin*-PAEKS (reprinted and adapted with permission from ref. 103. Copyright 2009 John Wiley and Sons), and b) the *per*-PAEKS (reprinted and adapted with permission from ref. 106. Copyright 2008 American Chemical Society)

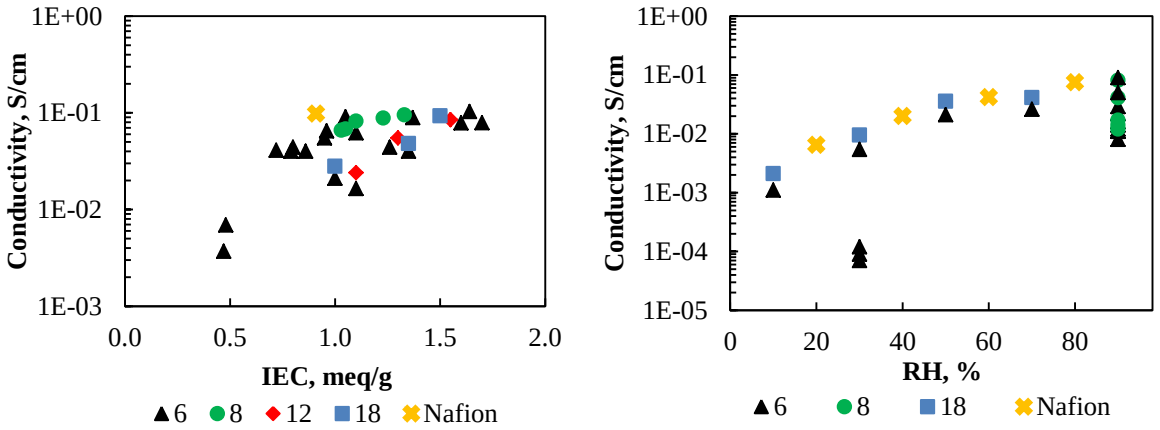

(a) (b)

Figure 1.23. Dependence of conductivity on: a) IEC (conductivity is measured in water at room temperature (20 – 35 °C), b) RH (conductivity is measured at 80 °C) [103-108]. Numbers in legends tell about the amount of sulfonic acid groups in proximity on bulky multiphenylene structures. Data for Nafion are copied from references 106 and 107

An important advantage of sulfonated multiphenylene structures is deduced from dependence of their conductivity on IEC (*Fig. 1.23 (a)*). Hydrocarbon polymers are known to require higher concentrations of ionic species in order to show high conductivity. Surprisingly, the copolymers *per*-PAEKS [106] with 6 and 8 sulfonic acid sites in proximity and IEC around 1.0 meq/g almost attain conductivity of Nafion, 10^{-1} S/cm. The same ionomers adjust comparable to Nafion 117 performance at reduced humidity (*Fig. 1.23 (b)*). Unfortunately,

little information is given for the polymers, described above, however accessible data justify the effectiveness of the multiple sulfonic acid location in proximity for the high performance at reduced humidity.

1.4. Polyaromatics with sulfonic acid on a long spacer

1.4.1. C(O)PhSO$_3$H and derivatives as pendent chains

As it was mentioned earlier, location of the sulfonic acid group on a pendent chain increases stability and conductivity of a polymer. However, the first studies of the group of Jannasch on introducing the sulfobenzoic acid to a poly(sulfone) (PSU) relieved the contrary results [110-112]. When they compared conductivities in water of polymers with sulfonic function directly bound to the main chain and those, having –SO$_3$H at a benzophenone spacer, of the same IEC (1.12 – 1.15 meq/g), the latter samples showed 10 times lower conductivities. Besides, from the SAXS data on interdomain spacing, these are polymers with –C(O)PhSO$_3$H protogenic group that did not respond with a visible ionomer peak, evidencing poor clustering of the current ionic sites.

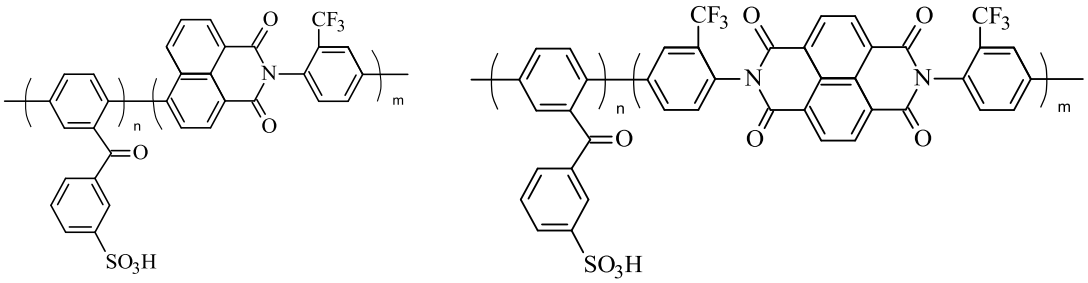

Figure 1.24. Polyimides, proposed by Zhang *et al.* [113]

Despite the discouraging trials, another group proposed to copolymerize poly-*p*-phenylene, bearing sulfobenzoic group, with polyamide [113], which, additionally, contained trifluoromethyl-groups for the improved stability (*Fig. 1.24*). Interesting fact in their research lies in comparison between chemical structures of the two copolymers proposed: the first one having a 'half'-imide plane, creating the asymmetric configuration of a structural unit that acquires higher free volume, higher conductivities and better hydrolytic and oxidative stabilities. At the same time the second series of symmetrical imides are characterized by higher rigidity, thus lower swelling even at high IECs, and, as a result, their performance in a conductivity test revealed the common results to the series of PSU of Jannasch *et al.*

Other mostly studied structures, which comprise blocks of poly-*p*-phenylenes (PPP), bearing sulfobenzoic groups, are shown in *Fig. 1.25* [114-117]. The common synthesis of a sulfonated PPP includes catalyst transfer condensation between molecules of the same monomer. A non-ionic block could be either PPP with –C(O)Ph lateral group, or PES. High degree of structuring into well-separated hydrophilic and hydrophobic domains at wide range of IEC (1.4 – 2.8 meq/g) was observed. However, the ionomers show lower performance, than the polyimides, mentioned above, at complete hydration. At reduced humidity the materials of IEC 1.82 meq/g over-performed Nafion in conductivity at > 70 % RH only.

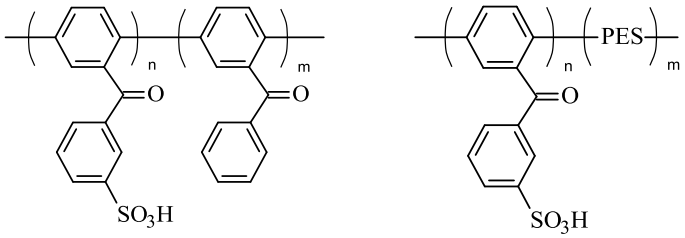

(a) (b)

Figure 1.25. The most studied polymers, having blocks of PPP with –C(O)PhSO$_3$H

It is known that the best property of PPP is stability: even at high values of IEC (> 2.0 meq/g) the oxidative stability of the current type of polymers overpasses several days at 80 °C in a 3 %-solution of H_2O_2 (Fenton reagent) or at room temperature in a 30 %-solution of H_2O_2. For comparison, other polymeric structures with different interaromatic bridges are susceptible to degradation already in several hours. In general, it seems that even with high concentration of sulfobenzoic specie as a pendent group of polyaromatics, the properties of these ionomers are not as promising as of the other materials, mentioned in the previous sections.

Jannasch *et al.* investigated the effect of prolongation of the –C(O)PhSO$_3$H group by introducing an additional naphthalene-ether linkage to a random PAES [110] (*Fig. 1.26*). Location of the sulfonic group at the end of the lateral chain played an important role: the sixth position appeared to be more favorable for higher performance. Such polymer with IEC 0.77 meq/g showed equivalent dependence of conductivity on temperature as a non-extended polymer with IEC 1.12 meq/g.

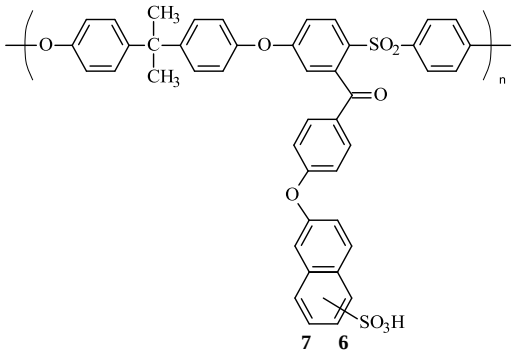

Figure 1.26. Chemical structure of PAES, bearing an extended ionic site [110]

When two or three sulfonic acids are present at the end of the multiphenylene-benzoic lateral chain performance of the ionomer increases. Among the two structures, presented in *Fig. 1.27*, the both show comparable conductivities at the same IECs. However, the ionomer, bearing two sulfonic acid groups per repeating unit, is considered being more efficient in formation of a connected network. On the contrary, the polymer, which has three ionic sites at the end of the lateral chain, is considered by authors as a one with too bulky side groups that prevents percolation of acid groups [118].

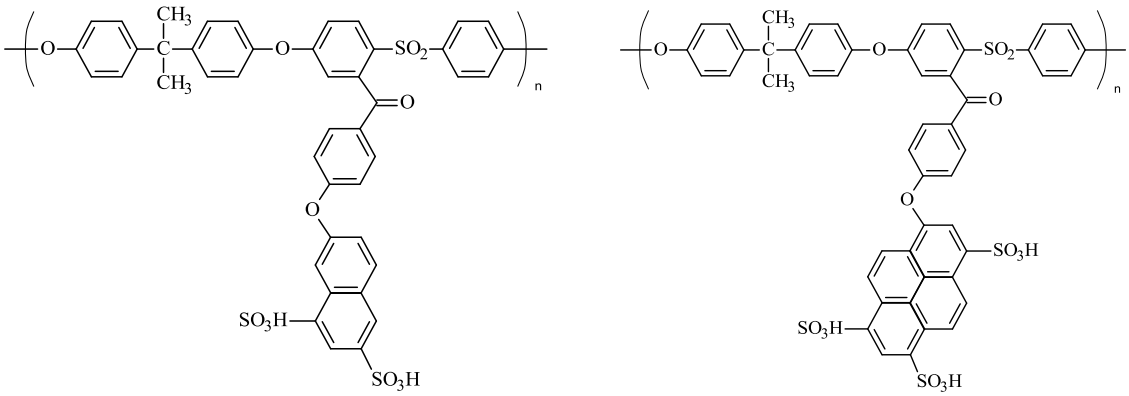

Figure 1.27. Chemical structures of PAES, bearing several sulfonic acid groups at the end of the prolonged benzophenone lateral chain [118]

1.4.2. $O(CH_2)_xSO_3H$ as a pendent chain

Random poly(imide)s (PI) of IEC around 2.0 meq/g were investigated [119, 120] by varying length of ethylene spacer to the sulfonic group. No visible trend on the conductivity or other properties was registered. The both groups clearly evidenced poor performance of these materials in the whole range of humidity. In the experiment of complete humidification the polymers did not reach the values of Nafion even at high concentration of ionic sites. At reduced humidity of 20 – 60 % RH the conductivities of 10^{-6} – 10^{-3} S/cm were registered. Materials of the highest degree of sulfonation (IEC = 2.3 meq/g) demonstrated values of 10^{-3}

– 10^{-2} S/cm at 40 – 80 % RH. Poor performance was explained by the method of scanning TEM, where absence of connectivity of hydrophilic sites was observed.

Guiver *et al.* [121] designed random PAES, bearing two to four ionic groups of the chemical structure $PhO(CH_2)_4SO_3H$. The ionomers of IEC 1.2 – 1.7 meq/g showed comparable and higher conductivities to Nafion, when immersed in water. Unfortunately, no data are given at reduced humidity. However, TEM images in dry state clearly showed clustering effect of ionic aggregates; therefore one may presume the ionomers to demonstrate high conductivity at reduced humidity as well.

Such difference in performance of ionomers, bearing similar pendent alkylsulfonic acid groups may be related to the main chain. In case of PI bulky structures are used to form a polymer backbone, whereas Guiver *et al.* investigated linear PAES.

1.5. Polyaromatics with sulfonic acid on a perfluorinated spacer

1.5.1. $Y(CF_2)_xSO_3H$ as a pendent chain*

All the ionomers, discussed above, were possessing simple sulfonic acid groups or attached to alkylated / phenylated structures that, basically, do not influence on acidity of the ionic site. Nafion is believed to have high values of conductivity, especially at reduced humidity, due to its superacid pendent specie, in particular. To implement the same idea for the polyaromatics, recently Yoshimura *et al.* modified commercial PAES with perfluorosulfonic acid (PFSA) groups [122]. Fluorine as a highly electro-negative element provokes strong withdrawing effect on the sulfonic group, thus decreasing electron density of the terminal. In such a way proton becomes a much easier leaving group: pK_a of the Nafion's acid was calculated to be −6, while sulfonated polyaromatics (type PEEK) bear sulfonic acid of pK_a −1 [123]. However due to several factors, such as high cost of fluorine-containing materials, high caution while working with F-reagents, and limitedness of commercial perfluorinated sulfonic species, research on PFSA ionomers for PEMFC applications is still in its initial stage.

An early work of Storey *et al.* [124] described production of a diphenylated monomer with a short difluoromethylenesulfonic pendent group and random poly(ether sulfone) thereafter (*Fig. 1.28*). First measurements of conductivity revealed the disadvantage of the rigid

* Y is a heteroatom or aromatic ring as a spacer

CF_2SO_3H structure: polymers of IEC 1.0 – 1.3 meq/g (0.5 – 0.6 of ionic part per unit) conducted 2.0-2.5·10^{-4} S/cm in water at 80 °C. For this reason further studies concern pendent R_FSO_3H, obligatory connected to a heteroatom.

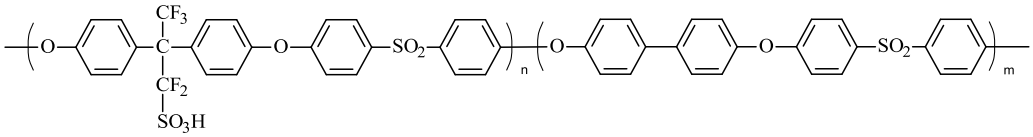

Figure 1.28. Random PAES, bearing short PFSA groups [124]

To study the impact of fluorinated species in the ionic chain Jang, Bae *et al.* [125] proposed comparison of ionomers with the same polymer backbone (PS) but different lateral substituents: i) PFSA (and corresponding ionomer is sPS-Rf), ii) alkylsulfonic group (corresponding polymer sPS-Rh), and iii) $–SO_3H$ (corresponding material sPS-SO_3H). *Fig. 1.29* illustrates dependence of these ionomers in the whole range of humidity, and Nafion 112 is proposed as a reference. Obviously, the polymer, bearing perfluoroalkylsulfonic lateral chains, shows the best performance with activation energy approaching that of Nafion. The other two materials are characterized by higher dependence on water content. It must be also taken to account that IEC of the sPS-Rf is the least out of all the three samples. This fact again proves that material with superacid ionic groups is more effective for proton conductivity.

The presented results are encouraging; however, one must admit that the main backbone is soft polymer PS. It may contribute to higher mobility of lateral chains, compared to polyaromatics.

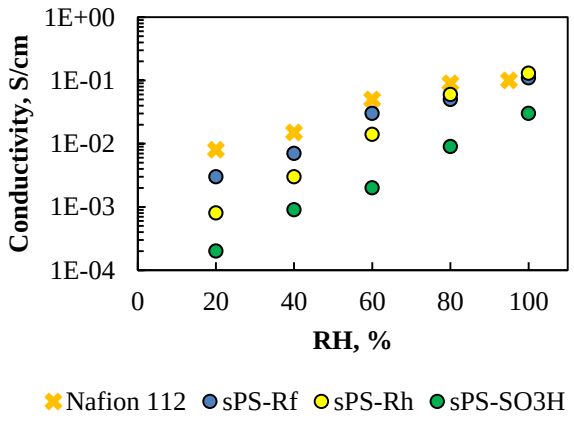

Figure 1.29. Comparison of the conductivity at reduced humidity for polystyrenes, bearing pendent PFSA groups (blue circles), alkylesulfonic chains (yellow circles), or sulfonic groups (green circles) [125]. Nafion 112 is presented as a reference

As a confirmation a group of Miyatake [126, 127] studied random and block-copolymers of PAE, bearing pendent chains $–(CF_2)_2O(CF_2)_2SO_3H$ on a fluorenyl specie. *Fig. 1.30* presents conductivity dependence on humidity for these structures. Random polymers are noted with a prefix '*r*' and a block-copolymer – with '*b*'. Suffixes give information about IEC of the polymers. Nafion 112 and sPS-Rf are presented as reference materials.

On the contrary to other ionomers described in previous sections random ionomers with PFSA side chains show better performance at reduced humidity than a block-copolymer. Taking to account presence of DFB as a comonomer in the structures of *r*-PAE, one may suppose better phase separation in the random polymer, compared to the block-copolymer with PEK-PES backbone.

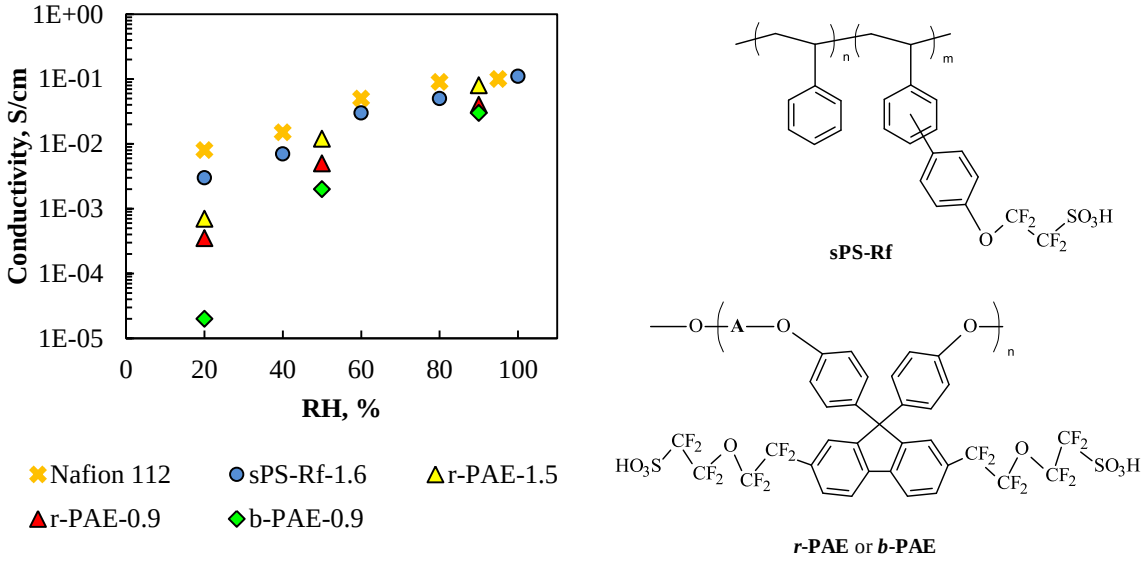

Figure 1.30. Comparison of PFSA ionomers' performance at reduced humidity and corresponding chemical structures of ionomers on the right

The structures of *r*-PAE and *b*-PAE contain longer PFSA chains, compared to sPS-Rf, but performance of the latter is higher. Hence, it is presumed that a more rigid polyaromatic fluorenyl-containing main chain restricts mobility of the lateral groups.

Iojoiu *et al.* developed further the idea of synthesis of a polyaromatic block-copolymer with PFSA pendent groups type $–(CF_2)_2O(CF_2)_2SO_3H$ [128]. The authors used a linear sequence of phenylated structures (*Fig. 1.31*).

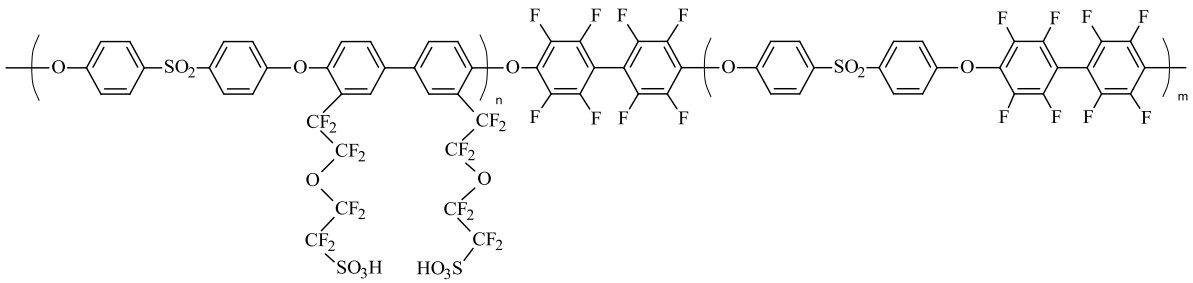

Figure 1.31. A block-copolymer, bearing $–(CF_2)_2O(CF_2)_2SO_3H$ pendent chains, proposed by a group of Iojoiu [128]

The ionomers showed prominent separation to ionic and non-ionic domains. Additionally, the samples demonstrated better conductivity in the whole range of humidity for the polymers of IEC 1.6 meq/g. The structures, having lower concentration of ionic groups, also show satisfactory performance, close to Nafion.

1.5.2. $Y(CF_2)_xSO_2NHSO_2CF_3$ as a pendent chain

Another family of superacid structures is a sulfonimide (SI) group. Due to delocalization of the negative charge over adjacent sulfoxides and thank to the strong electon-withdrawing effect of fluorinated alkyls, the proton of SI acquires even higher acidity than that of PFSA group. However, synthesis of the current organic specie is a demanding process, therefore not much research has been dedicated to ionomers, bearing SI chain.

Important contribution towards development of the SI synthesis procedure was done by D.D. DesMarteau and his colleagues [129-135]. Little attention was paid, though, to the production of ionomers thereafter. To our knowledge, there exist only four groups, who published their research on SI-containing proton-conducting membranes. The first one, already mentioned above, DesMarteau *et al.* [136] compared performance of Nafion in its sulfonate and sulfonimide ionic states (with IEC close one to another). They concluded higher conductivity of SI-bearing polymer to a traditional Nafion at reduced humidity due to the better water retention of the former structure. However, at immersed state this is Nafion-sulfonate that overperforms Nafion-SI.

The same observation was evidenced in a group of C. Iojoiu [137], where a modified PES UDEL (*Fig. 1.32 (a)*) was under investigation (SI-PSF). By comparing polymers of the same IEC (both per weight or per volume), one may observe better performance of ionomers with SI pendant chains, especially at higher temperatures. Additionally, these ionomers are characterized by higher WU. This phenomenon made the authors propose that SI species form

larger hydration shells due to the delocalized negative charge in the structure. The same explanation was revealed earlier by the group of Watanabe [138] to a polymer SI-PPMS, which is sketched in *Fig. 1.32 (b)*. However initially, DesMarteau proposed the presence of internal pore or channel structure that has no connection to water coordination around acid sites [136].

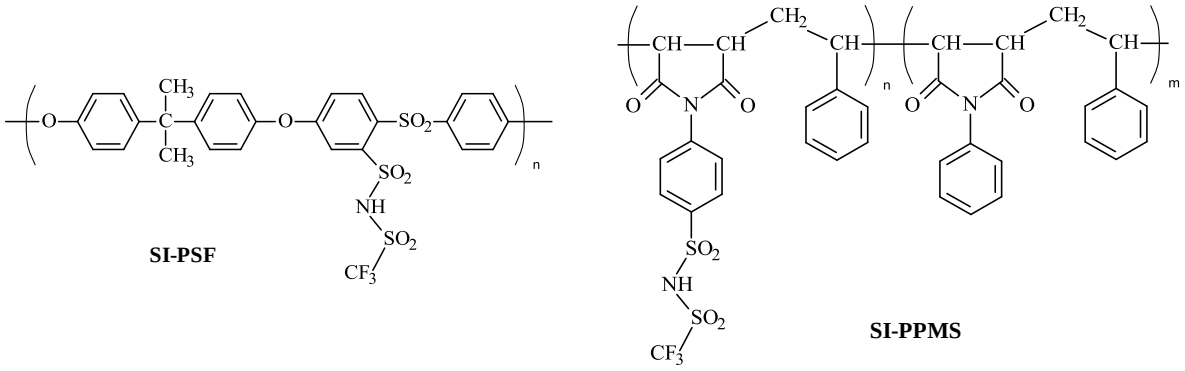

(a) (b)

Figure 1.32. Chemical structures of ionomers with SI pendent chains : a) SI-PSF [137] and b) SI-PPMS [138]

Whatever the reason for higher water retention is, the fact that SI dissociation, thus solvation, is higher compared to PFSA unit, is obvious. Another important point is that no ionomer, containing SI pendent chains on the polyaromatics or polyalkylenes, could achieve the performance of Nafion, which is plotted in *Fig. 1.33*.

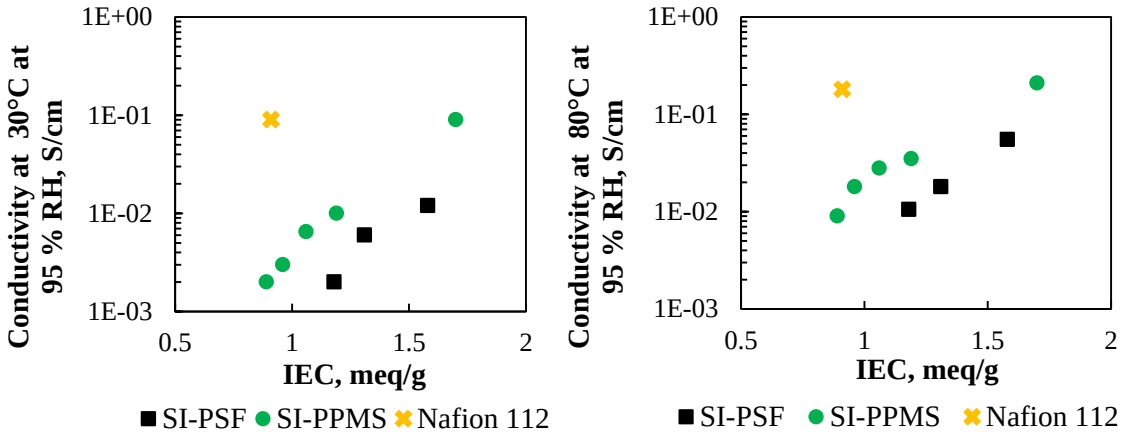

Figure 1.33. Dependence of conductivity on IEC for the ionomers from the references 137 and 138 to Nafion 112

Unfortunately, the results of McGrath *et al.* [139], who worked with PAES (just as the group of Iojoiu), cannot be plotted in *Fig. 1.33*, since their measurements were done exclusively in water. However, even at those conditions their polymers could not achieve performance of Nafion of IEC 0.9 meq/g.

Based on literature analysis, proposed in the current chapter, one may conclude:

i) Ionomers with sulfonic acid groups, directly attached to a polyaromatic backbone, show promising performance in terms of proton conductivity at both reduced at complete humidity. Block-copolymer structures are preferential to random.
ii) Polymers, bearing sulfonic functions through a long alkylated spacer, do not show outstanding results, even though ionic groups are believed to have higher accessibility one towards another.
iii) Materials, having sulfonated groups, concentrated on a multiphenylene moiety, perform in a way, similar to Nafion. Such behavior reveals an optimal organization of polymer chains with formation of highly connected ionic channels.
iv) Ionomers with PFSA lateral groups show promising conductivities in the whole range of humidity and temperature. Superacidity of the sulfonic site, thus better dissociation of the proton in water medium and higher hydration of the polar site, is believed to contribute to better performance of the current materials. Polymers of this type are not extensively studied for the moment.

Therefore, synthesis and characterization of ionic polymers, bearing PFSA pendent groups, are chosen to be the main objectives of the current dissertation. Previous investigation in our group considered post-modification of a polyaromatic chain with a $–(CF_2)_2O(CF_2)_2SO_3H$ specie [128]. The materials appeared to show high conductivity even at reduced humidity and promising organization of the polymer chains (a detailed study on morphology is given in ref. 140).

In order to change synthesis strategy, the current work deals with production of ionic monomers, bearing PFSA groups, and their further polycondensation with commercial non-ionic monomers. Such strategy avoids post-modification of the hydrophobic backbone with ionic species, which results in better control of sulfonic acid distribution.

Chapter 2. Synthesis part. Discussion

This chapter is focused on synthesis of different monomers and ionomers and is divided to parts:

i) Synthesis of monomers. Since the idea of an ionic monomer synthesis is new, detailed explanation on conditions and problems, appearing through the syntheses, will be described. In total, three monomers, bearing PFSA groups, are considered.

ii) Synthesis of polymers thereafter. The new ionic monomers are polymerized with commercial non-ionic monomers in order to get polymers of high enough molecular weight. The materials are then cast to membranes. Analysis on correspondence between theoretical ion exchange capacity (IEC) of the polymers and those obtained by nuclear magnetic resonance (NMR) and acid-base titration is presented. The difficulty to totally acidify several types of membranes is then discussed.

2.1. Synthesis of monomers

We report on synthesis of three different monomers of the general view, presented in *Fig. 2.1*. The basic principle, uniting all these structures is the presence of three functional groups in *meta*-position one to another: two of them are polymerizable sites, the third one is a PFSA chain. The monomer **2** has Fluorines as polymerizable sites, which make it an electrophile in subsequent polymerization. The monomers **3** and **4** contain –OH groups that would act as nucleophiles in polycondensation. The monomers **2** and **3** contain PFSA, directly attached to an aromatic center, while the monomer **4** contains a sulfanyl-bridge between the PFSA and a phenyl.

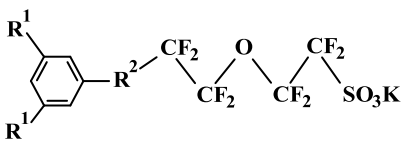

Monomer **2**: R^1 = F, R^2 = -

Monomer **3**: R^1 = OH, R^2 = -

Monomer **4**: R^1 = OH, R^2 = S

Figure 2.1. Schematic representation of the synthesized monomers

Syntheses of all the three ionic monomers are presented in *Fig. 2.2*. The first step is common for all the products – hydrolysis of a molecule **1**. The only side of the molecule that has to react is a fluorosulfonyl-end. It must be transformed into sulfonate prior to grafting of the perfluorosulfonic chain on the aromatic ring, because $–SO_2F$ does not resist harsh conditions during a monomer synthesis and can lead to many side products. At the same time, the

reaction of the iodine-terminated side has to be avoided during the hydrolysis, since it is the reactive site for subsequent copper-mediated coupling (in case of the monomers **2** and **3**) or nucleophilic substitution (for the monomer **4**). For this reason hydrolysis of $–SO_2F$ must be carefully conducted.

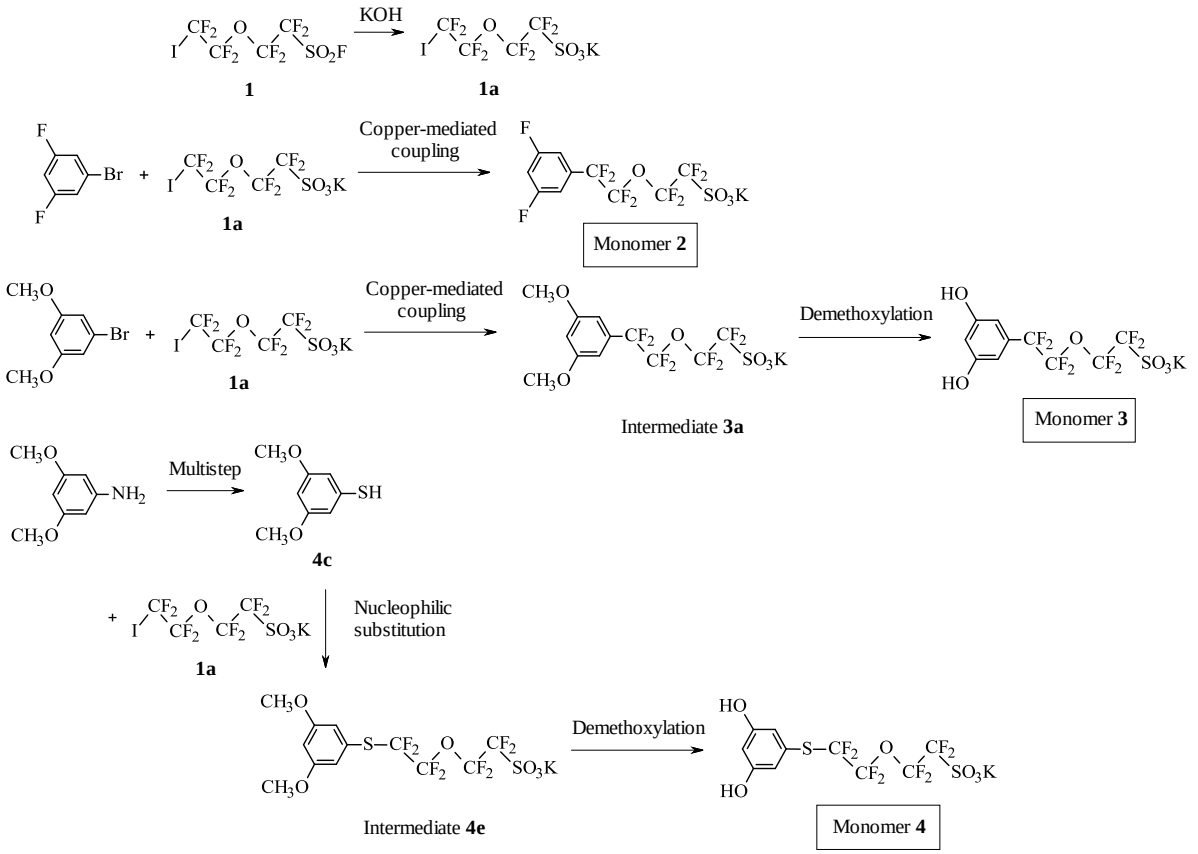

Figure 2.2. Overall synthesis routes to obtain three ionic monomers **2**, **3** and **4**

The monomer **2**, containing difluoro-polymerizable groups, is then synthesized in a one-step process by $Cu^{(0)}$-mediated coupling between a 3,5-difluoro-1-bromobenzene and the ionic function **1a**, produced in the previous step. The monomers **3** and **4**, having dihydroxy-polymerizable groups, are produced in several-step syntheses. In order to obtain the monomer **3** copper-mediated coupling between 3,5-dimethoxy-1-bromobenzene and **1a** is performed with subsequent demethoxylation-hydrogenation reaction. The monomer **4** is obtained by nucleophilic substitution of 3,5-dimethoxy-1-thiobenzene with **1a** and further deprotection of methoxy-groups. Presence of protective groups $–OCH_3$ in place of polymerizable hydroxyls during intermediate reactions is indispensable condition to avoid secondary product formation. Detailed discussion on problems during all the reactions is proposed below.

*2.1.1. Synthesis of an ionic function **1a***

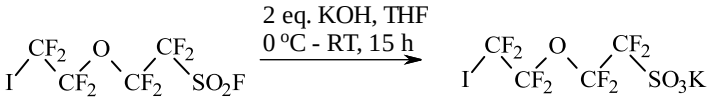

1 **1a**

Figure 2.3. Reaction of hydrolysis of a molecule **1** – preparation of an ionic precursor **1a**

Hydrolysis of a molecule **1** is conducted with 2.2 equivalents of KOH in THF as solvent (*Fig. 2.3*). The excess of the base is calculated in order to use its 1 equivalent for transformation of $–SO_2F$ into $–SO_3K$, another equivalent for neutralization of HF that is produced inevitably, and additional 0.2 equivalents of excess to assure the totality of the two previous reactions. As it was mentioned earlier, the terminal iodine function could also react with KOH. Therefore the objective was to find the best reaction conditions to minimize this secondary attack. The terminal iodine group was found to be sensitive to light and high temperature in particular. Great decrease of side products is observed if the reaction is started in an ice bath and then continued at room temperature overnight, compared to those started immediately at room temperature. Supposedly, addition of the strong base provokes an important local increase of the solution temperature and decrease of selectivity of the reaction. For this reason it is necessary to start the reaction at 0 °C and to keep it cold for the first several hours. After the initial attack of the base on the molecule **1** is complete (during these first several hours), the dissipation of heat becomes more effective and the reaction vessel may be left at room temperature overnight; the reaction finishes in totally more than 10 h. Taking to account the mentioned precautions for the conditions of hydrolysis, yield of the reaction reaches 97-98 %.

In case of the de-iodination taking place, a product **1b** is formed. It is shown in *Fig. 2.4* with its ^{1}H and ^{19}F NMR spectra. The latter measurement is done in a mixture with **1a**, therefore the signals, corresponding to **1b**, are marked with blue arrows with numbers corresponding to the atoms in a molecule. To summarize, the following chemical shifts characterize the secondary product **1b**:

^{1}H NMR: δ (ppm, acetone d_6) = 6.51, 6.34, 6.16 (*t-t-t*, 1H, $CF_2\underline{H}$). ^{19}F NMR: δ = −139.19 and −139.37 (*t-t*, $C\underline{F_2}H$); −118.71 (*s*, $C\underline{F_2}SO_3K$), −89.65 (*m*, $C\underline{F_2}O$); −82.66 (*m*, $C\underline{F_2}O$).

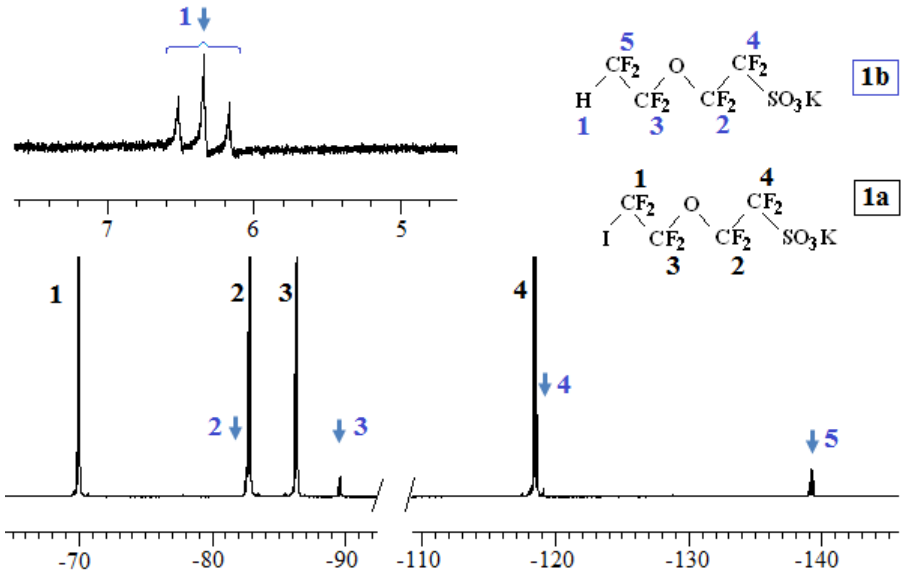

Figure 2.4. ^{1}H and ^{19}F NMR spectra of the deiodinated product **1b**, shown above the spectra. Fluorine spectrum presents the mixture of **1a** (also represented above the spectra) and **1b**, thus, the signals of **1b** are pointed with blue arrows

Mechanism of the secondary product appearance is investigated further. In literature there exist three suppositions for dehalogenation-hydrogenation of iodoperfluorosulfonates, supporting ionic, radical or electron transfer mechanism.

In order to better understand the nature of the secondary attack, further down we present the observations, concluded from additional reactions performed by our group, and we compare them with the literature results. Firstly, we noticed that the reaction depended considerably on quantity of the reagents. When the hydrolysis is performed with 1-2 g of **1**, no secondary products are produced and no overheating is observed. Probably, due to the low volume of the reaction mixture the heat is easily evacuated. Therefore, the small-scale syntheses were conducted without an ice bath. Working with higher quantities of 10-30 g required lowering the reaction temperature.

Secondly, type of the base influences amount of the product **1b** to be formed. When investigating batches of **1** of 10 g, two reactions were launched simultaneously without using an ice bath: with LiOH in form of powder and with KOH in form of pellets. Formation of up to 1 % of **1b** with the former base and up to 10 % with KOH was registered in the end of the reaction. Due to a bigger cation, thus better dissociation, KOH is a slightly stronger base, than LiOH. Presumably, their activity might be also different because of the surface area of the base: in case of KOH in form of pellets the reaction takes place on the surface of the base before the complete dissolution of the latter, while lithine, being in dispersed state, reacts faster and does not create local overheating points.

Concerning the basicity of the reactive Huang *et al.* [141] reported on use of a weak base, such as M_2SO_3 where M can be K, Na, etc. in reaction of transformation IR_FSO_2F into IR_FSO_2M. They performed the procedure at temperatures 75-80 °C and in aqueous solvents; and small amounts of HR_FSO_2K were registered. However, when at the same reaction conditions stronger bases were used, such as pyridine or trimethylamine (act also as solvents) [141], or reagents KOH, NaOH [142], up till 80 % of deiodinated-hydrogenated product were observed [143].

Same authors [141] pointed that presence of radicals in reaction of iodoperfluoroalkylsulfinate hydrolysis provokes the deiodination. Thus, they added 2-3 % of AIBN to the reaction mixture of IR_FSO_2F with sulfite, and observed formation of 80 % of HR_FSO_2M. These results were interpreted by authors as those, evidencing a pure radical mechanism of the reaction. However, when the reaction was conducted without any addition of radicals, still formation of HR_FSO_2M was registered.

Our investigation by heating the product **1** in the reaction solvent only (THF, at 60 °C overnight) proves no degradation of the product. But when KOH is added to the same solution and again heated – formation of **1b** is observed in several hours. Hence, we suppose that the secondary reaction does not follow uniquely radical mechanism, but rather ionic, where water is the reactant, attacking the iodine-terminated side.

Mainly, researchers report on the reaction of deiodination pursuing radical-anionic mechanism (SET) [144, 145] (*Fig. 2.5*). Following the activity of radical-anionic intermediate, the reaction continues through radical or ionic pathway. The most comprehensive work, on our opinion, was conducted by Howell *et al.* [146]. Their research concerned iodinated perfluoroalkanes in reaction with methylated sodium. The authors clearly pointed that: i) the reaction occured at low temperature in the presence of radical species only, following the radical path (if no radicals presented in the system, no reaction happened); ii) at temperature, higher than RT, in absence of radical species the reaction proceeded by anionic mechanism. For the latter case a question appeared: where proton comes from to regenerate perfluorinated anion. The same group of researchers conducted a supplementary test, using the same system of IR_F with CH_3ONa in methanol, changing the protons of the solvent to deuterium either in methyl-group or instead of acidic proton. They remarked that when reaction takes the thermal path, this is deuterium in place of acidic proton of methanol that is engaged in hydrogenation of R_F^-.

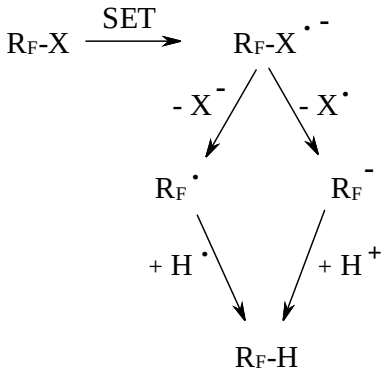

Figure 2.5. Schematic representation of mechanism of transformation IR_FSO_2F to HR_FSO_xM, proposed by Meinert and Brune [144]

In case of the reaction, studied in the current work, we propose that the proton for hydrogenation of perfluorosulfonate comes from water by the next scheme:

$IR_FS^{\delta+}O_2F + K^+HO^- = IR_FSO_3H + KF$ (1)

$IR_FSO_3H + KOH = IR_FSO_3K + H^+HO^-$

$HO^- + IR_FSO_3K = {}^-R_fSO_3K + HOI$ (unstable, decomposes to H(or K)I and H(or K)IO_3) (2)

${}^-R_FSO_3M + H^+ = HR_FSO_3M$

Based on these results one may conclude that the reaction of deiodination-hydrogenation for the molecule **1** in the current research, most probably, happens by thermal mechanism: i) no secondary reaction occurs in the reaction mixture IR_FSO_2F / KOH / THF at 0 °C, ii) no secondary reaction takes place even at high temperature in the system IR_FSO_2F / THF, when we assume the presence of iodine radicals, eliminating from the **1**, and iii) secondary reaction happens at high temperature in presence of base. According to the same research of Howell *et al.* [146], it is acidic proton that is contributed for the HR_FSO_3M. Since water appears to be a product of the reaction, it is supposed to give its proton.

2.1.2. Copper-mediated coupling

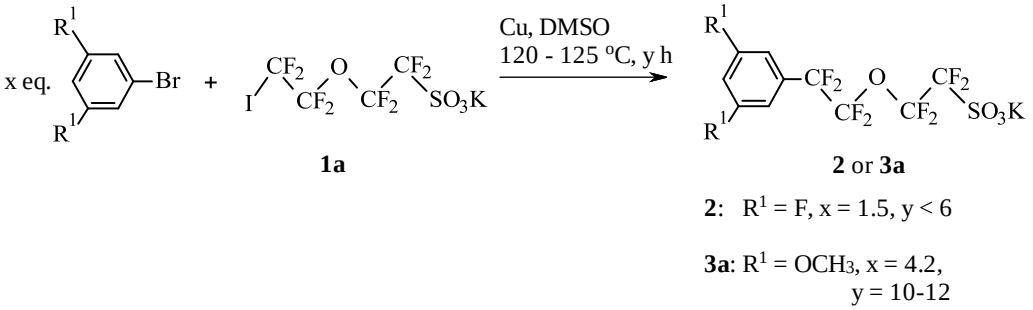

1a

2 or **3a**

2: R^1 = F, x = 1.5, y < 6

3a: R^1 = OCH_3, x = 4.2, y = 10-12

Figure 2.6. Reaction of copper-mediated coupling of a molecule **1a**

Copper-mediated coupling is performed between the iodinated perfluoroalkylsulfonate **1a** and aromatic bromide (*Fig. 2.6*) in order to obtain the monomer **2** (final yield 76 %) or intermediate **3a** (yield is 83 % with sufficient purity, as for an intermediate product). For the former product 1-bromo-3,5-difluorobenzene (DFBB) is used as an aromatic halogenide, for the latter one – 1-bromo-3,5-dimethoxybenzene (DMBB). The conditions of the reactions differ by two main factors: excess of the aromatic bromide and time of the reaction. The best ones are determined to be: 1.5-fold excess of DFBB and time less than 6 h in case of the reaction with **2** as a final product; 4.2-fold excess of DMBB and longer time of 10-12 h in case of the reaction with **3a** as a target product.

The aromatic bromide must be taken in excess to **1a** in order to avoid the formation of $H(CF_2)_2O(CF_2)_2SO_3K$ (**1b**). Since the secondary product is polar, just as the target molecule, difficulties in purifying are foreseen. Lower excess of DMBB was studied (1.5, 2.5 eq.), but the expected **3a** was always obtained in small quantity together with several additional series of ionic products (estimated by ^{19}F NMR). Therefore, 4.0-4.2 eq. of DMBB were determined as optimal for successful synthesis.

For these reactions it was observed that temperature of the reaction and time were very important parameters. McLoughlin and Thrower [147] reported that copper-mediated reactions with iodinated perfluoroalkylsulfonates are sensitive at temperature higher than 128 °C, they tend to form **1b** as a secondary product. At the same time, the current work revealed that no reaction happens at $T < 110$ °C. For this reason, the reactions of coupling between **1a** and aromatic bromides in DMSO in presence of $Cu^{(0)}$ must be kept in the temperature range 110-128 °C.

An interesting observation for the coupling DFBB / **1a** is registered: time of the reaction depends much on quantity of products introduced to the reaction mixture. For example, 1 g (2.16 mmol) of **1a** reacts with DFBB in 4 h at 128 °C, whereas the reaction of 15 g (32.47 mmol) of **1a** proceeds for 3 h at 125 °C. Additionally, the reaction must be stopped immediately after the total consummation of **1a** in order to avoid the excessive formation of another secondary ionic product **2a**, which will be discussed further. On the contrary, the reaction between **1a** and DMBB is much longer; it lasts during 10-12 h, at 120-128 °C and does not depend on the quantity of the initial products. Moreover, no secondary ionic product formation is observed, therefore the reaction may be stopped not immediately, but during the next several hours without no bad effect on the resultant product. Such dependences indicate that the coupling is facilitated for DFBB, rather than DMBB. With a closer look on electron

density distribution over the phenyls of the aromatic halogenides (*Fig. 2.7*), one may observe that both fluorine- or methoxy-substituents in *meta*-positions to the reactive site show the *–I*-effect. However, in the former case due to the Fluorine high electronegativity the electron-withdrawing force is higher, than that of Oxygens. Therefore electron density on the Carbon, participating in a copper-mediated reaction, is more depleted in DFBB, rather than in DMBB. It means that for such type of a reaction the reactive site of an aromatic halogenide is more active, when it carries lower electronegativity.

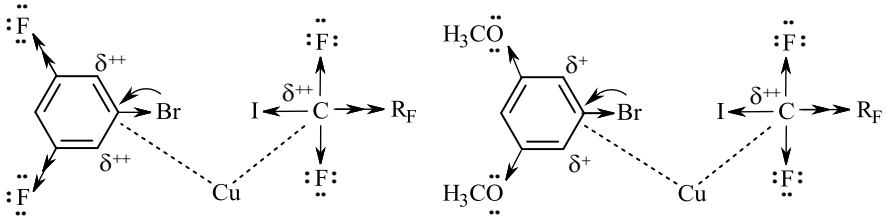

Figure 2.7. Electron density distribution in DFBB and DMBB, and in iodoperfluorosulfonate **1a**

Since the both reactive Carbons of the aromatic compound and IR_FSO_3M are depleted in negative charge, we presume that it is $Cu^{(0)}$ that mediates the partially positive charge by its one electron in *s*-orbital (electron configuration of copper is $3d^{10}4s^1$), therefore *Fig. 2.7* shows dashed lines between the three reactive species.

Another observation, evoked from the reaction between DFBB and **1a**, is the formation of the secondary product **2a**, which is schematically shown in *Fig. 2.8* together with its ^{1}H NMR and ^{19}F NMR spectra. The product is in mixture with the monomer **2**, therefore its signals are marked with blue arrows and numbers of corresponding atoms. Chemical displacements of peaks are summarized as following:

^{1}H NMR: δ (ppm, acetone d_6) = 6.51, 6.34, 6.16 (*t-t-t*, $CF_2\underline{H}$). ^{19}F NMR: δ = −118.57 (*s*, $C\underline{F_2}SO_3K$), −114.21 (*t*, $C\underline{F_2}Ar$); −112.52 (*d*, Ar-$C\underline{F_2}$); −110.96 (*t*, Ar-Ar-$C\underline{F_2}$); −88.17 (*m*, $C\underline{F_2}O$); −82.52 (*m*, $C\underline{F_2}O$).

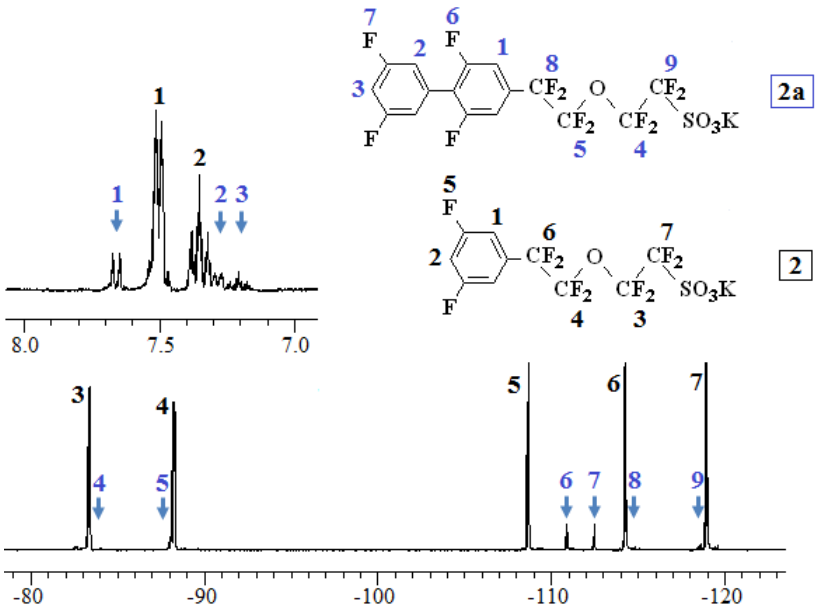

Figure 2.8. ^{1}H and ^{19}F NMR spectra of the secondary product **2a**, shown above the spectra. The both spectra additionally contain signals of **2**, thus, the peaks of **2a** are pointed with blue arrows

As it was mentioned before, the undesired product **2a** is formed even when the reaction is stopped immediately after the total consummation of **1a**. At this time, 1-3% of **2a** is observed for the batches of 1 – 30 g (2.16 – 60.48 mmol, respectively) of **1a**. Longer reaction time leads to important increase amount of **2a**. In order to be able to control the consummation of **1a** and to stop the reaction, when the least quantity of **2a** is formed, the reaction procedure is verified after 1 h from its start, and the approximate time of its totality is calculated. This is done, since with increasing the quantity of introduced reagents the reactions, both main and secondary, become faster, therefore the time and temperature must be attentively controlled. Additionally, it must be taken to consideration that formation of **2a** happens much more slowly, if IR_FSO_3M is used in its Li^+-counterion form. The latter phenomenon is, probably, connected to lower dissociation of lithiated sulfonate, but we are not able to explain the exact mechanism.

In order to understand the reason of **2a** formation, mechanism of the overall reaction of copper-mediated coupling must be studied. In litterature there exist several suppositions for that, but most of them concern Ullmann coupling between aromatic and / or alkylated halogenides. In the current case alkylhalogenides are replaced by perfluorinated ones, therefore different mechanism might occur.

Ullmann reaction has been investigated since decades, but even now no confirmative conclusion on its mechanism is given. Many groups propose the combination of several pathways, among which: i) nucleophilic substitution, ii) radical mechanism, and iii) formation

of organometallic complex by simple sorption and subsequent desorption of the reacted species. The first mechanism for Ullmann reaction was supported by Fanta [148], and suppose nucleophilic attack by the metallic copper (M) at the activated position may be an initial and rate determining step. These corroborate with our results and can explain while the reaction of DFBB with IR_FSO_3K is faster, than that of DMBB with IR_FSO_3K, considering the electron distribution in aromatic rings (*Fig. 2.7*).

Radical mechanism for Ullmann reaction was supported by Flynn *et al.* [149], who conducted temperature programmed desorption of toluene, formed on $Cu^{(0)}$ surface by reaction between phenyliodide and iodomethane. The authors were confident in a procedure by radical mechanism at low temperatures (120-180 K) only, when the Ullmann coupling happens between gaseous and/or surface accommodated species. At higher temperatures (> 350 K), when the reaction occurs between both copper-surface bound species, Langmuir-Hinshelwood mechanism is proposed, which does not follow a pure radical path.

Therefore, very often authors, investigating the mechanism of Ullman reaction, could not give exact explanation on electron behavior of the reacting species, and the frequent supposition is formation of organometallic intermediate ($ArCu(L_3)R$), where L is ligand. The ligands may be pyridine and DMSO [150, 151].

In order to understand, why the main and the secondary reactions are taking place in the current research on Cu-mediated coupling of aromatic and perfluorinated halogenides, and based on results of other groups on Ullmann coupling, another mechanism is proposed – a multistep single-electron transfer (SET). *Fig. 2.9* shows schematic representation of three main steps of the reaction. Firstly, metallic copper, possessing an odd number of free electrons at the outer orbital (Cu $3d^{10}4s^1$) gives its one electron to the phenylehalogenide. Simultaneously it combines with a C-Br site, creating a radical anionic intermediate and itself acquiring a positive charge. In the same way another equivalent of $Cu^{(0)}$ transfers its electron to a iodinated perfluoroalkylesulfonate, but no further distribution of charge takes place, therefore iodine is cleaved off. A free radical $^{\bullet}R_FSO_3M$ is formed and copper (I) iodide is eliminated. The both steps follow SET mechanism. The last step is the recombination of two reactive intermediates.

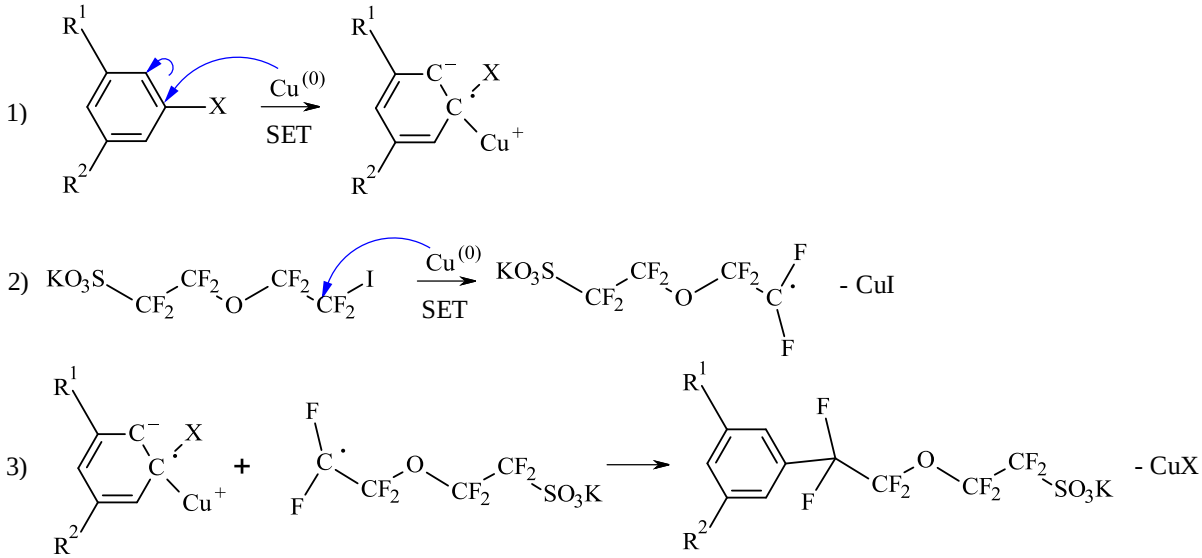

Figure 2.9. A proposed three-step mechanism for the copper-mediated coupling of aromatic with perfluoroalkylsulfonate halogenides

In the first step metallic copper donates its electron to the poorest in electronegativity aromatic carbon. In case of DMBB it is a C-Br site: both bromine and methoxy-substituents reveal *–I*-effect, but the strength of electron-withdrawing force of the halogen is more important. In case of DFBB these are two C-F sites (carbons # 3 and 5). However, Guo *et al.* [152] reported on impossibility of formation of an ion-radical at C-F or C-Cl sites. Among the other aromatic carbon sites, these are C-Br and the one in-between the two C-F (C4), which are electronically the poorest in DFBB. The latter atom undergoes strong *–I*- and *–M*-effects from adjacent fluorines, whereas C1 has a direct influence of inductive withdrawing force of bromine. Additionally, C4 is decreased in reactivity by steric hindrance of fluorines, and C1, being attached to the halogen, is easily adsorbed on copper surface. For all these reasons, main attack of $Cu^{(0)}$ happens at C1, therefore the monomer **2** is produced. However, due to high acidity of C4, the product **2** may further physically adsorb on copper surface, taking its electron and creating a radical center at C4. Recombination of this specie with the radical ionic product from the first step of the proposed mechanism results in the secondary product **2a**. This explanation is an assumption, proposed as alternative to the mechanisms of the Cu-mediated coupling, reported by other authors. It gives more evidence on formation of the main products, as well as the secondary product **2a**.

It is known that ligand is usually used in order to activate a catalyst and accelerate a reaction. Several authors proposed formation of an intermediate complex $ArCu(L_3)R$ during the copper-mediated coupling reaction. Some researchers report [147] on using of different polar aprotic solvents (as ligands) and their influence on reaction to proceed. In the current work DMSO as a solvent is constantly used. However, to investigate influence of a ligand 2,2′-

bipyridine is introduced to the reaction between DMBB and **1a**. After the first several hours of the reaction, formation of a few series of secondary products is registered. When totality of **1a** is consumed, all the secondary polar products are still present in the system. Lowering the reaction temperature does not result in purer yield. Therefore, one might indeed expect important influence of ligands, but on accelerated formation of secondary products, rather than of a required molecule. However, when a reaction is fast enough, there exists no need of ligand introduction.

*2.1.3. Synthesis of the S-containing ionic intermediate **4e***

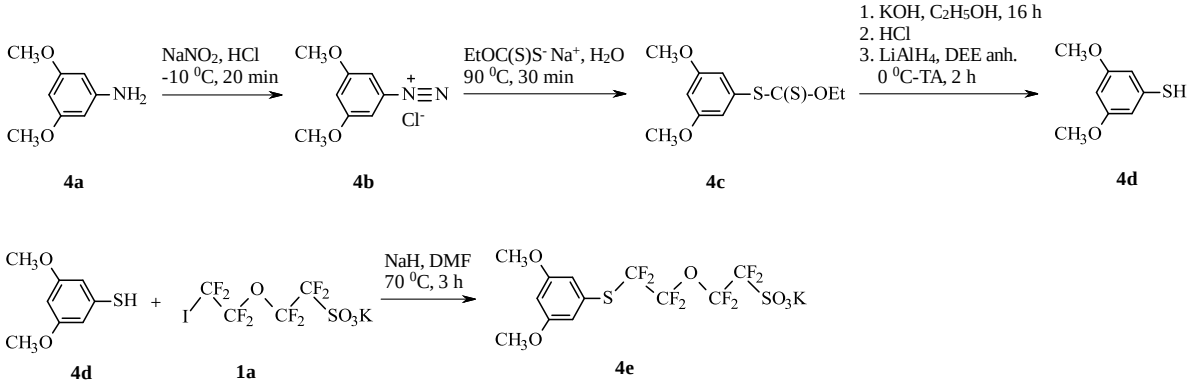

Figure 2.10. Synthesis of an intermediate **4e**

Synthesis of **4e** is comprised of two main steps: 1) a multistep synthesis of 3,5-dimethoxy-1-thiobenzene, and 2) nucleophilic substitution of sodium thiolate (*Fig. 2.10*). **4d** compound exists commercially as a milligram-stocked reagent of high price; therefore the up-scale synthesis was developed in the laboratory. The basic reaction is mercapto-diazoniation from the correspondent aromatic amine (*Fig. 2.10*). The procedure consists of the diazonium-ion formation in the acidic environment; and further sulfur introduction with the help of xanthate salt. The latter, having delocalized electron charge, is easily hydrolyzed to the thiolate. Initial products of reaction between **4c** and ethanol contain the mixture of **4d** and its dimer, for this reason the latter is subjected to reduction to **4d** with help of $LiAlH_4$. The total yield of transformation of **4a** to **4d** is 58 %.

Product **4b** is not stable at temperature > 4 °C and at low concentration of acid in the solution. At the same time if temperature of the **4b** solution is lowered less, than −20 °C, formation of high amount of solid is observed. Therefore, accurate control on temperature must be carried, when producing a diazonium salt, with the most appropriate range −15...−5 °C. Additionally, it is advised to prepare the solution of potassium ethyl xanthate simultaneously with the solution of diazonium salt in order to diminish the period of existence of the latter. As soon as

the diazonium chloride is formed, it is transferred to the solution of ethyl xanthate by small quantities of 10 mL to avoid the diazonium decomposition.

Reaction between 3,5-dimethoxybenzenethiol **4d** and iodinated ionic function **1a** proceeds through nucleophilic substitution; the reaction goes fast at medium temperature and with high yield (85 %). Subsequent separation of the product from dimethylformamide (DMF) by the usual mixing with water does not result in a pure product. Due to its high polarity it stays highly solvated by DMF. Drying the product under the reduced pressure at temperature of DMF boiling still does not eliminate the majority of the organic solvent.

Instead, two methods are proposed: modified column chromatography and solvent extraction with low boiling organic solvents. The first method yields in lower amounts of final product, the second method consumes more solvents and time. Modified column chromatography is provided manually: a 500 mL filtering funnel is filled with silica and connected to a recipient Büchner flask. The product **4e** (in mixture with DMF) is poured on top of silica and washed several times with dichloromethane (DCM) under the pressure. To collect the product, further washing with 60 / 40 acetonitrile (ACN) / DCM is provided. Such method of fast product purification lets extract the non-solvated **4e** and avoid big losses on the silica. Another method of DMF extraction is washing of the mixture **4e** and DMF with non-polar solvents that are partially miscible with DMF and do not solubilize **4e**. The most appropriate found to be hexane with progressive increase in percentage of diethyl ether (DEE) from 5 to 20 %. The washing procedure follows: adding hexane (and mixture of hexane with DEE for further washings), of approximately 5-fold volume excess with respect to the product, leaving the mixture at 35 °C-heating upon fast stirring for 1 h, then decanting the solvent phase and repeating the same procedure several times more. The final product solidifies.

The purification over silica phase seems to be more appropriate method in terms of time and cost. The overall yield of the procedure, starting from **4a** and finishing with ionic intermediate **4e** is 50.9 %.

*2.1.4. Demethylation-hydrogenation of ionic intermediates **3a** and **4e***

Demethylation or, in other words, deprotection, is a frequently used reaction in organic synthesis. Methoxy-groups at an aromatic ring are highly stable to oxidation, but may be easily transformed to hydroxyls by several methods, discussed further. The most common way is using a Lewis acid, in particularly BBr_3, $AlCl_3$, $BeCl_2$. Bearing a free electron orbital these compounds adopt an electron doublet of oxygen of the methoxy-group, creating a partly

positive charge on the oxygen. This destabilization of electronic distribution provokes weakening of benzene-oxygen bond, and even a weak base causes its rupture.

The majority of demethylation-hydrogenation reactions proceeds with non-ionic products, therefore a low-polar or medium-polar solvents, such as benzene, toluene, dichloromethane are usually used as a reaction medium [153, 154]. They are excellent regarding non-reactivity towards Lewis acids and non-miscibility with water. In addition, DCM and hexane have low boiling temperatures and they are broadly used as solvents for commercial solutions of Lewis acids. However, when one intends the deprotection reaction on polar products, it does not happen, presumably because of the inability of the reaction to proceed at the interface of the non-solvent / reactant.

A number of researches proposed the use of demethylation reagents in pair with highly polar solvents. The majority of these reactions were conducted on **3a** (*Fig. 2.11*). *Table 2.1* summarizes all these trials.

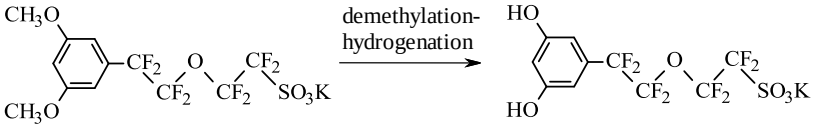

3a **3**

Figure 2.11. General scheme of demethylation-hydrogenation of **3a**

Table 2.1. Trials on demethylation of **3a**

Reactant	**Solvent**	**Temperature, °C**	**Observations**	**Reference, remarks**
Hydrobromic acid	Acetic acid	80 °C	▪ formation of side products	153, 154
Iodocyclohexane	Dimethylformamide	150 °C	▪ 20-fold excess of the reactant does not lead to the total demethylation ▪ formation of side products	155
Boron tribromide	Acetonitrile / dichloromethane	50-80 °C	▪ very long (more than a week) and does not lead to the total demethylation	156 (used AlI_3 instead of BBr_3)
Boron tribromide / thiourea	Acetonitrile / dichloromethane	50-80 °C	▪ 20 h at 80 °C ▪ demethylated product is received for batches of 1 g of **3a** ▪ demethylation does not proceed till the end for batches of > 5 g ▪ difficulties in purifying a demethylated product	157 (a modified Fujita method)

The first three reactions were repeated at least twice to assure that changing the conditions of the reactions does not give a more favorable result. The forth reaction was studied more in detail. It is a modified version of Fujita method, which is based on the reaction with a pair of strong Lewis acid / weak nucleophile. Normally, thiol is used as a latter reagent that is characterized by strong bad odor. The authors proposed thiourea instead [157].

The reaction of demethylation of **3a** was conducted with a BBr_3 / thiourea pair. In a first step BBr_3 in DCM (1 eq., commercial solution) is let reacting with thiourea (1.2 eq.) for 20 min; then the solution of **3a** (0.2 eq.) in ACN (3 times more than DCM) is carefully introduced and temperature is raised till 80 °C with subsequent evaporation of DCM. The reaction continues for 20 h and the demethylated product is received. The reaction is repeated several times with batches of different amount of **3a**. As it is mentioned in *Table 2.1*, low-scale reactions proceed with the total conversion into **3**, but higher amounts (> 5 g) of **3a** are not demethylated totally. Besides, purification is sophisticated at low-scale and unsuccessful, when the **3a** is not demethylated in totality.

Since the reaction of the polar molecule deprotection in polar solvents does not result in a required product, it is proposed to lower polarity of the initial ionic product. For that increasing bulkiness of a cationic site with the help of amines is suggested. Tetrabutylammonium (TBA^+) and ethyl-diisopropylammonium ($DIEA^+$) are chosen for comparison. They differ gravely in symmetry and ability to form a free amine (*Fig. 2.12*). TBA^+ is a symmetric stable quaternary ammonium that is coordinated through ionic forces, while $DIEA^+$ is non-symmetric and its coordination happens by hydrogen forces.

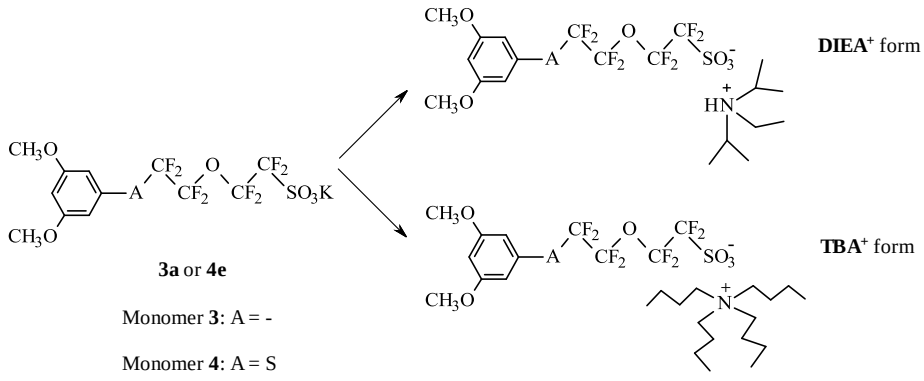

Figure 2.12. $DIEA^+$- and TBA^+-neutralized forms of **3a** and **4e**

The products **3a** and **4e** in both TBA^+- and $DIEA^+$-forms are soluble in DCM, thus their demethylation with the commercial solution of BBr_3 in DCM becomes possible. The reactions are conducted at room temperature and during several hours only (see *annex 3* and *4*). The

both cationic forms result in a totally demethylated product. However, it was not possible to transform the latter from its TBA^+-form to a K^+-one in the end of the demethylation-hydrogenation reaction. The cationic exchange was done in aqueous, either water / methanol solution of saturated KCl, but increasing content of organic solvent increased probability of the product extraction from the solution as well. But totality of TBA^+- to K^+-exchange was never achieved. A demethylated molecule in its $DIEA^+$-form, on the contrary, eliminated free DIEA during the demethylation reaction. Thus, the reaction of deprotection of the **3a** and **4e**, passing by their $DIEA^+$-intermediates, is presented further in detail (*Fig. 2.13*).

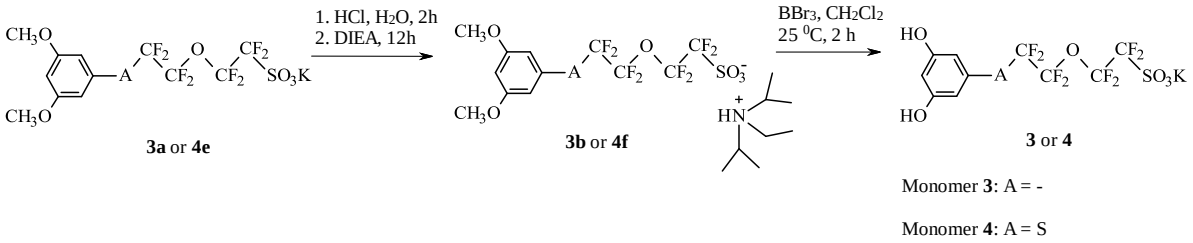

Figure 2.13. Demethylation-hydrogenation reactions in order to obtain monomers **3** and **4**

Firstly, a dimethoxy-protected molecule (**3a** or **4e**) is acidified and then neutralized with a bulky $DIEA^+$-cation. The intermediate in its ammonium form (**3b** or **4f**) is washed from excess of DIEA. An interesting observation is that DIEA is poorly miscible with water, but once **3b** or **4f** is washed with water, no excess of DIEA is seen at the ^1H NMR spectrum (*Fig. 2.14*, the spectrum of **3b** only is presented).

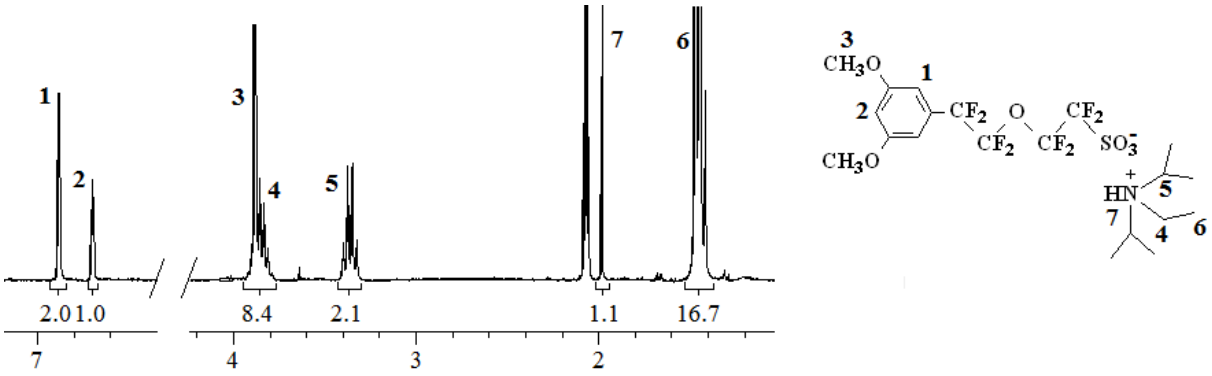

Figure 2.14. ^1H NMR spectrum of the intermediate **3b** (a non-integrated signal at the spectrum corresponds to the deuterated solvent acetone d_6)

$DIEA^+$-neutralized intermediates are then subjected to 2.5-3 eq. of BBr_3 / DCM. The advantage of using small excess of Lewis acid decreases much the cost of the reaction. Remarkably, during demethylation of **3b** precipitation of clear solid in the brown solution is observed. In the case of **4e** the whole reaction mixture solidifies, therefore it is necessary to use a mechanical stirrer. Precipitation / solidification during the reaction points on formation

of a more polar product, which is not soluble in DCM any more, – demethylated molecules. Totality of the deprotection is verified by disappearance of a peak, corresponding to protons # 3 (see *Fig. 2.14*).

The reaction mixture is neutralized with a strong base (KOH) – it destructs the excess of BBr_3 and HBr, which inevitably forms, when boron tribromide comes in contact with air moisture. At the same time the base transforms the newly formed monomer **3** or **4** into a three-potassium salt (*Fig. 2.15*). As a highly polar product it is soluble in water and may be purified by less polar, non-miscible with water solvents, such as DCM.

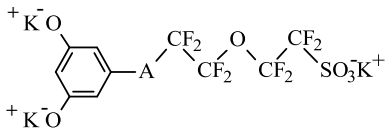

Monomer **3**: A = -

Monomer **4**: A = S

Figure 2.15. Three-potassium salt, produced after neutralization of the demethoxylation reaction mixture

Further on, the three-salt is transformed to a di-phenol mono-salt by acidification. It is worth mentioning that –OH groups, bound to an aromatic ring, are sometimes shielded in the ^1H NMR spectrum by the possible coordination of solvent molecules, therefore the control of the transformation to a diphenol is performed by pH-measurement. Concentration of protons in aqueous solution of **3** or **4** corresponds to that of phenol. Phenol is slightly acidic, its pH is approximately 3. Hence, acidification of three-salts to corresponding monomers **3** and **4** is performed until pH of the monomers' solutions becomes 3. It is important not to overpass the acidity (pH not lower than 3) to avoid acidification of the sulfonate group.

Purification of both monomers **3** and **4** is provided by the same method of modified column chromatography, described in *paragraph 2.1.3*. Since silica, as a non-mobile phase, may contain traces of other cations (such as Na^+) due to its production procedure, the ionic monomers are susceptible to attrap them. Thus, after purification of the **3** and **4** over silica they are subjected to long-term stirring in saturated aqueous solution of KCl to assure that totality of the product is in K^+-form.

Yields of the demethylation reactions comprise: 71 % for transformation of **3a** to **3**, and 55 % for deprotection of **4e** to **4**. Lower values of the latter might be connected to errors in calculation of the amount of introduced reagent **4e**, since ionic intermediates in both multi-step syntheses of **3** or **4** are never purified totally. The strategy is to obtain the most pure

intermediate without losing much product during purification process. Therefore, **4e** could still coordinate molecules of solvent, which give an error in weight of the introduced reagent.

2.1.5. Purity of the monomers

Purity of a monomer is crucial for polycondensation to reach the equilibrium and to result in a polymer of high molecular weight and of required theoretical composition. In addition to NMR analysis of chemical structures of newly synthesized organic molecules, elemental analysis was performed. *Tables 2.2*, *2.3* and *2.4* propose to compare theoretical and experimental composition of monomers **2**, **3** and **4**, respectively.

Table 2.2. Elemental analysis of the monomer **2**

Atom	Theoretical, %	Experimental, %
C	26.79	25.35 ± 0.3
F	42.38	38.30 ± 1.3
H	0.68	0.64 ± 0.2
S	7.15	6.88 ± 0.3
K	8.72	8.55 ± 0.2

Table 2.3. Elemental analysis of the monomer **3**

Atom	Theoretical, %	Experimental, %
C	27.03	27.18 ± 0.3
F	34.21	34.45 ± 1.0
H	1.13	1.12 ± 0.2
S	7.22	6.83 ± 0.3
K	8.80	7.99 ± 0.2

Table 2.4. Elemental analysis of the monomer **4**

Atom	Theoretical, %	Experimental, %
C	25.21	24.60 ± 0.3
F	31.91	31.47 ± 1.0
H	1.06	0.94 ± 0.2
S	13.46	12.23 ± 0.4
K	8.21	8.24 ± 0.2

All the monomers show coherent quantities of hydrogen to theoretical values, which presumes the products to be dry and coordinating no water. However, amount of carbon (in **2** and **4**), as well as fluorine (in **2**) and sulfur (in **4**) deviate largely from the allowed limits. The measurements are not repeated, therefore it cannot be assured, either the error comes from the measuring technique, or from the impurity of the monomers. However, since the NMR spectra of ^{1}H and ^{19}F of all the monomers synthesized show neat signals with expected

integration values and since the polycondensation reactions proceed in the previewed equilibrium, it is assumed that the molecules do have sufficient purity.

The three monomers are additionally characterized by differential scanning calorimetry (DSC), illustrared in *Fig. 2.16*. Neat background and clearly resolved melting endotherms again indicate the products to be pure. *Table 2.5* summarizes information, extracted from the DSC curves, such as melting temperature, enthalpy of melting and degradation temperature.

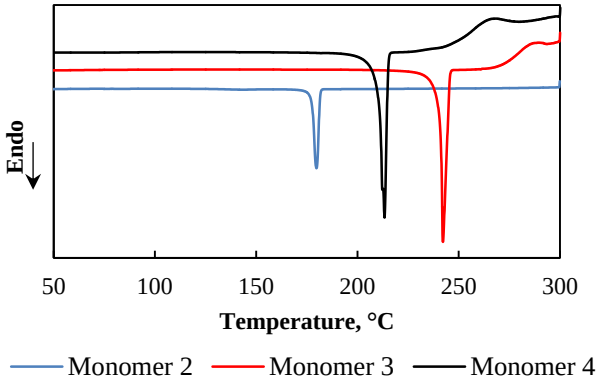

Figure 2.16. DSC thermograms of the monomers **2**, **3** and **4**

Table 2.5. Thermal characterization of the newly synthesized monomers

Monomer	**$T_{melting}$, °C**	**$\Delta H_{melting}$, J/g**	**$T_{degradation}$, °C**
2	179.8	34.4	> 300.0
3	242.2	113.1	265.0
4	213.3	95.0	245.0

The monomer **3** is characterized by the highest melting temperature (242 °C), the monomer **2** – by the lowest (180 °C). The melting enthalpy of the products follows the same trend: **3** > **4** > **2**. The monomers **3** and **4** show degradation exotherms, starting from 265 °C for the monomer **3** and from 245 °C for the monomer **4**. Presumably, degradation of these molecules is related to the dehydration of dihydroxyl groups. Such a conclusion is based on comparison of degradation temperatures of the monomers **2** and **3**. Both products have the same chemical structure, but differ in polymerizable substituents: the monomer **3**, being a dihydroxylated molecule, shows a lower T_d, than the difluorinated structure.

Likewise to **3**, degradation of the monomer **4** might also start through the –OH groups. However, its T_d is 20 °C lower, than that of the monomer **3**. In the case of monomer 4 the degradation can start also by the sulfanyl function how it was reported by Paillard *et al* [158] for similar compound. When comparing the electronegativity on the hydroxyl sites of both monomers, **3** and **4**, sulfanyl group in *meta*-position provides with lower electron-

withdrawing effect, than the CF_2. For this reason electronegativity on hydroxyls of the monomer **4** is higher, than that of the monomer **3**. It might provoke their higher activity towards reciprocal condensation.

The three monomers **2**, **3** and **4** were successfully produced. Main synthesis problems, related to: i) finding appropriate conditions for copper-mediated synthesis and demethylation reactions, ii) purification of polar monomers from secondary polar (or ionic) products, are succeded and described in detail. Additional information on protocol of all the reactions is presented in annexes with additional data of NMR chemical shifts. Elemental analysis shows coherent to theoretical values of atom contents which lets assume the monomers to have high enough purity for further reactions of polycondensation.

2.2. Synthesis of polymers

Polycondensation reactions, realized here between the newly synthesized ionic monomers **2**, **3** and **4** and commercial non-ionic monomers, are the second order nucleophilic aromatic substitutions (S_N2Ar), which proceed through formation of the anionic intermediate of the Meisenheimer complex. However, roles of the difluorinated monomer **2** and the dihydroxylated monomers **3** and **4** in nucleophilic substitution are different: the first one is an electrophile, the latter two are nucleophiles.

In order to understand the feasibility of the current polycondensations, a closer look on electron distribution in aromatic rings of the novel molecules is provided. *Fig. 2.17* presents all possible substitutions of polymerizable sites, which are marked as P. A chemical structure (**d**) corresponds to generalized formula of monomers, studied in the current work.

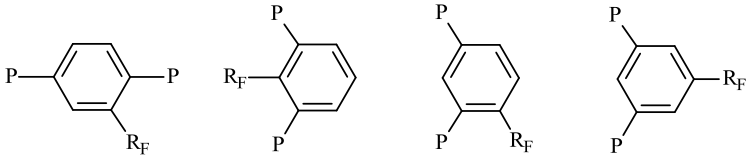

Figure 2.17. Schematic representation of possible arrangement of polymerizable substituents P at the aromatic ring

If one considers the fluorines are polymerizable sites P, then in case of the structure (**a**) the first phenate (nucleophile) attacks a *meta*-positioned (to R_F) P-site. Oxygen of the substituting phenate creates poorer *–I*-effect, than fluorine. Additionally, it shows *+M*-influence on the non-substituted second C-P-site, which increases electronegativity on the latter. For these reasons substitution of the second polymerizable group is deactivated. Besides, R_F-group creates steric hindrance, which becomes even more prominent in (**b**) case. Substitution of the P-sites in a structure (**c**) is favorable in terms of electron distribution. However adjacent neighborhood of R_F to one of the polymerizable groups might create a steric hindrance factor. Still this phenomenon is less influencing, than in case of the structure (**a**), due to a higher angle between the R_F and the plane of the polymer: in (**a**) structure polymerization proceeds by *para*-groups, forming a linear polymer, whereas the (**c**) structure has *meta*-positioned P-sites that, taking to account the formation of low molecular weight cyclic secondary products (discussed further), must provide angular polymers. Hereof, the (**d**) molecule is the most convenient in terms of electron distribution and steric factors for nucleophilic substitution, if P-sites are fluorines.

In spite of the easiest possibility for polycondensation of the structure (**d**), high temperatures are still required in order to substitute the fluorines. The group of Fossum [159-163] extensively studied (poly)condensation reactions of the di-*meta*-fluorinated aromatic molecules, having different electron-withdrawing groups (phenylketone, phenylsulfoxide, diphenylphosphoxide) in the third *meta*-position (case, shown in *Fig. 2.17 (d)*). The authors found that electron-withdrawing force of the non-polymerizable substituent influences activation energy for the nucleophilic substitution: sulfoxide is a stronger activating group, than ketone and phosphoxide, thus the first substitution takes place already at 75 °C and polymerization proceeds at 150 °C, while for the latter two cases the first substitution starts not earlier than at 150 °C and the polymerization at 185 °C. Unfortunately, no comparison to structures, containing a perfluoroalkyle-substituent (R_F), was given. Presumably, R_F-group in *meta*-position to P-sites, has a similar or slightly lower *–I*-effect, than sulfoxide.

In the case of the monomers **3** and **4** these are hydroxyls as polymerizable groups P (*Fig. 2.17*). In substitution reaction they are transformed to phenates in order to enhance their nucleophilic character. The reactivity of a phenate depends on the electron density, higher it is higher is its reactivity. Thus, *−I*-substituents in an aromatic ring do not have positive influence on reactivity of phenates, in general. Taking to account that in the (**d**) structure all the substituents are situated in *meta*-position one to another, no additional mesomeric effect may be detected, therefore again, the (**d**) structure is considered as the most reactive towards S_N2.

When comparing the two dihydroxylated monomers **3** and **4**, for both of them the ionic function (PFSA and S-PFSA) has *–I*-effect on aromatic ring and thus on phenate group. However, in case of the monomer **4** the sulfanyl-group, having two unpaired electrons, additionally reveals *+M*-effect (*Fig. 2.18*). Therefore, aromatic ring in the monomer **4** is less depleted in electron density, compared to the one in the monomer **3**, which presumes higher nucleophile reactivity of the former in S_N2 reactions.

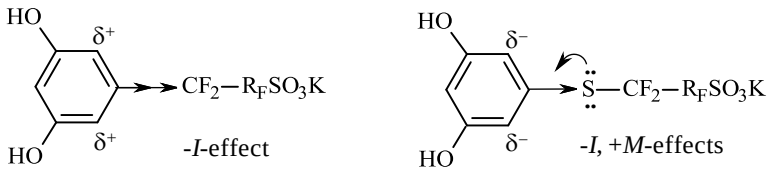

(a) (b)

Figure 2.18. Electron distribution in the monomers **3** (a) and **4** (b)

Monomers with *meta*-positioned polymerizable substituents are known to form cyclic low molecular weight products during the reaction of polycondensation [159-163]. Such a secondary

reaction is possible due to the angular location of the functions, participating in polymerization. The low molecular weight products in mixture with high molecular weight polymers either disable casting polymers to membranes, or, if a membrane could be produced, influence its thermo-mechanical properties. In addition, when more than two monomers are subjected to polymerization, formation of cyclic materials disrupts the previewed stoichiometry. For this reason precaution must be taken in polymer production, and conditions for cycle formation must be studied.

The following paragraphs give detailed discussion on nucleophilic substitution reactions for all the three ionic monomers with commercial ones. Description on production of random and block-copolymers is presented. Problems, when casting polymers to membranes, are also discussed.

The last paragraph proposes a new strategy of concentrating ionic lateral chains in a polymer by condensation of two monomers, bearing PFSA side groups. The method is innovative, thus, only one polymer of this type is synthesized for the moment.

*2.2.1. Polymerization of the monomer **2***

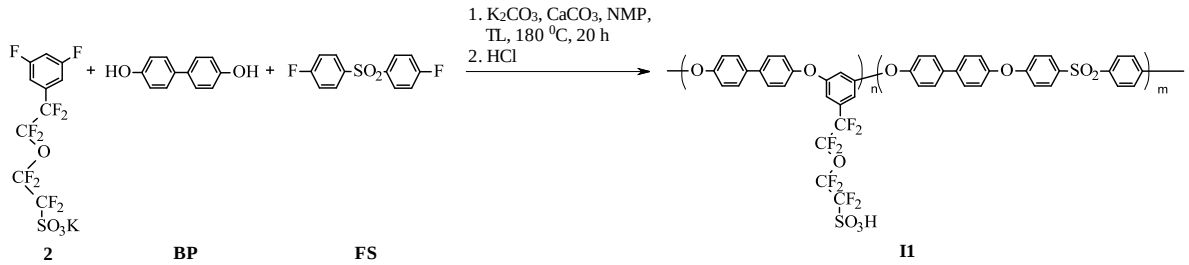

Figure 2.19. Polymerization of the monomer **2** – production of **I1**

The current paragraph presents series of random ionomers **I1**, produced by polycondensation of the **2** with 4,4′-biphenol (BP) and 4,4′-difluorodiphenylsulfone (FS) (*Fig. 2.19*). Ratio of the introduced monomers is varied (*Table 2.6*) in order to synthesize polymers of different ionic content (IEC 1.0 – 1.8).

As it was mentioned earlier polycondensation of the *meta*-positioned fluorines requires high temperatures. Therefore, two parameters were implied to avoid polymer chain scission during the reaction: i) drying the reaction mixture with the help of a Dean-Stark trap, filled with toluene, and ii) using the second salt of calcium carbonate for better precipitation of fluoride-anions, eliminating during the phenate attack. The reaction procedure is monitorized by disappearance of ^{19}F NMR peak, corresponding to aromatic F=fluorines at −108.1 ppm.

It is observed that the reaction mixture acquires high viscosity. Due to this phenomenon droplet precipitation of the polymer solution into acidic water (in order to stop the reaction) is not possible. Dilution of the reaction mixture with N-methyl-2-pyrrolidone (NMP) does not decrease significantly the solution viscosity. In order to precipitate such material, it is transferred to acidic water with a spatula, while forcing very viscous solution to disperse.

Table 2.6. IECs of **I1** and amounts of the introduced monomers for **I1** synthesis

Ionomer	**IEC (theor.), meq/g**	**IEC_{NMR}, meq/g**	**Introduced reactants, parts**		
			2	**BP**	**FS**
I1-1.0	1.05	1.05	1.0	2.0	1.0
I1-1.3	1.26	1.16	1.7	2.7	1.0
I1-1.5	1.48	1.54	3.3	4.3	1.0
I1-1.8	1.80	–	1.0	1.0	–

The obtained polymers are analyzed by ^{1}H and ^{19}F NMR spectra, which are presented in *Fig. 2.20*. Numbers, written above each peak, correspond to protons or fluorines of the same numerical indication at the chemical structure in the right upper corner. Integrals of peaks at the ^{1}H NMR spectrum may be compared to the introduced amounts of monomers in the following way:

i) peaks # 1 and 3 correspond to protons of the FS monomer in the ionomer. Since the signal # 1 is better separated from other peaks, it will be investigated further. From *Table 2.6* FS implies with 1.0 part to the polymer composition, hence 4 protons, corresponding to the peak # 1 will give integral 4.0.

ii) The monomer **2** is characterized by two types of protons, numbered 5 and 6 at the ^{1}H NMR spectrum. They contain three protons of the monomer **2**. Therefore integral of the peaks # 5 and 6 will correspond to multiplication of the part of **2**, noted in *Table 2.6*, by three (e.g., for the **I1-1.0** integral of the peaks # 5 and 6 will be (1.0·3), which is equal to 3.0, and which is close to the value 2.9, shown at the spectrum).

In the similar way estimation of IEC of each ionomer from the ^{1}H NMR spectrum may be done, using the following formula:

$$IEC_{H\text{-}NMR} = \frac{1000}{((\frac{I_1}{4}) \cdot MW_{[FS-BP]} + (\frac{I_{5+6}}{3}) \cdot MW_{[2-BP]}) / (\frac{I_{5+6}}{3})} \quad (3)$$

where I_1 is the integral of the peak # 1 and I_{5+6} is the integral of the peaks # 5 and 6 (shown in *Fig. 2.20*); $MW_{[FS\text{-}BP]}$ is molecular weight of the non-ionic structural unit between FS and BP

(which is equal to 400.5 g/mol) and $MW_{[2\text{-BP}]}$ is molecular weight of the ionic structural unit between the monomer **2** and BP (which is equal to 556.4 g/mol). Results of these calculations are shown in *Table 2.6*.

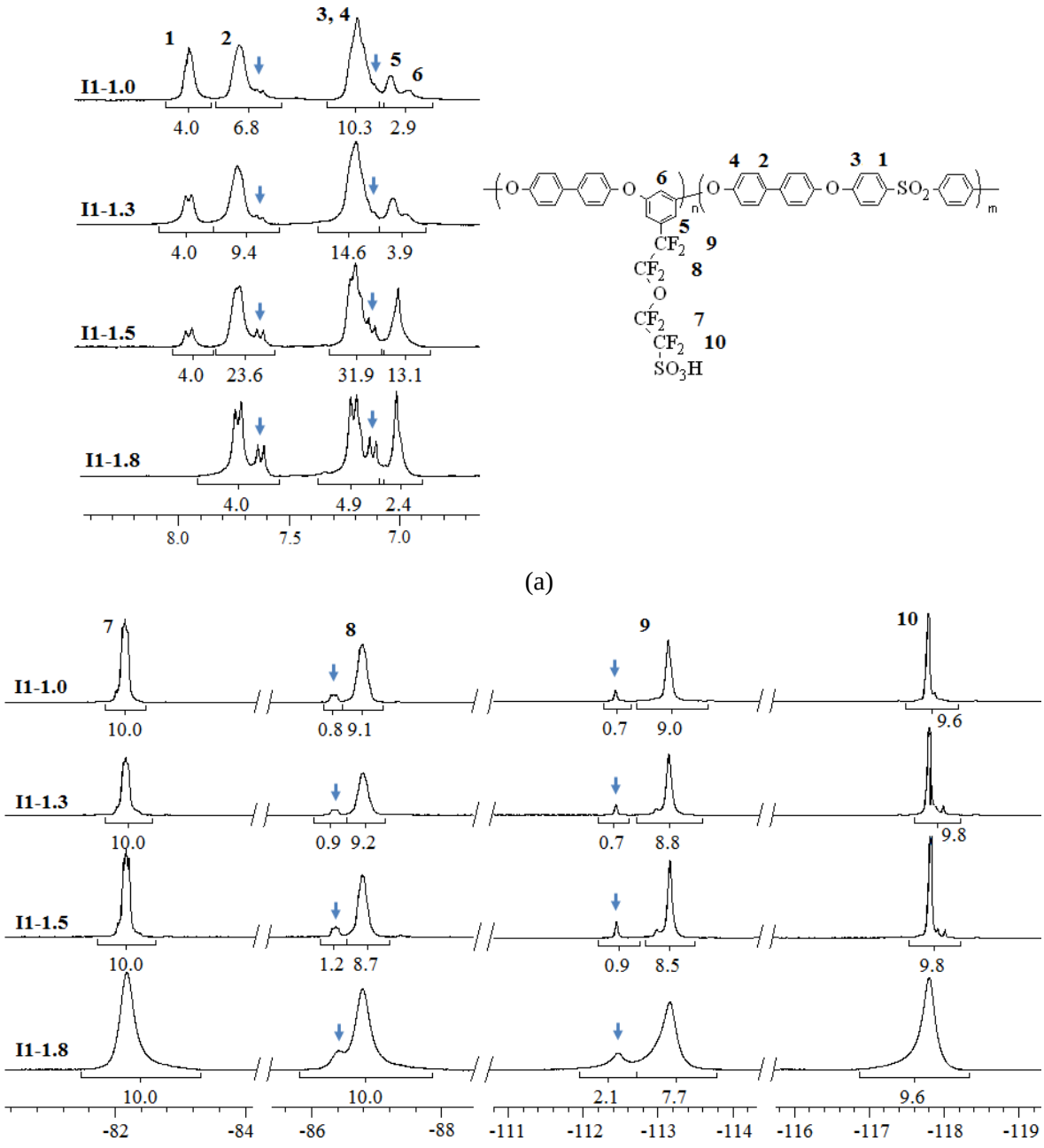

Figure 2.20. NMR spectra of the series **I1**: a) ^{1}H NMR and b) ^{19}F NMR spectra. Blue arrows point on the minor fraction, which is assumed to be cyclic oligomers

Other information extracted from the NMR spectra of the ionomers **I1** is the presence of two series (at least) of products: one major corresponds to the required polymer and another, pointed with blue arrows, to secondary products. Amount of the latter serie increases with higher IEC, thus higher amount of ionic monomer introduced to the reaction mixture.

Presumably, these secondary products are cyclic oligomers, formed during the high-temperature polycondensation of *meta*-polymerizable sites.

In order to study this phenomenon washing of the **I1** powders with alcohol (propan-2-ol) is performed. Alcohol phase is changed three times in order to make extraction more effective. *Fig. 2.21* shows NMR spectra of the ionomer **I1-1.3**: pristine, before its washing with propan-2-ol (spectrum (**a**)), the products washed with alcohol (spectrum (**b**)), and the part of the polymer that did not solubilize while washing (spectrum (**c**)).

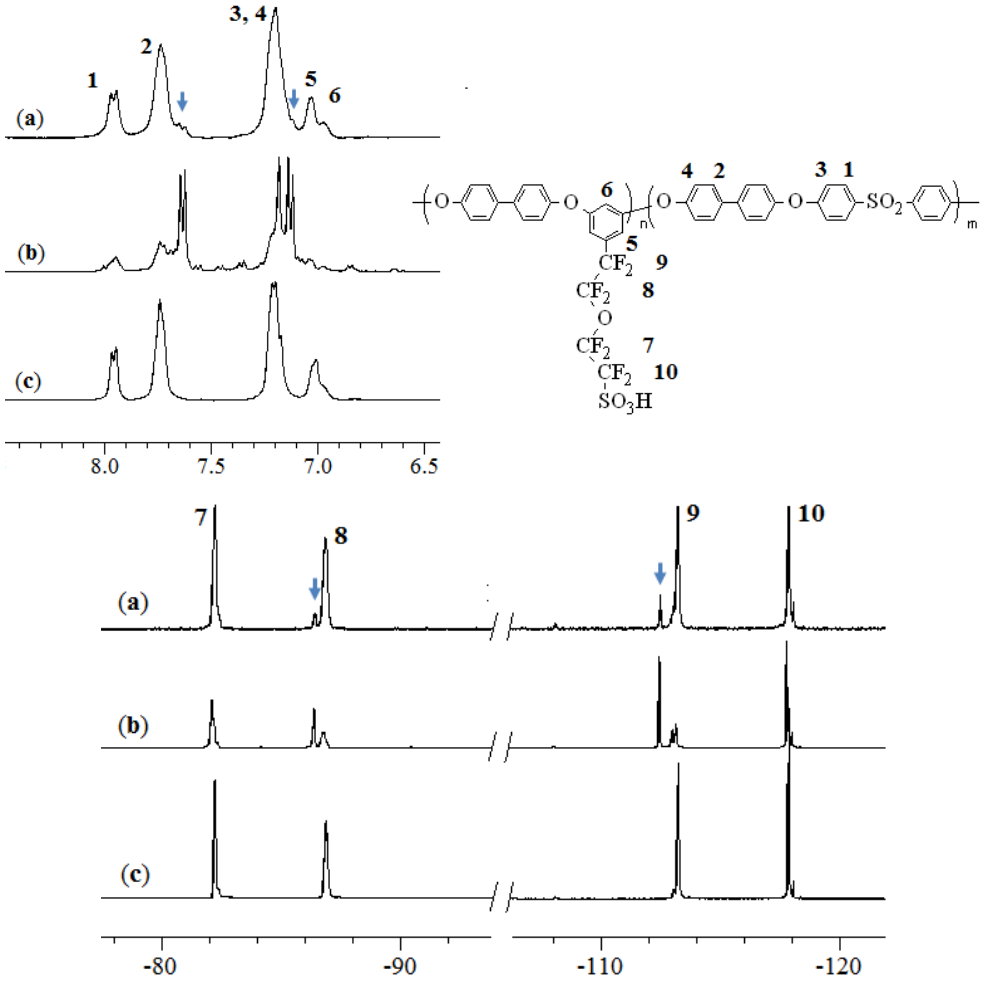

(b)

Figure 2.21. ^{1}H (upper part) and ^{19}F (down part) NMR spectra of the **I1-1.3**: a) pristine polymer, b) low molecular weight products, extracted with propan-2-ol, c) the part that is not soluble in alcohol – the pure polymer

Blue arrows on the spectra (**a**) in *Fig. 2.21* point on peaks, corresponding to the secondary product. Taking to consideration chemical shifts of the extracted by alcohol product (spectra (**b**)), one may presume that oligomers contain BP and **2** species only, which is schematized in *Fig. 2.22*.

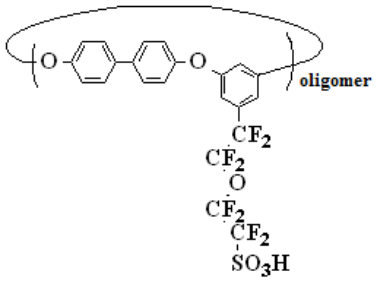

Figure 2.22. Assumed chemical structure of low molecular products, formed during the synthesis of **I1** and that could be washed from the polymer with propan-2-ol

When analyzing the fluorine spectra in *Fig. 2.21* we are not able to conclude if one or two series of secondary products are present. Peaks # 8 and 9 at (**b**) spectrum clearly show two types of products. But one of them has the same chemical shifts as the polymer. Therefore, it is impossible to accurately quantify amount of oligomers produced during the polycondensation. However, to estimate dependence of amount of cycles, formed during polycondensation, on IEC we make an approximation that only one type of oligomers is present. Then *Fig 2.20* is again analyzed: we calculate the ratio of integral of the small peak # 2, marked with the blue arrow, to the overall integral of the peak # 2 in the ^{1}H NMR spectrum, and ratio of the small peak # 8, marked with the blue arrow, to the overall integral of the peak # 8 in the ^{19}F NMR spectrum. The results are summarized in *Table 2.7*.

Table 2.7. Analysis on amount of oligomers, formed during polymerization of **I1**

Ionomer	**Amount of oligomers, %**		**Washing with propan-2-ol**	**IEC (titr.), meq/g**
	From ^{1}H NMR	**From ^{19}F NMR**		
I1-1.0	10.5	8.0	+ *	0.9
I1-1.3	8.0	9.0	+ *	1.2
I1-1.5	16.5	12.0	almost soluble	1.3
I1-1.8	22.0	21.4	soluble	–

* Polymer may be used further

I1-1.5 and **I1-1.8** gradually dissolve during the washing procedure; therefore they will not be investigated further. *Table 2.7* also proposes values of IEC of the polymers, containing no oligomers. Estimation of IEC was provided by titration of acidic polymer solutions in organic solvent. Since cyclic structures contain the ionic monomer, difference exists between experimental and theoretical values. However, due to low content of oligomers this difference is not considerable.

Membrane elaboration

Casting of **I1** polymers into membranes is performed in two ways. The first one is the production of films from the polymers, which contain cyclic oligomers, therefore the **I1** ionomers of all IECs are cast. The second way is membrane elaboration of exclusively **I1-1.0** and **I1-1.3** powders, which were thoroughly washed with alcohol to eliminate the low molecular weight products. For the first case the polymers in their Li^+-neutralized form are used, while for the second case – in both K^+- and Li^+-forms. The mentioned problem of high solution viscosity impedes formation of homogeneous materials. Different solvents are tested in order to find the best one to dissolve the ionomers. Dimethylsulfoxide (DMSO), dimethylacetamide (DMAc), NMP, and their mixtures with water, ACN, chloroform (up to 20 % maximum) are checked, but no amelioration is reported. Therefore, the polymer solution (10 % w/v) in DMAc is prepared, then filtered with a 0.45-μm filter, and cast to a Petri dish. Evaporation of solvent lasts for 2 days at 60 °C. The dry material is immersed in water for 2 days to wash out the residual organic solvent. The self-standing membranes in their salt-forms are received, while protonated samples are obtained by additional acidification with 1 M solution of HCl.

*2.2.2. Polymerizations of the monomers **3** and **4***

All the polycondensations of the monomers **3** and **4**, presented in the current work, are based on their reactions with decafluorobiphenyl (DFB), which is a highly reactive electrophile due to the totally delocalized electron density on the outskirts' fluorines of the aromatic rings. Two main series of ionomers are presented in the current work: poly(arylene ether)s PAEs and poly(arylene ether sulfone)s PAESs, differing in type of a third comonomer used – either BP or HS, respectively (*Fig. 2.23*).

In case of PAEs random copolymers only are presented. No corresponding block-copolymers could be synthesized due to the insolubility of the non-functionalized oligomers in any polar aprotic solvent. PAESs, however, will be further described in both their forms of random and block-copolymers. *Table 2.8* presents summarized information on types of comonomers used and attributed names to the resulting ionomers.

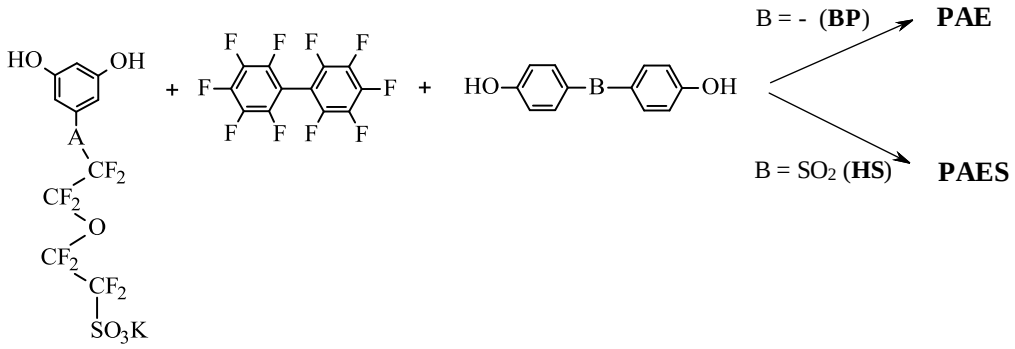

Figure 2.23. General scheme of polymerizations of the monomers **3** and **4**

Table 2.8. Generalized information on the ionomers, synthesized from the monomers **3** and **4**

Ionic monomer	Co-monomers		Ionomer type		Synthesis type	Ionomer name
3	DFB	BP	PAE	random	one-pot	I2
		HS	PAES	random	one-pot	*r*-I3
				block-copolymer	one-pot	*b*-I3
					copolymerization of separated blocks	*sb*-I3
4		BP	PAE	random	one-pot	I4
		HS	PAES	random	one-pot	*r*-I5
				block-copolymer	one-pot	*b*-I5

*2.2.2.1. PAEs **I2** and **I4***

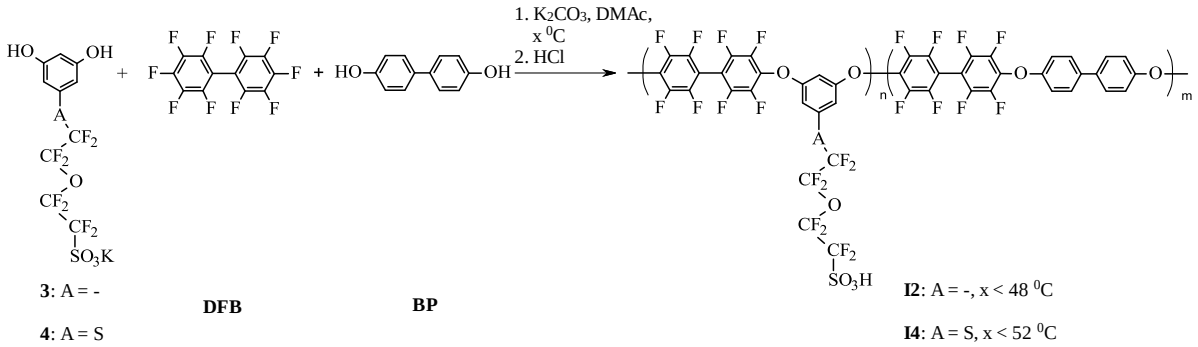

Figure 2.24. Polymerization of the monomers **3** and **4** with formation of PAEs

Polymerizations of the monomers **3** and **4** with DFB proceed at temperatures lower, than 48 °C and 52 °C, respectively. Higher operating temperatures provoke multiple substitutions at *ortho*- and *meta*-fluorine sites of the DFB. Series of **I2** and **I4** are produced, varying concentration of PFSA lateral chains in the ionomers. The products of polycondensation between the ionic monomers and DFB only result in maximal IEC 1.4 meq/g for both series.

To decrease concentration of acidic sites BP as a third comonomer is introduced. Additional IECs are previewed to be 1.2 meq/g (for both **I2** and **I4**) and 1.1 meq/g (for **I2**, when 1.0 meq/g for **I4**). For better explanation it will be further marked the series number together with IEC of the ionomer in suffix.

Table 2.9. Ratio of monomers introduced and time of synthesis of PAEs series **I2** and **I4**

Ionomer	**IEC (theor.), meq/g**	**IEC_{NMR}, meq/g**	**Introduced reactants, parts**			**Reaction time, days**
			3 or **4**	**DFB**	**BP**	
I2-1.1	1.05	1.07	1.9	2.9	1.0	3
I2-1.2	1.20	1.21	3.6	4.6	1.0	4
I2-1.4	1.43	1.43	1.0	1.0	–	5
I4-1.0	1.00	1.02	1.8	2.8	1.0	1
I4-1.2	1.20	1.21	4.8	5.8	1.0	2
I4-1.4	1.37	1.37	1.0	1.0	–	3

Reaction time is dependent on reactants' loading (*Table 2.9*): lower the concentration of BP introduced (higher the IEC), longer the time of polycondensation is. Such dependence reveals higher reactivity of BP as a phenate, compared to the ionic monomers **3** and **4**. Delocalization of electron density in the ionic monomers due to *–I*-effect of PFSA (or (S)-PFSA) in *meta*-position to polymerizable sites decreases the reactivity of the phenate. Moreover, the first substitution with a molecule of DFB decreases the reactivity of the second phenate site even more. On the contrary, the first substitution in BP does not create any impact on reactivity of the second phenate, since it is situated at long distance in *para*-position of another aromatic ring.

Polymerization is considered to be finished, when the reactive solution becomes viscous enough. No precise reaction time in hours is given, because no instant gain in viscosity is detected. Nevertheless, polymers of sufficient molecular weight for excellent film-forming properties are obtained that will be proved below with size exclusion chromatography (SEC). Moreover, when polymers of low to medium molecular weight (oligomers) are also present, they give additional signals of their end-chains, which are easily detectable by ^{19}F NMR. *Fig. 2.25* presents two spectra of Fluorine atoms of an ionomer **I2-1.4**: in case (**a**) the ionomer polymerization lasted 3 days, in (**b**) case polycondensation was left for 5 consecutive days. Low molecular weight products at the spectrum (**a**) are marked with blue arrows and are characterized by following chemical displacements: −139.4 ppm (2 F_{Ar}), −152.9 ppm (1 F_{Ar}), and −163.3 ppm (2 F_{Ar}). No membrane might be formed out of the polymer powder, presented in *Fig. 2.25 (a)*.

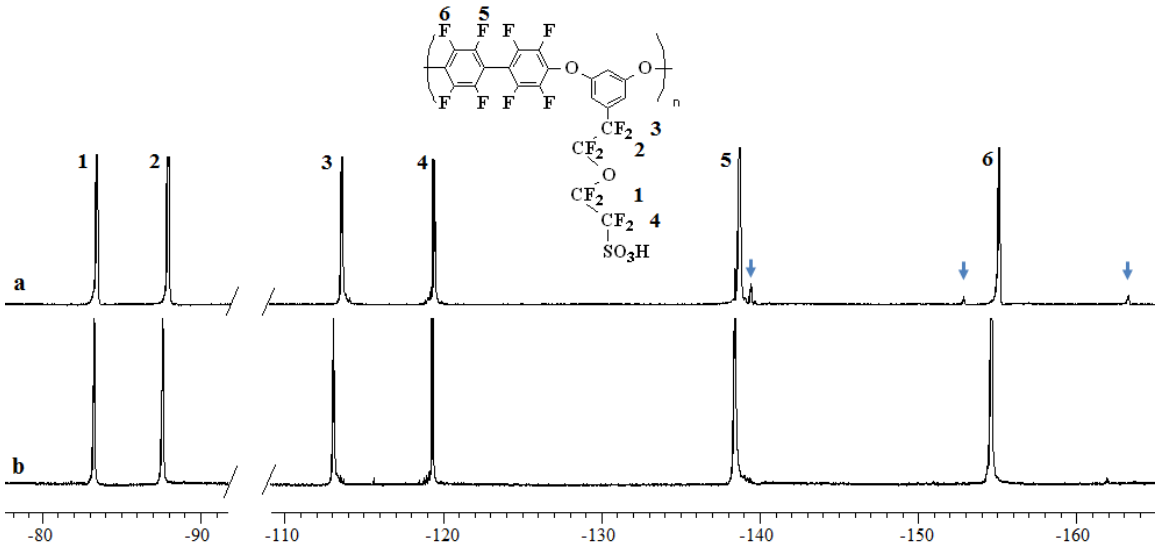

Figure 2.25. ^{19}F NMR spectra of **I2-1.4**; polymerization time is: a) 3 days, b) 5 days. Blue arrows point on the ends of polymer chains of low molecular weight

Fig. 2.26 and *2.27* present ^{1}H and ^{19}F NMR spectra of all the ionomers series **I2** and **I4**. Numbers, attributed to each peak, correspond to hydrogens and fluorines of the chemical structures, shown in the right upper corners. Spectra of ionomers **I2-1.4** and **I4-1.4** evidence the presence of electron delocalization towards the fluorinated phenylenes of DFB. In the initial monomers **3** and **4** protons # 2 are the most deshielded (due to the strong electron-withdrawing effect of the PFSA chain in the vicinity). After polymerization to ionomers **I2** and **I4** hydrogens in-between *meta*-oxygens become the most deshielded, thus protons #1 are subjected to the stronger effect of the decrease of electron density (due to the electron withdrawing effect of DFB) as compared to their state in the monomers.

IEC may be estimated separately from ^{1}H and ^{19}F NMR spectra. Analyzing the ^{1}H NMR spectrum, for the both series of ionomers peaks # 2 and 3 correspond to hydrogens of the aromatic ring bearing the ionic function and of the BP, respectively. The peak # 2 is related to two hydrogens and the peak # 3 to four atoms. From the integration values of these characteristic signals IEC may be calculated, using the following formula:

$$IEC_{H\text{-}NMR} = \frac{1000}{\left(\frac{I_3}{4}\cdot MW_{[BP-DFB]} + \frac{I_2}{2}\cdot MW_{[3(4)-DFB]}\right)/\left(\frac{I_2}{2}\right)} \qquad (4)$$

where I_3 is the integral of the peak # 3 and I_2 is the integral of the peak # 2 (shown in *Fig. 2.26* and *2.27*); $MW_{[BP\text{-}DFB]}$ is molecular weight of the non-ionic structural unit resulted by the condensation between BP and DFB (which is equal to 480.3 g/mol) and $MW_{[3(4)\text{-}DFB]}$ is

molecular weight of the ionic structural unit resulted by the reaction between the monomer **3** or **4** and DFB (which is equal to 700.3 and 732.4 g/mol, respectively).

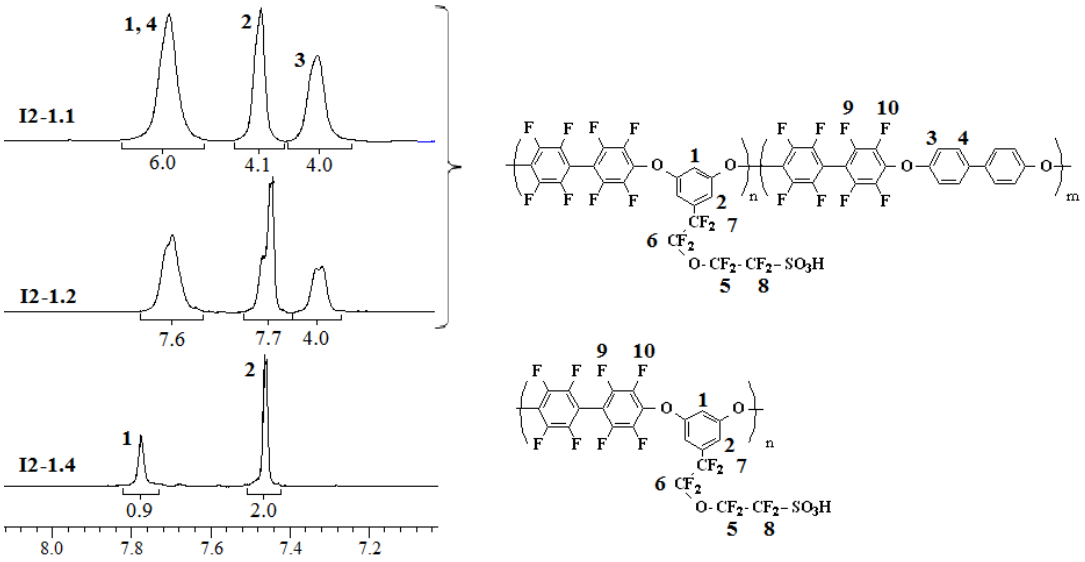

(a)

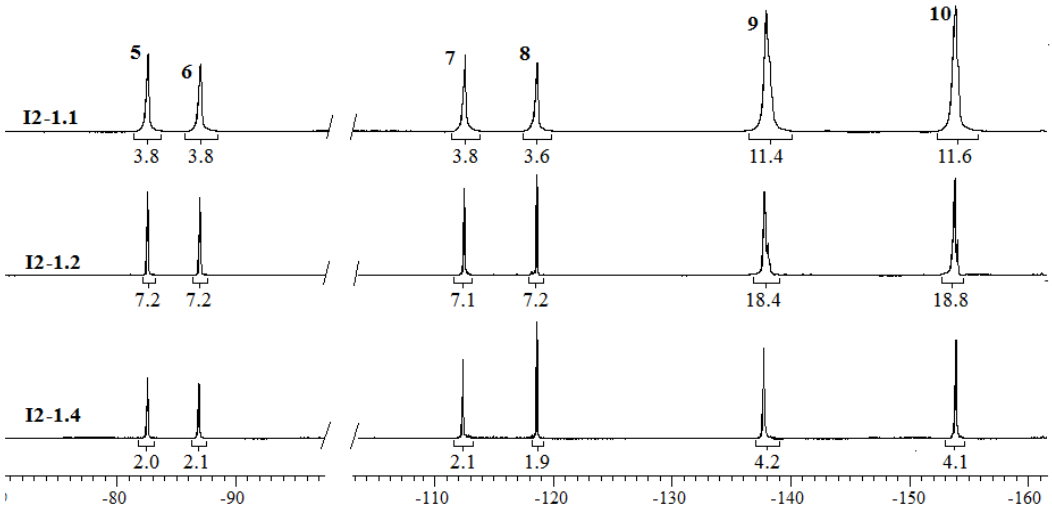

(b)

Figure 2.26. ^{1}H NMR (a) and ^{19}F NMR (b) spectra of the ionomers series **I2**

Analyzing the ^{19}F NMR spectrum, for the both series of ionomers peaks # 5, 6, 7 and 8 correspond to fluorines of the PFSA function and # 9 and 10 – of the DFB. For example, peak #5 is considered further, which is related to two fluorines in the ionic function and peak – # 9 to four atoms of DFB. But it must be noted that total integral of the peak # 9 contains DFB bound to the ionic monomer and to the BP specie. Therefore to evaluate the integral of the peak # 9 exctraction of the integral of DFB, connected to the ionic monomer must not be forgotten. From the integration values of these characteristic signals IEC may be calculated, using the following formula:

$$IEC_{F\text{-}NMR} = \frac{1000}{\left(\frac{(I_9 - 2 \cdot I_5)}{4} \cdot MW_{[BP-DFB]} + \frac{I_5}{2} \cdot MW_{[3(4)-DFB]}\right) / \left(\frac{I_5}{2}\right)} \quad (5)$$

where I_5 is the integral of the peak # 5 and I_9 is the integral of the peak # 9 (shown in *Fig. 2.26* and *2.27*). Results of these calculations are shown in *Table 2.9*. Since the identic values of IEC, calculated from the ^{1}H and ^{19}F NMR spectra, are obtained, both of them are noted in one column in the table as IEC_{NMR}. **I2-1.4** and **I4-1.4** are exceptionally calculated based on ^{19}F NMR only, since they do not contain any BP specie to be analyzed by ^{1}H NMR.

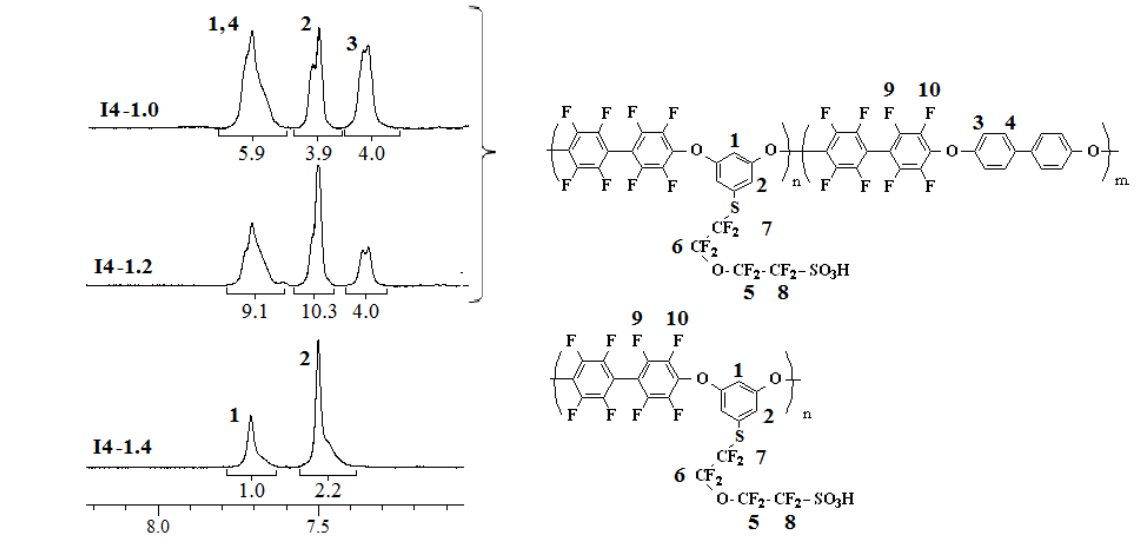

(a)

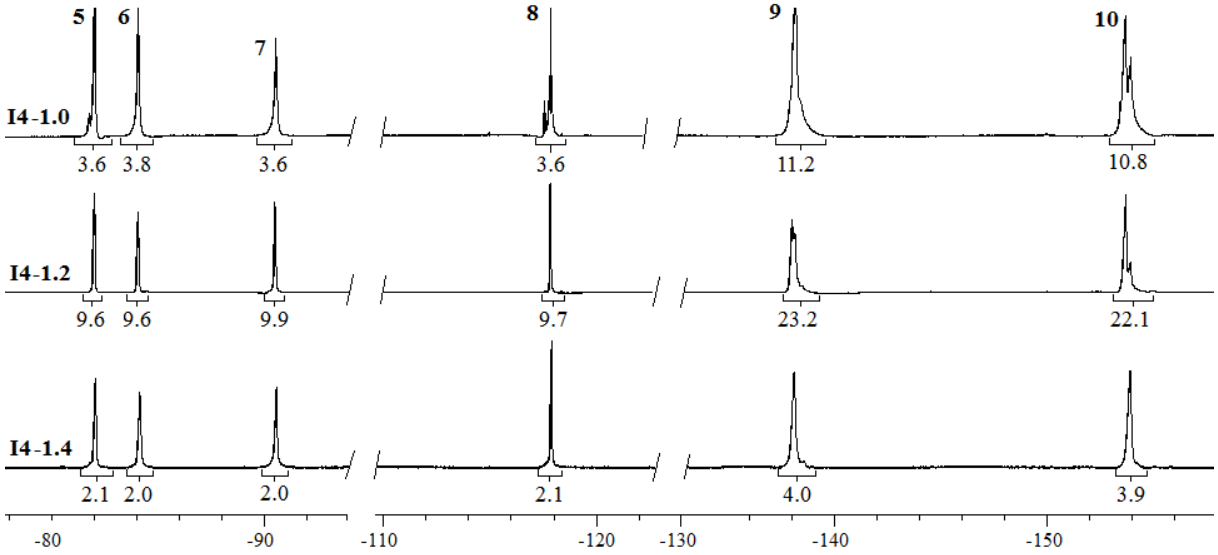

(b)

Figure 2.27. ^{1}H NMR (a) and ^{19}F NMR (b) spectra of the ionomers series **I4**

Table 2.10 presents data on molecular weights (MW) of polymers **I2** and **I4**, determined by size-exclusion chromatography (SEC). The polymers **I2-1.1** and **I4-1.0** show the highest values of polydispersity index (Mw/Mn) among the other samples of the series.

Table 2.10. Molecular weights of the ionomers series **I2** and **I4**, measured by size exclusion chromatography coupled with light scattering

Ionomer	Mn, $\cdot 10^3$, g/mol	Mw, $\cdot 10^3$, g/mol	Mw/Mn
I2-1.1	60.4 ± 4.2	193.1 ± 0.6	3.2 ± 0.2
I2-1.2	69.2 ± 2.9	128.6 ± 2.1	1.9 ± 0.1
I2-1.4	61.7 ± 2.7	118.8 ± 1.6	1.9 ± 0.1
I4-1.0	106.4 ± 2.0	448.2 ± 3.6	4.2 ± 0.1
I4-1.2	51.8 ± 1.0	103.6 ± 0.5	2.0 ± 0.1
I4-1.4	N/A *	N/A *	N/A *

* Sample blocks a pre-filter of a measuring device

Tests on block-copolymer syntheses are also realized. The strategy consists in production of an ionomer, bearing monomers **3** (or **4**) and DFB in a hydrophilic block and monomers BP and DFB in a hydrophobic block. The choice of monomers is stipulated, based on series of random ionomers **I2** and **I4**. The programmed synthesis path is illustrated in *Fig. 2.28*.

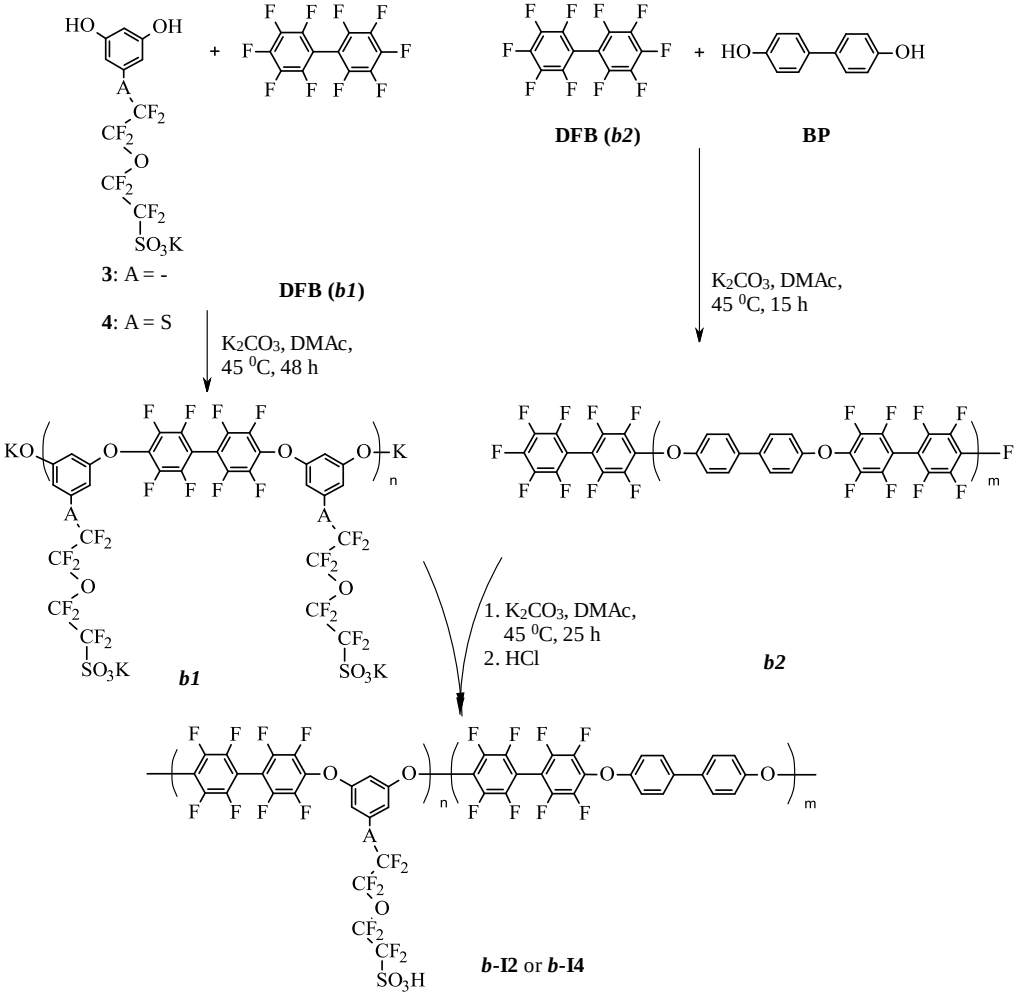

Figure 2.28. Unsuccessful copolymerization of the monomers **3** and **4** in order to produce block-copolymers of PAEs

However, hydrophobic oligomer (***b2*** in *Fig. 2.28*) is insoluble in DMAc as a reaction solvent; neither it is in other polar solvents that may be used for further condensation of blocks. Due to this phenomenon no block-copolymer may be produced with the ionic monomers **3** or **4** and non-ionic comonomers BP and DFB.

Membrane elaboration

I2 series is further studied for casting into membranes. It is known that polymers, containing superacid groups, are cast to membranes from their salt forms. In this way two possible degradation events, which become possible due to interaction with the superacid lateral group, are avoided: the first is the polymer scission through the ether-bond and the second is degradation of the casting solvent. To study the influence (if any) of a counter-ion all the ionomers series **I2** are neutralized overnight in 1 M solutions of three bases: LiOH, KOH, and trimethylamine (TEA). Excess of bases is washed out with deionized water, the polymers are dried and then solubilized in DMAc (10 % solution w/v). Polymer solutions are then filtered over 0.45 μm filter, degased, and cast to Petri dishes; solvent is evaporated during 2 days at 60 °C. Membranes are then transferred to water overnight to wash out traces of solvent. Further on this method of membrane preparation is called *method A*.

The first observation on membranes, containing ionic groups neutralized by alkaline cations (Li^+, K^+), is the difference in their appearance: those containing higher amount of BP are the least transparent, almost white-colored, whereas the membranes based on ionomers of the highest IEC (containing no BP) are totally transparent. The second observation is evoked from the tests on protonation of the membranes. Acidification proceeds in 1 M HCl aqueous solution overnight. Afterwards, membranes are washed until neutral pH, dried at 50 °C overnight and analyzed for ion-exchange capacity (IEC) by forward titration of the polymer solution in organic solvent (see chapter on characterization techniques in the end of the dissertation).

Results on the IEC of the membranes **I2** measured after this acidification protocol, are presented in a *Table 2.11*. The best salt ion-to-proton exchange is observed for the membranes cast from their Li^+ initial form, which comprises 85 % of exchanged ionic functions. Meanwhile the membranes, acidified from their K^+ initial salt form, show 77 % of protonation and from the TEA^+ initial salt form 14 – 41 % (for different IECs) only. Notably, the degree of protonation from the latter salt form is dependent on the ionomer's IEC: the acidification increases with the increase of ionic sites. Non-totality of salt-to-proton exchange presumes

poor accessibility of ionic groups; moreover, bigger the cation is, worse the acidification proceeds.

It was proposed to increase the strength of the acidifying environment, thus to change hydrochloric acid to a superacid trifluoromethanesulfonic one. From *Table 2.11* Li^+-to-H^+ exchange is evaluated to be complete. However, the K^+ and TEA^+ forms still have partial protonation: 65 % for the samples, acidified from K^+-form, and 34-56 % (depending on IEC) for the TEA^+-to-H^+ ionomers.

Table 2.11. Ion exchange capacity* of the ionomers **I3**, when acidified by a strong and a super-acids

Ionomer	**IEC (theor.) meq/g**	**Initial salt form**	**HCl, 1M**		**Triflic acid, 1M**		**Density, g/cm^3**	**IEC$_V$, meq/cm^3**
			IEC (titr.), meq/g	**Conversion salt-to acid, %**	**IEC (titr.), meq/g**	**Conversion salt-to acid, %**		
I2-1.1	1.1	Li^+	0.9	85	1.0	99	1.6	1.7
		K^+	0.8	77	0.7	65		
		TEA^+	0.1	14	0.4	34		
I2-1.2	1.2	Li^+	–	–	1.2	100	1.7	2.0
		K^+	–	–	0.8	65		
		TEA^+	–	–	0.5	44		
I2-1.4	1.4	Li^+	1.2	85	1.4	100	1.7	2.5
		K^+	1.1	77	–	–		
		TEA^+	0.6	41	0.8	56		

* All data on IEC and density of polymers will be presented with one decimal, since we are certain that manual techniques used for the current measurements do not allow to precise the two decimals

Based on these results we suppose that the nature of the cation influences considerably the morphology of the membranes. The counter-ions play important role in the lateral chain organization, which guides the overall packing of polymer chains. Due to these phenomena, probably, some ionic ends become isolated and not accessible to acidic water, which results in non-totality of salt-to proton acidification.

In order to verify this assumption the organization of polymer chains in the membranes as a function of cation nature and the accessibility of cation to acidified water we solubilize the membrane in a solvent (DMAc) and precipitate such as thin filaments directly in acidic water (1M HCl). **I2-1.1** was chosen, which, even after acidification with trifluoromethanesulfonic acid from its TEA^+-form, results in 34 % of protonated PFSA only (refer to *Table 2.11*). The measurement of IEC of its filaments (after washing and drying), resulted by precipitation, shows almost twice increase in protonation (63 %), though the totality is still not achieved.

The current results corroborate with the hypothesis that morphology of the membranes, produced by the *method A*, does not assure full accessibility and connectivity of the ionic domains. It is known that annealing of the dry membranes leads to reorganization of ionic domains and enhances significantly their connectivity [48].Therefore the strategy of film elaboration is changed to a *method B*. It consists of: i) polymer in its salt form being solubilized in DMAc (10 % w/v solution), ii) polymer solution being filtered at a 0.45 μm filter under pressure and degassed, iii) polymer solution being cast to a Petri dish and subsequent solvent evaporation at 60 °C during 2 days, iv) a membrane being annealed at 150 °C for 12 h at least, and v) a membrane being washed from traces of organic solvent by water at 35-40 °C during 2 days.

Protonation of the newly elaborated membranes, particularly of the polymer **I2-1.4**, is done in1 M aqueous solution of HCl, changing acidifying media two times. IECs of the prepared samples are shown in *Table 2.12*.

Table 2.12. Ion exchange capacity of the ionomers **I2-1.4**, being cast by different methods

Ionomer	**IEC (theor.), meq/g**	**Initial salt form**	***Method A*, titration**		***Method B*, titration**	
			IEC (titr.), meq/g	**Conversion, %**	**IEC (titr.), meq/g**	**Conversion, %**
I2-1.4	1.4	Li^+	1.2	85	1.3	92
		K^+	1.1	77	1.4	96

Increased conversion of salt-to-acid form of the membranes **I2-1.4** is registered. It confirms that morphology of the samples is changed upon annealing, and accessibility of ionic domains is increased.

Based on the results, described above for the series **I2**, *method B* is chosen for membrane elaboration. Further series of ionomers, produced in the current work, are studied with K^+- and Li^+-counter-ions only. Acidification is performed with 1 M HCl, changing the solution 3 times to remove gradually the eliminating KCl or LiCl, thus achieving higher probability for total protonation.

Consequently, ion-exchange properties of the series **I4** are presented in *Table 2.13*. The conversions of cation exchange are higher than 95% for all the studied membranes. The polymers' densities and IECs per volume are very close to those of the series **I2** (*Table 2.11*), thus the membrane properties of the two series may be easily compared by their properties, what is discussed in the next chapter.

Table 2.13. Ion exchange capacities of the ionomers series **I4**

Ionomer	IEC (theor.), meq/g	Initial salt form	IEC (titr.), meq/g	Conversion, %	Density, g/cm^3	IEC$_V$, meq/cm^3
I4-1.0	1.0	Li^+	1.0	100	1.7	1.7
		K^+	1.0	100		
I4-1.2	1.2	Li^+	1.1	95	1.7	2.0
		K^+	1.1	94		
I4-1.4	1.4	Li^+	1.4	100	1.8	2.4
		K^+	1.5	100		

The experimental data of IEC in *Table 2.13* are in good agreement with theoretical values that makes us believe the conditions for membrane production are adapted.

*2.2.2.2. PAESs **I3** and **I5***

The current paragraph describes production of both random (***r*-I3** and **r-I5**) and corresponding in IEC block-copolymers ***b*-I3**, ***sb*-I3** and ***b*-I5**. General schemes of synthesis of all these types of PAES are shown in *Fig. 2.29*, *2.30* and *2.31*.

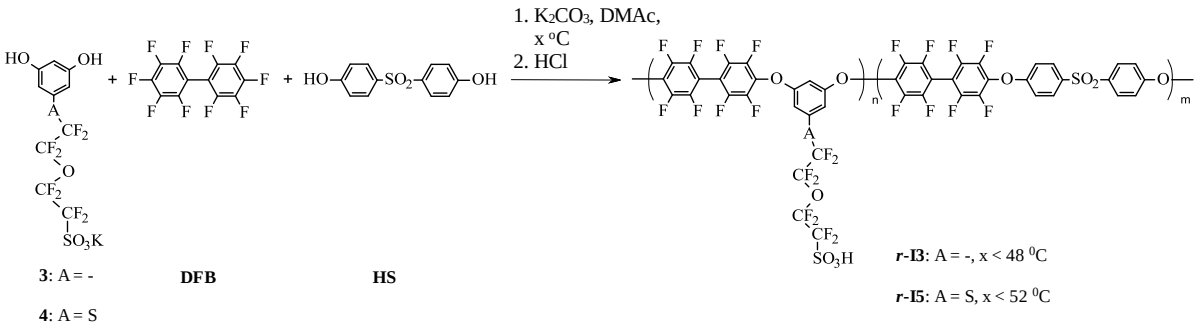

Figure 2.29. Synthesis scheme of random PAES ***r*-I3** and ***r*-I5**

The reactions proceed between the ionic monomers **3** and **4** and non-ionic difluorinated monomer DFB and dihydroxy-terminated molecule 4,4′-dihydroxydiphenylsulfone (HS). Temperatures of polycondensation are not higher than 48 °C and 52 °C for the series **I3** and **I5**, respectively. On the contrary to the syntheses of PAEs, polymerizations in presence of HS leads to faster increase in viscosity, which would result in a hardly soluble polymer, thus inhomogeneous membranes thereafter. For this reason, control of the reaction time is important, and it is given in hours (*Table 2.14*).

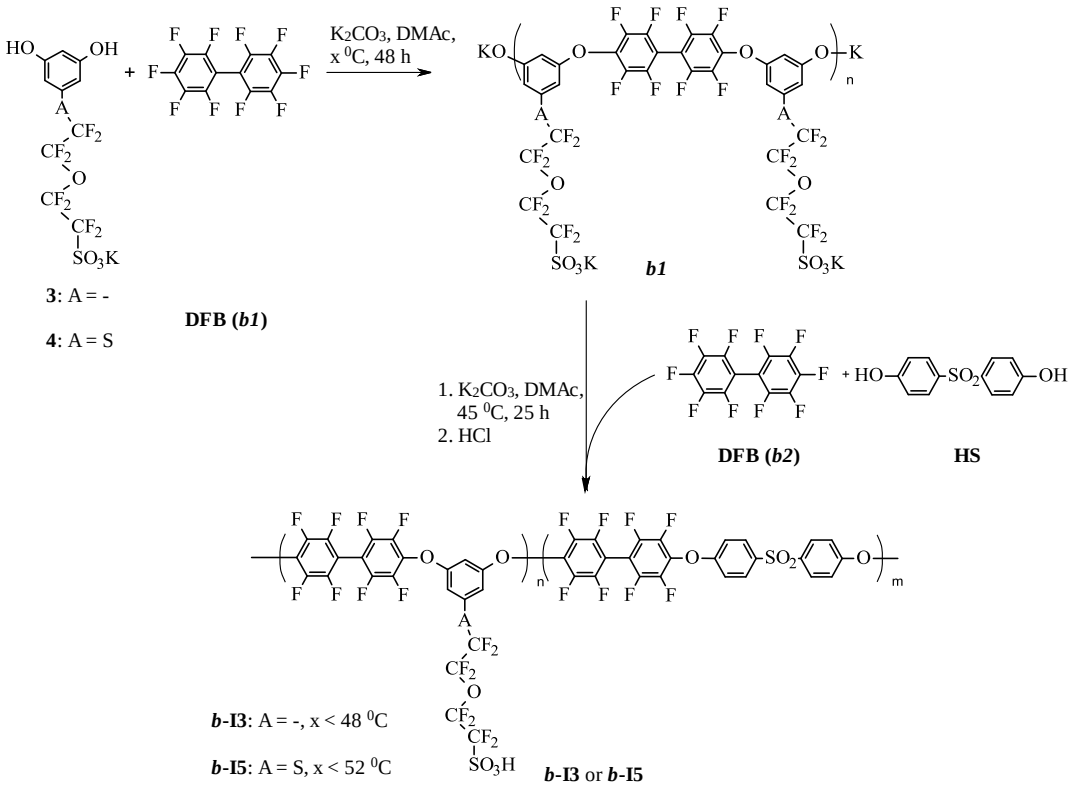

Figure 2.30. *S*ynthesis scheme of block-copolymers series **I3** and **I5**, produced by a method 'one-pot'

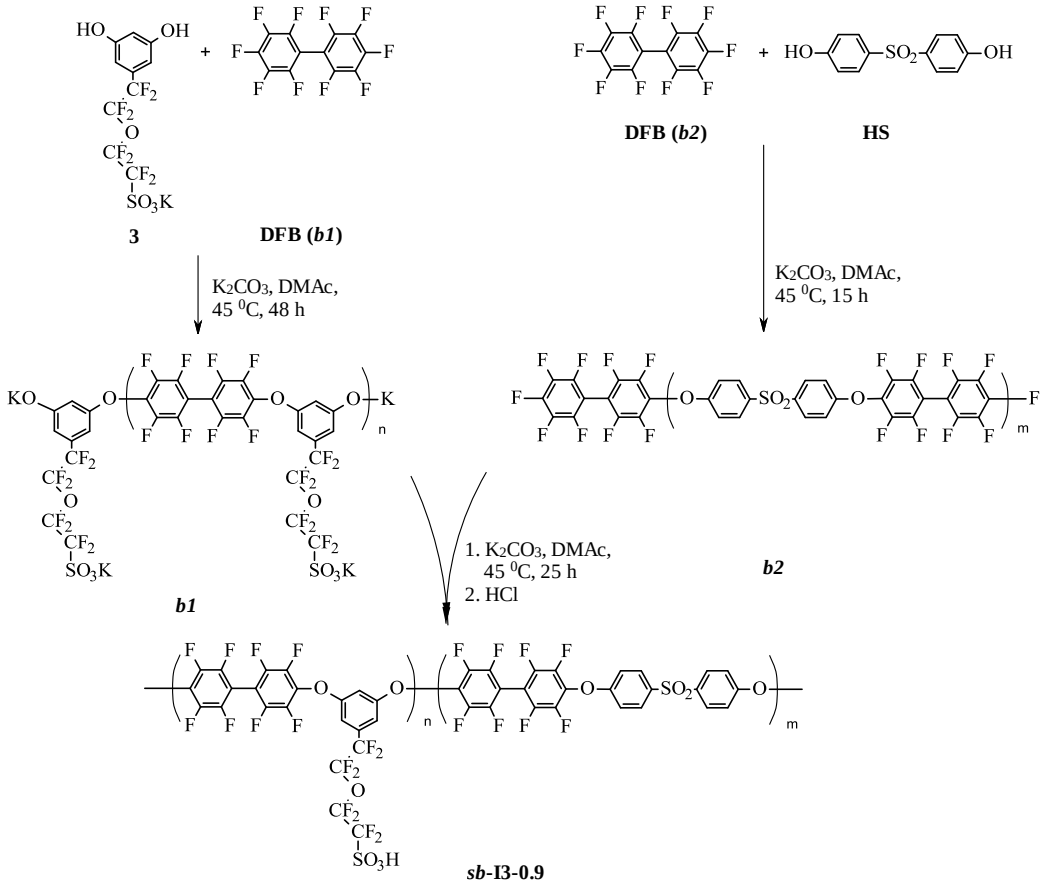

Figure 2.31. *S*ynthesis scheme of block-copolymers series **I3**, produced from separate blocks

Random and block-copolymers of the series **I3** and **I5** are synthesized in order to obtain materials of IEC in the range 0.9 – 1.1 meq/g. *Table 2.14* presents all the samples produced; IECs are mentioned as suffixes in the names of each material. Block-copolymers of IEC 0.9 meq/g (***b*-I3-0.9**, ***sb*-I3-0.9** and ***b*-I5-0.9**) have blocks of equal lengths of the main chain. It means that molecular weights (MW) of the hydrophobic block and of the backbone of the hydrophilic block are the same, 10 kDa.

Fig. 2.32 schematically illustrates how calculations of MW of the hydrophilic blocks were performed, and shows further procedure for quantification of the introduced reagents. When synthesizing a block one of the monomers (terminating the block) must be taken in excess. To estimate the ratio (r) between the introduced monomers Carother's equation is applied:

$$MW_{\text{block}} = \frac{(1+r)}{(1-r)} \cdot \frac{1}{2} MW_o + MW_{end} \qquad (6)$$

where MW_{block} is previewed molecular weight of a block, MW_{o} is molecular weight of a structural unit, MW_{end} is molecular weight of a terminating monomer. Amounts of the monomers, used in the reactions, are summarized in *Table 2.14*.

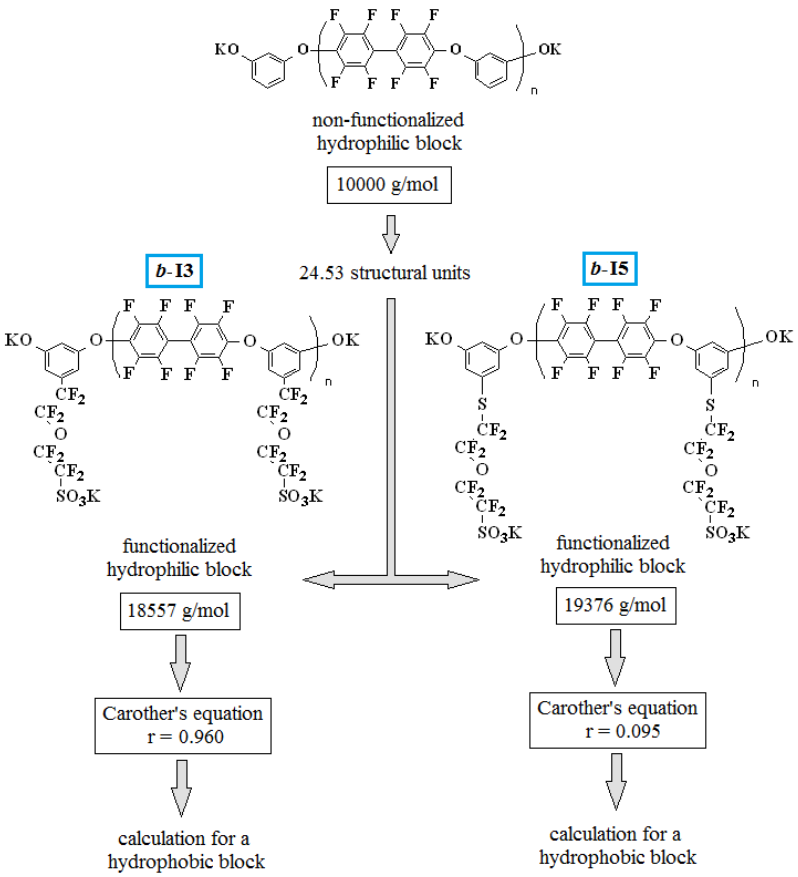

Figure 2.32. Scheme of calculations of the ratio between the introduced monomers for synthesis of hydrophilic blocks of block-copolymers series **I3** and **I5**

Reactions of block-copolymerization are performed in two ways: i) by 'one-pot' polycondensation (case of ***b*-I3**, ***b*-I5**), where a hydrophilic block is synthesized in a reaction flask, and then the monomers for a hydrophobic block are introduced to the solution of the first block; and ii) by condensation of separate blocks (case of ***sb*-I3**), when a hydrophilic and a hydrophobic blocks are separately synthesized and then are mixed to react between each other.

Each of the synthesis methods has advantages and drawbacks. For the first method the advantage is related to the synthesis facility, in one pot. However, the monomers are added to the solution of a hydrophilic block, polydispersity of the lengths of a hydrophobic block cannot be controlled. However, it may be supposed, that the monomers, introduced to the solution of the hydrophilic block, will firstly react between each other (due to the higher concentration and higher mobility) and then condensate with a polar block. Effectiveness of one-pot strategy was confirmed by our group earlier [140]. The second method allows to control MW of each of the blocks and to directly proceed to condensation in-between the two blocks. But it implies consummation of more solvent and more time.

Table 2.14. Ratio of monomers introduced and time of synthesis of PAESs series **I3** and **I5**

Ionomer	**IEC (theor.), meq/g**	**IEC_{NMR}, meq/g**	**Introduced reactants, parts**			**Reaction time, hours**
			3 or **4**	**DFB**	**HS**	
r-I3-0.9	0.90	0.89	1.33	2.33	1.00	30
b-I3-0.9		0.80	1.31	2.31	1.00	25
sb-I3-0.9		0.87	1.31	2.31	1.00	25
r-I3-1.1	1.13	N/A	2.95	3.95	1.00	30
r-I5-0.9	0.92	0.89	1.43	2.43	1.00	40
b-I5-0.9		0.78	1.44	2.44	1.00	9

Fig. 2.33 and *2.34* present ^{1}H and ^{19}F NMR spectra of all the ionomers series **I3** and **I5** of IEC 0.9 meq/g, and *Fig. 2.35* illustrates the both spectra of the random **I3** of IEC 1.1 meq/g (***r*-I3-1.1**). Numbers, attributed to each peak, correspond to hydrogens and fluorines of the chemical structures, shown in the right upper corners. For the both series of ionomers peaks # 1 and 3 correspond to hydrogens of the ionic monomer specie and of HS, respectively. Peak # 1 is related to one proton and peak # 3 to four protons. From the integration values of these characteristic signals IEC may be calculated, using the following formula:

$$IEC_{H\text{-}NMR} = \frac{1000}{((\frac{I_3}{4}) \cdot MW_{[HS-DFB]} + (\frac{I_1}{1}) \cdot MW_{[3(4)-DFB]}) / (\frac{I_1}{1})} \quad (7)$$

where I_3 is the integral of the peak # 3 and I_1 is the integral of the peak # 1 (shown in *Fig. 2.33, 2.34* and *2.35*); $MW_{[HS\text{-}DFB]}$ is molecular weight of the non-ionic structural unit between HS and DFB (which is equal to 544.4 g/mol) and $MW_{[3(4)\text{-}DFB]}$ is molecular weight of the ionic structural unit between the monomer **3** or **4** and DFB (which is equal to 700.3 and 732.4 g/mol, respectively).

Analyzing the ^{19}F NMR spectra, for the both series of ionomers peaks # 5, 6, 7 and 8 correspond to fluorines of the PFSA function and # 9 and 10 – of the DFB. For example, peak #5 is considered further, which is related to two fluorines in the ionic function and peak – # 9 to four atoms of DFB. But it must be noted that total integral of the peak # 9 contains DFB bound to the ionic monomer and to the HS specie. Therefore, to evaluate the integral of the peak # 9 exctraction of the integral of DFB, connected to the ionic monomer must not be forgotten. From the integration values of these characteristic signals IEC may be calculated, using the following formula:

$$IEC_{F\text{-}NMR} = \frac{1000}{\left(\frac{(I_9 - 2 \cdot I_5)}{4} \cdot MW_{[HS-DFB]} + \frac{I_5}{2} \cdot MW_{[3(4)-DFB]}\right) / \left(\frac{I_5}{2}\right)} \quad (8)$$

where I_5 is the integral of the peak # 5 and I_9 is the integral of the peak # 9 (shown in *Fig. 2.33, 2.34* and *2.35*). Results of these calculations are shown in *Table 2.14*. Since the identic values of IEC, calculated from the ^1H and ^{19}F NMR spectra, are obtained, both of them are noted in one column in the table as IEC_{NMR}.

Block-copolymers ***b*-I3-0.9** and ***b*-I5-0.9** give the biggest difference between the theoretical and experimental (from NMR spectra) values of IEC, as compared to the ***sb*-I3-0.9** or random ionomers. It seems like during the ionomer synthesis some part of the ionic segments (oligomer of the monomer **3** or **4** with DFB) does not participate in coupling with a hydrophobic block and is washed out from the material by acidic water.

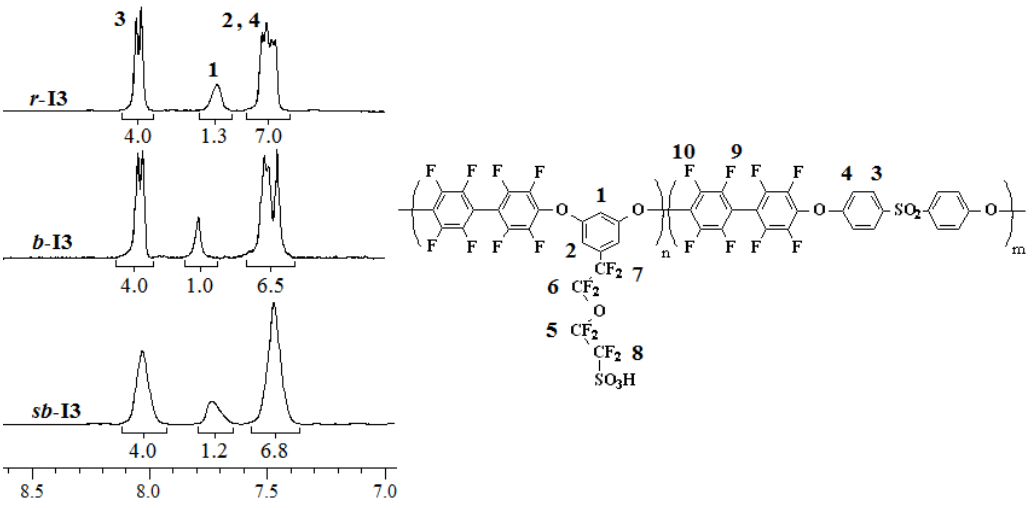

(a)

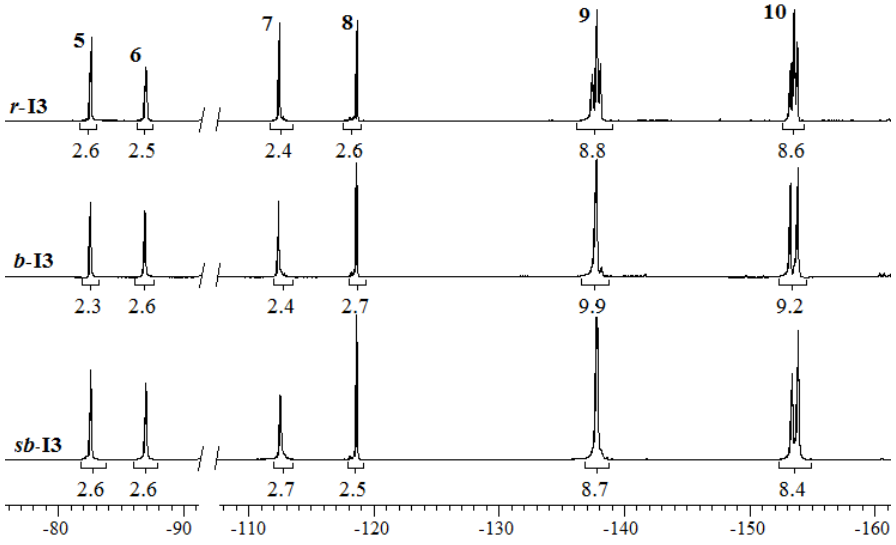

(b)

Figure 2.33. ^{1}H (a) and ^{19}F (b) NMR spectra of the random and block-copolymers series **I3**, IEC 0.9 meq/g

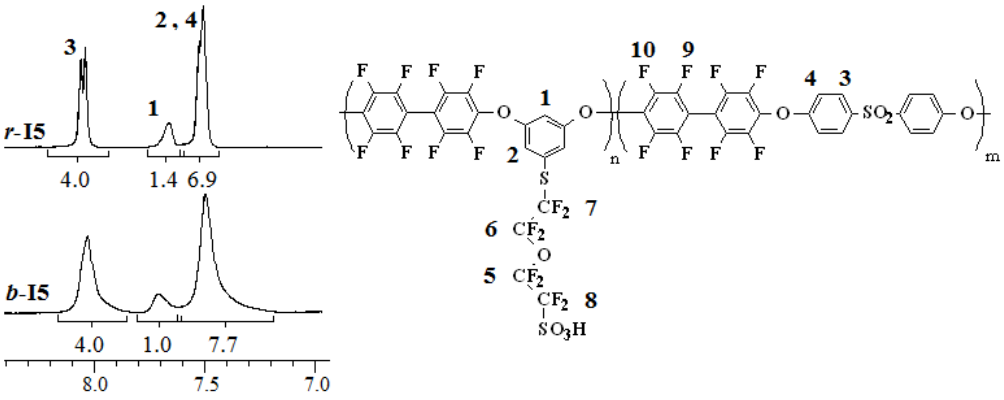

(a)

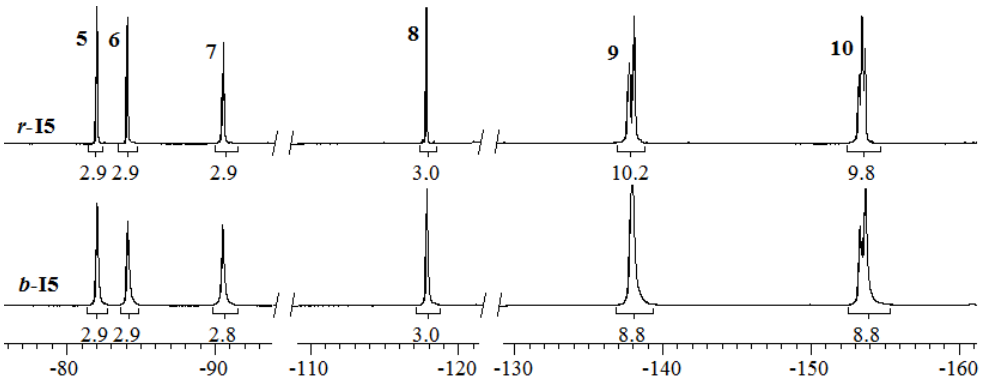

(b)

Figure 2.34. ^{1}H (a) and ^{19}F (b) NMR spectra of the random and block-copolymers series **I5**

Figure 2.35. ^{1}H (a) and ^{19}F (b) NMR spectra of the copolymer ***r*-I3-1.1**

Referring to the ^{19}F NMR spectrum of the ionomers series **I3** (of IEC 0.9 meq/g) (*Fig. 2.33 (b)*), difference in coupling is observed for the peaks # 9 and 10 between the random and block-copolymers. The same behavior is registered for the polymers series **I5** (*Fig. 2.33 (b)*). The zoomed images on the characteristic peaks # 9 and 10 are shown in *Fig. 2.35*.

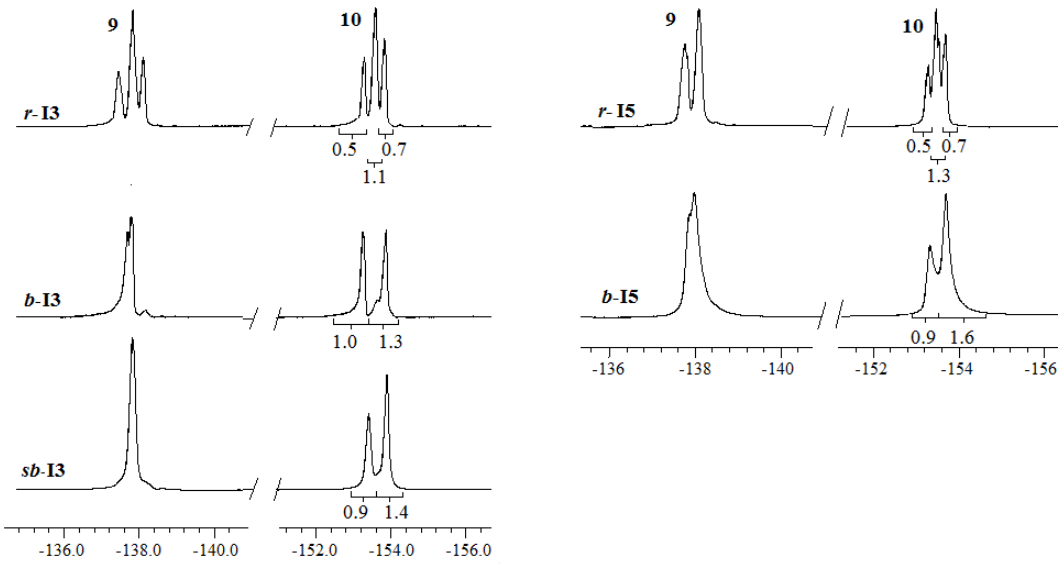

(a) (b)

Figure 2.35. Enlarged scale image of peaks # 9 and 10 of the ionomers series **I3** (a) and **I5** (b) of IEC 0.9 meq/g

Analyzing *Fig. 2.35 (a)*, a peak # 10 corresponds to the Fluorines of the DFB, adjacent to the ether bridges. For ***r*-I3** it appears as a triplet, since three possible connections of DFB in a polymer chain exist: i) to the monomer **3** from both sides, ii) to the monomer HS from both sides, iii) to the monomer **3** from one side and to the monomer HS from another side. For the

block-copolymers ***b*-I3** or ***sb*-I3** the peak # 10 appears as a doublet, since only two connections of DFB in a polymer chain are possible: i) to the monomer **3** from both sides (case of the hydrophilic block), ii) to the monomer HS from both sides (case of the hydrophobic block). For this reason the middle signal of the triplet of the random copolymer **I3** corresponds to atoms of DFB, which is bound to two different monomers from two sides. Moreover, statistically this signal must be the most intensive in the triplet, what is observed here.

In order to refer the other two peaks of the triplet # 10 of the random copolymer **I3**, two strategies are employed:

1) The studied peak is compared to chemical shift of the peak # 10 of the ionomer **I2-1.4** (see *Fig. 2.26 (b)*). In this polymer DFB is connected exclusively to the monomer **3**, therefore its peak # 10 at −153.9 ppm corresponds to Fluorines, being adjacent the ether-bridge with ionic monomer **3**. In the triplet # 10 of ***r*-I3** this is the most right signal that has the same chemical shift.

2) Since ***b*-I3** has discrepancies between theoretical and experimental IEC (deduced from the discussion on ^{1}H NMR), ^{19}F NMR spectrum of ***sb*-I3** is considered further for comparison. Integration of both peaks of its doublet # 10 corresponds to ratio 0.9 / 1.4. Taking to account ratio of the introduced HS and **3** as 1.0 / 1.3 (from *Table 2.14*), a more deshielded signal of the doublet # 10 (−153.5 ppm) corresponds then to Fluorines of DFB being connected to HS, thus situating in the hydrophobic block. The signal at −154.0 ppm is related to the Fluorines of DFB attached to the **3** in the hydrophilic block.

By both strategies the same attribution of peaks of the triplet # 10 of the random copolymer **I3** is evoked. In addition, the same strategies are applied for analysis of the peak # 10 from the ^{19}F NMR spectra of ***r*-I5** (*Fig. 2.35 (b)*). Again a more deshielded peak corresponds to Fluorines of DFB between two HS (integration value 0.5), and a more shielded one is for Fluorines of DFB between two monomers **4** (integration 0.7). The middle peak of the triplet is related to atoms of DFB, being connected to HS from one side and to **3** from another side.

A closer look on peaks # 9 (*Fig. 2.35*) evidences difference in their splitting for the random and the block-copolymers as well. However these peaks can not be analyzed in the same way as the peaks # 10, because the correspondent Fluorines are not adjacent to the ether-bridges.

From analysis of the ^{1}H and ^{19}F NMR spectra of the series **I3** and **I5**, we claim that production of block-copolymers by the method of separate block synthesis is more preferential for the current ionomers.

The molecular weights of the synthesized ionomers series PAES are analyzed by SEC-MALLS, results of which are presented in *Table 2.15*. All the materials are characterized by high molecular weights. The block-copolymers contain very long chains that result in partial dissolution of the material in DMF (+ $NaNO_3$) as a solvent for SEC-MALLS technique. This provoked blocking of the pre-filter of the measuring column and inaccurate determination of the sample concentration. As a result, the plots of molecule size exclusion do not show Gaussian curves.

Table 2.15. Properties of the ionomers series **I3** and **I5**: molecular weights, measured by size exclusion chromatography coupled with light scattering; IECs and densities

Ionomer	**Mn, $\cdot 10^3$, g/mol**	**Mw, $\cdot 10^3$, g/mol**	**Mw/Mn**	**IEC (theor.), meq/g**	**Density, g/cm^3**	**IEC$_V$, meq/cm^3**
r-I3-0.9	117.5 ± 28.0	263.4 ± 29.8	2.2 ± 0.6	0.9	1.7	1.6
b-I3-0.9	76.8 ± 3.5	1650 ± 377.9	21.5 ± 5.0			
r-I3-1.1	90.6 ± 5.6	512.2 ± 7.4	5.7 ± 0.4	1.1	1.7	1.9
b-I3-1.1	1818.0 ± 53.0	6175.0 ± 340.2	3.4 ± 0.2			
r-I5-0.9	135 ± 3.6	655.9 ± 17.7	4.9 ± 0.2	0.9	1.7	1.5
b-I5-0.9	89.2 ± 2.1	1209 ± 188.6	13.6 ± 2.1			

Membrane elaboration

Based on the results, observed from the series PAEs (*paragraph 2.2.2.1*), all the membranes series PAESs are produced by the *method B*. To remind, the method applies annealing of dry membranes at 150 °C overnight (at least) as an additional step to the common procedure.

Random materials are easily solubilized and cast into membranes. The solutions of block-copolymers (***b*-I3** and ***b*-I5**), however, appear as highly viscous gel-like, when concentration of the polymer in DMAc comprises 10 % (w/v). They are then solubilized until 5 %-solution and filtered under pressure over a 0.45 μm filter. Then the polymer solutions are cast in Petri dishes and the solvent evaporation procedure is applied, as it was described earlier for the series PAEs.

The membranes in their Li^+- and K^+-forms are then acidified with 1 M solution of HCl, changing the protonating medium twice. Then the samples are washed until neutral pH of water and dried at 50 °C during 48 h.

Verification of IEC by titration in organic solvent is performed. All the samples series **I3** and **I5** show values identical to theoretical values of IEC. Such results again confirm that membrane elaboration procedure is well adapted. On the contrary to IEC measurement by NMR (*Table 2.14*), ***b*-I3** and ***b*-I5** did not show lower IEC, than the theoretically programmed. However, one must take to account that the method of titration is less accurate than that of NMR analysis.

2.2.3. Synthesis of ionomers by copolymerization of two ionic monomers

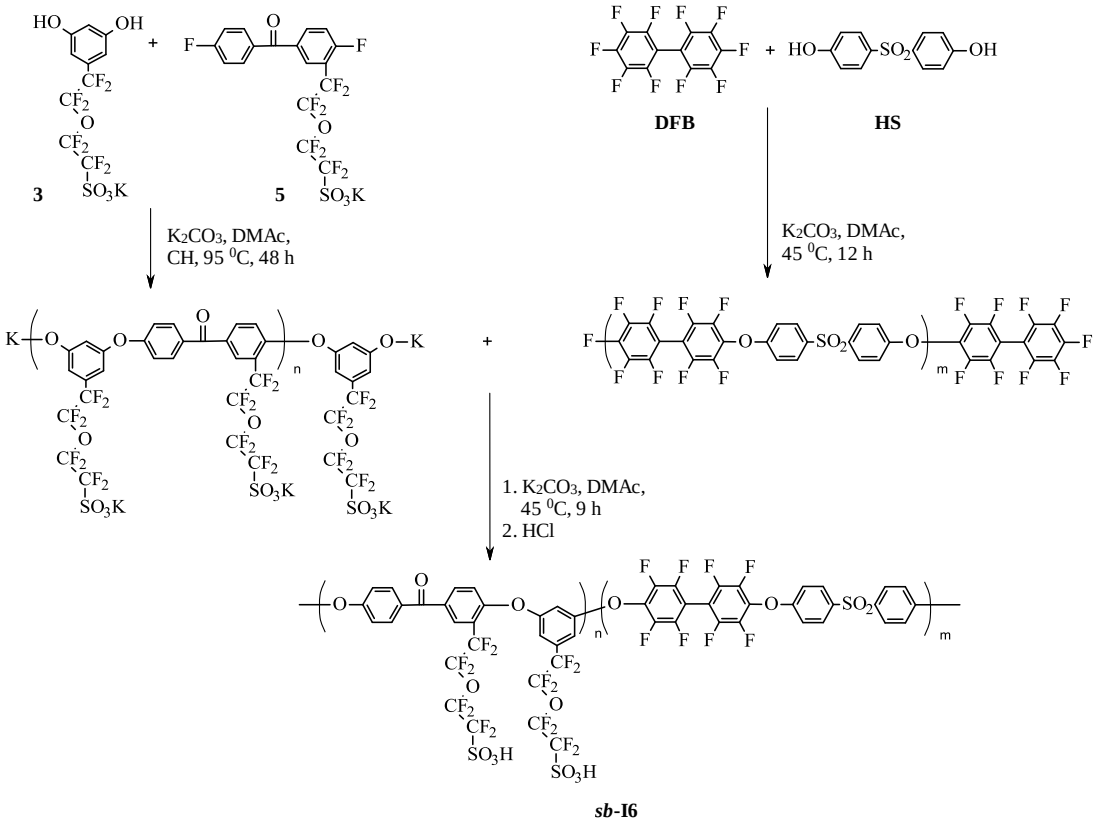

Figure 2.36. Synthesis of a block-copolymer ***sb*-I6-1.4**

Fig. 2.36 presents a new and unique strategy of a block-copolymer synthesis by producing a hydrophilic block from condensation of two ionic monomers, bearing PFSA lateral chains. Prior to description of the overall synthesis of this block-copolymer (***sb*-I6**) a new ionic monomer **5** must be introduced. It is produced in terms of the NMHT project by a collaborative group IMP at UMR CNRS 5223.

Production of ***sb*-I6** proceeds through the syntheses of separate blocks (hydrophilic and hydrophobic) and their further condensation. Fluorine-terminating hydrophobic block of MW 10.0 kDa is previewed. Its synthesis, precipitation and overall treatment are described in *annex 10*, and are identical to those for the hydrophobic block of the material ***sb*-I3**.

Since a hydrophilic block, constituting of the ionic monomers **3** and **5**, is highly functionalized, its precipitation in acidic water will never be successful. For this reason the control of formation of the hydrophilic block is monitorized by ^{19}F NMR. Initially it is programmed to produce an OH-terminated hydrophilic block with the legth of the polyaromatic backbone as 5.0 kDa (*Fig. 2.37*). However, the molecular weight of the hydrophilic block with two PFSA lateral groups per unit is 16.8 kDa. After that Carother's equation (6) is applied to calculate ratio between the monomers, which must be introduced for formation of the hydrophilic block.

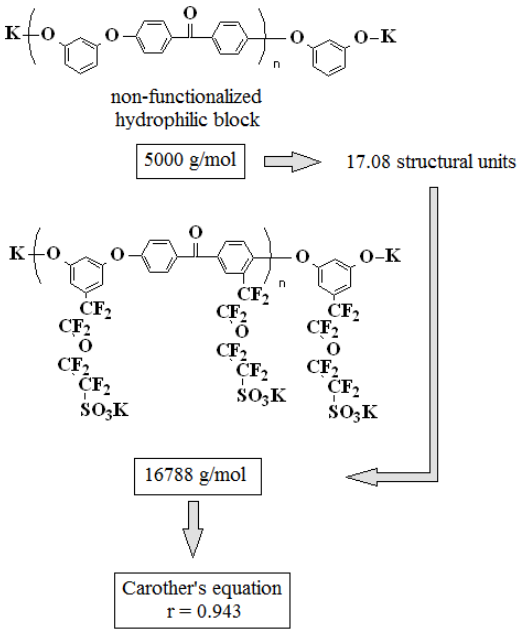

Figure 2.37. Scheme for calculation of the MW of the hydrophilic block in ***sb*-I6-1.4**

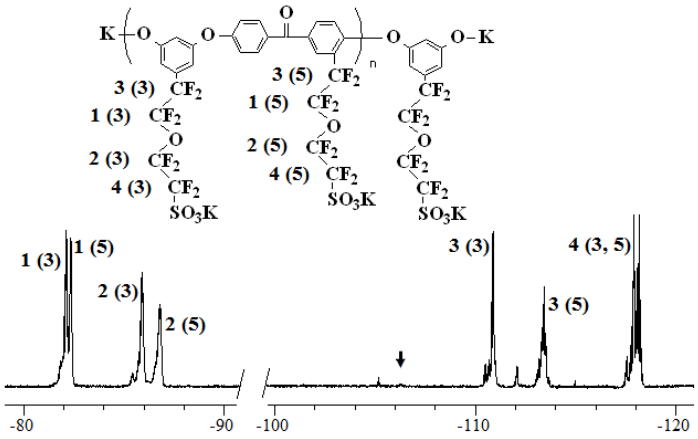

Figure 2.38. ^{19}F NMR spectrum of the hydrophilic block of the block-copolymer ***sb*-I6-1.4**, synthesized by condensation of the monomers **3** and **5**. A black arrow shows condensable Fluorines of the monomer **5**

Fig. 2.38 illustrates ^{19}F NMR spectrum of the hydrophilic block in reaction mixture. The monomer **3** is programmed to be taken in excess, thus the hydrophilic block must not have fluorines at the end of the chain. Hence, disappearance of a peak of condensable fluorines of the monomer **5** (chemical shift at −106.2 ppm, shown with a black arrow in *Fig. 2.38*) proves the hydrophilic oligomer formation. Splitting of peaks at ^{19}F NMR spectrum is related to different location of the PFSA side chain on the main chain: either in *ortho*-position to the ether-bridge (in moiety of the monomer **5**), or in *meta*-position to the ether-bond (in the monomer **3**).

When the reaction between **3** and **5** is complete, a ready dry hydrophobic block is solubilized in DMAc and added to the reaction mixture. Due to DFB, situating at the ends of the hydrophobic block, the condensation of the blocks happens at 45 °C. The reaction is stopped when the reaction solution becomes viscous enough to resume formation of a high molecular weight polymer.

After precipitation of the polymeric solution in acidic water it is additionally washed with ethanol several times. The polymer is characterized by ^{1}H and ^{19}F NMR, shown in *Fig. 2.39*.

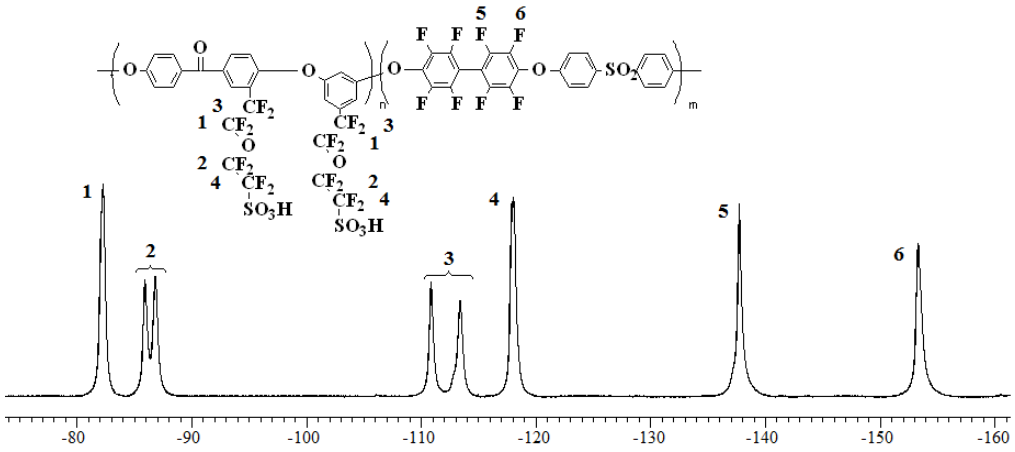

Figure 2.39. ^{1}H and ^{19}F NMR spectrum of the block-copolymer ***sb*-I6-1.4**

Theoretical IEC of the synthesized block-copolymer ***sb*-I6** is 1.4 meq/g. Its molecular weights comprise: $117.5 \cdot 10^3$ g/mol for number average MW and $498.0 \cdot 10^3$ g/mol for weight average MW, thus PDI results in 4.2.

Another type of condensation of ionic monomers was previewed – between the monomers **2** and **3**. Previously it was already described the difficulties in eliminating the second fluorine of the monomer **2**, which is situated in *meta*-position to the PFSA group and to the first substituted phenate. High temperatures are required that result in material degradation or formation of cyclic oligomers. To avoid all these inconveniences it was decided to synthesize

a three-mer of the monomer sequence **2-3-2** (*Fig. 2.40*). In such case only one fluorine of the monomer **2** must be substituted, which happens at lower temperature. Further on this three-mer is subjected to polymerization with BP to produce a hydrophilic oligomer.

The reaction between two equivalents of **2** and one equivalent of **3** was supposed to proceed at medium temperatures (90-100 °C), but it is not until 160 °C, when the substitution starts to proceed. ^{19}F NMR analysis at a *Fig. 2. 41* shows that at such harsh conditions formation of the secondary product is provoked, which is marked with a blue arrow at chemical shift −124.0 ppm. It is presumed that a secondary product comes from degradation of the PFSA group. Moreover, when the reaction is assumed to finish (the complete displacement of the condensable Fluorines), ratio between the two Fluorines at the ends of the three-mer and the fluorines in the PFSA side chains is not correct. Therefore, reaction between ionic monomers **2** and **3** is not possible.

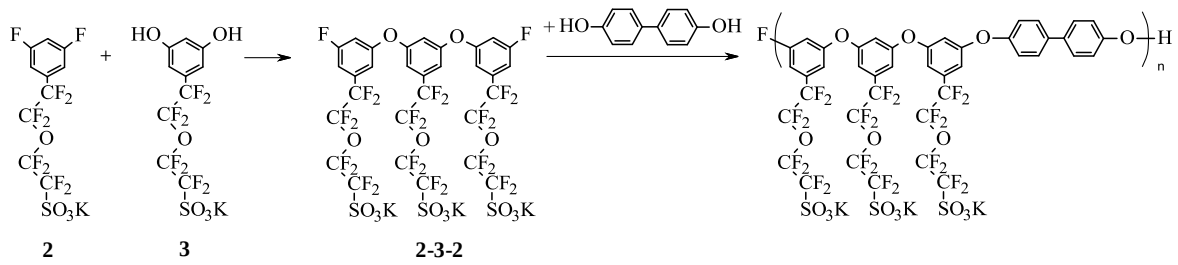

Figure 2.40. Combination of the monomers **2** and **3** in a three-mer and subsequent condensation with BP

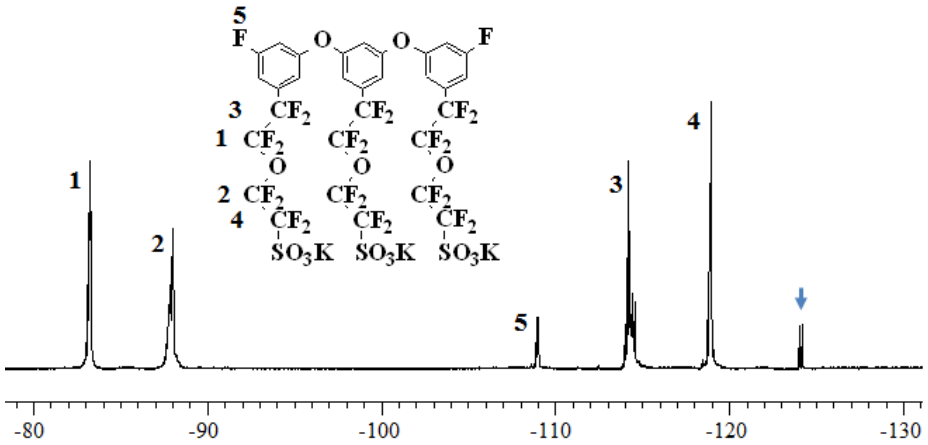

Figure 2.41. ^{19}F NMR spectrum of the specie **2-3-2**. A blue arrow points on a secondary product, which is referred to degradation of the PFSA

Theoretically, the monomer **4** is more reactive than **3**, but it is assumed that its activity is not enough to decrease the temperature of nucleophilic substitution with **2** to less than 100 °C. However, its condensation with the monomer **5** is presumed to be effective.

Based on the information, presented in the current chapter, it may be concluded:

i) Three ionic monomers and six series of ionic polymers thereafter are successfully synthesized.
ii) The optimal protocols of synthesis and treatment are established to result in products of the highest yield and purity.
iii) The most appropriate strategy of membrane production out of the synthesized polymers is proposed.
iv) The theoreally programmed IEC of each ionomer is verified; the density, thus volumic IEC, are determined.

Each series of polymers, presented in the current chapter, might be enlarged when varying IEC. For random copolymers it is performed by introducing higher amounts of non-ionic monomer with the same terminating groups as the ionic one. For block-copolymers it is possible by changing the ratio between lengths of blocks. Additionally, the block-copolymers may have be studied of the same IEC, the same ratio between the block lengths, but different lengths of blocks themselves.

Chapter 3. Characterization of ionomers

This chapter is focused on characterization of the ionomers series **I1** – **I6** in their form of membranes. For better comparison of properties, the pairs of polymers are presented in the following sequence:

i) random poly(arylene ether)s series **I2** and **I4**, synthesized from the ionic dihydroxylated monomers **3** and **4**;

ii) random and block poly(arylene ether sulfone)s series **I3** and **I5**, synthesized from the ionic dihydroxylated monomers **3** and **4**;

iii) random poly(arylene ether sulfone)s series **I1** and **I3**, synthesized from the ionic difluorinated and dihydroxylated monomers **2** and **3**, respectively.

The last, forth, subchapter presents characteristics of the block-copolymer ***sb*-I6** only, since its structure, containing two ionic PFSA groups in proximity, differs from the other polymers, proposed here.

Each sub-paragraph firstly deals with thermo-mechanical reply of the membranes in their salt and protonated forms in order to obtain the first idea on their bulk morphology. Further detailed description is presented with help of X-ray scattering techniques (except the series **I1**). Consequently, their water uptake and conductivity characteristics are presented and correlated to results on morphology. Lastly, stability of several samples to radical treatment is registered.

3.1. Properties of the (PAE)s series I2 and I4

General structure of the series of random poly(arylene ether)s **I2** and **I4**, synthesized by polycondensation of dihydroxylated ionic monomers **3** and **4**, is reminded in *Fig. 3.1*.

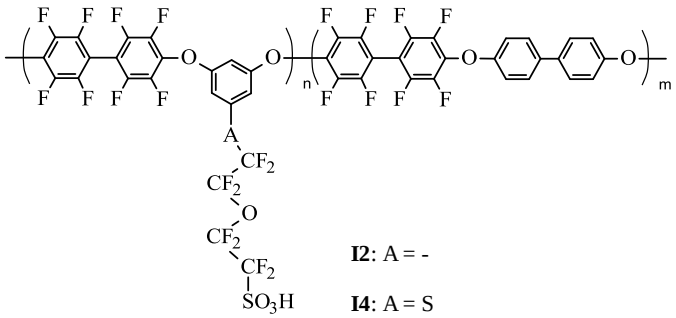

Figure 3.1. General structure of the PAEs **I2** and **I4**

The current paragraph proposes comparison of the main properties of these series. Additional explanation of relation between the method of membrane elaboration and properties of the polymers is reported. First, the materials are characterized in terms of their thermal stability and thermo-mechanical properties; then morphology of the membranes is studied more in detail. Finally, the PAEs are checked for dependence of swelling in water and conductivity in temperature and humidity, and for stability in highly oxidative medium.

3.1.1. Thermal stability

Analysis of the weight loss in temperature indicates material's stability, while heated in its static state. *Fig. 3.2* represents thermogravimetric curves of the relative weight loss in temperature for the membranes series **I2** and **I4**. Solid lines show the behavior of their K^+-neutralized form, dotted lines – of the Li^+-form and dashed ones – of the H^+-form. The colors of the curves are consistent with the IEC values: blue is for the lowest IECs (1.0 – 1.1 meq/g), red is responsible for the ionomers of IEC 1.2 meq/g, and black is for IEC 1.4 meq/g.

Potassium-neutralized forms are the most thermally stable. That comes from the size of a cation: $K^+ > Li^+ > H^+$; bigger the cation is, stronger Coulomb forces retain the highly dissociable PFSA chains. Therefore higher the decomposition temperature is, faster the degradation proceeds. An interesting observation is made for the series **I4** in their K^+-form – the origin of decomposition changes with IEC: lower the latter (higher the concentration of the BP comonomer), lower the degradation temperature is. Since no similar behavior is registered for the series **I2**, it is presumed that the decomposition occurs due to the presence of a sulfanyl spacer in **I4**. Additionally, **I4-1.4**, containing no BP moiety in its structure, shows immediate one-step weight loss. These two factors in combination result that **I4-1.0** and **I4-1.2** have the first degradations at 310 and 330 °C respectively due to the simultaneous presence of the sulfanyl spacer and the BP specie. We are not able to explain such dependence.

Possibly, the similar decomposition dependence on IEC is not observed for Li^+- and H^+-forms, because their degradation starts at temperature lower, than 300 °C. However, degradation region of the curves, corresponding to the protonated **I4** series, seems to be not steep but 'wavy' at 210-220 °C, and the curves of the lithiated **I4** series do not have a visible end of the degradation decline. This behavior may testify the presence of more than one degradation series. In general, degradation of the series **I4** in all their neutralized forms happens at lower temperatures, than that for the series **I2**. For better analysis of thermal resistance of the poly(arylene ether)s, we refer to *Table 3.1*.

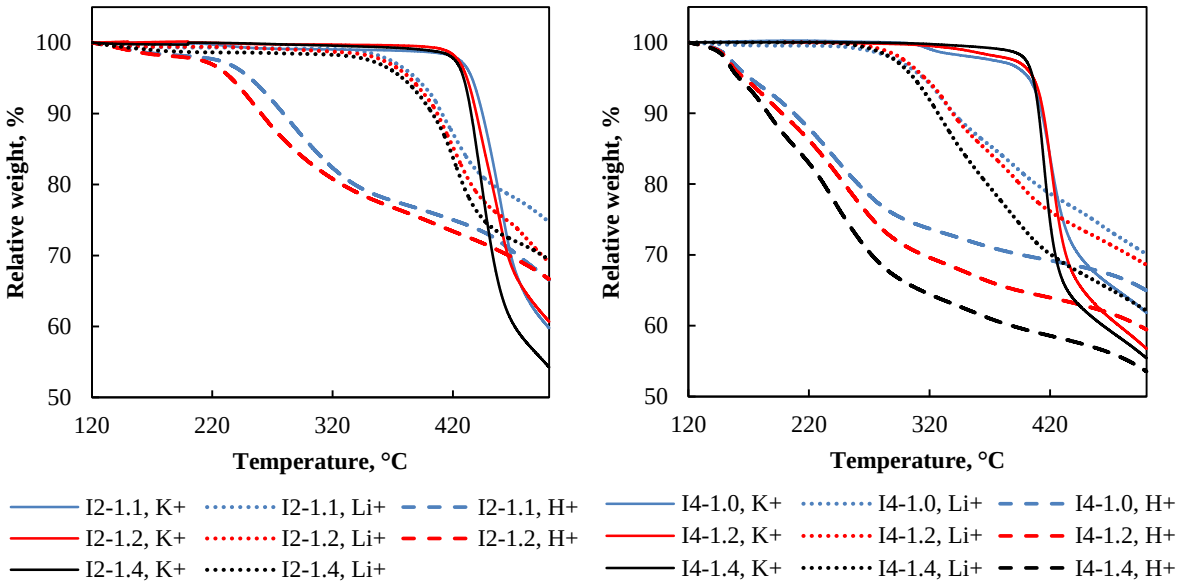

(a) (b)

Figure 3.2. Thermogravimetric curves of the PAEs series: a) **I2** and b) **I4**

Lithiated and protonated ionomers are much more hygroscopic, than potassed. It is important to mention that the sample preparation for the TGA measurement is realized at ambient conditions, and no preheating in the TGA chamber is done before the measurement.

In order to have higher precision in calculations, thermal degradation onset is determined as a point on the initial plateau of a TGA curve in the most proximity to the curve decline. The thermal degradation endset is equally specified at a point nearly after the end of the steepest decline of a curve. With the help of these two points, the value of a polymer loss is estimated and referred to the molecular weight (noted as molecular weight loss or MWL). The latter operation is done with the help of the following equation:

$$MWL = \frac{RWL}{100} \cdot ((MW_{[3(4)-DFB]} \cdot 1) + (MW_{[BP-DFB]} \cdot x)) \qquad (9)$$

where *RWL* is relative weight loss (see *Table 3.1*); $MW_{[3(4)\text{-DFB}]}$ is molecular weight of the ionic structural unit between the monomer **3** or **4** and DFB (which is equal to 700.3 and 732.4 g/mol, respectively); $MW_{[\text{BP-DFB}]}$ is molecular weight of the non-ionic structural unit between BP and DFB (which is equal to 480.3 g/mol); *x* is equivalent of the non-ionic structural unit [BP-DFB], taking the ionic structural unit [**3**(**4**)-DFB] as equivalent 1.

Additionally, molecular weights of the pendent chains are given in the last column in *Table 3.1* to compare them to values of MWL.

Table 3.1. Analysis of polymer thermal degradation for the series **I2** and **I4**

M^+-form	**Ionomer**	**Thermal degradation onset, T_d, °C**	**Thermal degradation endset, °C**	**Relative weight loss, %**	**Molecular weight loss, g/mol**	**Molecular weight of X-PFSA-M^+side chain *, g/mol**
K^+-form	I2-1.1	400	470	30.5	300.9	332.0
	I2-1.2			31.9	278.0	
	I2-1.4			39.4	290.9	
	I4-1.0	310	450	31.5	327.0	367.3
	I4-1.2	330		35.6	310.2	
	I4-1.4	390		38.1	293.5	
Li^+-form	I2-1.1	350	440	17.4	166.0	303.0
	I2-1.2			20.3	170.4	
	I2-1.4			22.6	159.6	
	I4-1.0	250	430	22.0	221.3	335.1
	I4-1.2			25.0	209.8	
	I4-1.4			31.0	237.6	
H^+-form	I2-1.1	215	335	18.1	171.7	297.1
	I2-1.2			17.9	149.2	
	I2-1.4			–	–	
	I4-1.0	130	300	25.0	250.0	329.2
	I4-1.2			28.8	240.0	
	I4-1.4			33.9	248.2	

* X is S in case of the ionomers series **I4** and X is nothing in case of the ionomers series **I2**

The **I4** ionomers are characterized by higher losses, than the correspondent in IEC and counter-ion samples of **I2** series. For all the ionomers clear dependence of the weight loss on IEC is observed: higher the IEC, bigger the weight loss. Undoubtedly, the decomposition happens at the lateral chains of the polymers. The K^+-neutralized materials lose almost the totality of their PFSA side chains with the non-degradable residue of 30-70 g/mol. The **I4** in their protonated form are characterized by similar non-degradable specie of 80-90 g/mol. Meanwhile, the lithiated polymers of both series and the protonated **I2** stay with approximately 110-140 g/mol of the non-degradable residue. Unfortunately, an in-lab device for thermal degradation measurement is not connected to the mass spectrum to detect precisely the chemical composition of the residue of the lateral chain for each sample. From results of the group of Miyatake [126, 127], who used the same type of the PFSA chain, we may presume that the protonated ionomers degrade with elimination of the same species SO, SO_2, CFO, CF_2.

3.1.2. Calorimetric analysis

The differential scanning calorimetry (DSC) is conducted by two to three times cycling in a crucible with a pierced cap in order to evaporate residual water during the first heating semi-cycles. For this reason they are never shown at the thermograms below. The maximal heating temperature in DSC measurements corresponds to (T_d-10) °C, where T_d is determined from the TGA analysis and is noted in *Table 3.1*.

Firstly, the study on membrane production technique is done by the DSC analysis on the series **I2**. *Fig. 3.3* presents thermograms of the membranes, produced by the *method A*, when evaporation of the DMAc is conducted at 60 °C during 2 days with no subsequent annealing. The first heating-cooling cycle is performed in the temperature range RT – 120 °C. All the ionomers in their both K^+- and Li^+-forms, except **I2-1.4-K$^+$**, show two distinct transition temperatures: a low-temperature transition at 120-150 °C (highlighted as light-red area) and a high-temperature one at 200-220 °C (light-blue area).

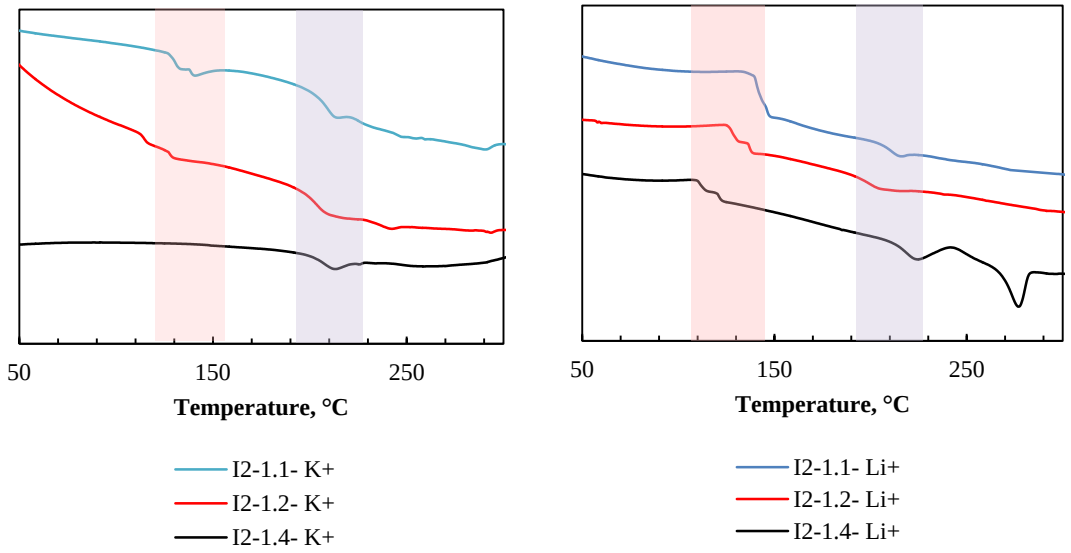

Figure 3.3. A second heating-cooling cycle of DSC curves for the membranes series **I2** in their: a) K^+-form, b) Li^+-form. The samples are produced by evaporation of the solvent at 60 °C during 2 days

With a closer look at the low-temperature reply (light-red area), one may refer the signals to the evaporation of residual water. Yet the ionomer **I2-1.4**, which contains the most of ionic functions (the highest IEC), in its K^+-form gives no change in enthalpy in this temperature range, though it reappears for its lithiated sample. To understand the nature of the low-temperature transition, two additional analyses are conducted: i) two types of polymer backbones, **PB2/4-1.4** and **PB2/4-1.0** (*Fig. 3.4*), containing no ionic functions, are

synthesized and investigated by DSC, and ii) membranes, in particular **I2-1.1-Li**$^{+}$, are subjected to annealing at different temperature and further measured for the calorimetric reply.

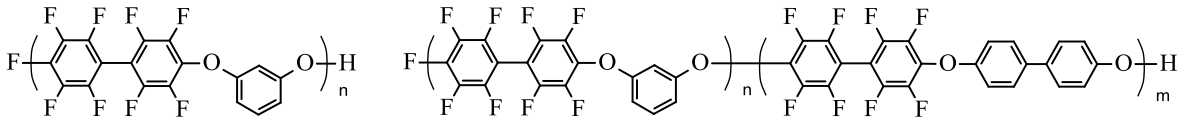

(a) (b)

Figure 3.4. Polymer backbones, containing no ionic lateral chains, of the ionomers: a) **I2-1.4** or **I4-1.4**, named **PB2/4-1.4**, and b) **I2-1.0** or **I4-1.0**, named **PB2/4-1.0**

In the first study, the chemical structure of **PB2/4-1.4** is identic to the main chain of the **I2-1.4** and **I4-1.4**, the polymer is prepared by polycondensation of equimolar amounts of 1,3-resorcinol and DFB. The random **PB2/4-1.0** is prepared by polycondensation of three monomers, 1,3-resorcinol, DFB and BP, having the proportion between monomers, approximate to the one, used for synthesis of the ionomers **I2-1.1** and **I4-1.0** (quantity of 1,3-resorcinol corresponds to the introduced amount of the monomers **3** or **4**). It must be noted that DSC is conducted on **PB2/4-1.4** in its membrane form, while on **PB2/4-1.0** as powder (filaments).

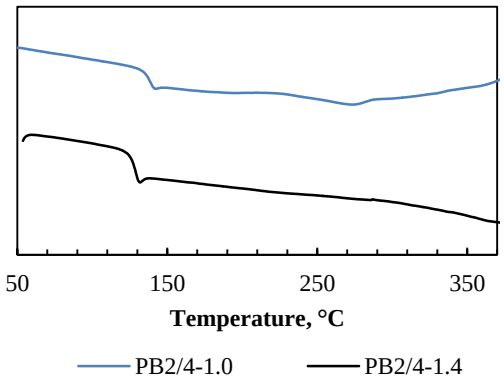

Figure 3.5. DSC thermograms of the non-ionic polymers **PB2/4-1.0** and **PB2/4-1.4**

The both non-ionic structures are fully amorphous materials, which thermograms are presented *Fig. 3.5*. **PB2/4-1.4** is characterized by one glass transition temperature at 129 °C. However, when BP is added to the chemical structure, an additional thermal reply appears at approximately 250 °C. At the same time the lower-temperature transition increases slightly in temperature, adjusting 137 °C. Consequently, the both transitions characterize movements of an aromatic backbone, but the one of lower temperature is, most probably, related to the impact of resorcinol part, which is a more mobile specie due to its *meta*-ether bridges, and the

other transition of higher temperature corresponds to the movements of *para*-connected moieties (DFB-BP).

Based on these results and returning back to interpretation of the thermograms in *Fig. 3.3*, it may be concluded that transitions, happenning in red-highlighted area, characterize local movements of the polymer and are provoked by the *meta*-ether bridges of the polymer main chain, and those in blue-highlighted area, are related to a long range polymer movements. Transitions that correspond to the movements of sulfonic acid groups are then not distinguished at the DSC curves. Undoubtedly, the low-temeprature transition is dependent on a PFSA lateral chain, since it is directly attached to the resorcinol-moiety. For this reason: i) ionomers, neutralized with bigger cations (e.g. $K^+ > Li^+$) show less intensive transition due to stronger interactions between the ionic heads, which impede the ether-bridges to move easily, and ii) intensity of the low-temperature thermal event decreases much with higher concentration of PFSA groups, which we refer to formation of the most energetically convenient conformation of the polymer. The latter idea was previously proposed in the *paragraph 2.2.2.1*, when acidification of the membranes was investigated. There, limited accessibility of the ionic clusters was presumed in order to explain the incapability of the total salt-to-proton exchange of the membranes. If this assumption is true, then DSC curves are a good confirmation: the ionomers of the lowest IEC have the most linear structure, since the distance between the angled *meta*-ether bridges is the longest. Thus applying heat (up to 150 °C) to these systems results in changing the conformation of the aromatic ring with PFSA chains, to a more energetically favorable state, probably, to orientation of ionic groups closer to each other. Increasing IEC to the maximal value, when only one monomer moiety (of DFB) creates linear connections between the angled *meta*-ether bridges, presumes a membrane to already achieve its preferrable conformation (close arrangement of ionic groups) to some extent. For this reason, when heat is applied, little transformation must be additionally done by polymer to complete its conformation change. To confirm or reject these assumptions, analyses of the following paragraphs on membrane morphology will give the answer.

Meanwhile, the complementary study with the help of DSC is provided. Membrane annealing was proposed as a better method (*method B*) for polymer to adjust its stable orientation (*paragraph 2.2.2.1*). Overpassing the high-temperature transition (light-blue area in *Fig. 3.3*) additionally assures the total dryness of the ionic functions. The sample **I2-1.1-Li$^+$** is investigated, when: i) a membrane undergoes three heating cycles of up till 210, 300 and 340 °C with the heating rate of 20 °C/min and isotherms of 2 min at the highest heating points directly in the DSC device; ii) a membrane is annealed at 200 °C under vaccum overnight and

the same three thermal cycles are conducted; iii) a membrane is annealed at 250 °C for 2 h at ambient atmosphere and the same DSC program is used. The difference between the first and the two last methods of membrane preparation is that in the former case a membrane is not subjected to high temperature for long time.

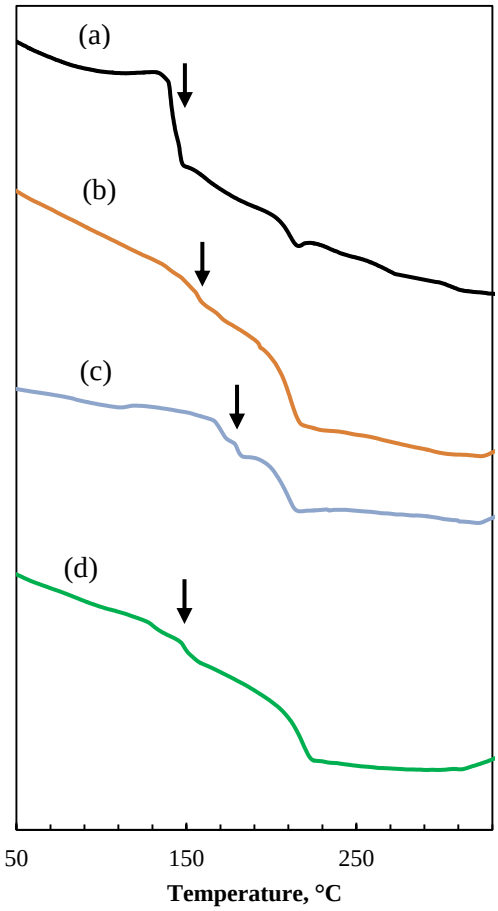

Figure 3.6. The DSC profile of the **I2-1.1** membranes in Li^+-form: (a) a membrane, produced by the *method A*, not having been subjected to any high-temperature treatment, except fast heating till 120 °C with the isotherm of 2 min in the DSC chamber, (b) a membrane, produced by the *method A*, and heated till 250 and 300 °C with the isotherms of 2 min in the DSC chamber, (c) an annealed sample at 200 °C under vacuum overnight with the same two thermal cycles as (b), (d) an annealed sample at 250 °C during 2 h at ambient conditions and the same two thermal cycles as (b) and (c)

Thermograms for these three samples are presented in *Fig. 3.6* as samples (b), (c) and (d). Aditionally, a membrane, produced by the *method A* without any high-temperature post-treatment, is shown as a sample (a) at the same figure for comparison. The low-temperature transitions are pointed with arrows; they happen at higher temperature (up till 180 °C) with increasing the time and temperature of the membrane exposure. But for the ionomer, annealed at 250 °C for 2 h thermal reply occurs again at barely the same temperature as for the non-

treated membrane. Meanwhile, the high-temperature transition is not dependent on the membrane treatment, and it always occurs at 210 °C.

The obtained results confirm the reorientation of the polymer backbone, supposedly at the *meta*-ether sites, while heated up till 200 °C. It must be always kept in mind that re-structuring of the polymer chains happens in a rigid frame of ionically interconnected sulfonic groups, which was previously reported by Moore *et al.* [164]. The observed weakening of forces in the hydrophobic matrix, when annealed at 250 °C, is a straightforward indication for the loss in mechanical properties. Indeed the sample becomes brittle. Such a result testifies, most probably, degradation of the material. It happens without elimination of gazeous products of degradation, since the results of thermogravimetric analysis (*paragraph 3.2.1*) showed the resistance of these samples up till 350 °C. In any case, losening of mechanical properties is not a good indication for the membrane, therefore annealing of the current samples at temperature higher, than 200 °C must be avoided.

Another way to understand the best temperature conditions of a membranes' preparation, is by comparing the second and the third heating cycles in DSC. If the transitions from both heatings coincide, then the membrane acquired its stable confirmation; when hysteresis is observed, the polymer chains keep reorienting to the conformation of the lowest energy.

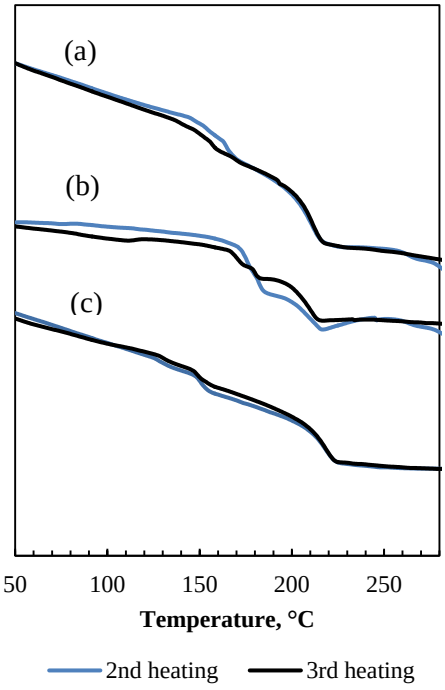

Figure 3.7. Second and third DSC heating semi-cycles of the membranes **I2-1.1-Li$^+$**: (a) received by the *method A*, (b) received by the *method A*, but additionally annealed at 200 °C overnight under vacuum, (c) received by the *method A*, but additionally annealed at 250 °C during 2 h

For the current investigation again the membranes **I2-1.1-Li**$^+$ are presented in *Fig. 3.7*. A membrane, which is not subjected to any long-term annealing (sample (a)), shows hysteresis in transition values at 150 °C. It means that the polymer structure continues reorganizing at repeated heatings. On the contrary, for the sample (b), being annealed overnight at 200 °C, the low-temperature relaxation appears at the same range at around 180 °C at both heatings. Interestingly, at the third cycle the transition signal separates to two thermal events – that is phenomenon we are not able to explain for the moment. Equally to the (b)-sample, the membrane, annealed at 250 °C, shows identic behavior of the two heating semi-cycles; however, as it was discussed earlier, the membrane becomes brittle, therefore not usable.

Hence, annealing time is important for the organization of the polymer chains. The sample, heated at 200 °C overnight, seems to have the most appropriate behaviour and shows the true value of the low-temperature transition. Nevertheless, when the membranes, annealed at 140-150 °C overnight, are measured at DSC, no hystereses between heating semi-cycles are observed either. Based on all these studies, the *method B* is established as the most appropriate for a membrane elaboration. It was described in the *paragraph 2.2.2.1* and reminded in *annex 11*, which we refer the reader to.

All the thermograms, presented above, cover the temperature region up till 300 °C. In *Fig. 3.8* two salt-forms of the ionomer **I2-1.4** are presented with the temperature axis till 380 °C. Clear endothermic signals on heating and exothermic peaks on cooling evidence the presence of the crystalline structure; summarized data on melting and recrystallization events are given in *Table 3.2*.

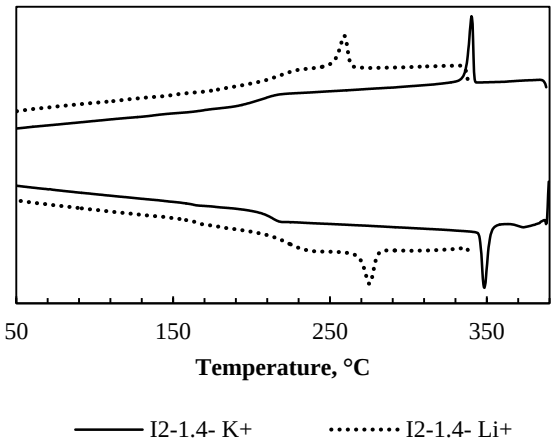

Figure 3.8. DSC curves on heating and cooling for the polymers **I2-1.4** in their K^+ and Li^+ forms

Table 3.2. Analysis of melting and recrystallization events for the ionomers **I2-1.4** in K^+ and Li^+ forms

Ionomer	**$T_{melt.}$, °C**	**$\Delta H_{melt.}$, J/g**	**$T_{recr.}$, °C**	**$\Delta H_{recr.}$, J/g**
I2-1.4-K^+	348	3.4	340	3.3
I2-1.4-Li^+	275	2.6	258	2.3

The sharper appearance of the melting peak for the K^+-neutralized polymer evidences the presence of crystals of more uniform size distribution. Higher enthalpies of melting and recrystallization for the potassed sample (see *Table 3.2*) also prove the higher amount of crystallites in the polymer. Additionally, melting of the potassed ionomer happens at 70 °C higher, than that of the lithiated one. Thus, bigger the counter-ion is, more organized and more homogeneous in size the crystalline structure becomes.

Unlike the Nafion membrane, crystallinity in **I2-1.4** ionomers is not a property acquired due to the fluorinated backbone, since the **PB2/4-1.4** non-ionic polymer is a fully amorphous material (as it was proved above). Therefore, we assume that lateral ionic groups provoke formation of crystallites. Such statement is firstly proposed by our group and it supports the obtained data from DSC analysis.

In order to approve this supposition, a closer look at thermograms of another series of PAEs – **I4** – is done. *Fig. 3.9* presents K^+-neutralized samples only, since the lithiated ionomers start to degrade at 250 °C, thus it is difficult to observe energy transitions of the polymers in the temperature range close to the degradation origin. All the membranes series **I4** are produced by the *method B*.

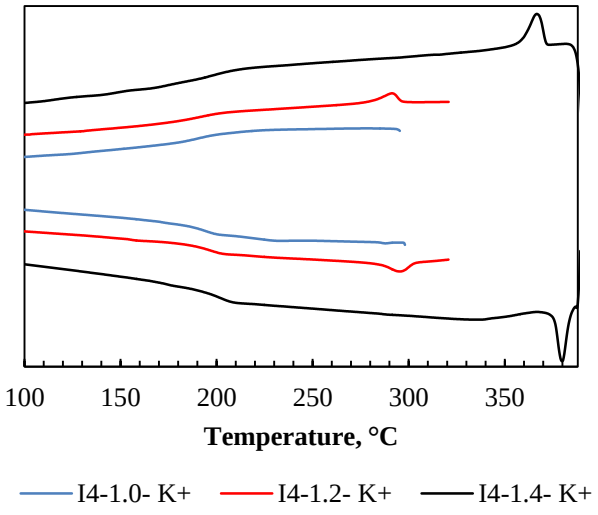

Figure 3.9. DSC curves on heating and cooling for the polymers **I4** in their K^+ form

Table 3.3. Analysis of melting and recrystallization events for the ionomers **I4-1.2** and **I4-1.4** in their K^+-form

Ionomer	**$T_{melt.}$, °C**	**$\Delta H_{melt.}$, J/g**	**$T_{recr.}$, °C**	**$\Delta H_{recr.}$, J/g**
I4-1.2-K^+	295	1.1	290	0.8
I4-1.4-K^+	379	2.8	367	2.4

Similarly to the series **I2**, semi-crystalline nature of the ionomers **I4-1.4** is observed, but their enthalpy of melting / recrystallization is slightly lower, than that of the **I2-1.4-K^+**. However it is important to admit that intensity of the melting endotherm of **I4-1.4-K^+** is higher and the width of the peak is narrower that those of **I2-1.4-K^+**. This observation points that the crystallites of **I4-1.4-K^+** are more homogeneous in size.

The ionomers of lower IEC, surprisingly, evidence the melting phenomenon as well: the broad endotherm at 295 °C for the **I4-1.2** and a slight energy change at 286 °C for the **I4-1.0** (which is seen at high magnification and not registered in *Table 3.3*). Obviously, the crystallinity of the **I4** ionomers increases with higher IEC values, thus higher amount of PFSA side chains in the structure. The difference in melting temperatures for the **I4-1.2** and **I4-1.4** comprises 84 °C, which might point on a structure with more homogeneous and bigger in size crystallites in the latter polymer. Additionally, the symmetric structure of the **I4-1.4** may help in the polymer organization.

From the thermal reply of both PAEs series of the **I2** and **I4**, it is certainly concluded that ionic chains guide the crystallization of the polymer. Such conclusion is surprising, because PFSA lateral groups are long and mobile, therefore they are believed to prompt the dezorganization of the polymer matrix.

With a closer look on the DSC profile of the polymers **I4** (*Fig. 3.9*) at temperature region 150-200 °C, several thermal events may be vaguely distinguished. The one, which has higher enthalpy contrast, is a high-temperature transition, and that, which is hardly observed, happens at slightly lower temperature. These two transitions are in analogy to the transitions of the **I2** series, but their enthalpy change is much lower, than for the **I2** membranes.

Thermograms of the protonated forms of ionomers **I2** and **I4** are shown in *Fig. 3.10*. The only transition, happening at 96-129 °C is related to movements of the whole polymer: PFSA chains feel no more strong ionic interactions (as in the case of their salt forms), but weak hydrogen forces. Therefore, less energy is required to break these bonds. The plasticizing effect of the PFSA chains is observed: glass transition temperature is lower with higher IEC. Presumably, higher concentration of the superacid groups in proximity lowers the energy

required for the lateral groups to interact with each other, forming the S(O)O(O)S bridges by dehydration of the two adjacent superacid sites.

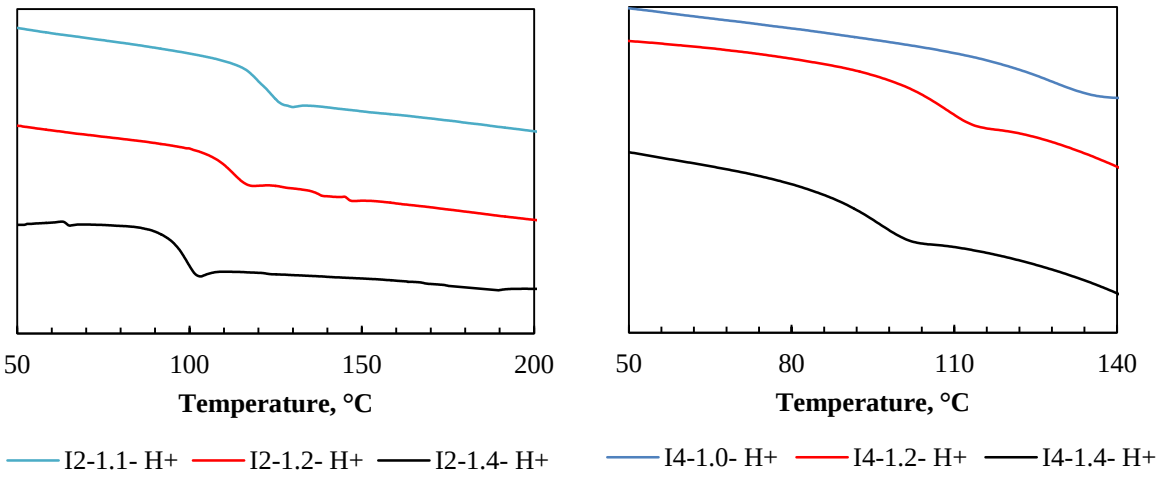

(a) (b)

Figure 3.10. DSC thermograms for the protonated forms of the ionomers series: **I2** (a), and **I4** (b)

Table 3.4. Summarized data of thermal events for the ionomers **I2** and **I4**, extracted from the DSC measurements

Ionomer		**DSC data**		
		T_m, °C	**T_{HT}, °C**	**T_{LT}, °C**
K^+-form	**I2-1.1**	–	207 *	138 *
	I2-1.2	–	203 *	125 *
	I2-1.4	349	209	152
	I4-1.0	–	195	–
	I4-1.2	295	194	–
	I4-1.4	379	198	–
Li^+-form	**I2-1.1**	–	210	179
	I2-1.2	–	198 *	137 *
	I2-1.4	278	222	172
	I4-1.0	–	–	–
	I4-1.2	–	–	–
	I4-1.4	–	–	–
H^+-form	**I2-1.1**	–	117	–
	I2-1.2	–	112	–
	I2-1.4	–	97	–
	I4-1.0	–	129	–
	I4-1.2	–	107	–
	I4-1.4	–	96	–

* Membranes, produced by evaporation of the solvent at 60 °C for 2 days (*method A*)

All the results of DSC analysis are generalized in *Table 3.4*. For the transitions, the following indications are used: T_m – melting temperature, T_{HT} – high-temperature transition, T_{LT} – low-

temperature transition. Since some samples of the series **I2** are cast into membranes exclusively by the *method A*, data of their measurements are marked with asterisks. One may preview, however, the low-temperature transition of these samples to occur at 20-30 °C higher after annealing.

Several prominent conclusions are marked, basing on the DSC measurements:

i) The synthesized ionic poly(ether)s are semi-crystalline polymers, when high amount of lateral PFSA groups is present. Such phenomenon evidences that ionic groups are a driving force for crystallite formation.
ii) The synthesized random PAEs show several transition regions, when neutralized by salts: one – at around 160-180 °C and the other – at 200-220 °C. The low-temperature event highly depends on the membrane drying procedure, hence, on orientation of polymer chains; whereas the high-temperature transition does not depend on a membrane treatment. The polymer's low-temperature reply is believed to exist due to the *meta*-arranged ether bridges in the aromatic backbone, the high-temperature transition is equally related to the main chain.
iii) The best procedure for membrane production is again studied; final annealing of dry membranes at 150-200 °C is confirmed to be the most appropriate complement in order to promote polymer chain structuring.

3.1.3. Thermo-mechanical analysis

When the thermal transitions in a static mode of an ionomer occur close to each other, the force is applied to the material and its reply in dynamic mode is registered (dynamic mechanical analysis (DMA)). Besides the better resoluted transitions, polymers' mechanical properties, such as storage (E') and loss (E'') moduli, are also estimated. T_g of a polymer in DMA appears as a peak on a curve of tan δ. Therefore, a more distinct determination of the T_g may be done, compared to DSC results. Moreover, in calorimetric analysis change of a polymer state is measured, whereas in dynamic analysis polymer relaxes at T_g and flows due to the applied force.

The samples are always measured in their dry state, however one must take to account the time of sample mounting to the device of DMA at ambient conditions. For this reason comparison between the results of DSC and DMA analyses takes to account the possible difference in transition (or relaxation) temperatures of 20 °C.

Fig. 3.11 presents dependence of storage modulus and tan δ on temperature of PAEs series **I2** and **I4** in K^+-form. The membranes in all range of explored IEC (1.1-1.4) show distinct separation to two phases, which is seen: i) from the curve of storage modulus that shows a several-step slope, and ii) from the curve of tan δ, where two peaks of relaxation are observed. A high-temperature relaxation, happening in the range 208-251 °C, is α-relaxation, and the one at lower temperature range (165-193 °C) is β-relaxation.

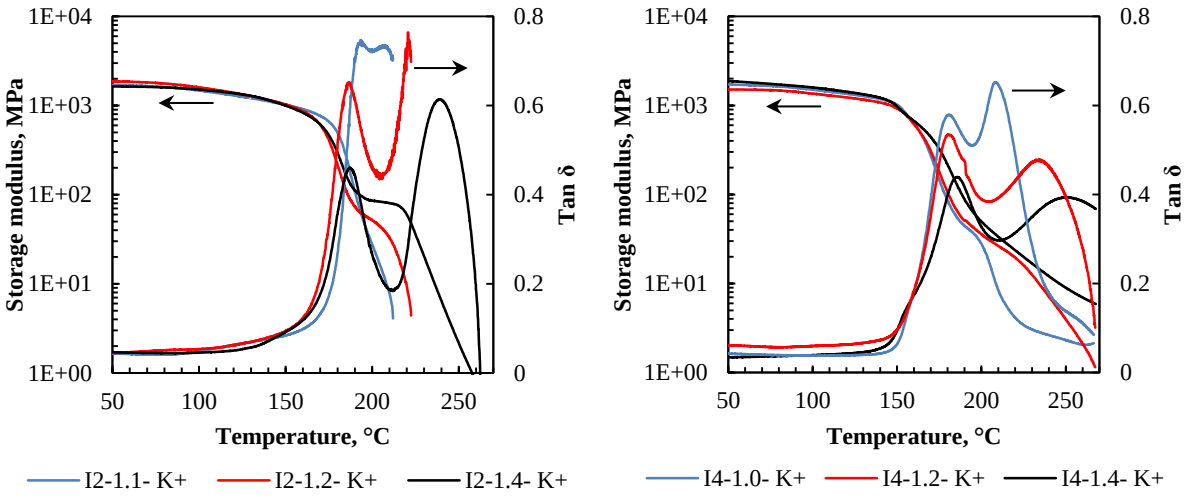

(a) (b)

Figure 3.11. DMA curves for the potassium-neutralized forms of the ionomers series: a) **I2**, and b) **I4**

Membranes show high mechanical stiffness with storage modulus between 1.6-1.8 GPa. When heated, the membranes partially lose their mechanical properties at T_β, but not till the total flowing of the polymer. These are strong ionic forces that keep polymers' integrity and preserve their mechanical strength at 30-80 MPa for **I2** and at 10-30 MPa for **I4** until the α-relaxation. Therefore, the β-relaxation of the polymer is related to its hydrophobic part of a polymer backbone and the high-temperature relaxation happens at the hydrophilic heads of the PFSA-K^+ groups, which provokes the flow of the whole polymer.

As another confirmation of such a supposition, the curve of tan δ is considered. For both series of PAEs an integral of the peak, responsible for β-relaxation, decreases with increasing IEC (it is estimated to decrease in intensity, while having minor changes in width). It points that lower the fraction of a hydrophobic polymer in a sample of the higher IEC, lower the integral of the corresponding signal on a tan δ curve. At the same time a peak of the high-temperature relaxation increases importantly in width, though decreasing slightly in intensity. In total, integration of the α-relaxation tends to increase with increase in concentration of ionic groups. Based on these observations, it is again confirmed, that the non-ionic phase of a

polymer backbone relaxes at 165-193 °C, and the ionic phase, bearing ionic PFSA chains, shows its T_g at 208-251 °C.

Additionally, temperature of α-relaxation is highly dependent on the ionic density: higher concentration of ionic groups is, more difficult it becomes to rupture the ionic forces, and higher T_α is. Another point that may influence the increase of T_α is presence of crystallinity in polymers of high IEC (in particular, **I2-1.4**, **I4-1.2**, **I4-1.4**). This phenomenon may create retardation in high-temperature relaxation and, undoubtedly, causes appearance of inhomogeneous population in a polymer, which contributes to broadening of the relaxation peak.

Thermo-mechanical behavior of the same series of PAEs in their Li^+-neutralized form is presented in *Fig. 3.12*. Two relaxations are again observed for all the ionomers, except **I2-1.4**. But a clear decline of its *E′* curve is observed at 240 °C together with the upturn behavior of the tan δ curve. It suggests that a second relaxation might happen at higher temperature, than 250 °C, if the polymer did not creep.

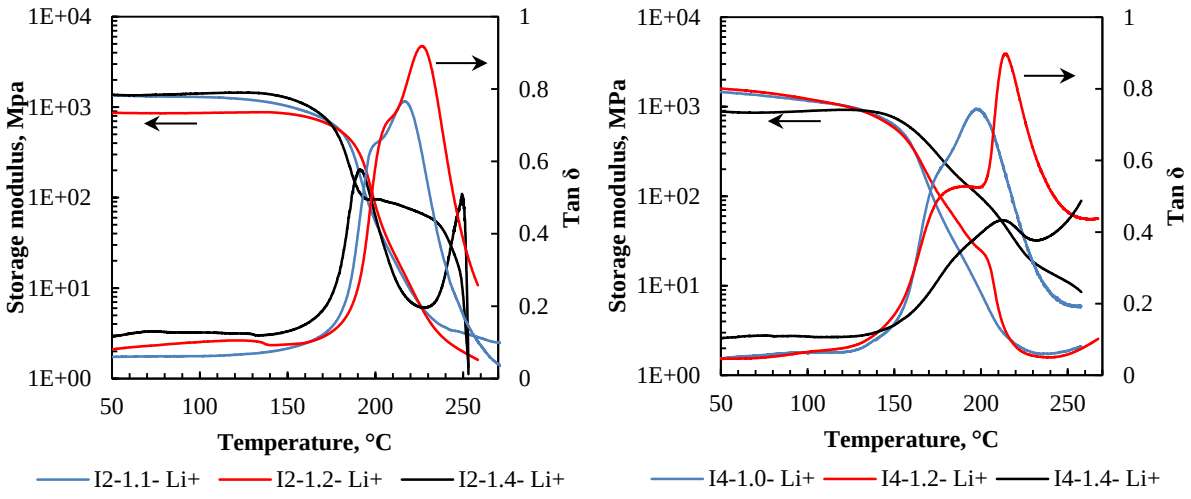

(a) (b)

Figure 3.12. DMA curves for the lithiated form of ionomers series: a) **I2**, and b) **I4**

All the polymers show high mechanical stiffness of 1.0-2.0 GPa up till 150-180 °C for the **I2** series and till 140-150 °C for the **I4** series. At higher temperature the storage modulus decreases in one step (except **I2-1.4**), down till 20-30 MPa. However, the loss in mechanical strength is not linear, but contains several phenomena, which are better distinguished by the tan δ curves.

An important observation is done on the **I4-1.0** and **I4-1.2** samples – their curves of storage modulus tend to rise after 240 °C. It means that even after the total creep of a polymer, there still exist minor interactions that tend to reply to applied force.

Analyzing the curves of tan δ, one may again confirm the presence of the phase separation phenomena for all the samples. Although the two relaxations overlap, still the lower-temperature event may be distinguished. However, the exact value of T_β together with the peak area may not be given with certainty. The difference in T_α for polymers of different IEC is not as big, as for the potassed samples. It is explained by lower counter-ion size of Lithium, therefore, lower free volume of the ionic aggregates in a polymer. The α-relaxation signals of the ionomers with IEC 1.0 – 1.2 of both series show the similar appearance of pics by width, but intensities are higher for the membranes with higher concentration of PFSA groups. Such result is in accordance with the potassed samples, and with the supposition that the high-temperature relaxation is provoked by ionic groups. Considering the ionomers of the highest IEC, the **I2-1.4** membrane seems to show its α-relaxation at temperature higher, than 250 °C, whereas the polymer achieves its maximum creep at this point. Therefore, its high-temperature relaxation signal may not be compared to other peaks of the same series of different IEC. The **I4-1.4** polymer is characterized by a broad signal of tan δ with a peak maximum at 224 °C. It seems as if this broad peak contains two signals, however, after the relaxation at 224 °C the curve of tan δ decreases in intensity and then again rises. At 250 °C the membrane achieves its maximum creep, hence, it may not be verified, if another relaxation happens at high temperature.

Performance of the protonated PAEs series **I2** and **I4** in dynamic mode is presented in *Fig. 3.13*. The membranes are characterized by high mechanical properties with storage modulus values around 1.0 GPa. A remarkable difference between *E′* curves of both series of PAEs is that **I2** ionomers show a one-step slope, starting at 92-107 °C, depending on IEC; whereas for **I4** polymers storage modulus decline, starting at 96-102 °C is followed by its rise after 123-138 °C for the samples of different ionic group concentration.

On the contrary to the low temperature relaxation of the K^+- and Li^+-neutralized membranes, the β-relaxation of the protonated ionomers is related to rupture of weak hydrogen forces between the sulfonic acid groups. A membrane then loses its initial mechanical integrity till the point, when: i) the aromatic main chain starts preserving its stiffness, either ii) crosslinking between two dehydrated sulfonic acid groups occurs with formation of sulfonic anhydride. Among two series of PAEs it is only **I4** that shows such behavior. The only difference between two series is the presence of the sulfanyl-bridge between an aromatic

backbone and the PFSA chain in **I4**, which increases mobility of ionic groups. Presumably, reciprocal access of superacid protons is then more favored in such series of polymers that allows the crosslinking to occur.

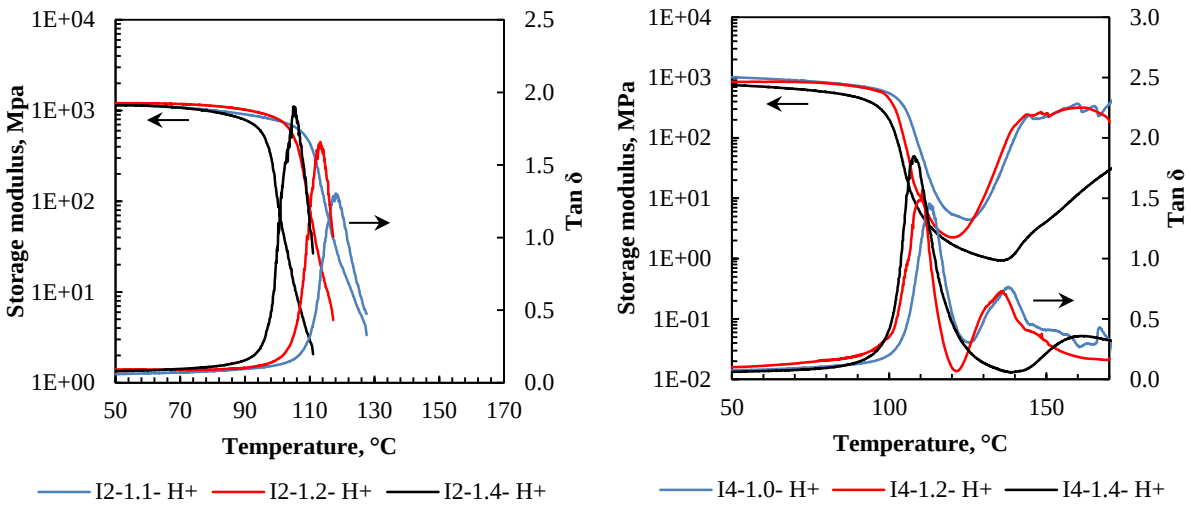

(a) (b)

Figure 3.13. DMA curves for the protonated form of ionomers series: a) **I2**, and b) **I4**

From the curves of tan δ the polymers' T_g may be compared: it decreases with higher IEC, thus, plasticizing effect of ionic chains is observed. Higher the concentration of superacid groups present in a polymer, shorter the distance between them, hence, less energy is required to approach them and make interacting by dehydration reaction.

As a conclusion, analysis on thermo-mechanical properties of the PAEs ionomers evidences:

i) random ionic polymers **I2** and **I4** show distinct phase separation in the whole range of studied IEC (1.0-1.4 meq/g), which is rarely observed for a material of a statistic structure;
ii) this phenomenon points on ionic and hydrophobic parts that tend to self-organize in a way to create well-distinguished domains.

In order to relate the results from DSC analysis to those from DMA, *Table 3.5* is presented. For the relaxations in DMA the following indications are used: T_α – high-temperature or α-relaxation, T_β – low-temperature or β-relaxation.

T_{HT} from the DSC data is the transition of the higher ΔH, it does not depend greatly on annealing procedure during the membrane preparation (see *paragraph 3.1.2*), therefore, even the values with asterisk may be considered as true values. On the contrary, T_{LT} depends much on the heating temperature during the preparation of the membranes, thus its values, marked

with an asterisk, may be 20-30 °C lower from those, when annealing is applied to a membrane. Earlier in the current work it was considered that T_{LT} and T_{HT} correspond to the movements of a polymer backbone. At the same time T_β from the DMA data is determined as relaxation of the polymer main chain. Then the results of two measuring techniques are in good agreement, when T_β is the average between T_{HT} and T_{LT}.

Table 3.5. Summarized data of thermal events for the ionomers **I2** and **I4** from the DSC and DMA measurements

Ionomer		**DSC data**			**DMA data**	
		T_m, °C	**T_{HT}, °C**	**T_{LT}, °C**	**T_α, °C**	**T_β, °C**
K^+-form	**I2-1.1**	–	207 *	138 *	208	193
	I2-1.2	–	203 *	125 *	222	186
	I2-1.4	349	209	152	246	185
	I4-1.0	–	195	–	210	181
	I4-1.2	295	194	–	235	181
	I4-1.4	379	198	–	251	183
Li^+-form	**I2-1.1**	–	210	179	217	201
	I2-1.2	–	198 *	137 *	229	206
	I2-1.4	278	222	172	250	195
	I4-1.0	–	–	–	210	185
	I4-1.2	–	–	–	216	183
	I4-1.4	–	–	–	222	202
H^+-form	**I2-1.1**	–	117	–	118	–
	I2-1.2	–	112	–	113	–
	I2-1.4	–	97	–	105	–
	I4-1.0	–	129	–	114	–
	I4-1.2	–	107	–	109	–
	I4-1.4	–	96	–	107	–

* Membranes, produced by evaporation of the solvent at 60 °C for 2 days (*method A*)

Such dependence is observed for the lithiated and potassed membranes series **I2**. Ionomers of the series **I4** in their K^+-form do not show a distinct T_{LT} at DSC curves, but their T_β is for 13-15 °C lower than the T_{HT}. The lithiated ionomers series **I4**, however, cannot be compared by different techniques, because DSC curves do not show distinct transitions. It could be related to the fact that the changes in energy state of the Li^+-neutralized **I4** membranes are too small and they happen close to the maximal temperature of the current measurement. Consequently, the α-relaxation of the salt-neutralized samples, happening in dynamic mode and responsible for the movements of ionic chains, does not have a correspondent transition in static mode, or it is not detected at a DSC curve.

The protonated PAEs series **I2** and **I4** show only one distinct and intense transition and relaxation. Undoubtedly, they are related to the change of energy state of the PFSA groups, since hydrogen bonds between superacid groups are ruptured faster and at lower temperature, than ionic forces between their neutralized forms. The values of both measuring techniques, presented in *Table 3.5* for the H^+-form ionomers, are in good agreement.

3.1.4. Bulk morphology

In order to better understand the bulk morphology of the membranes series **I2** and **I4**, differing in the way of PFSA attachment to the polymer backbone (directly or through the sulfanyl specie), measurement of small angle X-ray scattering (SAXS) is provided below. The current section is subdivided by the three effects studied: 1) effect of the counter-ion; 2) effect of protonation; 3) effect of IEC and water uptake.

Effect of the counter-ion

From the previous results of thermo-mechanical properties, dependence of the membrane behavior on the nature of counter-ion is registered. Therefore, the first measurements of SAXS are conducted on the samples of the highest IEC (**I2-1.4** and **I4-1.4**), neutralized by potassium and lithium. *Fig. 3.14* illustrates the obtained results for the dried samples: red markers correspond to ionomers with K^+-bearing PFSA groups, green markers – to Li^+-neutralized polymers. The baseline is the background signal from the cell windows (Kapton).

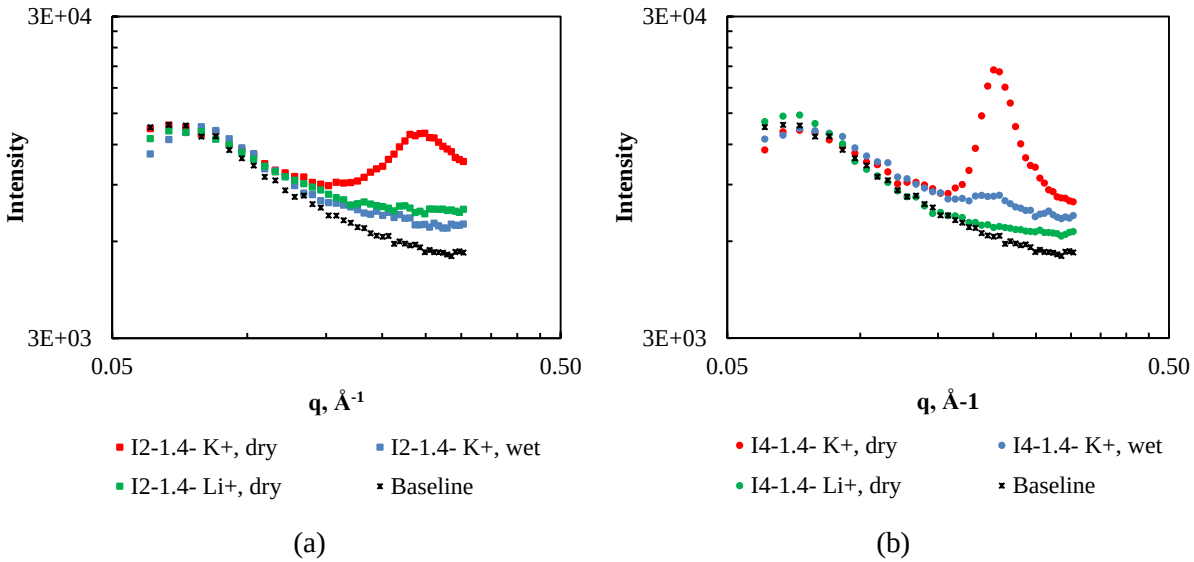

Figure 3.14. SAXS spectra of the Li^+- and K^+-neutralized forms of: a) **I2-1.4** and b) **I4-1.4**. The K^+-form is presented in both dry and wet states

From the spectra of both samples it is evidenced that the dry K^+-neutralized polymers show the presence of a well-defined intense correlation peak, at 0.24 and 0.20 $Å^{-1}$ for **I2-1.4** and **I4-1.4**, respectively. This peak is not present in the lithiated materials. Hence, it is sensitive to the nature of the counter-ion and, therefore, is related to the organization of the ionic phase, so-called 'ionomer peak'. Additionally, when humidifying the ionomers, bearing PFSA-K^+ lateral chains (shown with blue markers in *Fig. 3.14*), we observe that intensity of the correlation peak decreases significantly, while the position is slightly shifted towards small *q*-vectors.

Generally, scattering maxima arise from the regular organization of domains with different electron density at the nanoscale. Changing the nature of the counter-ion and/or adding few water molecules change(s) the electronic contrast between hydrophobic polymer domains and ionic domains, containing ions and water. With a closer look at samples **I2-1.4** and **I4-1.4** in their K^+-form, in a dry state ionomer peaks present electron difference between the ionic head of $–SO_3K$ and the perfluorinated segment (either aromatic in a backbone of the DFB specie, or the PFSA lateral chain), which is big enough to result in a well-resoluted peak. When the ionomers are humidified, water molecules increase electron density of the ionic groups, at the same time decreasing the difference between the electron densities of the ionic and perfluorinated parts. Hence, the signal fades upon water treatment. The lithiated ionomers do not show characteristic peak in dry state due to the low contrast between Li^+ and the polymer chain, which may not be distinguished among the other atoms around. Unfortunately, no test on humidification of these membranes was conducted.

Another important observation for the dry potassed samples is that **I4-1.4** gives a more intensive and narrower ionomer peak, than **I2-1.4**. Such property is probably related to a better organization of the ionic phase, when PFSA is attached by the sulfanyl bridge. Referring to the melting endotherms (*Table 3.2* and *3.3*), ionomer the **I2-1.4-K^+** is characterized by higher crystallinity, than **I4-1.4-K^+**, however the crystallinity of the latter ionomer is more homogeneous. Presumably, th latter parameter has stronger influence on the organization of the ionic phase, which results in ionomer peak of much higher intensity.

The characteristic distance between scattering objects can be obtained from the position q_{max} of the ionomer peak, as:

$$d = \frac{2\pi}{q_{max}} \qquad (10)$$

Table 3.6. Characteristic distances of the dry ionomers in their K^+-form

Ionomer	q_{max}, $Å^{-1}$	d_1, Å
I2-1.4- K^+	0.2431	25.8
I4-1.4- K^+	0.2007	31.3

The results for dry potassed polymers are indicated in *Table 3.6*. The characteristic distance *d* corresponds to a mean separation distance between ionic domains. A possible organization at the nanoscale is depicted in *Fig. 3.15*, which shows the segregation between ionic domains and polymer domains. *d*-distance must correspond to two lengths of the PFSA groups and two lengths of the aromatic ring the PFSA chain is bound to (the double length of the specie, marked with blue arrows in *Fig. 3.15*). To check this validity *Table 3.7* presents calculations of the bond lengths in both ionomers **I2-1.4** and **I4-1.4**. Based on these results *d*-distance for **I2-1.4** is 28.5 Å and for **I4-1.4** is 32.8 Å. The data are slightly higher than those, determined from the SAXS (*Table 3.6*). This discrepancy may come from the fact that lateral groups are not linear when dry and exhibit angular arrangement.

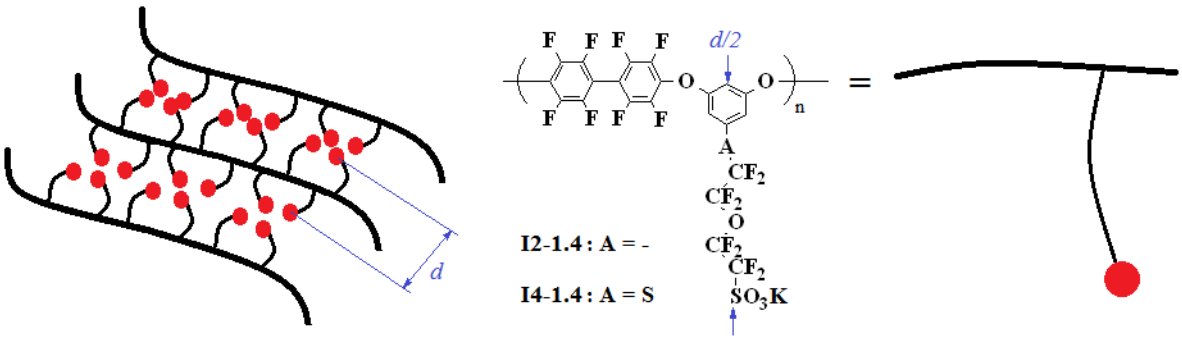

Figure 3.15. Schematic illustration of ionomer chains and *d*-distance between the ionic groups

Table 3.7. Calculations of bond distances between the blue arrows, marked in *Fig. 3.15*, for the ionomers **I2-1.4** and **I4-1.4**

Bond in moiety of the ionic monomer	Bond length	Number of bonds		Lengths of bonds in moiety of the ionic monomer, Å		Length of moiety of the ionic monomer, *d*/2, Å	
		I2-1.4	I4-1.4	I2-1.4	I4-1.4	I2-1.4	I4-1.4
C-C (*para* in benzene)	2.80	1	1	2.80	2.80	14.23	16.41
$C_{arom.}$-C	1.40	1	0	1.40	–		
$C_{arom.}$-S	1.76	0	1	–	1.76		
C-C	1.54	2	2	3.08	3.08		
C-O	1.82	2	2	3.64	3.64		
C-S	1.82	1	2	1.82	3.64		
S-O	1.49	1	1	1.49	1.49		

Conclusively, the presented results show that: i) the structures of the ionomers **I2** and **I4** are organized (presence of the ionomer peak), and ii) the ionomer peak of the dry membranes is registered for the polymers with the bigger counter-ion, but it vanishes at humidification due to zero-contrast point.

Effect of the protonation

The effect of protonation of membranes on their morphology is studied. The both samples of the highest IEC are acidified separately from their K^+- and Li^+-neutralized state and swollen in water overnight at 40 °C. Just as in the case of lithiated samples, the acidified ionomers do not show correlation peak in dry state, thus, to attain the contrast humidification is inevitable.

Fig. 3.16 illustrates the measurements by small angle neutron scattering (SANS). Basically SAXS and SANS techniques provide the same structural information, but the principle lying in the measuring method is defferent: in SANS neutrons interact with nuclei, while in SAXS X-rays interact with electrons. In both techniques the scattered intensitites are proportional to a contrast term.

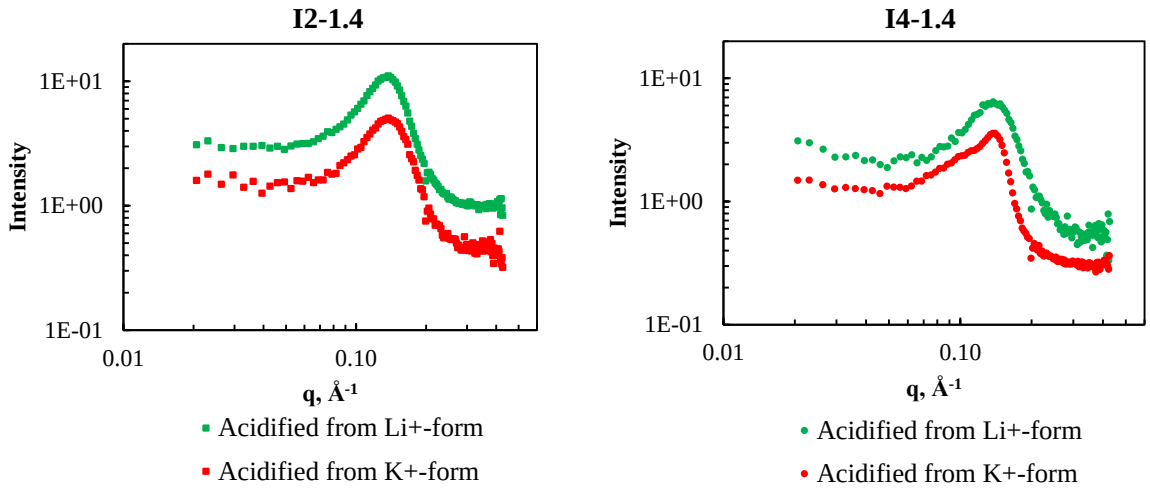

Figure 3.16. SANS spectra of the membranes acidified from Li^+- and K^+-neutralized forms of: a) **I2-1.4** and b) **I4-1.4**

Well-defined intense ionomer peaks are clearly observed for all the samples. They appear at very similar *q*, therefore the characteristic distances are almost identic and comprise approximately 46 Å for the **I2-1.4** and 45 Å for the **I4-1.4** (*Table 3.8*). Taking to account the similar swelling for the samples, acidified from different cationic forms, it may be concluded that the initial salt state has no effect on distance between the scattering objects, hence, between the ionic domains.

Table 3.8. Characteristic distances of the wet ionomers in their protonated form

Ionomer form	I2-1.4			I4-1.4		
	q, Å^{-1}	d, Å	λ, H_2O/SO_3H	q, Å^{-1}	d, Å	λ, H_2O/SO_3H
Acidified from Li+-form	0.1344	46.7	19.8	0.1410	44.5	22.4
Acidified from K+-form	0.1377	45.6	19.4	0.1373	45.7	21.4

The ionomer **I4-1.4** acidified from its K^+-form does not have a Gaussian-type curve. With a closer look on the plot (*Fig. 3.17*) two maxima are evoked, associated to characteristic distances of 45.7 Å (q = 0.1373 Å^{-1}), and 61.9 Å (q = 0.1015 Å^{-1}) (the both peaks are extrapolated to x-axis with black lines).

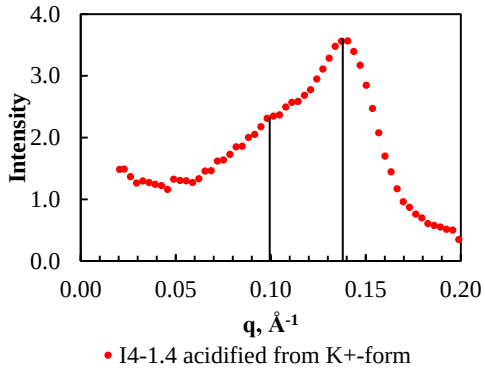

Figure 3.17. Enlarged SANS spectrum of the **I4-1.4** acidified from K^+-form

The peak at q = 0.1373 Å^{-1} is sharp and intense, while the other is broader and lower in intensity. We can hypothesize that there exist two types of organized structures, and possibly two types of ionic domains. Taking to account the presence of homogeneous crystallinity (from the DSC data), it is assumed that one type of ionic domains is formed by the crystallites, whereas the other one – by amorphous chains. The former due to the rigidity of the crystalline structure swells much less, than the latter; therefore it gives characteristic peak at higher q-values. Moreover, appearance of the peak evidences a more regular structure.

Three other ionomers, presented in *Fig. 3.16*, two of which were verified by DSC for the presence of the crystalline part (**I2-1.4-K$^+$** and **I2-1.4-Li$^+$**), show symmetric and broad ionomer peaks. Presumably, both types of the ionic domains are hidden in one signal; in order to separate them different amount of water must be incorporated to the membranes. This study is described in the next subdivision.

Effect of IEC and water uptake

Here, the protonated ionomers, being swollen in water at three different temperatures – 40, 60 and 80 °C – are studied by SAXS. The samples series **I2** and **I4** of the highest and the lowest

IEC are depicted in *Fig. 3.18.* All the polymers, except **I4-1.4**, are acidified from their lithiated state. **I4-1.4**, protonated from K^+-form is represented due to the lack of measurement of the series, acidified from the lithiated state. However, these studies are previewed shortly. Hence, for comparison **I4-1.4** of the K^+-to-H^+ protonation is given here. As it was registered in *Fig. 3.16 (b)*, in case when there are two characteristic peaks, this is the one of the highest intensity that coincides by scattering vector with that of the Li^+-to-H^+.

All the ionomers from *Fig. 3.18* show the presence of a typical ionomer peak at scattering vectors q = [0.10; 0.17]. *Table 3.9* presents the dimensions of ionic domains for the ionomers, swollen in water overnight at the predetermined temperature. Polymers with the highest IEC are not subjected to swelling at 80 °C due to their solubility at such high temperature.

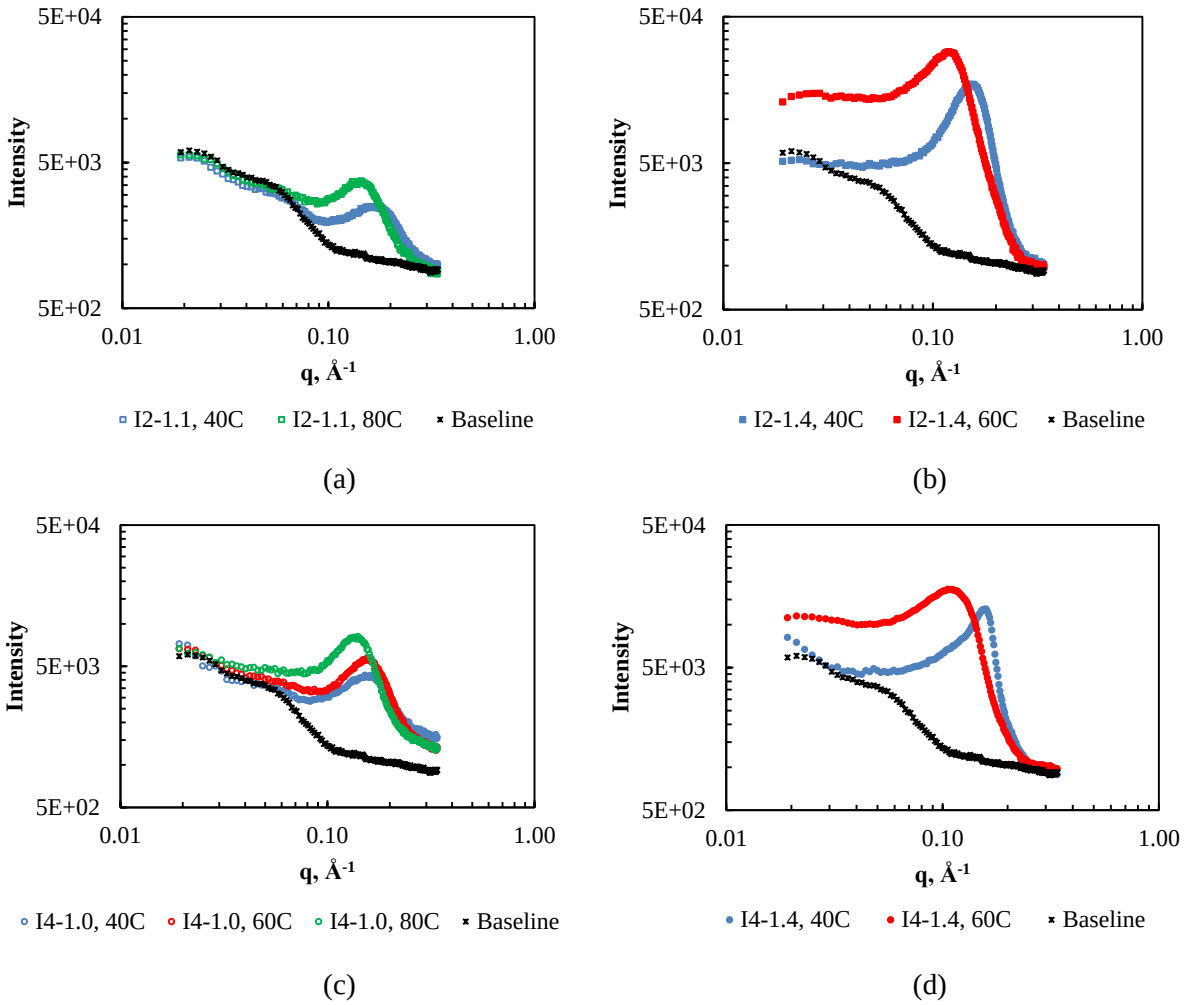

Figure 3.18. SAXS spectra of the protonated ionomers: a) **I2-1.1**, acidified from Li^+-form, b) **I2-1.4**, acidified from Li^+-form, c) **I4-1.0**, acidified from Li^+-form, d) **I4-1.4**, acidified from K^+-form. In the name of each sample temperature of water for swelling is given

Ionic domains of the studied polymers series PAE increase in size, when swelling the material at higher temperature. **I2-1.4** and **I4-1.4** are characterized by bigger interionic distances, when

swollen at 60 °C, than **I2-1.1** and **I2-1.4**, when swollen at 80 °C. Comparing the *d*-distances of **I2-1.4** and **I4-1.4** between SANS (*Table 3.8*) and SAXS (*Table 3.9*) results, the latter technique evokes slightly lower values. However, one must admit that estimation of q_{max} is performed by eye; since the peak is broad the value may differ little.

Table 3.9. Characteristic distances of the protonated ionomers, swollen at different temperatures

Ionomer	40 °C			60 °C			80 °C		
	q, Å^{-1}	d, Å	λ, H_2O/SO_3H	q, Å^{-1}	d, Å	λ, H_2O/SO_3H	q, Å^{-1}	d, Å	λ, H_2O/SO_3H
I2-1.1	0.1518	41.4	10.4	N/A	N/A	12.2	0.1326	47.4	15.4
I2-1.4	0.1422	44.2	19.8	0.1115	56.3	37.0	–	–	–
I4-1.0	0.1441	43.6	10.4	0.1441	43.6	12.3	0.1287	48.8	16.5
I4-1.4	0.1479	42.5	21.4	0.0980	64.1	48.0	–	–	–

In order to illustrate dependence of ionic domain size on water incorporation, a parameter of water fraction (Φ_{water}) is introduced. It is deduced from the results of the water uptake by the membranes, discussed in the next paragraph. Water fraction is calculated by an equation:

$$\Phi_{water} = 1 - \frac{V_{polymer}}{V_{polymer} + V_{water}} \qquad (11)$$

where $V_{polymer}$ is volume of a dry polymer, and V_{water} is volume of water in membrane at particular temperature.

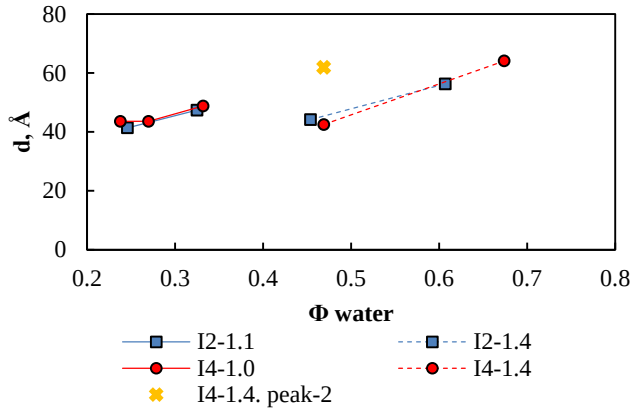

Figure 3.19. Dependence of interionic distance on water fraction of PAEs series **I2** and **I4**

The ionomers of the IEC 1.0 – 1.1 meq/g are characterized by interionic distances of 4.1 – 4.9 nm at water fraction 0.23 – 0.33 (*Fig. 3.19*). Materials with the highest IEC swell more (**I4** > **I2**), thus have wider sizes of the ionic domains, up till 6.4 nm. From the previous sub-paragraph we concluded that semi-crystaline ionomers might show two characteristic peaks: the one at higher *q*-values corresponding to the ionic domains surrounded by crystallites, when the other of the lower *q*-value is related to the ionic domains in amorphous phase. These

two peaks might be hidden in one broad peak. For the **I4-1.4** sample, protonated from the K^+-form and swollen at 40 °C, separation of these peaks is however observed. Extracting the value of *d*-distance, calculated from the scattering vector of the second peak with q_{max} = 0.1015 $Å^{-1}$ (which characterizes ionic domains in amorphous phase), and plotting it in *Fig. 3.19*, reveals a point on the prolongated lines of the **I2-1.1** and **I4-1.0** samples. Therefore, more studies must be performed in order to be able to separate the characteristic peaks of the ionic domains of different nature.

Based on the results of SAS together with previous knowledge of PAEs' behavior in terms of thermo-mechanical properties, the bulk morphology of the newly synthesized ionomers is studied. The following conclusions are made:

i) All the materials have highly organized structures, which are confirmed by the presence of a well-defined scattering maximum, labeled as ionomer peak, and attributed to phase separation at nanoscale. This signal evidences organization of polymer chains to ionic and non-ionic phases.
ii) If a polymer is semicrystalline and highly organized, two types of ionic phases exist: the one, where ionic clusters are surrounded by crystallites, the other, where ionic aggregates are dispersed in amorphous phase.
iii) Higher organization of the ionic polymer is registered for the material, having more homogeneous in size crystallites (case of **I4-1.4- K^+**), rather than higher crystallinity in general (**I2-1.4- K^+**).

3.1.5. Water uptake

A proton conducting membrane must swell in water enough to create the connected channels for sufficient proton conduction. At the same time, a membrane must not lose its mechanical properties that are keeping its initial appearance, no dissolution or over-swelling must occur, giving the highly breakable material.

It is known that higher the IEC of the material, higher its water uptake. In a fuel cell a membrane is always subjected to water vapor; however the test of membrane swelling is conducted in liquid water as the extreme case. *Fig. 3.20* shows results of the water uptake test and the dependence of calculated lambda-values (amount of water molecules per ionic site) on temperature. **I4** ionomers have higher ability of water uptake, compared to the **I2** series. This might be related to presence of the sulfanyl moiety, which increases mobility of the lateral chains, thus increases probability of water uptake.

Amount of water molecules per ionic site, adsorbed by **I4-1.0**, resembles that of **I2-1.2** at RT – 60 °C. At higher temperatures it is **I2-1.2** that takes water more brusquely. Such behavior testifies better water accessibility to ionic sites due to their higher concentration, at least. The membranes of IEC 1.2 meq/g swell in water at high temperatures so fast that at 90 °C the weight of the polymers becomes more than twice higher their dry state.

For the membranes of even higher IEC of 1.4 meq/g temperatures more than 50 °C are drastic for swelling. However, a closer look on their performance at reduced humidity must be taken.

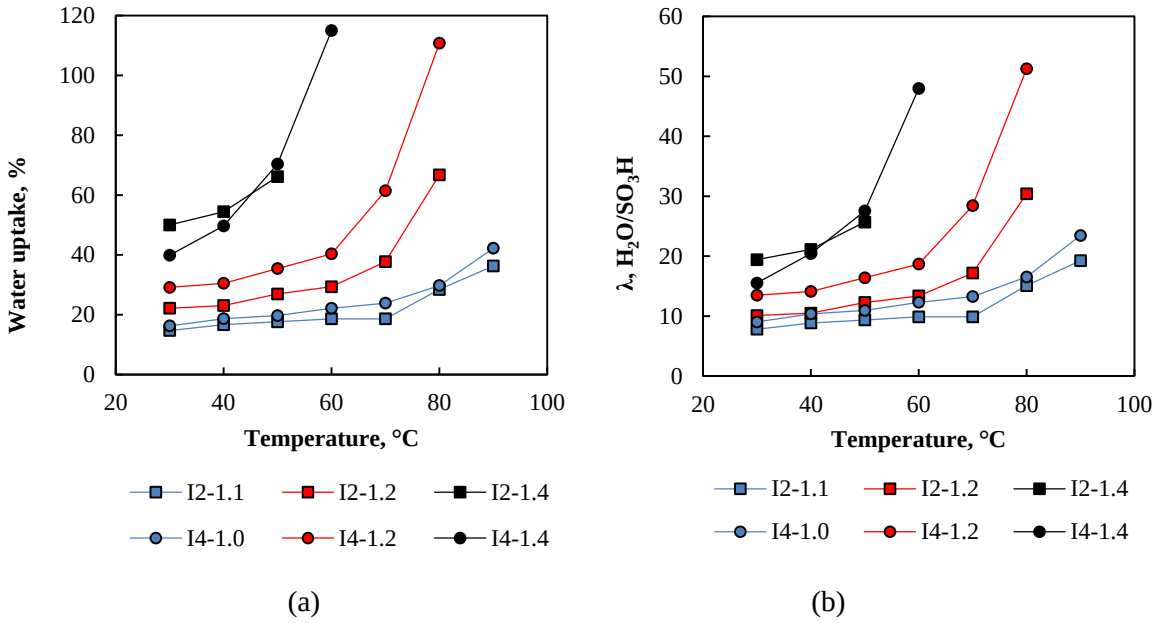

Figure 3.20. Swelling of **I2** and **I4** ionomers in water in the temperature range 30-90 °C: a) dependence of WU, and b) dependence of number of water molecules per sulfonic group

3.1.6. Conductivity

Unlike the previous measurement, impedance is registered at reduced humidity: at 95 %RH in the temperature range 30 – 90 °C and at 20-80 % RH at 80 °C. Unfortunately, the conditions for the current analysis do not allow conducting it in water that would be comparable to the water uptake measurements. However, information of ionomer conductivity at reduced humidity is much more important in terms of further utilization in a real fuel cell, than data on conductivity in water.

Fig. 3.21 shows dependence of conductivity (σ) on temperature for the series **I2** and **I4**, acidified from their Li^+-salts. Conductivity increases with temperature and with higher IEC of a polymer. Comparing the two series of ionomers, **I2** and **I4**, of the lowest IEC, the latter polymer shows twice higher conductivity, than **I2**. It must be reminded that IEC of **I2-1.1** is slightly higher than that of **I4-1.0**, therefore the difference in performance is not related to the

amount of the ionic sites. Additionally, no big difference in bulk morphology between the two samples is observed: sizes of ionic clusters of both polymers are comparable. Therefore, the difference in conductivity might occur because of the better connectivity of ionic domains in **I4-1.0**.

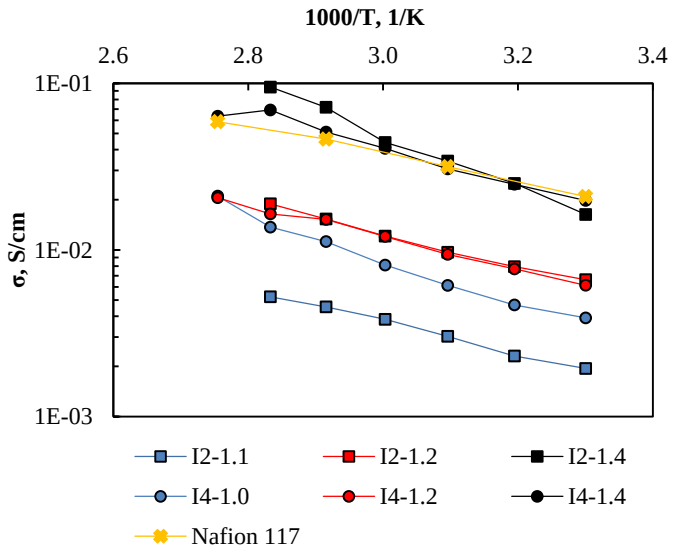

Figure 3.21. Conductivity of **I2** and **I4** ionomers in temperature at 95 %RH

On the contrary, the ionomers of IEC 1.2 meq/g show comparable performance in the range $6 \cdot 10^{-3} – 2 \cdot 10^{-2}$ S/cm at 30-90 °C. And the polymers of the highest concentration of ionic sites give similar conductivities to Nafion 117.

Nafion 117 is characterized by IEC 0.9 meq/g and IEC_V 1.9 meq/cm^3. With a look at *Tables 2.10* and *2.12*, these are polymers of the ionic content 1.2 and 1.4 meq/g, whose IECv overpass the one of Nafion 117 (their values are 2.1 meq/cm^3 for **I2-1.2** and **I4-1.2** and 2.4, 2.5 meq/cm^3 for **I2-1.4** and **I4-1.4**, respectively). Hence, Nafion 117 contains the amount of ionic groups that is an average value of the ionic contents of **I2-1.1** (**I4-1.0**) and **I2-1.2** (**I4-1.2**). Additionally if one compares the values of water uptake of Nafion 117 and of the currently described (PAE)s, the former material adsorbs 20 – 30 % of water (in ratio to its initial weight) at 30 – 80 °C. These values lie in the same region of water uptakes of **I2-1.1** (**I4-1.0**) and **I2** (**I4**)**-1.2** polymers. But conductivity of Nafion 117 is far higher, than that of the **I2-1.1** (**I4-1.0**) and **I2** (**I4**)**-1.2** membranes. Such dependence may indicate that Nafion has a structure more favorable for the proton passage. During the discussion on the morphology it was concluded that ionic domains of PAEs are well-organized. Lower conductivity of the membranes of IEC 1.0-1.2 meq/g may be explained by higher tortuosity of the proton channels. Such phenomenon could be related to higher rigidity of the main chain.

The results of SAS in *paragraph 3.1.4* showed difference in ionomer morphology, whether acidification was realized from K^+- or Li^+-neutralized forms. In order to see, how this property may influence conductivity, *Fig. 3.22* illustrates performance of **I2-1.4** and **I4-1.4**, protonated from both ionic forms. It is evident that conductivity of the membranes, acidified from their lithiated states, are higher, than those, transformed from the potassed ionomers. Additionally, higher slope of **I2-1.4**, compared to **I4-1.4**, says about its higher activation energy. It is known that lower activation energy points on lower energy barrier for protons to pass through the ionic channels.

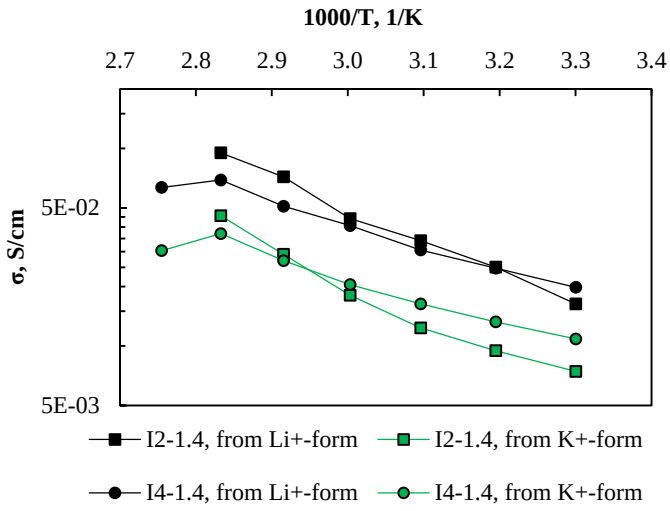

Figure 3.22. Conductivity of **I2-1.4** and **I4-1.4** ionomers, protonated from K^+- or Li^+-form

Fig. 3.23 shows dependence of proton conductivity on humidity for the **I2** and **I4** series of ionomers. The membranes of the lowest IEC, **I2-1.1** and **I4-1.0**, are acidified from their lithiated states; the membranes of the highest IEC, **I2-1.4** and **I4-1.4**, are protonated from the both forms that is noted in the legend. **I2-1.1** shows high resistances at humidity lower than 60 %RH, therefore no data are presented on the graph. On the contrary, **I4-1.0** ionomer conducts well at $6.03 \cdot 10^{-4}$– $8.02 \cdot 10^{-3}$ S/cm in the range 20-80 %RH. In general, performance of the ionomers of the lowest IEC is lower than that of Nafion. Moreover, difference in conductivity between Nafion 117 and aromatic polymers of IEC 1.0-1.1 meq/g increases with higher humidity.

Analyzing the ionomers of the highest IEC, again, the samples acidified from their Li^+-initial forms show much higher conductivity at reduced humidity, compared to those acidified from the potassed state. Performance of **I2-1.4**, protonated from its Lithium salt, is similar to that of Nafion 117 at high humidities, and shows tendency to increase at humidity < 60 %RH. The similar behavior is observed for **I4-1.4**: at 80 %RH its conductivity is twice higher than that

of Nafion 117 and the difference increases when lowering humidity. The samples of the highest IEC, protonated from their potassed salts, have slightly lower conductivity than Nafion 117, at 50-80 %RH. At < 50 %RH their performance becomes comparable to the reference material (**I2-1.4**) or up till 3-4 times higher at 30 %RH (**I4-1.4**).

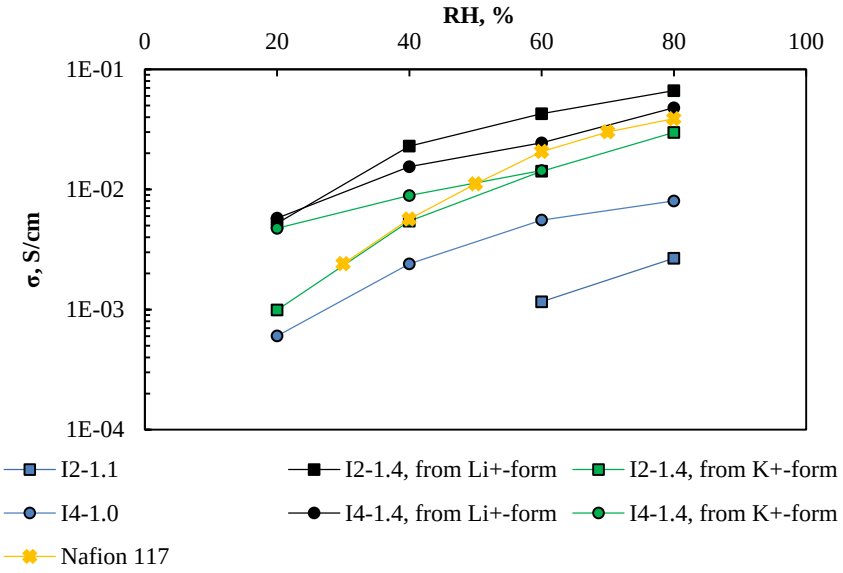

Figure 3.23. Conductivity dependence on relative humidity for the PAEs **I2** and **I4**

From the data, described in the current section, ionomers **I2** and **I4** of the highest IEC show performance comparable to Nafion 117 at highly humid conditions (> 80 %RH), and even better, than the reference, at 20-60 %RH. Such results are promising, and make us presume that water retention in conductive channels of these ionomers is highly effective. Due to difference in organization of ionic domains, when casting the membrane in its lithiated or potassed form, performance of these materials differs as well.

The ionomers of the lowest IEC do not reach performance of the reference material. Compared to the ionomers of the highest IEC, **I2-1.1** and **I4-1.0** have smaller ionic clusters (at least when humidified at temperature higher, than 40 °C) (refer to SAS results), and worse connected to conducting channels.

3.1.7. Oxidative stability test (OST)

In a real fuel cell a membrane is constantly subjected to the presence of free radicals that might cause a polymer chain rupture. In the *chapter 1* nature of the radical attack was explained in detail. To verify the stability of the PAEs series **I3** and **I7** the polymers in their protonated form are heated in a Fenton reagent, which is 3 % solution of H_2O_2 with 3 ppm of Fe^{2+}. In the literature no unique procedure for the Fenton test is protocoled: some groups

made the analysis at heating at 80 °C and plotted the dependence of the weight loss in time by counting each hour, the others heated samples at the same conditions during 1 h and then analyzed the values of molecular weight. Also there is a group of researchers, who used 30 % solution of H_2O_2 (with or without Fe(II) salt), and provided the measurement at RT.

For the current work the solution of H_2O_2 of lower concentration is used. The membranes are heated at 50 °C, since higher temperatures result in fast (less than 1 h) dissolution of statistic materials. The polymers of lower IEC are taken to avoid fast dissolving in hot water as well.

Among the PAEs, **I3-1.2** and **I7-1.0** are tested for the oxidative stability. Firstly, the polymers are equilibrated in water at 50 °C overnight, the weight is registered, and the membranes are transferred to a newly prepared solution of oxygenated water, preliminary heated in an oven at 50 °C during 30 min. Each hour the membranes are weighted. On the contrary to the previous Fenton tests, the ionomers, investigated in this work, do not lose in weight, but gain a little, while becoming brittle (noted as time of OST in a *table 3.10*). We presume that there occurs a main polymer chain scission on ether-bridges with further their oxidation. If there happened a rupture of lateral chains only, the polymer would still guard its integrity, while decreasing in weight. In order to verify our supposition, a measurement of SEC is provided in *Table 3.10*.

Table 3.10. Results of the OST for the PAEs

Ionomer	**Time of OST, h**	**Mn (before OST), $\times 10^3$, g/mol**	**Mw (before OST), $\times 10^3$, g/mol**	**PDI (before OST)**	**Mn (after OST), $\times 10^3$, g/mol**	**Mw (after OST), $\times 10^3$, g/mol**	**PDI (after OST)**
I3-1.2	8	69.0	128.6	1.9	16.5	23.9	1.4
I7-1.0	15	106.0	448.0	4.2	13.2	15.5	1.2

The both measured PAEs (**I3-1.2** and **I7-1.0**) show significant deterioration in molecular weight, therefore we assure the cleavage of the polymer backbone. The NMR spectra are also presented in a *Fig. 3.24*.

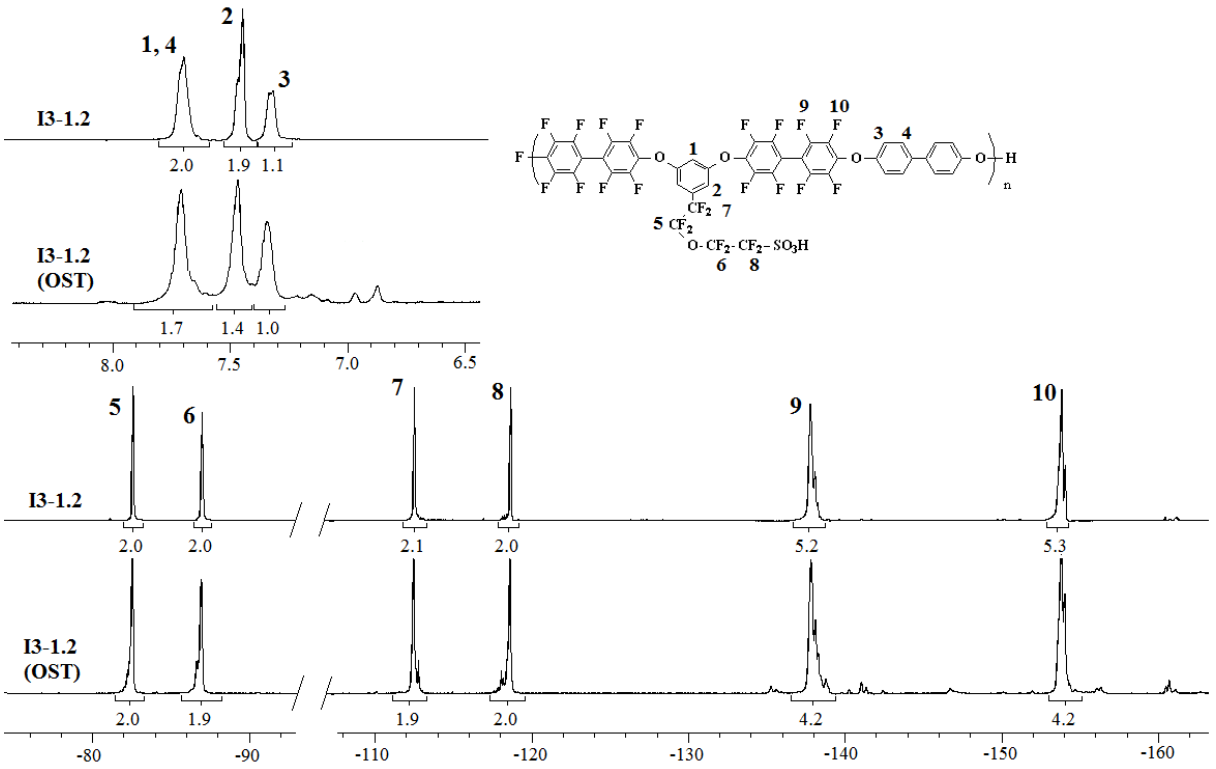

(a)

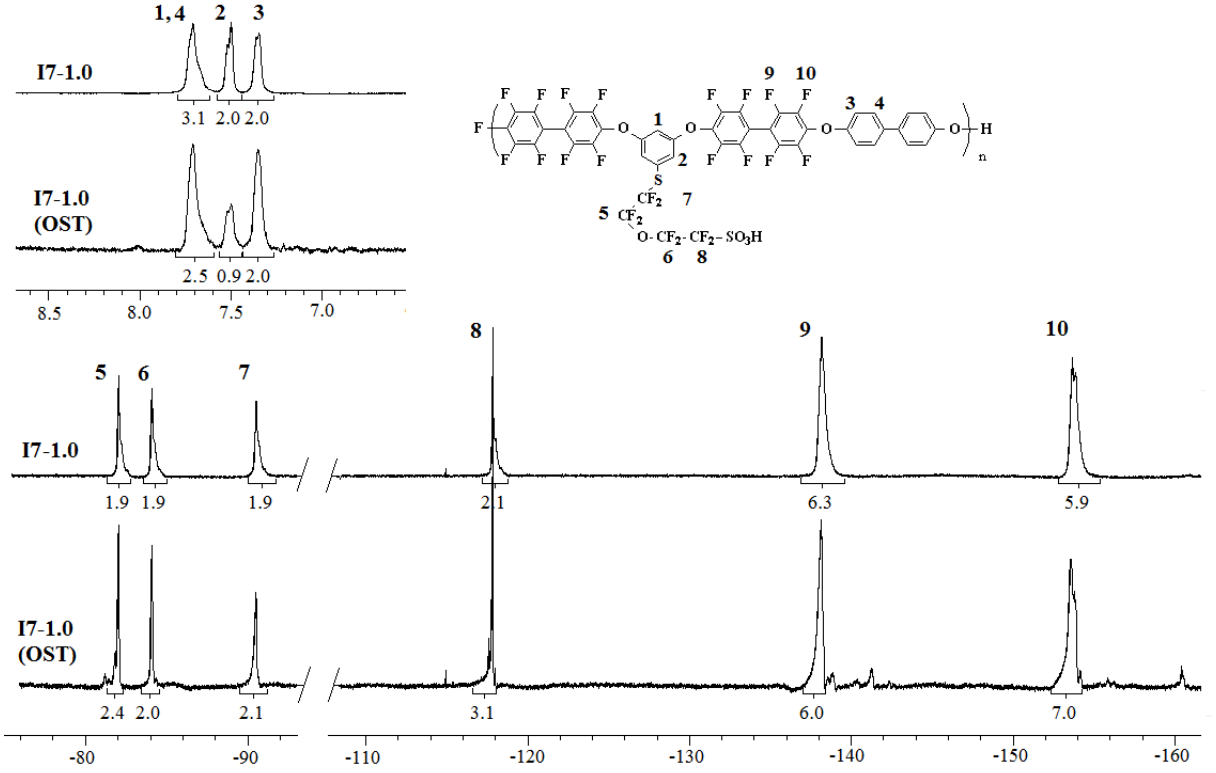

(b)

Figure 3.24. ^{1}H NMR and ^{19}F NMR spectra of the ionomers before and after OST (the latter indicated in parentheses at the spectra) during the time, noted in *Table 3.10*. a) Spectra for **I3-1.2** and b) spectra for **I7-1.0**

In both ionomers there appear more fluorines in both DFB zone and PFSA region, which evidences again the segmentation of a polymer chain. Comparison of the peak integration of ^{1}H NMR spectra before and after OST shows the decrease in the amount of ionic monomer, which might testify the dissolution of the small highly polar segments in the H_2O_2 solution. Another observation from the proton spectra is appearance of additional signals (for **I3-1.2**) or a 'noisy' background (for **I7-1.0**) in the zone of chemical displacement 6.8-7.3 ppm. Supposedly, the PAEs are stable enough, but, to our opinion, testing conditions, which avoid the presence of water are more credible. In this case there appears no problem of dissolution of a statistic polymer of high molecular weight at high temperature. If the dissolution (material deterioration visible with an eye) at reduced humidity is happening, it certainly testifies the degradation of a polymer. Besides, such conditions would approach more the real testing conditions in a fuel cell.

3.2. Properties of random and block-(PAES)s series I3 and I5

General structure of the ionomers studied in the current section is illustrated in *Fig. 3.25*. Compared to the series of random poly(arylene ether)s **I2** and **I4**, described in the previous paragraph, PAES **I3** and **I5** contain additional sulfoxide interarylene bonds in the main chain. Both random and block-copolymer structures of the unique IEC 0.9 meq/g are presented here. For the series **I3** two methods of block-copolymer production are chosen: i) by one pot two reactions, where the length of the hydrophobic block may not be estimated in advance by spectral techniques (***b*-I3-0.9**); and ii) by synthesis of separate blocks, being subsequently condensated (***sb*-I3-0.9**).

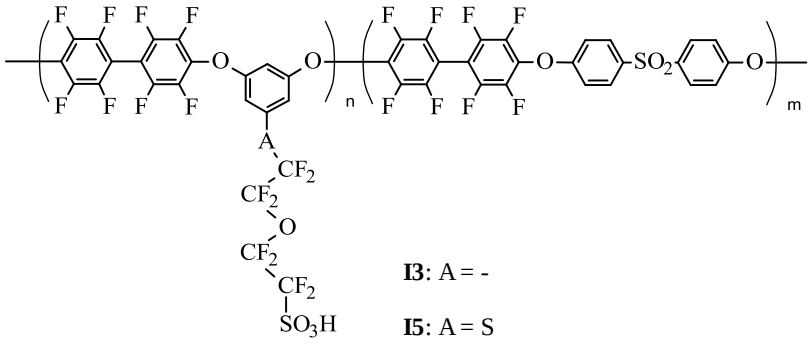

Figure 3.25. General structure of the PAESs series **I3** and **I5**

The main differences in properties of the polymers with random distribution of ionic sites to those with localized highly polar phases are presented. In addition, the samples are compared to the PAEs of the lowest IEC (**I2-1.1** and **I4-1.0**), described above.

3.2.1. Thermal stability

Analysis of the weight loss in temperature on random and related block-copolymers of IEC 0.9 meq/g series **I3** and **I5** is proposed. *Fig. 3.26* shows the thermograms and *Table 3.11* summarizes the data from the graphs. Thermograms contain: solid lines displaying the behavior of K^+-neutralized polymers, dotted lines – of their Li^+-form and dashed one – of the H^+-form. Black curves present the random polymers, green curves are for the block-copolymers.

Just as it was previously described for the ionomers PAEs, potassium-neutralized forms are the most thermally stable, lithiated samples are less stable and protonated are the least resistant to thermal degradation.

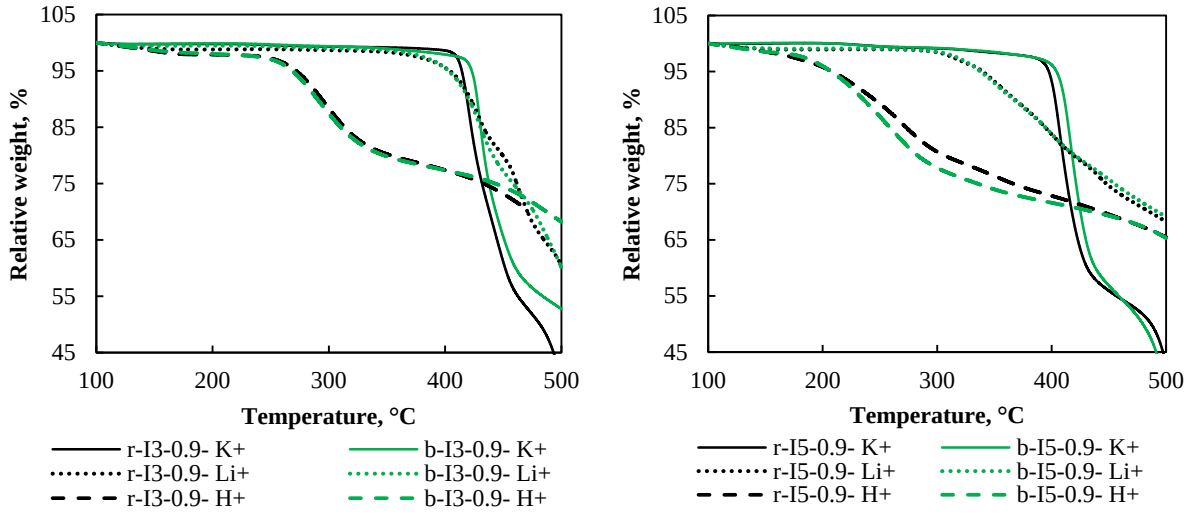

(a) (b)

Figure 3.26. Thermogravimetric curves for the PAESs of IEC 0.9 meq/g series: a) **I3** and b) **I5**

Table 3.11. Analysis of polymer thermal degradation

M^+-form	**Ionomer**	**Thermal degradation onset, T_d, °C**	**Thermal degradation endset, °C**	**Relative weight loss, %**	**Molecular weight loss, g/mol**	**Molecular weight of PFSA-M^+side chain, g/mol**
K^+-form	*r*-I3	400	470	45.4	521.4	332.0
	b-I3	414		39.6	457.9	
	r-I5	382	450	41.7	480.2	367.3
	b-I5	395		39.5	451.9	
Li^+-form	*r*-I3	370	500	36.7	409.7	303.0
	b-I3			36.0	404.7	
	r-I5	298		29.8	333.6	335.1
	b-I5			28.9	321.4	
H^+-form	*r*-I3	250	350	16.9	187.7	297.1
	b-I3			16.5	184.5	
	r-I5	165	300	17.2	191.5	329.2
	b-I5			19.7	217.9	

Relative weight loss is calculated between the two points on thermal degradation onset and endset. These values are related to molecular weight loss with the help of the following equation:

$$MWL = \frac{RWL}{100} \cdot ((MW_{[3(4)-DFB]} \cdot 1) + (MW_{[HS-DFB]} \cdot x)) \qquad (11)$$

where *RWL* is relative weight loss (see *Table 3.11*); $MW_{[3(4)\text{-DFB}]}$ is molecular weight of the ionic structural unit between the monomers **3** or **4** and DFB (which is equal to 700.3 and 732.4 g/mol, respectively); $MW_{[\text{HS-DFB}]}$ is molecular weight of the non-ionic structural unit between HS and DFB (which is equal to 544.4 g/mol); *x* is equivalent of the non-ionic structural unit [HS-DFB], taking the ionic structural unit [**3**(**4**)-DFB] as equivalent 1.

The block-copolymers in their K^+-form start degrading 10-15 °C later, than the random ionomers. Such behavior is probably related to the different organization of the material, where ionic segments are trapped in the shell of hydrophobic blocks, which preserves thermal stability of the block-copolymers. Degradation of K^+-neutralized ionomers happens immediately along the lateral and main chains. It is estimated from experimental molecular weight loss that exceeds greatly the real molecular weight of the PFSA-K^+ groups.

The Li^+-neutralized materials do not show degradation endset up till 500 °C. For the series **I3** deterioration of the main backbone starts in this range (relative weight loss is 100-110 g/mol higher, than the molecular weight of the lateral chain), whereas the polymers ***r*-I5** and ***b*-I5** seem to lose the exact moiety, corresponding to the PFSA-Li^+.

Analysis on protonated samples shows that ionomers of the series **I3** have a distinct steep weight loss in the range 250-350 °C and those of the series **I5** – in the range 165-300 °C. Presuming again that firstly the degradation occurs at the lateral chains, its residue comprises 110-140 g/mol after the degradation event, just as in case of the series **I2** and **I4**. Thermal behavior of the acidic ionomers is probably connected to partial degradation and subsequent cross-linking of the non-degradable residues of the PFSA lateral chains.

Comparing thermal stabilities of the series **I3** and **I5**, the latter is characterized by faster degradation. Such behavior is related to the presence of the sulfanyl bridge between the PFSA lateral chain and the polymer backbone. Undoubtedly, the C-S bond enthalpy is much lower, than the C-C one, which provokes the faster deterioration of an ionomer. The same observation was registered for the PAEs **I2** and **I4**.

3.2.2. Calorimetric analysis

It is important to remind that all the membranes series **I3** and **I5** are produced by the method of solvent evaporation at 60 °C and subsequent annealing at 150 °C overnight. Therefore, all the polymers may be compared. Calorimetric analysis is conducted, as usually, with a pierced capsule upon several heatings. The first cycle for salt-forms of the ionomers are performed in the temperature range RT – 250 °C, for the protonated samples – till 180 °C. The maximal temperature for the next two cycles is chosen, according to the degradation data from *Table 3.10,* counting (T_d-10) °C.

The DSC thermograms are presented in *Fig. 3.27*, the transition temperatures are summarized in *Table 3.12*.

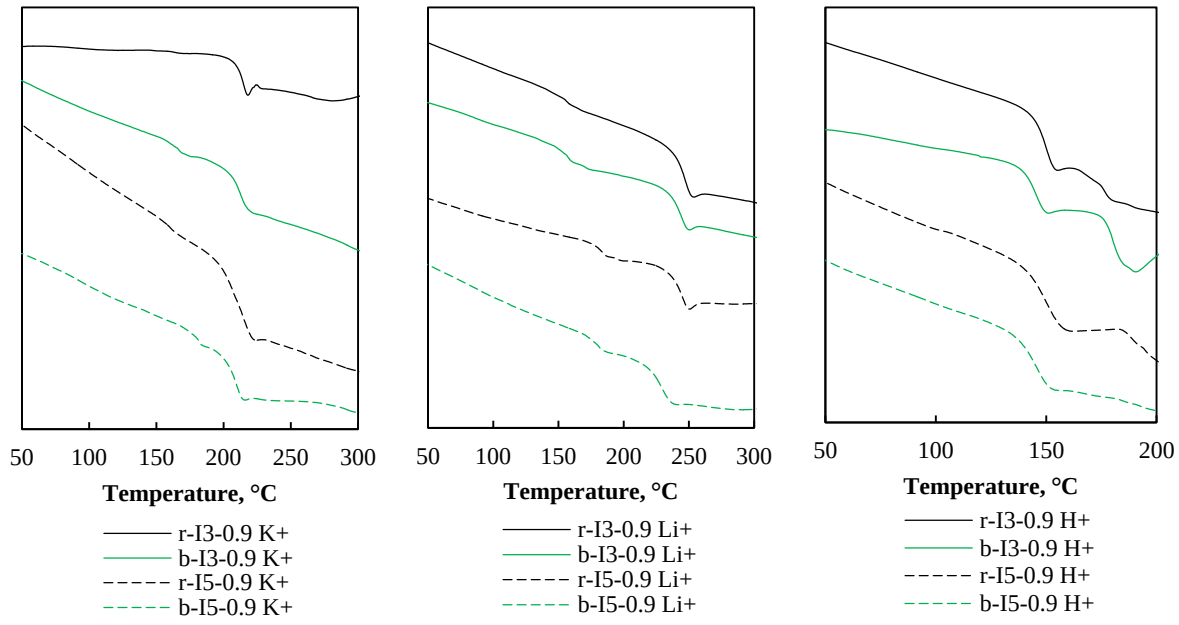

(a) (b) (c)

Figure 3.27. Thermogravimetric curves for the PAESs of IEC 0.9 meq/g series **I3** and **I5**: a) in K^+-form, b) in Li^+-form, c) in H^+-form (acidified from lithated samples)

Random copolymers ***r*-I3** and ***r*-I5** in their K^+-form show high-temperature transitions (T_{HT}) at 212 and 208 °C, respectively. The corresponding block-copolymers ***b*-I3** and ***b*-I5** give similar values. Apart from T_{HT}, all the block-copolymers are characterized by additional low-temperature transition (T_{LT}) at 165 °C for ***b*-I3** and at 178 °C for ***b*-I5**. Both random and structures in block of the lithiated ionomers, however, give two distinct thermal events: transitions at T_{LT} = 156-182 °C and at T_{HT} = 228-247 °C. Moreover, when T_{HT} is similar for the both series **I3** and **I5**, T_{LT} is 15-25 °C lower for the **I3** series (random and block-copolymers), than for the other one.

The nature of the transitions was discussed in detail for the series PAEs, taking to account the results from thermal reply of the ionomers in both static and dynamic modes. It was assumed, that both LT and HT transitions are related to the movements of the polymer chain due to softening of the main backbone: T_{LT} might be provoked by local movements, initiated by a part of the polymer chain of higher mobility (around *meta*-ether connections); T_{HT} is dependent on higher order transitions through the whole aromatic main chain. Undoubtedly, LT transition is dependent on nature of the counter-ion, since the PFSA chain is attached to the main polymer chain by the aromatic ring between the *meta*-ether bridges.

From *Fig. 3.27* LT transition for the lithiated series of polymers is more distinct, than for the potassed one. PFSA-Li^+ lateral groups are less dissociated than PFSA-K^+, which makes them being less immobilized by Coulomb forces. T_{LT} of the block-copolymers in K^+-form is

registered, probably, due to localized distribution of ionic functions, which makes the signal to be detected. Whereas the transition for random copolymers, which have PFSA-K^+ groups being dispersed throughout the polymer chain, is not evident.

Comparing protonated ionomers of the both series **I3** and **I5**, transitions at similar temperatures (140-150 °C) are registered for all the samples. This thermal event is provoked by rupture of hydrogen forces between the ionic groups (see the explanation for the series PAEs). Since all the samples PAES, studied here, bear the same amount of PFSA groups, which is estimated by the IEC, transition temperature must be also similar. ***r*-I3** and ***b*-I3** show additional large endothermal event in the temperature range 170-183 °C. It may be related to transition of the aromatic polymer backbone, but for better resolution thermo-mechanical analysis must be provided.

Table 3.12. Summarized data of thermal events for the ionomers series **I3** and **I5**, extracted from the DSC measurements

Ionomer		**T_m, °C**	**T_{HT}, °C**	**T_{LT}, °C**
K^+-form	*r*-I3-0.9	–	212	–
	b-I3-0.9	325	210	165
	r-I5-0.9	–	208	–
	b-I5-0.9	302	207	178
Li^+-form	*r*-I3-0.9	–	245	156
	b-I3-0.9	–	242	160
	r-I5-0.9	–	240	182
	b-I5-0.9	–	228	179
(Li)-H^+-form	*r*-I3-0.9	–	150	–
	b-I3-0.9	–	145	–
	r-I5-0.9	–	148	–
	b-I5-0.9	–	145	–
(K)-H^+-form	*r*-I3-0.9	–	149	–
	b-I3-0.9	N/A	N/A	N/A
	r-I5-0.9	N/A	N/A	N/A
	b-I5-0.9	N/A	N/A	N/A

All the block-copolymers series **I3** and **I5** contain hydrophilic blocks that are identic in chemical structure to **I2-1.4** or **I4-1.4**. The latter materials in their potassed form were characterized by presence of crystalline part. *Fig. 3.28* presents the DSC thermograms of ***b*-I3-0.9**, ***sb*-I3-0.9** and ***b*-I5-0.9** with the temperature scale up till 360 °C. Crystallinity of these samples is also observed, but in much lower amount, than for the PAEs. Values of ΔH are not given, since they are too small to be measured correctly.

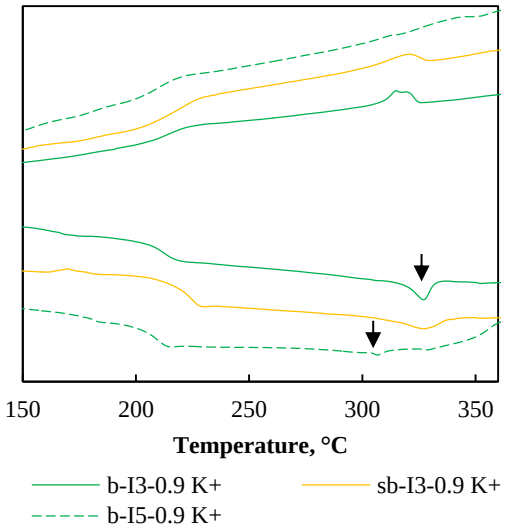

Figure 3.28. DSC spectra for the semi-crystalline block-copolymers ***b*-I3-0.9**, ***sb*-I3-0.9** and ***b*-I5-0.9**

The highest degree of crystallinity (by eye estimation) is attributed to ***b*-I3-0.9**. Interestingly, ***sb*-I3-0.9**, having identic chemical composition, but having been synthesized in a different way, shows larger and lower in intensity melting peak, which points on lower homogeneity of crystalline structure, compared to ***b*-I3-0.9**. Since the only difference between the two block-copolymers is the synthetic route, and during the elaboration of ***sb*-I3-0.9** all the blocks were controlled for the chemical composition, this is ***b*-I3-0.9** only that might have a shorter hydrophobic block. Presumably, the hydrophilic block in the reaction solution during the copolymerization guides the formation of the hydrophobic block of the most appropriate length. Then, when working on production of ***sb*-I3-0.9**, it could happen that the lengths of separate blocks were not equal, therefore when the blocks are copolymerized, a non-symmetric structure is formed. On the contrary, when applying a one pot technique, it is a hydrophilic block only that is synthesized, afterwards the hydrophibic block is formed and immediately copolymerized with the hydrophilic one. Therefore, this is the hydrophilic block that decides the switching between these two processes of block formation and of condensation between the blocks.

***b*-I5** does not show a distinct melting event, but a small variation in enthalpy at 302 °C. Compared to T_m of **I4-1.4** (379 °C) it is 77 °C lower. Besides, the DSC thermogram of ***b*-I5** shows exothermic rise after 330 °C, which might be related to the polymer degradation. Then the value of the T_d, released in *Table 3.11*, is overestimated. Out of these results we conclude that the true melting peak might appear at higher temperature, than 330 °C, and it can not be detected due to the partial degradation of the polymer.

Based on the results, obtained from DSC measurements, one may conclude:

i) Lithiated samples of series **I3** and **I5** show two transitions, called low-temperature LT and high-temperature HT, which were previously described for the series **I2** and **I4** as well. Potassed samples are expected to have the same transitions, but LT lower in enthalpy due to stronger electrostatic bonds between the PFSA-K^+ groups. For the block-copolymers in their potassed state this transition is better detected due to concentrated localization of the ionic sites.

ii) Presence of crystalline part in the block-copolymers is related to the hydrophilic blocks, having the exact composition of the semicrystalline PAEs **I2-1.4** and **I4-1.4**. Problems in detection of T_m for ***b*-I5** might be connected to the partial degradation of the polymer, which was not evident at TGA curves.

3.2.3. Thermo-mechanical analysis

Thermal reply of the ionomers series **I3** and **I5** to applied mechanical force is presented in the following section. Firstly, behavior of the random ionomers ***r*-I3-0.9** and ***r*-I5-0.9** together with correspondent block-copolymer, synthesized by one pot two reactions method, ***b*-I3-0.9** and ***b*-I5-0.9**, in their K^+-neutralized form are demonstrated in *Fig. 3.29 (a)*. Here, black curves present the random copolymers, and green curves – the block-copolymers. From the plots of storage modulus change in temperature it is observed that ***r*-I3-0.9** starts losing its mechanical properties at approximately 10 °C later, than ***r*-I5-0.9**. Meanwhile the block-copolymers of both series show similar loss of mechanical properties in temperature. Another observation from the storage modulus curves is related to the second plateau: it evidences, how material preserves its mechanical properties after the relaxation has occurred. The block-copolymers keep slightly higher values of the second plateau, which may be related to the strength of the ionic bonds of the hydrophilic block. In order to check this assumption, tan δ is analyzed further. Indeed the block-copolymers do not respond with one peak, but with several that overlap. Besides, the high-temperature signal (between 200 and 250 °C) is large and the exast value of this relaxation can not be determined. However, the presence of two separated phases is confirmed for the block-copolymers, and its absence – for the random materials.

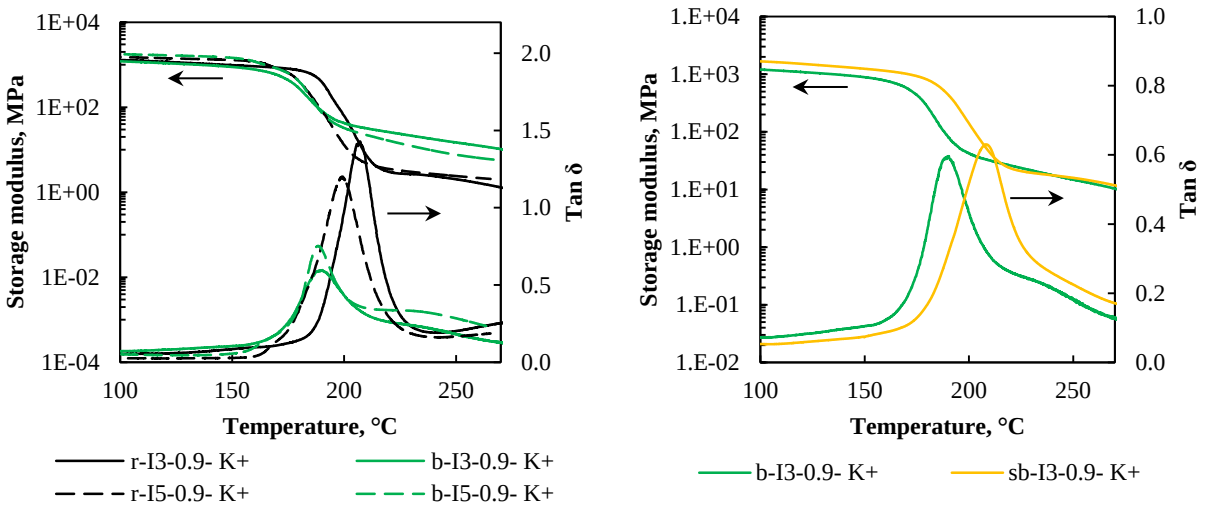

(a) (b)

Figure 3.29. DMA curves for the potassium-neutralized forms of the ionomers series **I3** and **I5**: a) random and block-copolymers, synthesized by one pot method, b) block-copolymers of **I3**, synthesized by one pot method and by condensation of separate blocks

To compare the block-copolymers, synthesized by different methods, *Fig. 3.29 (b)* is illustrated. It shows that ***sb*-I3-0.9** starts losing its thermo-mechanical stability at approximately 10 °C higher, than ***b*-I3-0.9**. However, the similar phase separation is observed for the both samples, which confirms their similar structure.

The lithiated samples, both random and in block, reply with one peak in tan δ, which does not reveal their phase separated morphology. This result is in accordance to the case of PAE series, where separation of ionic and non-ionic structures of the lithated membranes was observed to be much poorer, than of the materials with K^+-counterion.The plots are not presented in the manuscript, but the data on relaxations is summarized in *Table 3.13*.

Protonation of the membranes is performed from both lithiated and potassed forms. *Fig. 3.30 (a)* and *(c)* demonstrate these samples of the random and block-copolymers, synthesized by one pot two reactions method. *Fig. 3.30 (b)* and *(d)* complete the information on the block-copolymers, synthesized by two different methods.

Just as in the case of PAE random copolymers series **I3** and **I5** do not show difference in thermo-mechanical behavior, depending on the initial salt cation. And, as it was observed before, ***r*-I3-0.9** is more stable in temperature under the applied force, compared to ***r*-I5-0.9**. With a closer look on the block-copolymers, however, one may estimate the difference in their thermo-mechanical reply, depending on the counter-ion present prior to protonation.

When acidification of the lithiated ***b*-I3-0.9** and ***b*-I5-0.9** is performed, the ionomers respond with one relaxation and at the same temperature 130-135 °C. But when potassium-neutralized forms are protonated, separation of phases is observed for the both. Moreover, these polymers ((K)-H^+) start losing their mechanical properties at lower temperature of 110-115 °C, than the samples acidified from Li^+-form; and this deterioration continues in a wide temperature range. Such behavior reveals the presence of several phases that relax at different conditions. At the same time ***sb*-I3-0.9** shows distinct phase separation when being acidified from either of two salt forms (*Fig. 3.30 (b)* and *(d)*). The T_α is invariant for both acidied forms of ***sb*-I3-0.9**, while β-relaxation (of lower temperature) dependes on the initial salt cation and happens at lower temperature (112 °C) for the ***sb*-I3-0.9, (K)-H^+**, than for ***sb*-I3-0.9, (Li)-H^+** (130 °C).

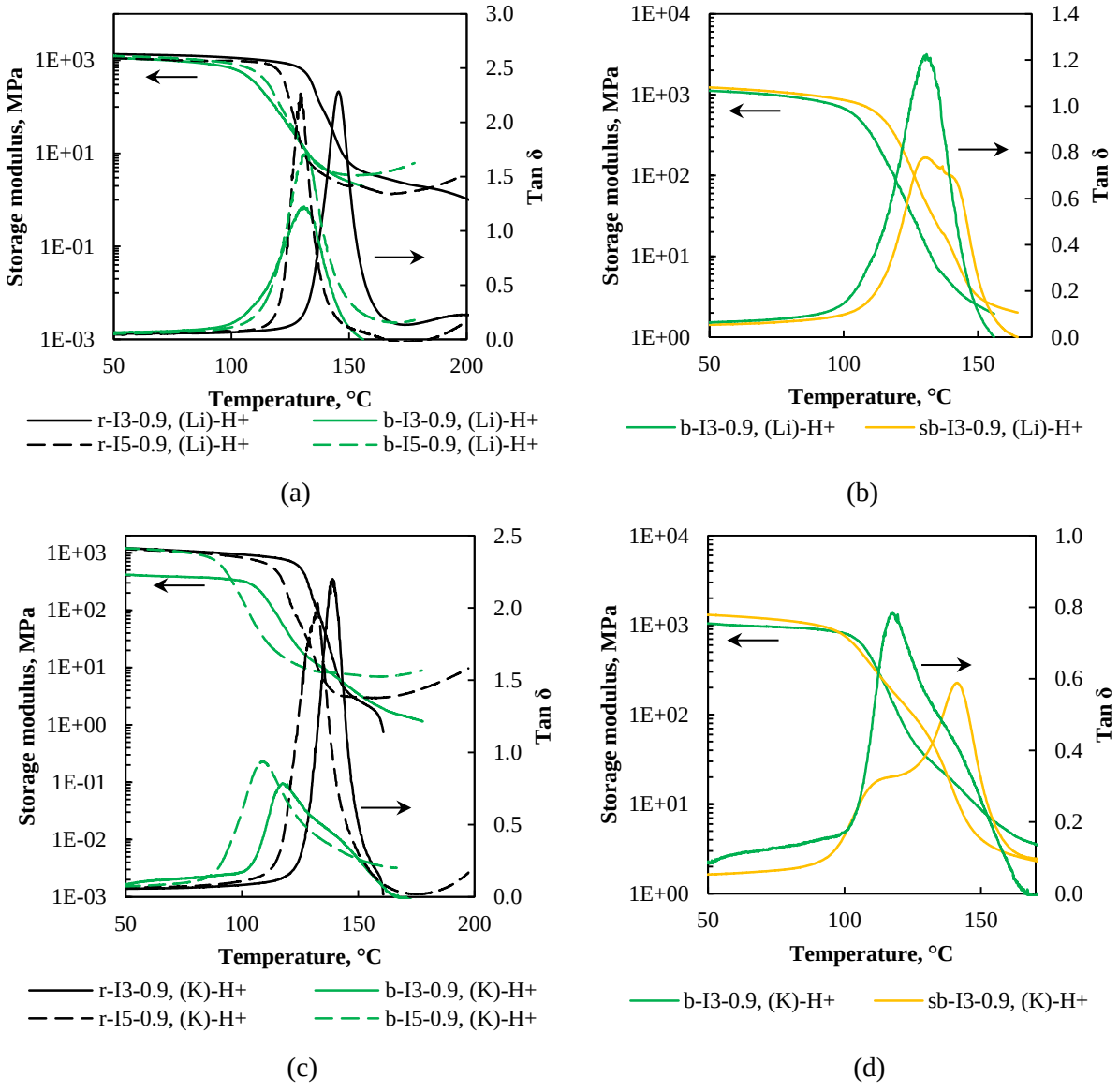

Figure 3.30. DMA curves for the protonated ionomers series **I3** and **I5**: a) and b) samples are acidified from their Li^+-form, c) and d) membranes are protonated from their K^+-form

Similarly to the series PAE, the β-relaxation of the protonated samples is related to the movements of the PFSA groups due to dehydration and loss of hydrogen bonds. If the robust polymer backbone is able to keep the integrity of the membrane, α-relaxation is observed as well. Neither of block-copolymers, protonated from lithiated state, except ***sb*-I3-0.9, (Li)-H$^+$**, is characterized by such behavior. Therefore it is concluded that the both relaxations happen at the same temperature for ***b*-I3-0.9, (Li)-H$^+$** and ***b*-I5-0.9, (Li)-H$^+$**. When acidification is performed from the bigger counter-ion of potassium the separation of the thermo-mechanical reply to the one of the ionic phase (T_β) and to the other, related to the hydrophobic phase (T_α) is observed.

When comparing the storage modulus curves of the ionomers series **I3** and **I5** (without taking to account the synthesis methods, and type of structures (random or in block)), the polymers of the latter series show tendency to rise. Since no similar behavior is observed for the **I3** series, one may conclude that sulfanyl-group contributes to some type of cross-linking of the polymers that preserves their mechanical properties for longer time.

The distinct themo-mechanical reply of the polymer phases may positively influence the polymer structuration and such properties as conductivity and proton diffusion through the well-separated from the polymer phase ionic channels. For this reason, the method of a block-copolymer synthesis by condensation of separate blocks is more preferential.

To compare the accordance between the results from DMA and DSC techniques for all the ionomers series **I3** and **I5**, we refer to *Table 3.13*. To remind the abbreviations: from the DSC results T_{HT} and T_{LT} are high-temperature and low-temperature transitions, from the DMA results T_α and T_β are high-temperature and low-temperature relaxations. For the salt forms of the ionomers T_{HT} and T_{LT} both correspond to the change of energy state of the polymer chain in the frame of strong ionic bonds; for the protonated samples only one transition was always observed, which we refer to T_{HT} and to enthalpy change of interactions between the PFSA-H$^+$ groups. T_α and T_β of the salt forms of the ionomers, on the contrary, estimate relaxations of the ionic groups (and the whole polymer thereafter) and of the polymer chain only in the frame of the ionic connections, respectively. For the protonated samples, sulfonic acid groups are not bound strongly by hydrogen forces, and they become responsible for the β-relaxation, while T_α characterizes creep of the whole polymer.

When comparing the K$^+$-neutralized ionomers between the DSC and DMA data, the same dependence, as for PAE series, is observed: β-relaxation happens at temperature average of T_{HT} and T_{LT}. In case when no T_β is registered (random copolymers ***r*-I3-0.9** and ***r*-I5-0.9**) α-

relaxation, containing performance of the both phases, corresponds to the only transition determined from the DSC.

For the lithiated samples T_{HT} of the ionomers are higher than those of the potassed-polymers, and are similar to T_{α}. Presumably, due to the fact that α-relaxation contains thermo-mechanical reply of the both phases) these values are no more the average of T_{HT} and T_{LT}, but closer to T_{HT}.

Table 3.13. Summarized data of thermal events for the ionomers **I3** and **I5** from the DSC and DMA measurements

Ionomer		**DSC data**			**DMA data**	
		T_m, °C	**T_{HT}, °C**	**T_{LT}, °C**	**T_{α}, °C**	**T_{β}, °C**
K^+-form	*r*-I3-0.9	–	212	–	206	–
	b-I3-0.9	325	210	165	~ 230	194
	sb-I3-0.9	327	220	172	~ 240	210
	r-I5-0.9	–	208	–	197	–
	b-I5-0.9	302	207	178	~ 230	188
Li^+-form	*r*-I3-0.9	–	245	156	247	–
	b-I3-0.9	–	242	160	N/A	N/A
	sb-I3-0.9	–	247	174	238	–
	r-I5-0.9	–	240	182	243	–
	b-I5-0.9	–	228	179	238	–
(Li)-H^+-form	*r*-I3-0.9	–	150	–	145	–
	b-I3-0.9	–	145	–	134	–
	sb-I3-0.9	N/A	N/A	N/A	~ 140	130
	r-I5-0.9	–	148	–	130	–
	b-I5-0.9	–	145	–	132	–
(K)-H^+-form	*r*-I3-0.9	–	149	–	139	–
	b-I3-0.9	N/A	N/A	N/A	~ 130	116
	sb-I3-0.9	N/A	N/A	N/A	141	112
	r-I5-0.9	N/A	N/A	N/A	132	–
	b-I5-0.9	N/A	N/A	N/A	~ 125	109

The protonated samples are in good agreement between the two measuring techniques. Unfortunately, no data is available for the DSC results of the ionomers, acidified from the K^+-form. Since the DMA measurements were repeated at least twice, the results of DMA are, however, credible.

As a conclusion of thermo-mechanical analysis of the PAES series **I3** and **I5**, one may evidence the advantage of the block-copolymer to random structure on the property of phase separation. The phenomenon is principally observed on the protonated samples: random copolymers present one relaxation, block-copolymers – mainly two. The effect of the block-

copolymer synthesis route is compared, and the difference in performance for the samples, synthesized by one pot or by condensation of separate blocks is revealed.

In order to compare the obtained results of thermo-mechanical behavior between the PAE and PAES series, two tables are proposed further. All the materials, presented in the current dissertation, bear the same type of the PFSA lateral group; the only difference is the connecting bridge to the main chain – either directly or through the sulfanyl specie. The samples of **I3** and **I5** series contain poly(arylene ether sulfone) backbone, and the series of **I2** and **I4** contain poly(arylene ether) main chain. Therefore, the effect of chemical structure of the polymer backbone is studied.

Table 3.14 presents comparison of the **I2** and **I3** ionomers. By the IEC values **I3** series is the closest to **I2-1.1**, however, the block-copolymers ***b*-I3-0.9** and ***sb*-I3-0.9** contain the hydrophilic blocks, identical to **I2-1.4**.

Table 3.14. Comparison data of thermal events for the ionomers **I2** and **I3**

Ionomer		**DSC data**			**DMA data**	
		T_m, °C	**T_{HT}, °C**	**T_{LT}, °C**	**T_α, °C**	**T_β, °C**
K^+-form	*r*-I3-0.9	–	212	–	206	–
	b-I3-0.9	325	210	165	~ 230	194
	sb-I3-0.9	327	220	172	~ 240	210
	I2-1.1	–	207 *	138 *	208	193
	I2-1.4	349	209	152	246	185
Li^+-form	*r*-I3-0.9	–	245	156	247	–
	b-I3-0.9	–	242	160	N/A	N/A
	sb-I3-0.9	–	247	174	238	–
	I2-1.1	–	210	179	217	201
	I2-1.4	278	222	172	250	195
(Li)-H^+-form	*r*-I3-0.9	–	150	–	145	–
	b-I3-0.9	–	145	–	134	–
	sb-I3-0.9	N/A	N/A	N/A	~ 140	130
	I2-1.1	–	117	–	118	–
	I2-1.4	–	97	–	105	–

The random copolymers ***r*-I3-0.9-K^+** show comparable behavior to **I2-1.1-K^+**, except no phase separation is registered. It may be proboked by higher rigidoty of the PAES main chain that relaxes at higher temperature, than PAE backbone. When comparing the potassed block-copolymers of the series **I3** to **I2-1.1-K^+**, great difference in T_α is detected, which is, however, similar to the one of **I2-1.4-K^+**. Additionally, the block-copolymers of the **I3** series show melting endotherms, as the **I2** polymer of the highest IEC, but at 22-24 °C lower. Therefore, one must conclude that the block-copolymers retain the properties of **I2-1.4-K^+** as a

hydrophilic part, but are also characterized by higher mechanical rigidity of the polymer backbone, which is estimated from the higher T_β in particular.

General trend of the lithiated samples consists in higher transition and relaxation temperatures, compared to **I2-1.1-Li$^+$**. It might be provoked by higher rigidity of PAES backbone as well due to interactions of the PFSA groups with the polar SO_2-bridge in the main chain. The same dependence is registered for the protonated samples.

Table 3.15 presents comparison of the **I4** and **I5** ionomers. By the IEC values **I5** series is the closest to **I4-1.0**, however, the block-copolymer ***b*-I5-0.9** contains the hydrophilic block, identical to **I2-1.4**. Very similar dependence between the series **I4** and **I5** is observed, as between **I2** and **I3**.

Table 3.15. Comparison data of thermal events for the ionomers **I4** and **I5**

Ionomer		**DSC data**			**DMA data**	
		T_m, °C	**T_{HT}, °C**	**T_{LT}, °C**	**T_α, °C**	**T_β, °C**
K^+-form	*r*-I5-0.9	–	208	–	197	–
	b-I5-0.9	302	207	178	~ 230	188
	I4-1.0	–	195	–	210	181
	I4-1.4	379	198	–	251	183
Li^+-form	*r*-I5-0.9	–	240	182	243	–
	b-I5-0.9	–	228	179	238	–
	I4-1.0	–	–	–	210	185
	I4-1.4	–	–	–	222	202
(Li)-H^+-form	*r*-I5-0.9	–	148	–	130	–
	b-I5-0.9	–	145	–	132	–
	I4-1.0	–	129	–	114	–
	I4-1.4	–	96	–	107	–

Based on all these analyses of data, it may be concluded:

i) PAES main chain contributes with higher mechanical stability to **I3** and **I5** ionomers, compared to PAEs.
ii) Behavior of block-copolymers PAESs is similar to random PAEs (especially of the highest IEC), which suggests that the latter series is not truly random.
iii) Type of the initial counter-ion prior to protonation plays an important role for the structures in block. It probably determines the size of the hydrophilic domains.

3.2.4. Bulk morphology

For a more detailed study of morphology of the random and block-copolymers series **I3** and **I5** of the same IEC 0.9 meq/g SAXS measurements are presented below. From the previous results of thermo-mechanical analysis it was determined that protonated samples of the random copolymers show similar behavior, whether being acidified from the K^+- or the Li^+-form. On the contrary, the block-copolymers perform differently.

In the current section the ionomers in their H^+-form only are under investigation: i) random copolymers in their Li^+-to-H^+ form, ii) block-copolymers in their Li^+-to-H^+ form, and iii) block-copolymers in their K^+-to-H^+ form. *Fig. 3.31* illustrates all these samples in their wet state, equilibrated in water at two different temperatures – 40 and 80 °C. For better comprehension of the spectra the following must be kept in mind: the baseline is the background signal from the cell windows (Kapton), samples humidified at 40 °C are represented with blue markers, those humidified at 80 °C are shown with green markers. The spactra on the left are for the series **I3**, on the right – for the series **I5**. The majority of the membranes are also measured after humidification at 60 °C, but the curves are not given in *Fig. 3.31* for better resolution. However, the results of these experiments are summarized in *Table 3.16*.

From *Fig. 3.31* all the ionomers show an intense and a well-defined correlation peak. It increases in intensity and shifts till smaller *q*-values, which evaluates higher characteristic distances between the scattering objects. The only ionomer, which does not show the same dependence, is the random **I5** copolymer; the sample must be re-measured. The values of q_{max} of the ionomer peaks are summarized in *Table 3.16*, characteristic distances (sizes of the ionic domains) and amount of water molecules per ionic site are also indicated for better comparison.

Comparing the *d*-distances of the ionomers series **I3**, it is observed that random copolymers, which have similar λ-values to those of the block-copolymers, protonated from the Li^+-form, show slightly smaller sizes of ionic domains. The block-copolymers, in their turn, differ in *d*-values as well, when they are protonated from different salt-cations: the K^+-to-H^+ polymer with a block structure swells much more, than ***b*-I3-0.9 (Li)-H^+** and, thus, has much bigger ionic domains – 5.2 nm compared to 4.5 nm at 80 °C. Remarkably, at 40 °C swelling, ***b*-I3-0.9 (K)-H^+** accommodates 15 molecules of water more, than ***b*-I3-0.9 (Li)-H^+**, but the sizes of the ionic domains are equal.

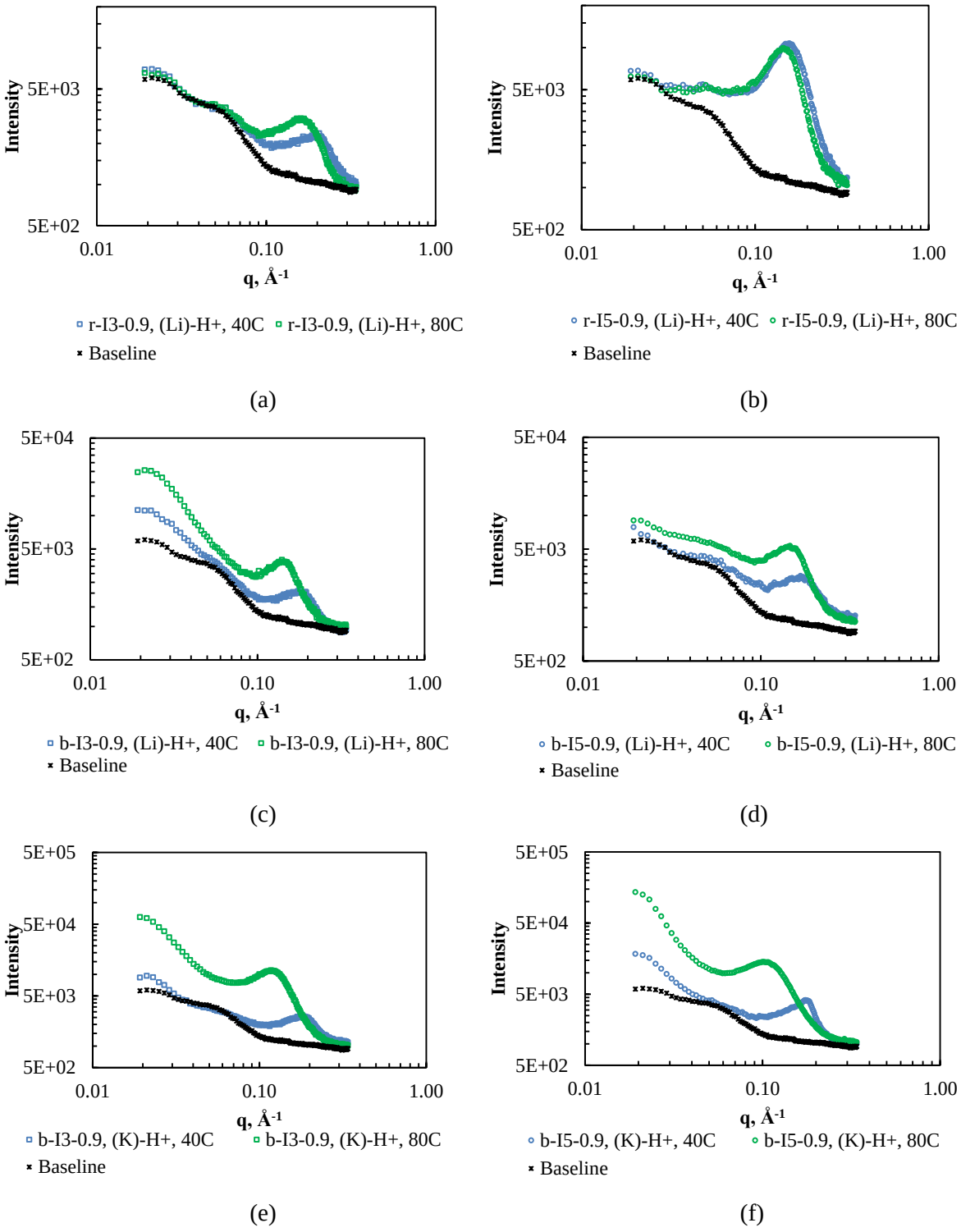

Figure 3.31. SAXS spectraof: a) and b) random copolymers series **I3** and **I5**, respectively; c) and d) block-copolymers series **I3** and **I5**, respectively, protonated from the Li^+-form; e) and f) block-copolymers series **I3** and **I5**, respectively, acidified from the K^+-form

Different dependence is registered for the **I5** series. The random copolymer accommodates similar amount of water and has the same size of the ionic domains, as ***b*-I5-0.9 (Li)-H^+** in the whole range of the studied swelling. The block-copolymer, protonated from the K^+-salt form,

behaves similarly to ***b*-I3-0.9 (K)-H$^+$**: it swells more than ***b*-I5-0.9 (Li)-H$^+$**, but its size of the ionic domains starts to surpass those of ***b*-I5-0.9 (Li)-H$^+$** at swelling higher, than 40 °C.

Table 3.16. Characteristic distances of the protonated ionomers, swollen at different temperatures

Ionomer	40 °C			60 °C			80 °C		
	q, Å^{-1}	**d, Å**	**λ, H_2O/SO_3H**	**q, Å^{-1}**	**d, Å**	**λ, H_2O/SO_3H**	**q, Å^{-1}**	**d, Å**	**λ, H_2O/SO_3H**
r-I3-0.9, (Li)-H$^+$	0.2036	30.8	8.5	N/A	N/A	10.4	0.1614	38.9	11.8
b-I3-0.9, (Li)-H$^+$	0.1844	34.1	8.5	N/A	N/A	10.9	0.1412	44.5	13.1
b-I3-0.9, (K)-H$^+$	0.1863	33.7	23.4	0.1614	38.9	31.2	0.1211	51.9	44.4
r-I5-0.9, (Li)-H$^+$	0.1575	39.9	9.9	0.1575	39.9	11.5	0.1460	43.0	13.8
b-I5-0.9, (Li)-H$^+$	0.1633	38.5	9.2	0.1652	38.0	11.2	0.1499	41.9	13.2
b-I5-0.9, (K)-H$^+$	0.1767	35.5	11.3	0.1460	43.0	14.5	0.1076	58.4	26.9

Based on the described results, random copolymers of both series **I3** and **I5** show similar segregation of ionic phase to the block-copolymers, acidified from the Li^+-form. The block-copolymers, protonated from the K^+-state accommodate much higher amount of water and are characterized by bigger ionic aggregates. Notably, ***b*-I5-0.9 (K)-H$^+$** requires twice less water to attain the same size of the ionic domains as ***b*-I3-0.9 (K)-H$^+$**. Therefore, organization of the polymer chains in ***b*-I5-0.9 (K)-H$^+$** is much more advantegous for better clustering of the ionic groups, than in its counterpart of the **I3** series.

The only curve from the SAXS spectra that is evidently non-symmetric and does not follow the Gaussian distribution is the one of ***b*-I5-0.9 (K)-H$^+$**, humidified at 40 °C. The ionomer peak contains several signals. With a closer look on the curve (*Fig. 3.31 (f)*) extrapolation of the possible peaks is shown with black lines. The current block-copolymer contains hydrophilic blocks of the structure identic to **I4-1.4**. In *paragraph 3.1.4* the unique morphology of this ionomer was studied by SANS technique, and it is again represented in *Fig. 3.32 (b)*. The scattering vectors of the assumed peaks do not match: in ***b*-I5-0.9 (K)-H$^+$** q_{max} are 0.1633 and 0.1806 Å^{-1}, while in **I4-1.4 (K)-H$^+$** q_{max} are 0.1015 and 0.1373 Å^{-1}. Characteristic distances, described by the ionomer peak in ***b*-I5-0.9 (K)-H$^+$**, are then lower than those in **I4-1.4 (K)-H$^+$**, which evidences smaller distance between the ionic domains in the block-copolymer. It happens due to the presence of the hydrophobic block, which does not swell, when wetted; therefore it restricts higher water uptake and increase of dimensions of the ionic aggregates of the hydrophilic block.

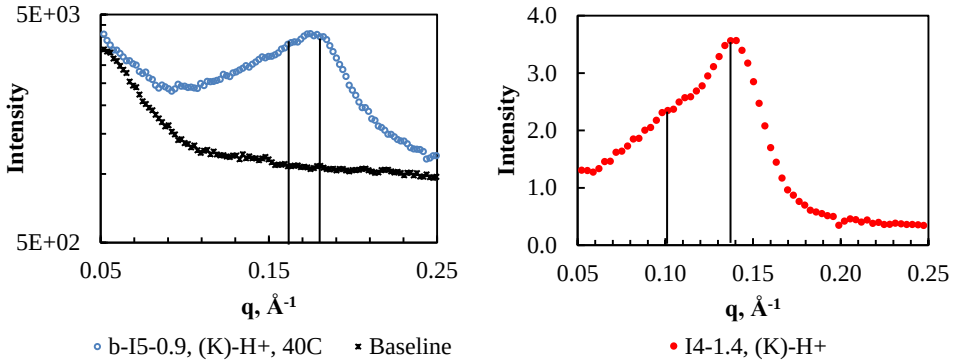

Figure 3.32. a) SAXS spectrum of ***b*-I5-0.9 (K)-H$^+$**; b) SANS spectrum of **I4-1.4 (K)-H$^+$**

Another piece of information that may be extracted for the block-copolymers from their SAXS spectra (*Fig. 3.32*) is the presence of a matrix peak – a signal, which characterizes bigger scattering objects at $q < 0.04$ Å^{-1}. Since it does not appear for random copolymers, it is referred to the repetitive block in the block-copolymer – a hydrophobic block. Comparing the spectra (c), (d), (e) and (f) in *Fig. 3.31*, no real peak may be registered, analyses at smaller angles must be provided. However from the behavior of the curves it is obvious that ***b*-I5-0.9 (Li)-H$^+$**does not show any trend for the matrix peak. The other three block-copolymers, ***b*-I5-0.9 (K)-H$^+$**, ***b*-I3-0.9 (Li)-H$^+$** and ***b*-I5-0.9 (K)-H$^+$** have high-intense upturn at $q < 0.04$ Å^{-1}. Hence, these ionomers might show the characteristic distance between the blocks, which confirms the presence of the block structure.

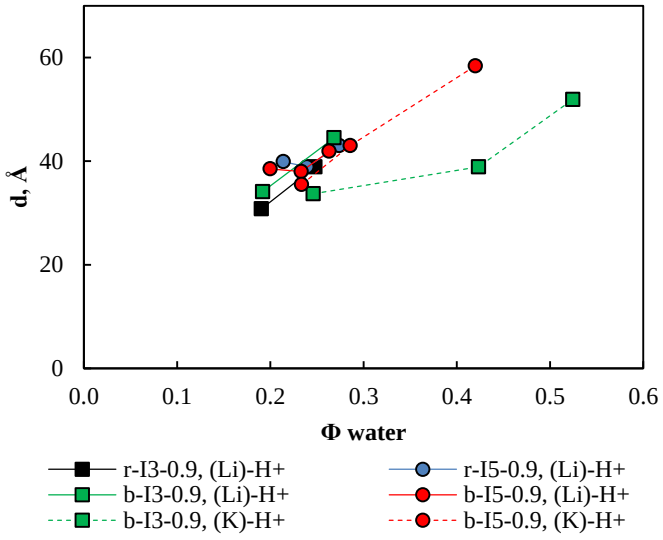

Figure 3.33. Dependence of characteristic distance *d* between scattering ionic objects on water fraction

Analysis of the size of ionic domains on the water fraction os illustrated in *Fig. 3.33*. All the ionomers of the random and block structures of the both series **I3** and **I5** have the same linear dependence. An exception is.***b*-I3-0.9 (K)-H$^+$**, which accommodates higher amount of water,

but reaches lower *d*-distances. To better understand the current phenomenon more points on the graph $\Phi_{water} = f(d)$ must be plotted.

3.2.5. Water uptake

In the current paragraph swelling behavior of the random and corresponding block-copolymers of the series PAESs is under investigation. The membranes are measured in their H^+-form. Since block-copolymers showed peculiar thermo-mechanical and morphological properties, when acidified from different salt forms, the materials of both protonation ways will be studied. The discussion on the random copolymers will include the samples, acidified from the lithiated ionomers only, because their behavior is identical to the one of the membranes, acidified from the potassed state.

Fig. 3.34 presents the swelling behavior of the series **I3** and **I5** with the same concentration of ionic groups, IEC = 0.9 meq/g. The polymers, acidified from the lithiated materials, are shown as filled markers with solid lines; the ionomers, protonated from their K^+-form, are presented as filled markers with dashed lines. The polymers with PFSA chains, directly connected to the polymer backbone, have square markers, the ones with sulfanyl bridges between the PFSA and a main chain are of round markers. Random copolymers are represented with black color, block-copolymers with green.

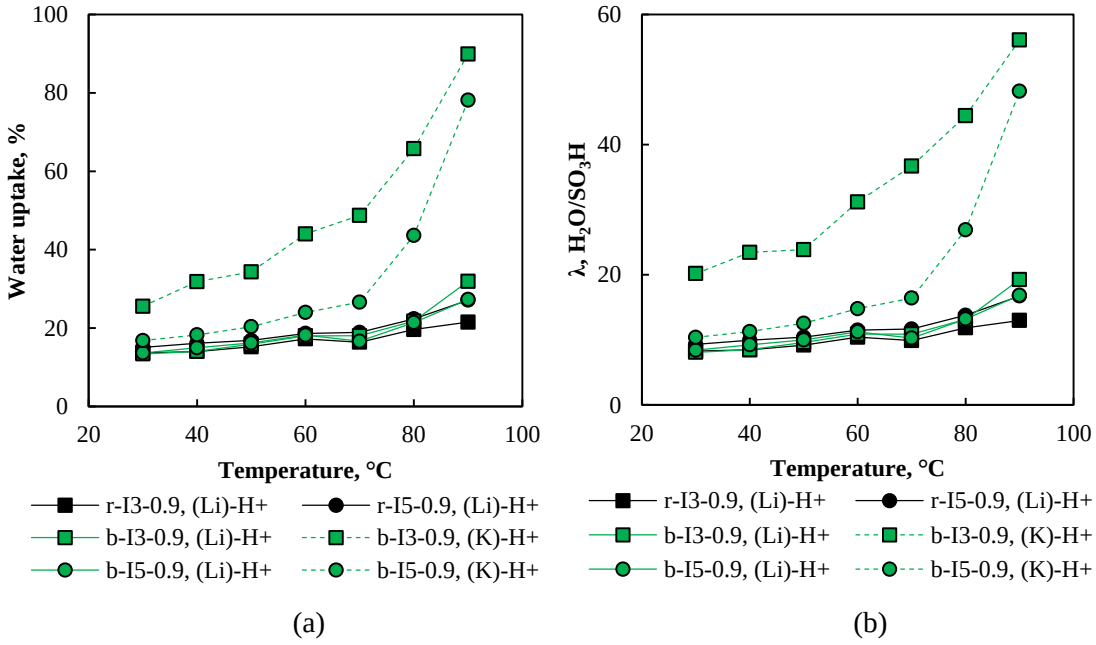

Figure 3.34. Swelling behavior of ionomers series **I3** and **I5** in water in temperature range 30-90 °C, represented as: a) water uptake in percent to the dry weight, b) lambda – amount of water molecules per an acid site

The random copolymers show similar water uptake as block-copolymers, acidified from the lithiated salts in the range 30-60 °C. At 70-90 °C the latter of the series **I3** gains up till 10 % more of water, than its random equivalent. Meanwhile the membranes ***r*-I5-0.9** and ***b*-I5-0.9 (Li)-H^+** continue overlaying when swelling.

Completely different behavior is observed for the block-copolymers, acidified from the K^+-form. ***b*-I8-0.9 (K)-H^+** moderately gains from 10 till 16 water molecules per sulfonic acid site at 30-70 °C. Then wetting continues in a steeper way – ***b*-I8-0.9 (K)-H^+** gains 32 water molecules till 90 °C. ***b*-I3-0.9 (K-H^+)** shows even more peculiar behavior: its high swelling occurs even at low temperatures. When all the other samples gain 13-16 % of water at 30 °C, ***b*-I3-0.9 (K-H^+)** already contains 25-26 %, which is twice more.

Such behavior of the block-copolymers, when acidified from their potassed salt, may be explained in relation to bulk morphology. It was previously discussed that the block-copolymers show a better phase separation, when protonated from K^+-state. It is related to both higher volume of K^+-ion, and better dissociation of the ionic chains, which, most probably, direct the organization of the polymer in general. In such a way, these materials might tend to form bigger hydrophilic aggregates, which cluster to larger domains. After acidification the cluster shell stays of the same size, but due to the lower volume of protons, compared to potassium, bigger free volume is created. This property provokes higher water uptake.

The block-copolymers, acidified from K^+-form, show different swelling behavior between the two series. Two reasons are proposed: 1) when producing a membrane, polymer solution of ***b*-I3-0.9-K^+** is too viscous and contains an important part of microgel structures; in a membrane they may provoke local overswelling compared to the other parts of the membrane; 2) morphology of the ***b*-I3-0.9-(K)-H^+** and ***b*-I5-0.9-(K)-H^+** is different, proved by SAS measurements – the latter ionomer has well-distinguished two ionic domains, one of which was proposed to be surrounded by homogeneous crystallites, which restrict excessive swelling.

When synthesizing the block-copolymer series **I3** by the method of separate block condensation, the crystallinity is much less developed (compare the DSC curves from *Fig. 3.8*). Additionally, the polymer solution of ***sb*-I3-0.9** in both salt forms, when producing a membrane, does not contain comparable quantity of microgles, as in its correspondent, synthesized by one pot two reactions. WU behavior of ***sb*-I3-0.9**, acidified from lithiated and potassed forms is compared to the other block-copolymers of the both series in *Fig. 3.35*. The

sample, protonated from the potassed ionomer, shows much lower WU, than the identic polymer, being synthesized by one pot method. Moreover, its swelling behavior is common to that of ***b*-I5-0.9 (K)-H$^+$** up till 70 °C. At 80-90 °C ***b*-I5-0.9 (K)-H$^+$** accommodates 7-14 water molecules more, than ***sb*-I3-0.9 (K)-H$^+$**.

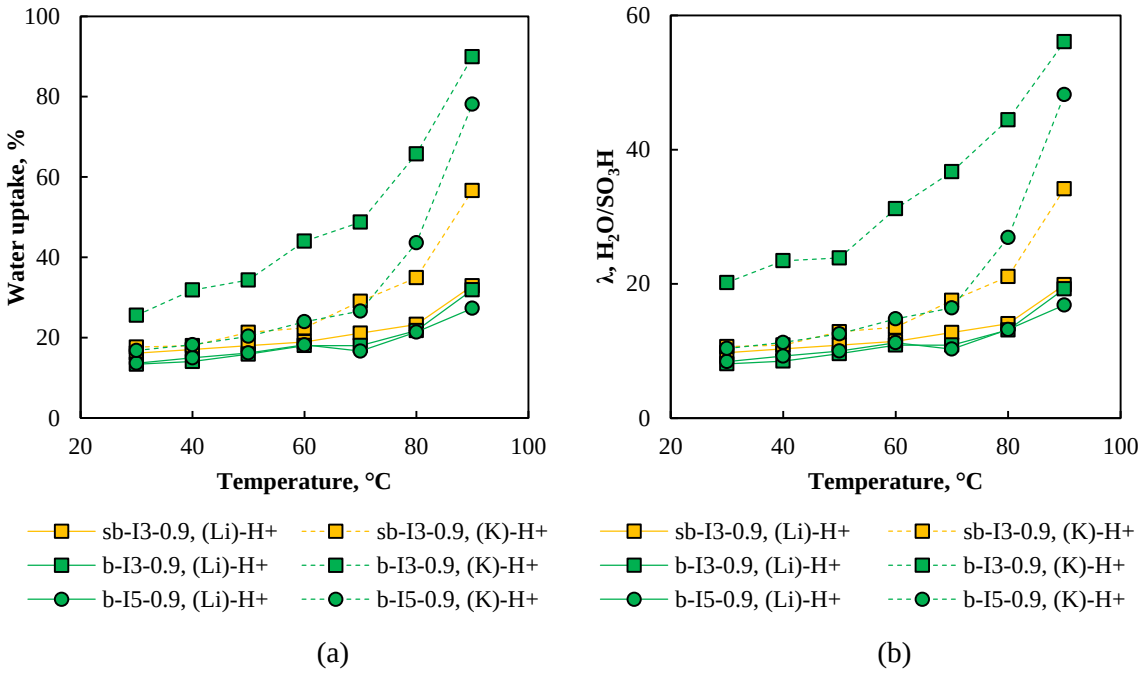

Figure 3.35. Swelling behavior of the block-copolymers series **I3** and **I5** in water in temperature range 30-90 °C, represented as: a) water uptake in percent to the dry weight, b) lambda – amount of water molecules per an acid site

In order to complete the study on swelling and to check the hypotheses of anomalous swelling of ***b*-I3-0.9-(K)-H$^+$**, its membrane must be produced, applying centrifugation of the microgel part.

3.2.6. Conductivity

Proton conductivity of random and block-copolymers of the series **I3** and **I5** is illustrated in *Fig. 3.36*. To remind, all the ionomers bear the same concentration of ionic sites (IEC 0.9 meq/g). For better resolution series **I3** are given in (a)-graph and series **I5** in (b)-plot.

First of all it is evident that all the synthesized ionomers conduct less than Nafion at 95 %RH in temperature range 30-90 °C. Comparing performance of random and block-copolymers series **I3**, the curve of the former ionomer shows a steeper slope in the range 1.0-5.3·10^{-3} S/cm. Basically, it "connects" the conductivity values of ***b*-I3-0.9 (Li)-H$^+$** at 30 °C and of ***b*-I3-0.9 (K)-H$^+$** at 90 °C. Such behavior is peculiar in terms of its validity for the series **I5** as well: ***r*-I5-0.9** shows conductivity range of 9.9·10^{-4}-1.1·10^{-2} S/cm, which is

comparable to performance of ***b*-I5-0.9 (Li)-H$^+$** at low temperature and of ***b*-I5-0.9 (K)-H$^+$** at high temperature. The physical meaning of the slope of the conductivity dependence on inverse temperature is activation energy: higher the slope, higher the activation energy for proton conduction. Therefore, the random copolymers are estimated to have higher activation energy for the conductivity event, than the block-copolymers. Such a result allows assuming that the block-copolymers have morphology, which facilitates protons to pass through the polymer, probably due to higher connectivity of the ionic domains.

When comparing conductivities between the two series, **I5** performs better, either of random structure or in block. Apart from having bigger in size ionic domains (that was determined by SAXS), it may also evidence the better connectivity between these domains. Such conclusion is revealed, taking to account the much lower WU of the **I5** polymers (especially of the block-copolymers, acidified from the potassed form). Again, referring to the chemical structure of the polymers, it may be related to the presence of the sulfanyl bond, which contributes with additional point of flexibility of the PFSA lateral chain.

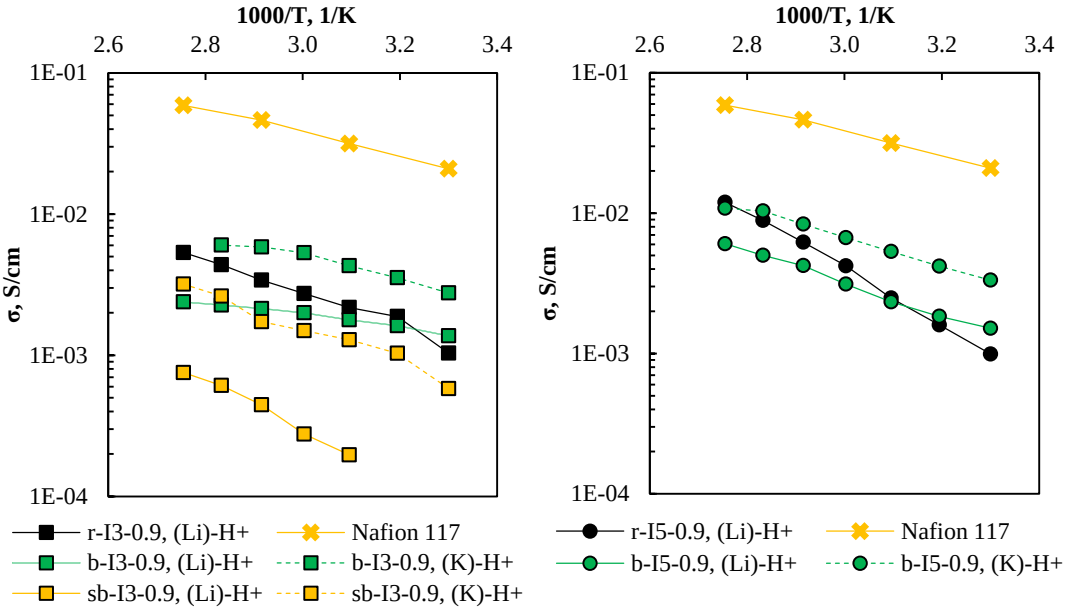

(a) (b)

Figure 3.36. Conductivity dependence on inverse temperature at 95 %RH for the ionomers series: a) **I3**, and b) **I5**

Fig. 3.36 (a) also illustrates the behavior of the ***sb*-I3-0.9** ionomer, synthesized by condensation of separate blocks. The material shows difference in conductivity, when acidified from Li$^+$- or from K$^+$-form, just as it was remarked for all the block-copolymers previously. However, the material of higher conductivity (protonated from the potassed sample) reaches conductivity of ***b*-I3-0.9 (Li)-H$^+$** only at high temperature. Referring to the

data of WU from the previous paragraph, swelling of ***sb*-I3-0.9 (Li)-H$^+$** is comparable to that of random and other block-copolymers, acidified from the lithiated state, while swelling of ***sb*-I3-0.9 (K)-H$^+$** is similar to that of ***b*-I5-0.9 (K)-H$^+$** and much lower than that of ***b*-I3-0.9 (K)-H$^+$**. Based on these observations, it is evidenced that ***sb*-I3-0.9 (Li)-H$^+$** has either small ionic domains or badly connected ionic channels. The recent results of SANS (not discussed in the previous paragraph) showed a highly organized material with ionic domains' size, comparable to that of the block-copolymers, synthesized by one pot method. Additionally, from the thermo-mechanical analysis a well-separated to phases structure was revealed. Therefore, it is, most probably, connectivity of the proton channels that results in low conductivity of the membrane.

Fig. 3.93 additionally illustrates conductivity study at reduced humidity at 80 °C. Random and block-copolymers, synthesized one pot, of the series **I3** have such high resistances that their conductivities may not be correctly estaimated. The only reference point may be plotted for ***b*-I3-0.9**, acidified form its K$^+$-form, at 80 %RH. Unexpectedly, the block-copolymer, synthesized by copolymerization of separate blocks and showing much lower conductivities at 95 %RH, than the other materials of the same series, overperforms at lower humidity. However, its conducitivity is still low, and it may not be measured at humidity < 60 %RH.

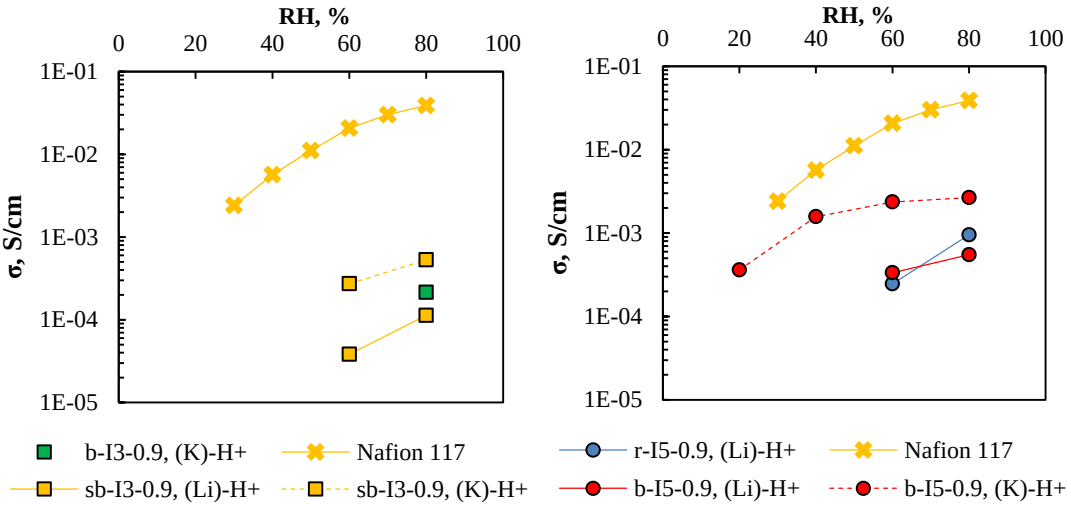

Figure 3.37. Conductivity dependence on relative humidity at 80 °C for the ionomers series: a) **I3**, and b) **I5**

On the contrary to PAES series **I3**, series **I5** shows more promising values of conductivity at humidity < 95 %RH. We were able to estimate conductivity of the random copolymers at RH = 60-80 %. Due to exclusively two points that were measured (at 60 and 80 %RH), it is not possible to assure, whether random copolymer indeed conducts better, than ***b*-I3-0.9 (Li)-**

H$^+$ at 80 %RH; additional measurements must be provided. However, the conductivities of the block-copolymer, protonated from the K$^+$-form, may be estimated in the whole range of measure relative humidity, it comprises $3.6 \cdot 10^{-4}$-$2.7 \cdot 10^{-3}$ S/cm at 20-80 %RH. So far, ***b*-I5-09 (K)-H**$^+$ is the only sample from all the series PAES of the IEC 0.9 meq/g that shows more or less satisfactory performance.

Hence, in order to compare proton conductive ability of the ionomers series PAES and PAE, ***b*-I5-09 (K)-H**$^+$ and **I4-1.0** are chosen (*Fig. 3.38*). The both materials have similar IEC, moreover, PFSA lateral group is attached by the sulfanyl bridge for the both polymers. **I4-1.0** overperforms the block-copolymer two timed at 20-40 %RH and almost three times at 80 %RH. These results show that actually the random PAEs may better retains water molecules in its structure, and, probably, their conductive channels are more developed and more connected.

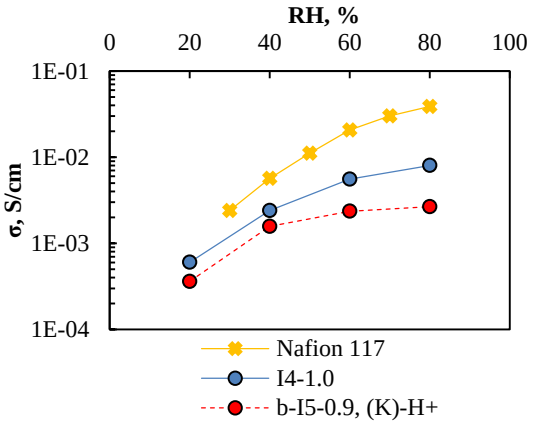

Figure 3.38. Conductivity dependence on relative humidity at 80 °C for the ionomers PAES and PAE

From the conductivity results the following conclusions are drawn:

i) PAES ionomers are characterized by much lower conductivity than PAEs in all rnage of temperatures and humidity;
ii) Block-copolymer structure does not seem to influence much the conductive properties of the ionomers;
iii) Great difference in a block-copolymer performance plays the initial salt cation, neutralizing the PFSA groups. Bigger the initial cation in the salt-state of an ionomer (Potassium *vs* Lithium), higher the conductivity of the subsequent acidified material.
iv) PAES series **I5**, both random and with a block structure, have more preferable organization of proton-conducting phases, than the series **I3**. It was explained from the point of higher mobility of PFSA chains due to the S-connectivity of the lateral group to a polymer backbone.

3.2.7. Oxidative stability test (OST)

The test of oxidative stability of PAES ionomers is conducted at the same conditions, as for the series PAEs. Again, little increase in weight occurs when a membrane becomes brittle, which means that, most probably, the degradation happens at the main chain. To verify such a supposition, the data on random and block-copolymers series **I6** and **I8** is presented in *Table 3.17*. During the OST it is enough for the molecular weight (Mn) of a polymer to lower down till 20 kg/mol for that material becomes breakable. The time for the PAESs degradation is approximate, but there exists a slight difference between **I6** and **I8**: the latter being more susceptible to oxidation.

Table 3.17. Results of the OST for the PAESs

Ionomer	**Time of OST, h**	**Mn (before OST), $\times 10^3$, g/mol**	**Mw (before OST), $\times 10^3$, g/mol**	**PDI (before OST)**	**Mn (after OST), $\times 10^3$, g/mol**	**Mw (after OST), $\times 10^3$, g/mol**	**PDI (after OST)**
I6	7	117.5	263.4	2.2	22.0	43.3	2.0
b-I6	7	76.8	1650.0	21.5	solubilizes		
I8	6	135.0	656.0	4.9	19.2	28.2	1.5
b-I8	6	89.0	1209.0	13.6	19.1	33.1	1.7

Such a result appears to be less expectable: it was assumed that sulfanyl bridge between the PFSA and a polymer backbone would capture the radicals and self-oxidize, avoiding the cleavage of a main chain or a lateral one. However, comparing the ^{19}F NMR spectra of the samples before and after OST, no S-C$\underline{F_2}$ signal displacement towards lower chemical shifts is observed (suppleme info). Additionally, similar to the series PAEs, there appear new peaks for fluorines, corresponding to the DFB zone. Integration of the signals evidences decrease of the DFB (peaks # 9 and 10 at ^{19}F NMR) and of HS species (peaks # 3 and 4 at ^{1}H NMR).

Interestingly, the oxidative degradation for the series PAEs showed the decrease of the ionic part, whereas the series PAESs have the radical attack happening in the non-ionic part of a polymer. Presumably, presence of the –SO_2– bridge in PAESs series creates high –*I*- and –*M*-effects, which delocalize electron doublets from the Oxygen in *para*-position. Such withdrawing force is stronger, than the force of PFSA or –S–PFSA groups in *meta*-position to the ether-link between DFB and an ionic monomer. For this reason PAESs are subjected to cleavage through the Oxygens between DFB and HS. Comparing to the PAEs series, no strong delocalization is provoked by BP moiety, therefore the –*I*-effect of the *meta*-localized (–S–)PFSA creates stronger withdrawing force, and Oxygens between DFB and monomers **3** or **4** are the most susceptible to radical attack.

3.3. Properties of the random (PAES)s series I1 and I3

The current section compares PAES of the series **I1** and **I3**, which structures are illustrated in *Fig. 3.39*. The main difference between the two samples lies in that **I1** series has a totally hydrogenated polymer backbone, while **I3** – a partially fluorinated.

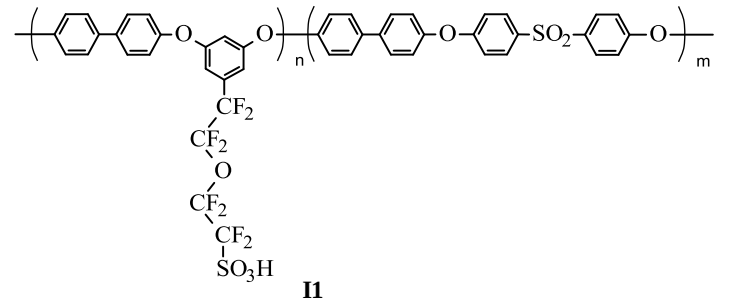

I1

(a)

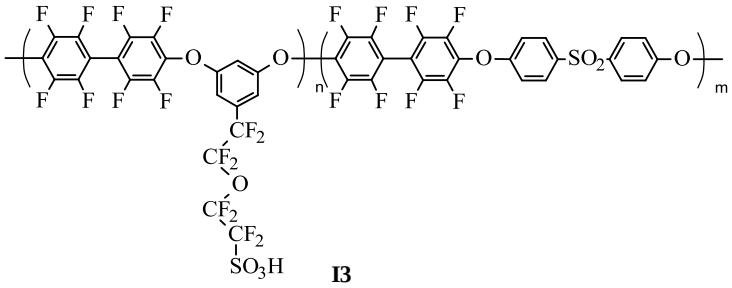

I3

(b)

Figure 3.39. Chemical structures of the random PAESs: a) series **I1** and b) series **I3**

Apart of this, the ionomers differ in:

i) The synthesis procedure – **I1** was copolymerized at 180 °C in NMP, while the polymerization reaction of **I3** proceeded at 45 °C in DMAc. In the previous chapter all the problems while treating the **I1** polymers were described in detail. High reaction temperature was assumed to be the main reason of these inconveniences.

ii) Polymer treatment prior to membrane elaboration – **I1** solution, being highly viscous, even after the filtration contained some part of microgels, which subsequently are present in membranes. **I3**, being viscous but homogeneous solution, was cast to a homogeneous membrane.

iii) Membrane elaboration – **I1** membrane were not studied in detail for the impact of a membrane heating on the polymer thermal and thermo-mechanical reply. Meanwhile, **I3** membranes are always annealed at 150 °C after complete evaporation of the solvent.

All these factors will influence the feasibility to compare the results between the series **I1** and **I3**. Supposedly, the last aspect of membrane annealing is the most important, as it was described for the PAEs in *paragraph 3.1*. Therefore, we reveal that the data on thermo-mechanical properties of the series **I1** may be lower, than if the membranes were annealed. However, the general trend of transition / relaxation temperature change may be still taken to account.

I1 ionomers of two different IECs are studied – **I1-1.0** and **I1-1.3**. Taking to account that some ionic part of the polymers is washed out with alcohol, when eliminating low molecular weight products (see *paragraph 2.2.1*), the real values of IEC are estimated as 0.9 and 1.2 meq/g. Therefore, **I1-1.0** may be compared to ***r*-I3-0.9** and **I1-1.3** to ***r*-I3-1.1**, as such having identic amount of ionic groups per gram.

3.3.1. Thermo-mechanical properties

The both series of random copolymers are analyzed by their reply in DSC and DMA analyses. The data are summarized in *Table 3.18.* First, it is evidenced that ionomers **I1**, having totally hydrogenated backbone, are more rigid, since their transitions / relaxations occur at higher temperatures. Then the thermal events may not be related to the movements of a polymer chain only, because, in general, partially fluorinated polymers are supposed to be more robust, than hydrogenated ones. Hence, the transitions / relaxations in *Table 3.18* are dependent on energy state change either movements of both polymer backbone and lateral groups.

Table 3.18. Thermo-mechanical properties of the PAES series **I1** and **I3**

Ionomer		**T_g, °C**	
		DMA	**DSC**
K^+-form	I1-1.0	212	120 / 215
	I1-1.3	239	120 / 245
	r-I3-0.9	208	213
	r-I3-1.1	203	213
Li^+-form	I1-1.0	249	–
	I1-1.3	241 / 289	–
	r-I3-0.9	249	230
	r-I3-1.1	226	213
H^+-form	I1-1.0	170	168
	I1-1.3	149	162
	r-I3-0.9	144	150
	r-I3-1.1	118	128

Remarkably that increasing IEC of the ionomers **I1** in both salt forms results in augmentation of glass transition temperature, whereas the contrary dependence is observed for the **I3** series of random copolymers. It is assumed that in **I1** polymers PFSA lateral chains have more probability to electrostatically interact with polar sulfone group in a backbone, than those in **I3** polymers, where presence of big Fluorine-atoms may restrict accessibility of the ionic groups towards SO_2-bridge.

The protonated materials of both **I1** and **I3** series show plasticizing effect of the PFSA side groups, presuming that in case of acidic lateral groups they prefer to interact between each other by hydrogen forces, rather than with sulfoxide of the main chain.

3.3.2. Water uptake and conductivity

In order to compare water uptake abilities of random copolymers series **I1** and **I3**, a reader is referred to *Fig. 3.40*. From the image (b) it is evident that the polymers from different series but of the same IEC accommodate identic amount of water molecules up till 60 °C. After that **I1** materials start swelling much more, than **I3**. Such behavior may be again explained from the point of the backbone chemical structure. Since **I1** polymers are less hydrophobic due to totally hydrogenated main chain, they swell more. Presumably, up till 60 °C the membranes swell in the same way, because water molecules occupy the vacant space in-between polymer chains. As soon as there is no free volume, membranes start to swell. Since **I1** are more affine towards water, than **I3**, they swell more.

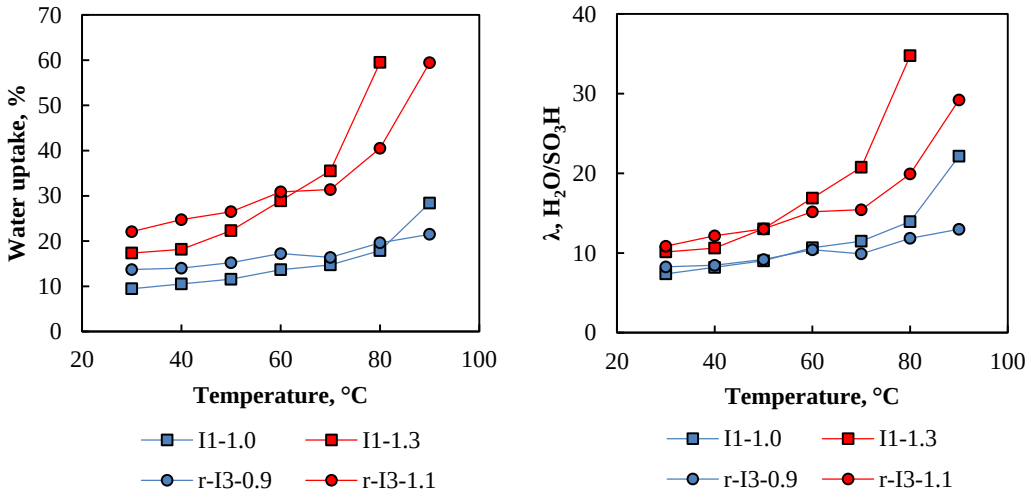

(3) (b)

Figure 3.40. Swelling behavior of random ionomers series **I1** and **I3** in water in temperature range 30-90 °C, represented as: a) water uptake in percent to the dry weight, b) lambda – amount of water molecules per an acid site

Conductivity was measures at 95 %RH in the whole temperature range that is illustrated in *Fig. 3.41*. Squared markers present **I1** series, round markers – **I3** series. The former materials show higher conductivity, than **I3**. These results are contraversive to the idea that high phase separation in a polymer favors its higher performance. **I3**, having fluorinated main chain must develop higher phase separation, compared to **I1** with fully hydrogenated backbone. For this reason a study on the ionomers' **I1** bulk morphology must be provided. Additionally, deeper analysis of the membrane elaboration technique has to be developed. In general, these ionomers show promising properties, but without complete understanding of the ionomer organization no affirmation on their structure-property relation may be concluded.

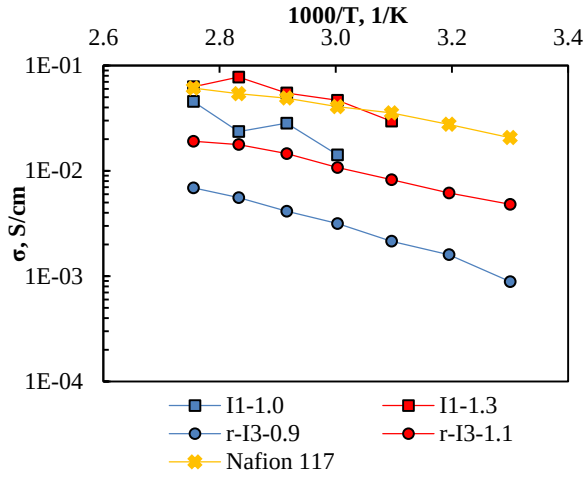

Figure 3.41. Conductivity dependence on temperature at humidity 95 %RH

Based on the analysis of the PAES series **I1** and **I3** it may be concluded that the former series is more interesting as a proton conducting membrane in terms of its higher T_g and conductivity. However, the study is not explicit, e.g. a better solution for membrane elaboration must be presented. Also a detailed analysis of the bulk morphology and its correlation to the one of the **I3** series must be given.

3.4. Properties of the ionomers by copolymerization of two ionic monomers

General structure of the block-copolymer ***sb*-I6** is represented in *Fig. 3.42*. To remind, its IEC is 1.4 meq/g, and the hydrophobic block has length twice as the length of the hydrophilic block.

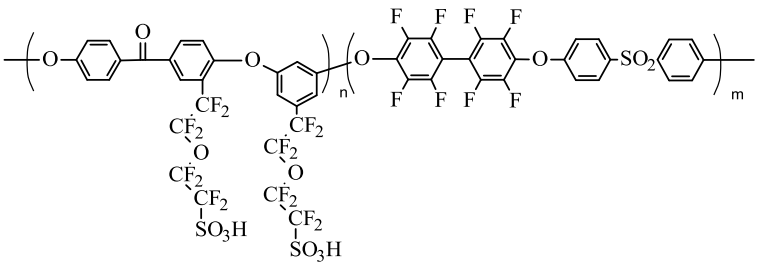

***b*-I6**

Figure 3.42. General structure of ***sb*-I6**

Similar to PAES block-copolymers, described in *paragraph 3.2*, the membranes ***sb*-I6** are also produced in the K^+- and Li^+-salts. Subsequently, the protonated samples exist equally in two forms: acidified from a potassed membrane and acidified from a lithiated membrane.

3.4.1. Thermo-mechanical properties, morphology

Thermal reply of all the four ionomers in static (from DSC data) and dynamic (from DMA data) modes are presented in *Table 3.19*. Relation between two measuring techniques is in good agreement. All the samples showed one thermal event, therefore no evident phase separation was observed. The T_g of the protonated samples is high enough to assure good thermo-mechanical properties of the membranes ***sb*-I6** in conditions of a real FC.

Table 3.19. Summarized data of thermal events for the ionomers ***sb*-I6** from the DSC and DMA measurements

Ionomer	**Transition / relaxation temperature, °C**	
	DSC data	**DMA data**
sb-I6-1.4, K^+	N/A	223
sb-I6-1.4, Li^+	254	254
sb-I6-1.4, (Li)-H^+	140	178
sb-I6-1.4, (K)-H^+	143	168

SANS analysis was provided in order to preview the bulk morphology of the membranes. For the moment measurement of the polymer, acidified from the Li^+-state only (equilibrated in water at 60 °C), is performed, and the data are plotted in *Fig. 3.43*. Similarly to the ionomers, studied earlier, the sample ***sb*-I6-1.4 (Li)-H^+** shows intense and well-defined ionomer peak at scattering vector q = 0.1210 $Å^{-1}$. It is related to characteristic distance between the scattering objects d that is equal to 51.9 Å.

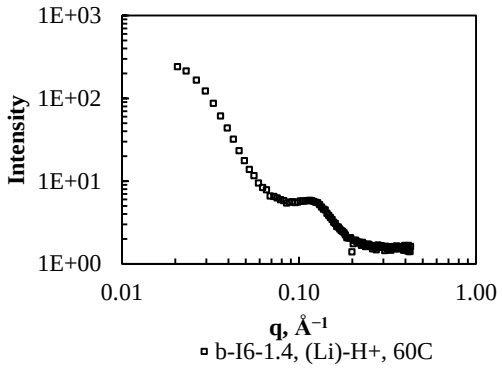

Figure 3.43. SANS measurement of the ionomer ***sb*-I6-1.4 (Li)-H^+**

We were interested in comparing the characteristic distance of ***sb*-I6-1.4 (Li)-H^+** to those of other ionomers: i) to block-copolymers, having identic hydrophobic block, but much less dense in PFSA groups hydrophilic block; besides, the main chain of the hydrophilic block also differs in chemical structure; ii) to the random PAE **I2-1.4**, having similar IEC. All the samples were equilibrated in water at 60 °C. This comparison (*Table 3.20*) shows that: i) ***sb*-I6-1.4 (Li)-H^+** accommodates similar amount of water and creates ionic domains of the size, comparable to those in random **I2-1.4** (> 5 nm), however the block-copolymer keeps its integrity at highly humidified conditions and at high temperatures, which is not the case for the random material; ii) presuming that ***b*-I3-0.9 (Li)-H^+** is characterized by the same *d*-distance, as ***b*-I3-0.9 (K)-H^+**, its value is more than 1 nm lower, than that of ***sb*-I6-1.4 (Li)-H^+**: ionic aggregation in the latter material is much more developed due to higher concentration and proximity of acidic functions.

Table 3.20. Comparison between the characteristic distances of several ionomers

Ionomer	**q, $Å^{-1}$**	**d, Å**	**λ, H_2O/SO_3H**
I2-1.4, (Li)-H^+	0.1115	56.3	37.0
b-I3-0.9, (Li)-H^+	N/A	N/A	10.9
b-I3-0.9, (K)-H^+	0.1614	38.9	31.2
sb-I6-1.4, (Li)-H^+	0.1210	51.9	35.6

Further study of bulk morphology of the sample, acidified from its potassed-state, must be provided. Inspite the fact that dynamic mechanical analysis did not show visual difference between the materials, acidified from different salt-forms, further measurements of water uptake and conductivity were conducted on both protonated forms.

3.4.2. Water uptake and conductivity

As in case of the block-copolymers series **I3** and **I5**, the ***sb*-I6-1.4** membranes gained differently in weight during the water uptake measurements, when protonated from K^+- either

Li^+-form (*Fig. 3.44 (a), (b)*). The former sample is characterized by 20-25 % higher values, than the latter one in the temperature range 30-90 °C. Additionally, the membranes are estimated for the difference in through-plane and in-plane swelling (*Fig. 3.44 (c)*). Anisotropy, reported for block-copolymers in a wide variety of publications, is also registered for the current ionomers. The gain of the membranes in thickness is approximately twice as much as their gain in length or width.

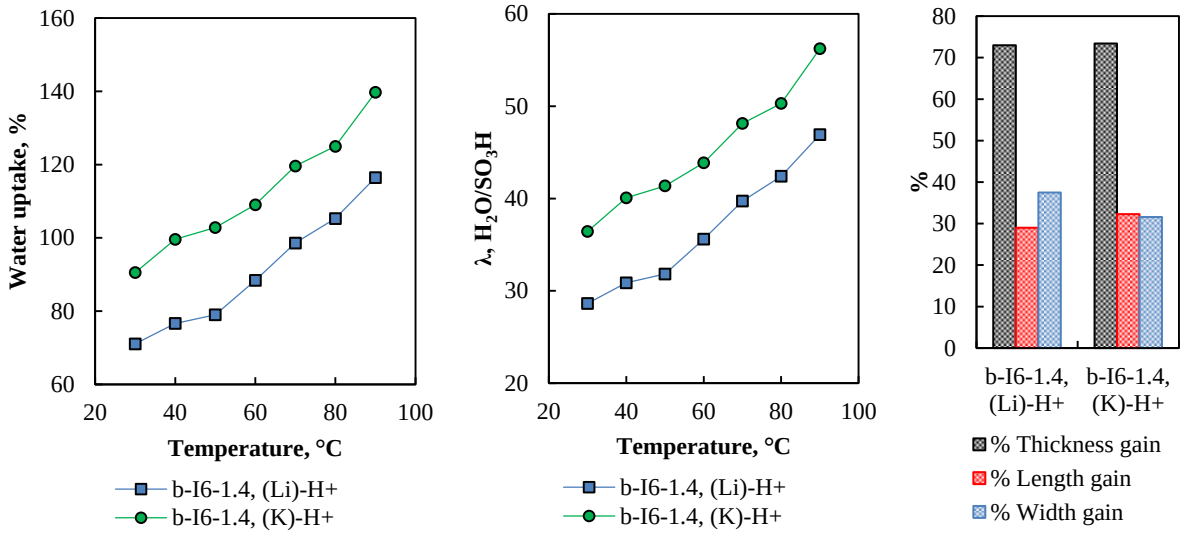

(a) (b) (c)

Figure 3.44. Swelling behavior of the membranes ***sb*-I6-1.4** in water in the temperature range 30-90 °C, represented as: a) water uptake in percent to the dry weight, b) lambda – amount of water molecules per an acid site. (c) Anisotropy of ***sb*-I6-1.4** swelling in water

Conductivity of the ionomers ***sb*-I6-1.4** was registered at 95 % RH in temperature range 30 – 90 °C (*Fig. 3.45 (a)*). Both protonated samples showed higher values, than Nafion 117: 3.6-$9.9 \cdot 10^{-2}$ S/cm for ***sb*-I6-1.4 (Li)-H^+** and $9.2 \cdot 10^{-2}$-$1.7 \cdot 10^{-1}$ S/cm for ***sb*-I6-1.4 (K)-H^+**. Slopes of the both materials are similar between each other and compared to Nafion. It may be presumed that activation energy for proton conduction in both polymers is close to the one in Nafion 117. Hence, the conductive channels of the synthesized ionomers might have the same structure as those in Nafion.

Measurement of conductivity at reduced humidity reveals higher performance of ***sb*-I6-1.4 (K)-H^+**, compared to Nafion and to ***sb*-I6-1.4 (Li)-H^+** (*Fig. 3.45 (b)*). Remarkably, that even at 20 %RH the current sample is still the best in conductivity. ***sb*-I6-1.4 (Li)-H^+** performs similarly to Nafion 117, but still slightly lower at humidity < 70 %.

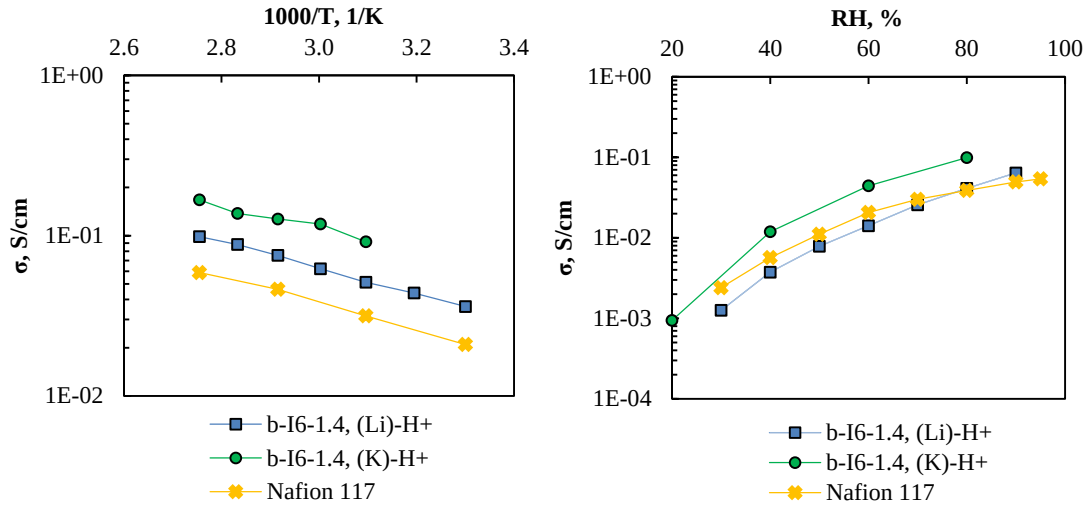

(a) (b)

Figure 3.45. Conductivity of ***sb*-I6-1.4** ionomers, represented: a) as a function on inverse temperature at 95 %RH, b) as a function on relative humidity at 80 °C

Based on the results of water uptake and conductivity measurements, it may be concluded that: i) there exists huge difference in performance of the block-copolymers series **I6**, protonated from K^+- or Li^+-states; ii) at 95 %RH the both samples have similar activation energy as Nafion 117, but at lower RH the new ionomers require overpassing higher energy barrier to achieve conductivity comparable to Nafion.

In order to complete analysis of this series, morphology study of the ionomer, acidified from its potassed-form, must be provided. Additionally, the impact of block length may be concluded, as well as variation of IEC. These manipulations are currently performed.

Conclusions

The general objective of the current dissertation work was to produce new types of proton conducting membranes for PEMFC applications. Based on literature research the required ionic polymer was determined as the one to contain aromatic backbone and long side chains of PFSA groups. Polycondensation was chosen as the most convenient method of the ionomer production. However, the common strategy of the ready polymer post-modification was changed to a more challenging one – condensation of the ionic and non-ionic monomers. Therefore, the current work was divided to three main tasks, which were successively solved:

1) Three new ionic monomers, bearing PFSA groups, were synthesized. The detailed protocols of synthesis and purification are proposed. The protocols are improved in order to receive the required monomers of the highest yield and of the least cost. Moreover, the production procedures are successfully repeated at high-scale (up till 30 g of the final product).

2) Several series of ionomers, synthesized by polymerization of the newly produced monomers with non-ionic commercial monomers, are elaborated. Three main types of ionomers are presented: random (series **I1**, **I2**, ***r*-I3**, **I4** and ***r*-I5**), block-copolymers, synthesized by 'one pot two reactions' (***b*-I3**, ***b*-I5**) and block-copolymers, synthesized by condensation of separate blocks (***sb*-I3** and ***sb*-I6**). All the series contain samples of different IEC to study its impact on the polymers' performance.

3) Characterization of the newly synthesized ionomers is provided. Thermal and oxidative stabilities, thermo-mechanical properties, bulk morphology, conductivity at reduced humidity in wide range of temperatures are studied. The ionomers of the different series are compared and the main features that differ or resemble for these polymers are discussed in detail.

It was revealed that all the ionomers, both random and in block, show highly organized structures, when moistured. The organization is related to presence of ionic aggregates (domains) that could better accommodate water molecules even at low humidity. Connectivity (percolation) of these ionic domains is another factor that may greatly influence conductivity.

It was assumed that several semi-crystalline ionomers contain two types of ionic domains: those in the more rigid shell of crystallites and the other, surrounded by amorphous phases. Such supposition is innovative and must be better studied. An important fact is that whenever

such structures are impregnated to other polymer compositions (the case of the block-copolymer, containing hydrophilic block of the described structure), the both ionic domains remain present.

It was observed that a great part of synthesized ionomers, both random and in block, additionally display well-defined phase separation between the polymer chain and the ionic groups. Such phenomenon was never observed for random materials before; therefore, it may be presumed that, in fact, they contain small blocks, enriched in ionic groups, and small blocks depleted or having no ionic groups.

Three polymers of IEC 1.4 meq/g (**I2-1.4, I4-1.4** and ***sb*-I6-1.4**) and one ionomer of IEC 1.3 meq/g (**I1-1.3**) were determined to have higher and/or comparable conductivities to those of Nafion 117 in humidity range 20-95 %RH and at temperatures 30-90 °C. These results are promising, but need further studying in terms of polymers' micro-nanoscale organization.

Notably, ionomers of the series **I6** are unique in terms of the synthesis strategy and arrangement of PFSA groups along the polyaromatic backbone: the hydrophilic block of the current block-copolymer contains three PFSA chains on four aromatic rings of poly(arylene ether ketone) backbone. Proximity of superacid species is believed to be one of the indicative factors for better proton conducting channels organization.

Perspectives

The tasks of the current dissertation work were innovative in terms of the overall process strategy: starting from the synthesis of a simple structural unit – a monomer, realizing the whole procedure to obtain a high molecular weigth product, which is further cast to a membrane, and ending with extensive analysis of the final product in order to predict the possible applied interest in it. Due to the vast objectives, we propose to pay further attention to the following tasks:

i) Synthesis of bigger variety of ionic monomers, bearing PFSA or sulfonimide superacid groups.
ii) Producing ionic polymers, using the already proposed in this work ionic monomers, of different types of the backbone. The current dissertation performed the initial study of poly(ether)s and poly(ether sulfone)s with partially fluorinated backbone. Further research may concern a fully hydrogenated main chain. The idea was briefly implemented, when producing the **I1** series, but a more deep study is preferential.
iii) Elaboration of block-copolymers of the same chemical composition in the main chain, but varying the concentration of the ionic PFSA groups per structural unit in the hydrophilic block in order to study the impact of proximity of the superacid heads on the structuration of the polymer.
iv) Producing series of block-copolymers of different lengths of blocks in order to study the impact of the block lengths.
v) Due to interesting properties of **I2-1.4** and **I4-1.4** ionomers (in particular, the presence of two different ionic domains), it is supposed that combination of the oligomer of the same chemical compositions as a hydrophilic block together with other hydrophilic and hydrophobic oligomers might result in a triblock-repetitive ionomer of promising structuration.
vi) A deeper analysis of the polymer organization must be provided in order to study the influence of the PFSA lateral chain on the overall behavior of the polymer.

Concerning the research, conducted in terms of the current dissertation, we evaluate that the measurement of water absorption at reduced humidity is lacking. Also the effect of solvent for casting might be studied: here, the membranes produced form their solutions in DMAc only are investigated, however, changing polarity and dielectric constants of the solvent medium might result in totally different polymer chain organization, thus different conductivity and overall performance.

Characterization techniques

1. Nuclear magmetic resonance (NMR)

NMR analysis is performed at Bruker AVANCE III HD spectrometer at frequencies 400.15 MHz for ^{1}H, 376.52 MHz for ^{19}F and 100.62 MHz for ^{13}C spectras. Data treatment is conducted with TopSpin 3.2 and MestRe-C 2.3a softwares.

The samples are analyzed in their solubilized state. The chemical shift (δ) is measured with the unit of parts per million (ppm). Several deuterated solvents are used for the samples preparation: dmso d_6 (δ_H = 2.50 ppm, δ_C = 39.52 ppm), acetone d_6 (δ_H = 2.04 ppm, δ_C = 29.80 ppm), chloroform d_1 (δ_H = 7.24 ppm, δ_C = 77.00 ppm). Multiplicities are reported as follows: *s* = singlet, *d* = doublet, *t* = triplet, q_4 = quadruplet, q_5 = quintuplet, *m* = multiplet, *d-d* = doublet of doublets, *t-t* = triplet of triplets.

Sample preparation. The studied product of minimum 10 mg is solubilized in approximately 0.4 mL of the appropriate deuterated solvent, and the solution is transferred to the tube for NMR analysis.

2. Elemental analysis

The current analysis is performed by Central Service of Analysis at the Institute of Analytical Science, in Villeurbanne, France.

Sample preparation. 25-30 mg of the product is dried overnight at 80 °C at reduced pressure. The sample is then transferred to the glove box, avoiding any contact with air, and closed firmly.

3. Size exclusion chromatography coupled multi-angle laser light scattering (SEC-MALLS)

SEC is performed at WATERS 515 HPLC, subsequent evaluation of the molecular weights is provided with the help of a differential refractometer SOPARES RI2000 and a light scattering detector WYATT DAWN EOS at 690 nm. Data treatment is conducted with ASTRA 6 software.

For SEC couplage 10 AGILENT 2xPLgel-Mixed-D is used as a column, DMF (Alfa aesar – HPLC grade 99.7%) with $NaNO_3$ (0.1 M) as a solvent. Injection of the solvent is performed

through the polypropylene filter of 0.2 μm, flow rate of the solvent is determined as 1 mL/min.

Molecular weights are calculated based on the signals of the light scattering detector and the refractometer, assuming that totality of the introduced product exits the column. The determined values are also verified in polystyrene equivalent.

Sample preparation. The polymer, either in the form of powder or as a membrane, is weighed in its dry state. It is then solubilized (1 % in weight) in the appropriate solvent for SEC analysis. The solution is then injected to the column through a disposable syringe-filter of PTFE 0.45 μm.

4. Thermogravimetric analysis (TGA)

TG analysis is performed at TGA 1 STAR^e instrument of METTLER TOLEDO. Data treatment is conducted with STAR^e software, data adjustment in Excel. The dry samples of average weight 20-25 mg are placed to the open crucilbles of aluminium oxide at ambient atmosphere and directly to the heating chamber. The analysis is programmed in atmosphere of compressed air of flowing rate 20 ml/min, at heating rate 5 °/min in temperature range 25-500 °C.

Sample preparation. The samples are dried prior to measurement under vacuum for 24 h at following temperatures: i) ionic polymers in their salt forms (K^+- and Li^+-forms) – at 150 °C, and ii) ionic polymers in their protonated state – at 50 °C.

5. Differential scanning calorimetry (DSC)

The current analysis is performed at DSC 1 STAR^e System of METTLER TOLEDO. Data treatment is conducted with STAR^e software, data adjustment in Excel. The dry samples of average weight 5-10 mg are encapsulated in the aluminium crucilbles at ambient atmosphere. The crucibles are holed and placed to the DSC chamber. An empty crucible is used as a reference, also placed to the DSC chamber. The analysis is programmed in atmosphere of nitrogen of flowing rate 150 mL/min around the DSC chamber and of 50 mL/min inside the chamber. Cooling is provided with liquid nitrogen.

Sample preparation. The samples are dried prior to measurement under vacuum for 24 h at following temperatures: i) ionic monomers in their potassium-neutralized form – at 80 °C, ii) ionic polymers in their salt forms (K^+- and Li^+-forms) – at 150 °C, and iii) ionic polymers in

their protonated state – at 50 °C.

The following programs are used to perform the DSC analysis of:

a) *Monomers in their potassium-neutralized state*. Two heating / cooling cycles with the first one in temperature range 25-180 °C at heating / cooling rate 20 °C/min and the second one in temperature range 25-300 °C at heating / cooling rate 5 °C/min.

b) *Ionomers.*Typically three heating / cooling cycles are performed:

1) to evaporate residual humidity of the sample – heating / cooling rate is 40 °C/min, temperature range is 25-210 °C for the ionic polymers in their salt-neutralized form and 25-180 °C for the ionic polymers in their protonated state;

2) to register the actual energy state changes of the polymers – heating / cooling rate is 20 °C/min, temperature range is 25-300 °C for the ionic polymers in their salt-neutralized form and 25-210 °C for the ionic polymers in their protonated state;

3) to check reproducibility of the obtained results – heating / cooling rate is 20 °C/min, temperature range is 25-(T_d-10) °C (where T_d is degradation temperature, determined from the TGA analysis).

6. Dynamic mechanical analysis (DMA)

DM analysis is performed at DMA Q800 device of TA Instruments. Data treatment is conducted with TA Universal Analysis software, data adjustment in Excel. The dry membranes of average dimensions 20-25 mm·4-7 mm·60-200 μm (L·W·T) are introduced to the clamp of film tension immediately after drying. The screw force applied to immobilize the membranes is chosen as 1.0 N·m. The following settings are chosen: multifrequency-strain mode, frequency 1.0 Hz, preload force 0.1 N, force track 150 %. Amplitude of the sample oscillation is determined by blank measurement for each sample independently; it varies between 5 and 45 μm. The analysis is programmed in atmosphere of compressed air at heating rate 2 °C/min in temperature range 30-270 °C for the ionomers in their salt-neutralized state and 30 – 180 °C for the ionomers in their protonated state.

Sample preparation. The membranes are dried prior to measurement under vacuum for 24 h at following temperatures: i) ionic polymers in their salt forms (K^+ and Li^+) – at 150 °C, and ii) ionic polymers in their protonated state – at 50 °C.

7. Small-angle X-ray scattering (SAXS)

SAXS analysis is performed at the in-lab constructed system with detector XXX at the Institute of Nanoscience and Cryogenics. Distance between the samples and the detector is determined as 80 cm. Data treatment is conducted with MNG.exe software, data adjustment in Excel.

Sample preparation. The membranes are cut to round discs of 4 mm in diameter. The samples in their salt-neutralized form are then either dried at 150 °C or equilibrated in deionized water (mentioned in the name of the sample). The protonated membranes are measured in their wet state only, therefore they are equilibrated in deionized water overnight at temperatures, indicated in the name of each measured membrane.

8. Small-angle neutron scattering (SANS)

SANS analysis is performed at PAXE spectrometer in the Laboratory CEA-CNRS Léon Brillouin, Orphée reactor, Saclay, France.

Sample preparation. The membranes in their protonated state are cut to squares of 10 mm^2. The samples are then put to deionized water overnight at temperature, indicated in the name of each measured membrane.

9. Impedance spectroscopy

Proton conductivity of the membranes is determined by measuring their resistances with the help of impedance spectroscopy method. The analysis is performed at Impedance analyzer Material Mates M^2 7260 in the frequency range 1 Hz – 10 MHz. Humidity and temperature control is attained in the climatic chamber VC 4018 of Vötsch Industrietechnik. Based on working capacities of the environmental chamber, the following conditions of measurement are applied: temperature range 30-90 °C (registering data each 10 °C after stabilization time of 7 h minimum) at humidity 95 %RH, and humidity range 20-80 %RH (registering data each 20 %RH after stabilization time of 5 h minimum) at temperature 80 °C.

The measurement of the membrane resistance is conducted through-plane with the help of the two in-lab constructed cells. The vertical cell contains one down electrode of big surface and three upper electrodes of the same diameter, 2 mm in one cell and 3 mm in another. The membrane is placed in-between the down and the upper electrode (stainless steel), the pressure is applied by the spring on the upper electrode of the same stiffness constant.

Sample preparation. The membranes in their protonated form are kept in dry (ambient) state before the measurement. On the contrary to a widely used method of the sample swelling in water prior to conductivity measurement, we presumed that equilibration of the membrane in conditions of the impedance measurement is more trustworthy.

10. Measurement of ion exchange capacity (IEC)

The protonated polymers in form of powder or a membrane are used for the current measurement. The samples are dried under reduced pressure at 50 °C overnight prior to the analysis. Two methods of IEC evaluation are applied: i) by forward titration of the polymer solution in organic solvent, and ii) by back titration of aqueous solution.

For the first method the polymer of known weight is solubilized in DEGME, methyl orange (2 drops) is added to the solution, and the latter is titrated with solution of NaOH in DEGME of known concentration. IEC (in meq/g) is then calculated from equation:

$$IEC = \frac{V_{NaOH} \cdot m_{solution\ NaOH}}{V_{solution\ NaOH} \cdot 40 \cdot m_{membrane}} \qquad (5)$$

where V_{NaOH} is volume of solution of NaOH in DEGME used for titration of the membrane solution; $m_{\mathrm{solution\ NaOH}}$ is weight of NaOH used for preparing the solution of NaOH in DEGME; $V_{\mathrm{solution\ NaOH}}$ is volume of the prepared NaOH solution in DEGME; 40 is molecular weight of NaOH; m_{membrane} is weight of the membrane solubilized in DEGME.

11. Measurement of polymer density

The analysis is performed with the help of a kit for density measurement for the balances, purchased from Mettler Toledo. The kit contains two weighting pans: one is situated at ambient, another is immersed in toluene. A dry membrane (dried at reduced pressure during 48 h at 50 °C) in its protonated form is weighed first in the pan at ambient, then in the pan in toluene. Density of the polymer (in g/cm^3) is then calculated with the help of equation XX.

$$\rho_{\mathrm{polymer}} = \frac{m_{ambient}}{m_{ambient} - m_{toluene}} \cdot \rho_{toluene} \qquad (XX)$$

where m_{ambient} is weight of the polymer at ambient, m_{toluene} is weight of the polymer in toluene, ρ_{toluene} is density of toluene.

12. Measurement of water uptake

To conduct a water uptake (WU) measurement the membranes in protonated form are dried at 50 °C during 48 h. The samples are weighed. Then they are immersed in deionized water and are left for equilibration at required temperature during 7 h minimum. The measured temperature range is 30-90 °C, providing the analysis each 10 °C.

After equilibration in water the membranes are wiped with Kimtech tissues (Kimberly Clark manufacturer) to remove excessive water from the surface and weighed again. WU (in percents) is calculated from the following equation:

$$WU = \frac{m_{wet} - m_{dry}}{m_{dry}} \cdot 100 \qquad ()$$

where m_{wet} is the weight of the membrane after equilibration in water at required temperature, m_{dry} is the weight of the membrane when dry.

To estimate the quantity of water molecules per acidic site (λ), the following equation is used:

$$\lambda = \frac{m_{wet} - m_{dry}}{18.01} \cdot \frac{1000}{IEC \cdot m_{dry}} \qquad ()$$

where 18.01 is molecular weight of water.

To estimate water fraction if the membrane (Φ), the following calculations are implied:

$$\Phi = \frac{\frac{m_{wet} - m_{dry}}{1.0}}{\frac{m_{wet} - m_{dry}}{1.0} + \frac{m_{dry}}{\rho_{polymer}}} \qquad ()$$

where 1.0 is density of water.

Swelling anisotropy, is measured at the same time as WU. The membranes are estimated for changes in thickness and in length / width with the help of a micrometer. Gain in either of these three parameters (in percents) is calculated with the help of the following equation:

$$Gain = \frac{x_{wet} - x_{dry}}{x_{dry}} \cdot 100 \qquad ()$$

where x_{wet} is one of these parameters (length or width or thickness) after equilibration in water, x_{dry} is the same parameter of the dry membrane.

13. Measurement of oxidative stability

Oxidative stability is also conducted with membranes in their protonated state. First, the sample is equilibrated in water at 50 °C for at least 7 h and weighed. 3 % aqueous solution of H_2O_2 with 3 ppm of $FeSO_4$ is prepared and put for 15 min to climatic chamber at 50 °C. The wet membrane is then transferred to this oxidative solution and the whole system is kept in climatic chamber at 50 °C. Each hour the measurement of weight is carried. As soon as the gain in weight is observed (usually the membrane becomes brittle at the same time), the membrane is dried with the help of Kimtech wipes and prepared for the NMR and SEC measurements.

In case the membrane does not show any degradation properties during the analysis day, the samples is eliminated from the oxidative solution, washed with deionized water and kept in water overnight. The next day the analysis is continued by immersing the sample to the oxidative solution again.

In case the sample solubilizes during the oxidative test, the oxidative solution is evaporated in the oven at 50 °C and exclusively NMR is conducted.

Annexes

*Annex 1. Synthesis of the ionic precursor – potassium salt of 1,1,2,2-tetrafluoro-2-(1,1,2,2-tetrafluoro-2-iodoethoxy)ethanesulfonate (**1a**)*

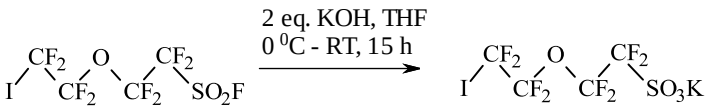

1 **1a**

30.700 g (0.0721 mol) of **1** is solubilized in 145 mL of THF and the reaction vessel is placed in an ice bath. 10.465 g (0.1588 mol) of potassium hydroxide is introduced to the solution and the reaction proceeds for 15 h at RT. The suspension is filtered once on the pore-filter from the excess of KOH and KF that is formed during the reaction. After the evaporation of THF at temperature not higher, than 40 °C, the obtained white-yellowish solid is resolubilized in ACN and refiltered at 0.2 µm filter. The transparent solution is dried to give white solid **1a** of

the yield 98 %. If the initial product **1** has non-transparent color, the product **1a** might possess yellowish color. To 'bleach' the potassium salt of iodoperfluoroalkanesulfonate it may be washed with DCM several times.

^{19}F NMR : δ (ppm, acetone d_6) = −118.60 (*s*, C$\underline{F_2}$SO$_3$K); −86.52 (*m*, C$\underline{F_2}$O); −82.94 (*t*, C$\underline{F_2}$O); −69.10 (*s*, IC$\underline{F_2}$).

*Annex 2. Synthesis of a monomer **2** – potassium salt of 1,3-difluoro-5-(1,1,2,2-tetrafluoro-2-(1,1,2,2-tetrafluoroethoxy-2-sulfonate)ethylbenzene*

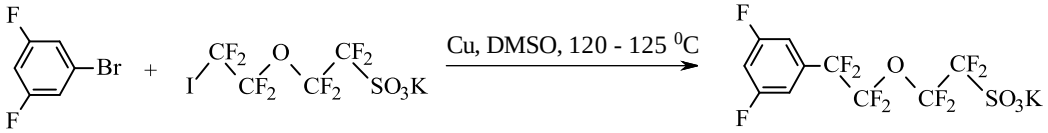

1a **2**

8.250 g (0.1298 mol) of copper powder, 7.500 mL (0.0649 mol) of 1-bromo-3,5-difluorobenzene and 10 mL of DMSO are placed to a flask equipped with a water condenser. The suspension is left at rigorous stirring at 115 – 120 °C for 1 h 30. Separately 15.000 g (0.0325 mol) of **1a** are solubilized in 17 mL of DMSO and the solution is added to the copper-containing suspension. The reaction is continued at 125 °C for 3 h.

The reaction mixture is cooled down to room temperature and filtered over the Celite ® filter with the help of 20 mL of acetone. The filtrate is evaporated from acetone and put to 200 mL of the saturated aqueous solution of KCl for 3 h at stirring. Then the product is extracted 3 times 150 mL of EA. The latter phase is dried over sodium sulfate and the solvent is evaporated to yield in a yellow solid. The latter one is mixed several times with hexane (until solvent stays colorless), then with TL and finally with DCM to result in white solid. The obtained product contains several percent of a secondary product, which is washed out by extraction with DCM / ACN in concentration from 90 / 10 till 80 / 20 while heating. The other way of the final product purification is the chromatography column with the alkylated silica (inverse phase silica) as a stationary phase and DW / ACN of 70 / 30 as eluents.

^{1}H NMR : δ (ppm, acetone d_6) = 7.34 (*t*-*t*, 1 H_{Ar}); 7.50 (*d*-*d*, 2 H_{Ar}). ^{19}F NMR : δ = −119.11 (*s*, C$\underline{F_2}$SO$_3$K); −114.34 (*t*, C$\underline{F_2}$Ar); −108.70 (*t*, 2 F_{Ar}); −88.38 (*m*, C$\underline{F_2}$O), −83.48 (*m*, C$\underline{F_2}$O).

*Annex 3. Synthesis of a monomer **3** – 1,3-dihydroxy-5-(1,1,2,2-tetrafluoro-2-(1,1,2,2-tetrafluoroethoxy-2-sulfonate)ethylbenzene*

a) synthesis of an intermediate product **3a** – 1,3-dimethoxy-5-(1,1,2,2-tetrafluoro-2-(1,1,2,2-tetrafluoroethoxy-2-sulfonate)ethylbenzene

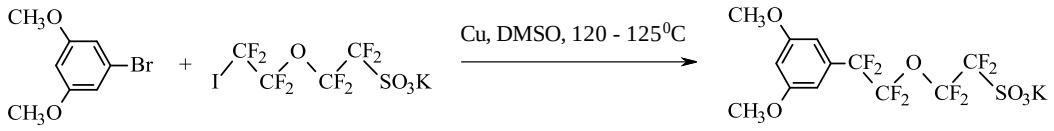

1a **3a**

25.024 g (0.3938 mol) of copper powder, 42.74 g (0.1969 mol) of 1-bromo-3,5-dimethoxybenzene and 35 mL of DMSO are placed to a flask equipped with an air condenser. The suspension is left at rigorous stirring at 115 – 120 °C for 1 h 30. Separately 21.664 g (0.0469 mol) of **1a** is solubilized in 22 mL of DMSO and the solution is added to the copper-containing suspension. The reaction is continued at 125 °C for 12 h.

The reaction mixture is cooled down to room temperature and filtered over the Celite ® with the help of 20 mL of acetone. The filtrate is evaporated from acetone and put to 200 mL of the saturated aqueous solution of KCl. The product is extracted with 3 times 150 mL of EA, the organic phase is dried over sodium sulfate and the solvent is evaporated. The obtained yellow solid is washed with 3 times 200 mL of hexane under the rigorous mixing. Then the paste is mixed with 200 mL of DW and the resulting suspension is washed 4 times 300 mL of DCM (until the phase of DCM stays uncolored); the product is collected from the aqueous phase by the extraction with EA (3 times 150 mL). The organic phase is dried over sodium sulfate and the solvent is evaporated. Since the product **3a** is an intermediate, no further purification is needed. The yield is 18.39 g or 83 %.

^{1}H NMR : δ (ppm, acetone d_6) = 3.88 (*s*, 2 OC$\underline{H}_3$), 6.68 (*t*, 1 H_{Ar}); 6.89 (*d*, 2 H_{Ar}). ^{19}F NMR : δ = −118.79 (*s*, C$\underline{F}_2$SO$_3$K); −113.94 (*s*, C$\underline{F}_2$Ar); −88.10 (*m*, C$\underline{F}_2$O), −83.32 (*m*, C$\underline{F}_2$O).

b) synthesis of the monomer – potassium salt of 1,3-dihydroxy-5-(1,1,2,2-tetrafluoro-2-(1,1,2,2-tetrafluoroethoxy-2-sulfonate)ethylbenzene (**3**)

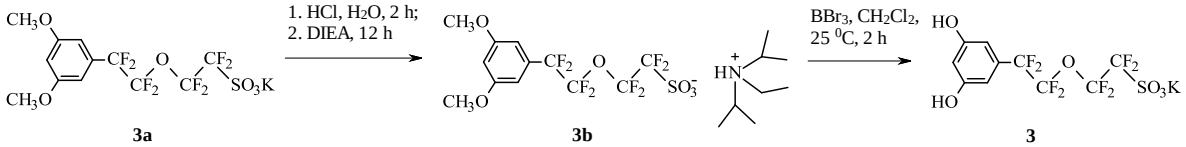

3a **3b** **3**

18.390 g (0.0389 mol) of **3a** is solubilized in 50 mL of 2 M HCl and the suspension is left at high agitation for 2 h until complete homogenization of the solution. The product is then extracted with 2 times 100 mL of EA, the organic phase is washed with 3 times 100 mL of DW to eliminate the excess of acid. The EA phase is then dried over Na_2SO_4 and the solvent is evaporated. The product **3a** in acid form is then put with 27 mL (0.1557 mol) of DIEA for 12 h at high agitation. The suspension is solubilized in 100 mL of EA and washed 1 time 150 mL of DW. The organic phase is dried over Na_2SO_4 and the solvent is evaporated. The product **3b** is light-yellow oil, which solidifies in time.

Characterization of the product **3b** by ^{1}H NMR gives the signals: δ (ppm, acetone d_6) = 1.43 (*d*, 5 C$\underline{H}_3$); 3.33 (*q_4*, C$\underline{H}_2$); 3.83 (*q_5*, 2 C$\underline{H}$); 3.88 (*s*, 2 OC$\underline{H}_3$); 6.69 (*t*, 1 H_{Ar}); 6.85 (*d*, 2 H_{Ar}) and by ^{19}F NMR δ = −118.73 (*s*, C$\underline{F}_2SO_3K$); −113.95 (*s*, C$\underline{F}_2$Ar); −88.03 (*m*, C$\underline{F}_2$O), −83.28 (*m*, C$\underline{F}_2$O).

19.426 g (0.0345 mol) of **3b** is then placed to a RB flask, equipped with a water condenser and flashed with argon, and solubilized in 8 mL of distilled DCM. 86.000 mL (0.0862 mol) of the BBr_3 solution in DCM is then introduced to the system, which is kept under the high agitation at RT. The reaction continues during 2 h, when the reacted product **3** is precipitating from the solution as fine white powder.

The reaction solution is then carefully neutralized with 250 mL of the 3 M water solution of KOH in an ice bath. The suspension is left at high agitation for 1 h to achieve the complete transfer of the colored product to the aqueous phase. The water phase is then washed 2 times 200 mL of DCM and acidified to pH 3. The aqueous solution is again washed with DCM (3 times 200 mL) and the product **3** is then extracted with 3 times 200 mL of EA, the organic phase is dried over sodium sulfate and evaporated from the solvent.

The purification of the product **3** may be realized in two ways: (i) with the modified type of a column chromatography under the pressure, (ii) with the true column chromatography with the inversed phase silica as a stationary phase. In the first case the actual laboratory glass column is changed for a pore-filter, the impure product **3** is deposited on the top of silica layer, which is then washed with pure DCM, and after that the required molecule **3** is extracted with 65 / 35 ACN / DCM. The collected product **3** as a grey powder is solubilized in 100 mL of the saturated aqueous KCl solution and is left for the agitation for 12 h. The product is then extracted with EA and dried over Na_2SO_4 and evaporated from the solvent. It is then washed with 4 times 200 mL of hot DCM to yield in white powder of 12.4 g or 71.7 %.

In the second purification case of **3** on the inverse phase silica, the true column is required with slow but immediately pure product extraction. The eluents are H_2O / ACN; no further cation exchange is needed.

Product **3** is characterized by the ^1H NMR : δ (ppm, acetone d_6) = 6.55 (*t*, 1 H_{Ar}); 6.72 (*d*, 2 H_{Ar}); 8.66 (*s*, 2 O<u>H</u>) and ^{19}F NMR : δ = −118.34 (*s*, C<u>F_2</u>SO_3K); −114.33 (*s*, C<u>F_2</u>Ar); −87.81 (*m*, C<u>F_2</u>O), −82.91 (*m*, C<u>F_2</u>O).

Annex 4. Synthesis of a monomer 4 – 1,3-dihydroxy-5-(1,1,2,2-tetrafluoro-2-(1,1,2,2-tetrafluoroethoxy-2-sulfonate)ethylsulfanylbenzene

a) synthesis of 1,3-dimethoxy-5-thiobenzene (**4d**)

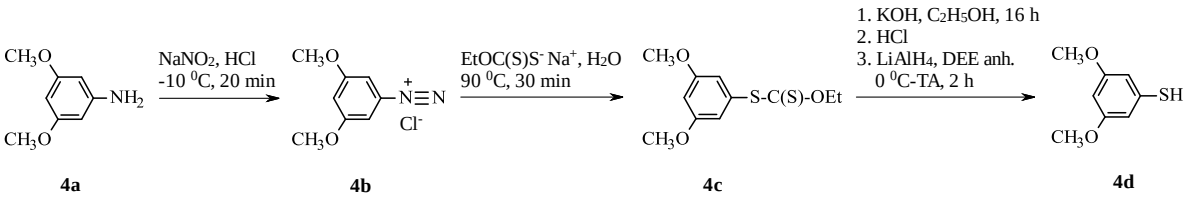

4a **4b** **4c** **4d**

In a RB flask, equipped with a mechanical agitator and the argon inlet, 25.000 g (0.1632 mol) of 3,5-dimethoxyaniline **4a** is dispersed in 80 mL of DW and 55 mL of HCl and the solution is cooled to −10 °C. Separately, 11.700 g (0.1696 mol) of sodium nitrite is solubilized in 55 mL of DW in an ice bath. The nitrite solution is slowly added to the suspension of **4a**, keeping the reaction temperature at −10 ..−15 °C and verifying the argon presence. The diazonium salt **4b** gives the characteristic dark brown color.

In a separate RB flask, equipped with a water condenser, 87.600 g (0.5465 mol) of potassium ethyl xanthate is solubilized in 190 mL of DW and the solution is heated till 90 °C. The diazonium salt solution is transferred to the potassium ethyl xanthate solution in small volume parts in order to keep the diazonium salt in cold conditions (its thermal stability range does not exceed 4 °C). By the end of combining the two solutions, the reaction is left to proceed during 30 min at 90 °C.

The product **4c** is then extracted from the cooled down water phase by 3 times 200 mL of DEE. The organic phases are combined and washed once with 200 mL of 0.5 M solution of NaOH and twice with DW. The organic phase is then dried over sodium sulfate and evaporated from the solvent. The obtained oil is solubilized in 180 mL of EtOH and 56.000 g (1.0000 mol) of KOH are introduced. The reaction solution is left at boiling for 16 h. After cooling down the solution to RT 180 mL of DW is added and the organic phase is evaporated

under reduced pressure. The obtained basic phase is washed 3 times 200 mL of DEE, then the aqueous phase is acidified till pH 1 and the product is extracted 3 times 200 mL of DEE. The organic phases are collected, dried over Na_2SO_4 and dried from the solvent.

The obtained oil is solubilized in 500 mL of anhydrous DEE, the solution is cooled down with an ice bath and it is kept under the argon atmosphere. 2.600 g (0.0685 mol) of $LiAlH_4$ are introduced to the solution and the reaction is left at RT during 2 h. The excess of hydride is neutralized with a 2 M solution of HCl and the product is then extracted with 3 times 200 mL of DEE. Organic phases are dried over sodium sulfate and the solvent is evaporated to result in 16.600 g or 59.83 % yield.

Product **4d** is characterized by the ^{1}H RMN: ($CDCl_3$) δ = 3.76 (*s*, 2 $OC\underline{H_3}$); 6.26 (*t*, 1 H_{Ar}); 6.42 (*d*, 2 H_{Ar}).

b) Synthesis of **4e** – 1,3-dimethoxy-5-(1,1,2,2-tetrafluoro-2-(1,1,2,2-tetrafluoroethoxy-2-sulfonate)ethylsulfanylbenzene

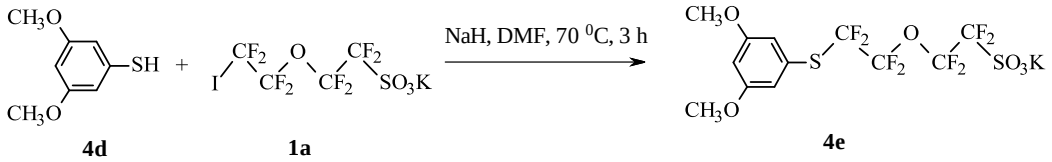

4d **1a** **4e**

16.600 g (0.0976 mol) of **4d** is solubilized in 140 mL of DMF, the solution is cooled down with an ice bath and it is kept under the argon atmosphere. 5.856 g (0.2440 mol) of sodium hydride is added in parts to avoid the overpressure. The suspension is left for 20 min at agitation at low temperature. Separately, in a RB flask equipped with an air condenser, 30.137 g (0.0651 mol) of **1a** are solubilized in 140 mL of DMF. To this solution the suspension of thiolate of sodium is introduced via the filtering paper. After that the reaction is left to proceed at 70 °C for 3 h.

The reaction mixture is cooled down to RT, mixed with 200 mL of DW and the product is extracted with 3 times 150 mL of EA. The organic phase is dried over sodium sulfate and evaporated from the solvent. The excessive solvent is extracted by 15 times 200 mL of hexane / DEE of proportion 80 / 20 until the solid product is obtained of 27.911 g or 85 % in yield.

The characteristic signals of the product **4e** by ^{1}H RMN are: (ppm, acetone d_6) δ = 3.85 (*s*, 2 $OC\underline{H_3}$); 6.67 (*t*, 1 H_{Ar}); 6.88 (*d*, 2 H_{Ar}); and by ^{19}F RMN : δ = −118.50 (*s*, $C\underline{F_2}SO_3K$); −91.60 (*t*, $C\underline{F_2}S$); −85.20 (*m*, $C\underline{F_2}O$); −82.65 (*m*, $C\underline{F_2}O$).

c) Synthesis of the monomer **4** – 1,3-dihydroxy-5-(1,1,2,2-tetrafluoro-2-(1,1,2,2-tetrafluoroethoxy-2-sulfonate)ethylsulfanylbenzene

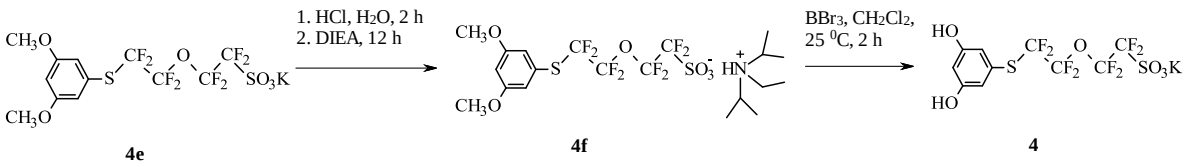

4e **4f** **4**

27.911 g (0.0553 mol) of **4e** is solubilized in 50 mL of 2 M HCl and the suspension is left at high agitation for 2 h until complete homogenization of the solution. The product is then extracted with 2 times 150 mL of EA, the organic phase is washed with 3 times 150 mL of DW to eliminate the excess of acid. The EA phase is then dried over Na_2SO_4 and the solvent is evaporated. The product **4e** in acid form is then put with 38.55 mL (0.2213 mol) of DIEA for 12 h at high agitation. The suspension is solubilized in 100 mL of EA and washed 1 time 150 mL of DW. The organic phase is dried over Na_2SO_4 and the solvent is evaporated.

The product **4f** is characterized by ^{1}H NMR: δ (ppm, acetone d_6) = 1.24 (*d*, 5 C$\underline{H}_3$), 2.97 (*q*$_4$, C$\underline{H}_2$), 3.49 (*q*$_5$, 2 C$\underline{H}$), 3.84 (*s*, 2 OC$\underline{H}_3$), 6.67 (*t*, 1 H_{Ar}), 6.85 (*d*, 2 H_{Ar}); and by ^{19}F NMR δ = −118.40 (*s*, C$\underline{F}_2SO_3K$), −91.56 (*t*, C$\underline{F}_2$Ar), −85.09 (*m*, C$\underline{F}_2$O), −82.71 (*m*, C$\underline{F}_2$O).

31.267 g (0.0525 mol) of **4f** is then placed to a RB flask, equipped with a mechanical agitator and a water condenser. The system is flashed with argon, and **4f** is solubilized in 15 mL of distilled DCM. 157.500 mL (0.1575 mol) of the BBr_3 solution in DCM is then introduced to the system, which is kept under stirring at RT for 2 h.

The reaction solution is then carefully neutralized with 250 mL of the 3 M water solution of KOH in an ice bath. The suspension is left at high agitation for 1 h to achieve the complete transfer of the colored product to the aqueous phase. The water phase is then washed 2 times 200 mL of DCM and acidified to pH 3. The aqueous solution is again washed with DCM (3 times 200 mL) and the product **4** is then extracted with 3 times 200 mL of EA, the organic phase is dried over sodium sulfate and evaporated from the solvent.

The purification of the product **4** is realized with the modified type of the column chromatography under the pressure, where the laboratory glass column is changed for the pore-filter. The impure product is deposited on the top of silica layer, which is then washed with DCM, and after that the required molecule **4** is extracted with 65 / 35 ACN / DCM. The product is collected from the latter eluent as grey powder or oil. The product is solubilized in 150 mL of the saturated aqueous KCl solution and left for the agitation for 12 h. The product

is extracted with EA and dried over Na_2SO_4 and evaporated from the solvent. It is then washed with 4 times 200 mL of hot DCM to yield in white-greyish powder of 13.75 g or 55.0 %.

Product **4** is characterized by the ^{1}H NMR : δ (ppm, acetone d_6) = 6.50 (*t*, 1 H_{Ar}); 6.72 (*d*, 2 H_{Ar}); 8.69 (*s*, 2 O<u>H</u>) and ^{19}F NMR : δ = −118.15 (*s*, C<u>F$_2$</u>SO_3K); −91.79 (*s*, C<u>F$_2$</u>Ar); −85.29 (*m*, C<u>F$_2$</u>O), −82.66 (*m*, C<u>F$_2$</u>O).

*Annex 5. Polymerization of the monomer **2**: ionomers **I1***

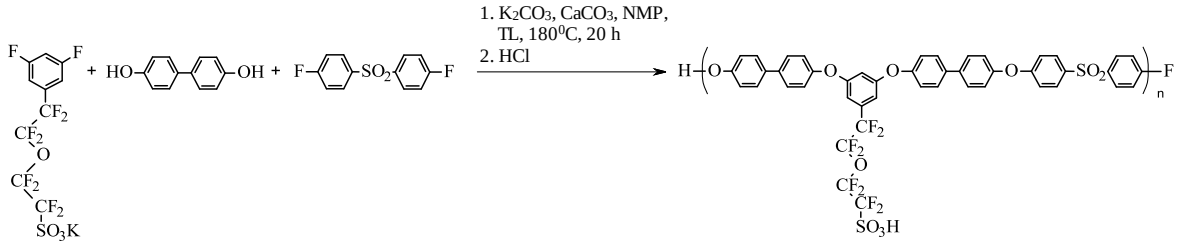

The specified amounts of reactants (see *Table A.1*) are introduced to a RB flask, equipped with a Dean-Stark trap with a water condenser, a mechanical stirrer, and slow argon flow. The system is left for 5 h for the azeotropic formation of TL / water, then TL is distilled off the system and the polycondensation reaction is left to proceed for 15 h more at 175 – 180 °C.

Table A.1. Amounts of reactants introduced for the syntheses of **I1**

Ionomer	**IEC (theor.), meq/g**	**Introduced reactants**											
		2		**BP**		**FS**		**K_2CO_3**		**$CaCO_3$**		**NMP**	**TL**
		mol	**g**	**mol**	**g**	**mol**	**g**	**mol**	**g**	**mol**	**g**	**mL**	**mL**
I1-1.0	1.0	0.003	1.345	0.006	1.117	0.003	0.763	0.018	2.484	0.012	1.200	12	8
I1-1.3	1.3	0.005	2.241	0.008	1.486	0.003	0.763	0.024	3.304	0.016	1.596	18	10
I1-1.5	1.5	0.005	2.241	0.007	1.210	0.002	0.381	0.020	2.691	0.013	1.300	15	9
I1-1.8	1.8	0.005	2.241	0.005	0.931	–	–	0.015	2.070	0.010	1.000	13	8

The viscous, gel-like reaction solutions are diluted with NMP (the same volume of solvent, used for the synthesis, is additionally introduced). Then they are precipitated with the help of a spatula in 400 mL of 1 M HCl solution and left upon stirring overnight. The precipitated polymer is then filtered and washed with DW until no free acid is detected. Then it is mixed with 300 mL of IP and the suspension is left for 15 h at high agitation. The IP is changed 2 times to assure the totality of low molecular weight products to be washed off. The obtained solid polymers are dried at 50 °C under reduced pressure overnight.

*Annex 6. Polymerization of the monomer **3**: ionomers **I2***

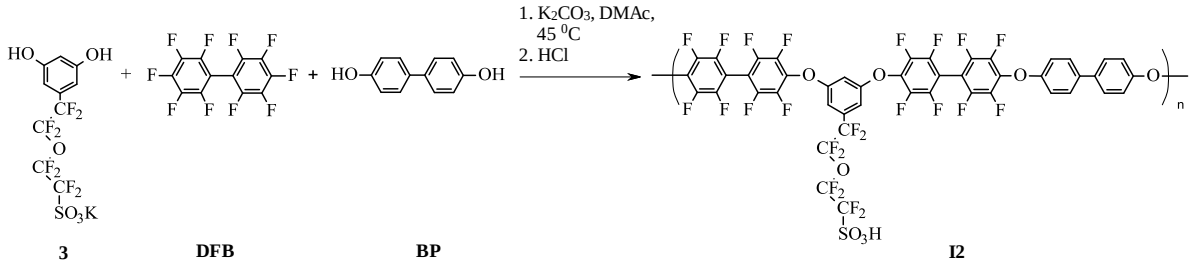

The specified amounts of reactants (see *Table A.2*) are introduced to a RB flask, equipped with an air condenser, a mechanical stirrer and slow argon flow. The reaction is left to proceed at 45 °C for the specified period of 3 to 5 days.

Table A.2. Amounts of the reactants introduced for the syntheses of **I2**

Ionomer	IEC (theor.), meq/g	Introduced reactants									Reaction time, days
		3		DFB		BP		K_2CO_3		DMAc	
		mol	g	mol	g	mol	g	mol	g	mL	
I2-1.1	1.1	0.0045	1.999	0.0068	2.280	0.0023	0.433	0.0209	2.877	20	3
I2-1.2	1.2	0.0045	1.999	0.0057	1.920	0.0012	0.232	0.0172	2.379	16	4
I2-1.4	1.4	0.0045	1.999	0.0045	1.504	–	–	0.0135	1.863	13	5

The reaction solution is then precipitated droplet in 300 – 400 mL of 1 M HCl solution at high stirring rate. The polymer is left in the acidic solution for a night, then filtered and washed with DW until no free acid is detected. The obtained polymer in the form of filaments is dried at 50 – 52 °C under reduced pressure for 48 h.

*Annex 7. Polymerization of the monomer **3**: ionomers **I3***

*a) random copolymers **r-I3***

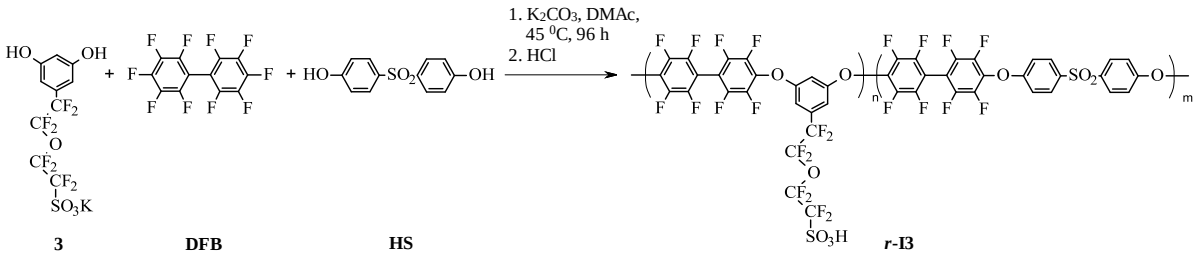

The specified amounts of reactants (see *Table A.3*) are introduced to a RB flask, equipped with an air condenser, a mechanical stirrer and slow argon flow. The reaction is left to proceed at 45 °C for 30 h.

Table A.3. Amounts of reactants introduced for the syntheses of ***r*-I3**

Ionomer	IEC (theor.), meq/g	Introduced reactants									Reaction time, hours
		3		DFB		HS		K_2CO_3		DMAc	
		mol	g	mol	g	mol	g	mol	g	mL	
I3-0.9	0.9	0.0045	1.999	0.0079	2.636	0.0034	0.848	0.0252	3.473	22	30
I3-1.1	1.1	0.0045	1.999	0.0060	2.013	0.0015	0.382	0.0164	2.257	16	30

The reaction solution is then precipitated and treated in the same way as the ionomers **I2**.

*b) block-copolymers **b-I3***

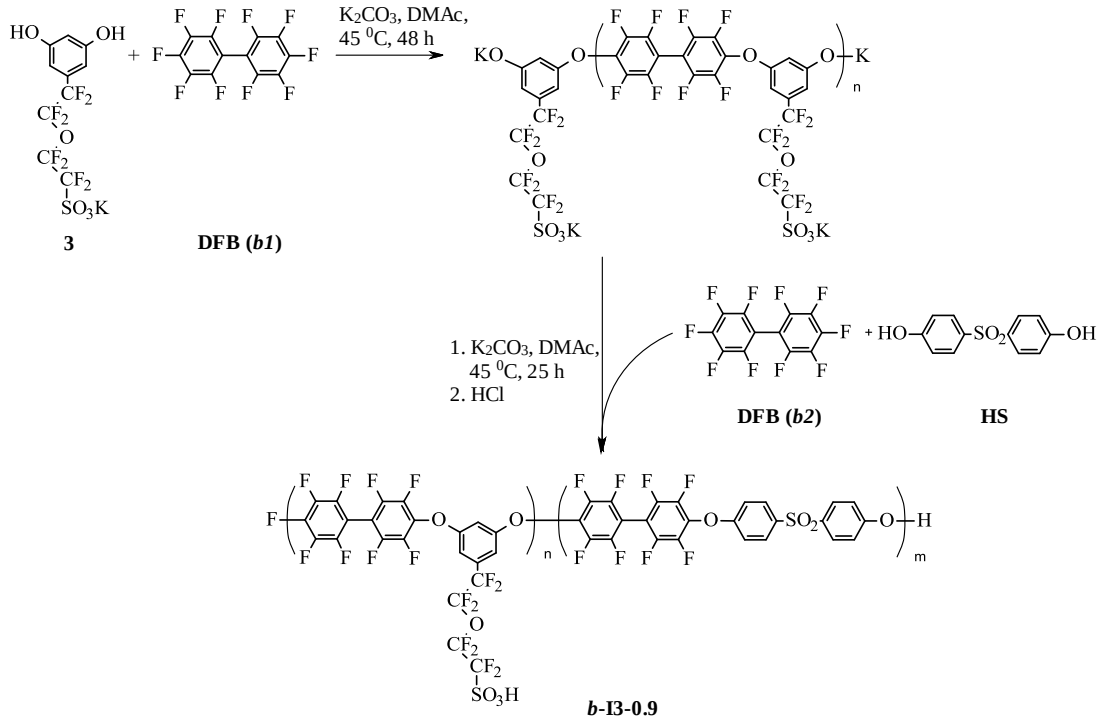

The synthesis of the block-copolymers ***b*-I3-0.9** proceeds in a one reaction vessel in two main steps. Firstly, the monomers **3** (0.0045 mol, 1.999 g) and DFB (*b1*) (0.0043 mol, 1.443 g), together with K_2CO_3 (*b1*) (0.0135 mol, 1.877 g) and 14 mL of DMAc (*b1*) are introduced in a RB flask, equipped with an air condenser, mechanical agitator and the slow argon flow. The reaction is left to proceed at 45 °C during 48 h. The completeness of a hydrophilic block (*b1*) formation is verified by ^{19}F NMR.

Then, the other two monomers of HS (0.0034 mol, 0.863 g) and DFB (*b2*) (0.0037 mol, 1.220 g)) together with K_2CO_3 (*b2*) (0.0219 mol, 3.022 g) and 7 mL of DMAc (*b2*) are introduced to the reaction mixture. The formation of the hydrophobic block (*b2*) together with a polymer chain growth continues at 45 °C for 25 h until the solution becomes viscous enough to suppose the presence of long polymer chains but not too viscous to avoid problems during its

precipitation. The reaction solution is then precipitated and treated in the same way as the ionomer ***r*-I3**.

c) *block-copolymer **sb-I3** via separate syntheses of blocks*

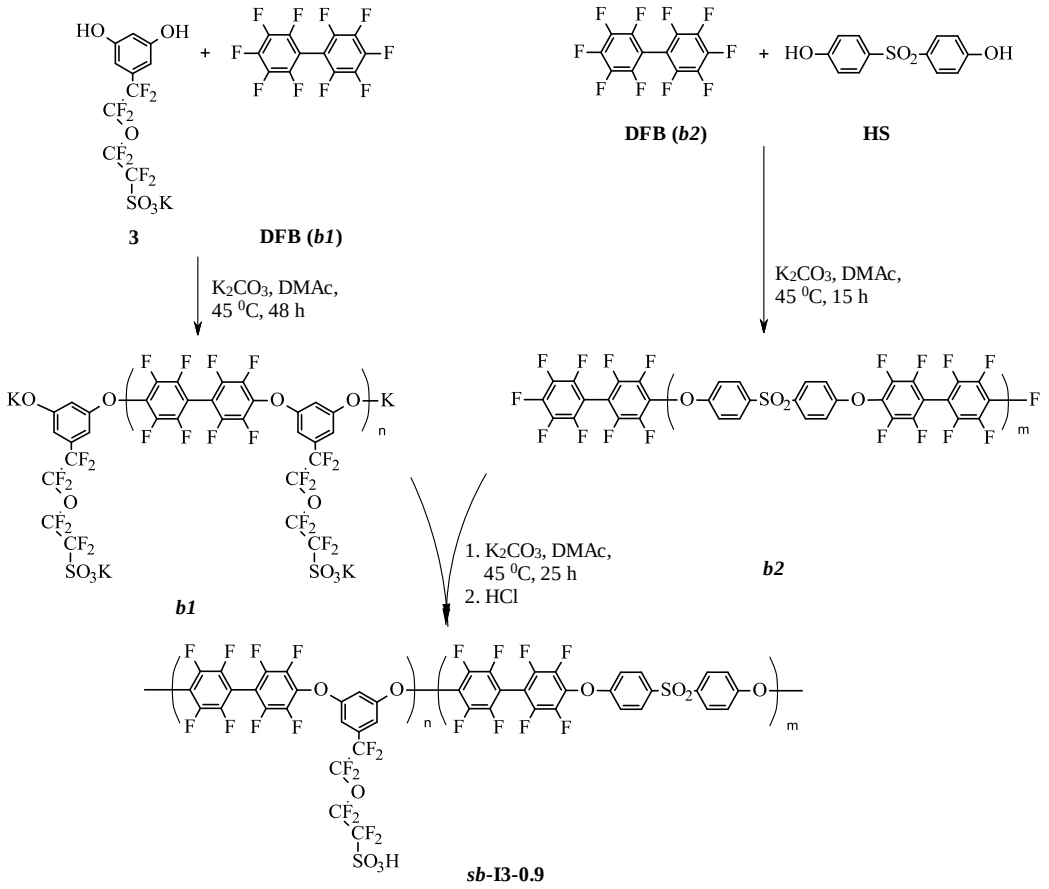

Lengths of blocks are predetermined to be 17.6 and $10.0 \cdot 10^3$ g/mol for a hydrophilic and hydrophobic, respectively.

Firstly, the hydrophobic block is synthesized by mixing 0.863 g (0.0034 mol) of HS, 1.220 g (0.0037 mol) of DFB, 3.022 g (0.0219 mol) of K_2CO_3 and 7 mL of DMAc. The reaction solution is kept at 40 °C overnight. Formation of the hydrophilic block of the required length is verified by ^{19}F NMR. The reaction solution is then precipitated droplet in a 1 M HCl solution and left overnight. The precipitated hydrophobic block is then washed thoroughly until the solution becomes neutral and it is dried at 70 °C for 48 h.

In a RB flask, equipped with an air condenser, a mechanical stirrer and slow argon flow 1.999 g (0.0045 mol) of **3**, 1.443 g (0.0043 mol) of DFB, 1.877 g (0.0135 mol) of K_2CO_3 and 14 mL of DMAc are mixed at 45 °C during 48 h. Formation of a hydrophilic block of the required length is also verified by ^{19}F NMR.

Then, the ready hydrophobic block is solubilized in 7-8 mL of DMAc and is introduced to the solution of the ready hydrophilic block. The reaction continues at 45 °C for 25 h more until the solution becomes viscous enough to suppose the presence of long polymer chains. The reaction solution is then precipitated and treated in the same way as the ionomer ***b*-I3-0.9**.

*Annex 8. Polymerization of the monomer **4**: ionomers **I4***

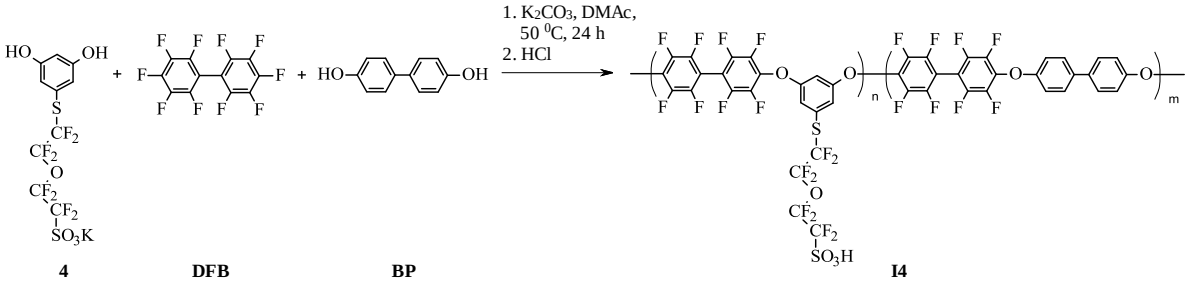

4 **DFB** **BP** **I4**

The specified amounts of reactants (see *Table A.4*) are introduced to a RB flask, equipped with an air condenser, a mechanical stirrer and slow argon flow. The reaction is left to proceed at 50 °C for the specified period of 1 to 3 days.

Table A.4. Amounts of the reactants introduced for the syntheses of **I4**

Ionomer	IEC (theor.), meq/g	Introduced reactants									Reaction time, days
		4		DFB		BP		K_2CO_3		DMAc	
		mol	g	mol	g	mol	g	mol	g	mL	
I4-1.0	1.0	0.0045	2.144	0.0070	2.342	0.0025	0.467	0.0209	2.877	20	1
I4-1.2	1.2	0.0045	2.144	0.0054	1.820	0.0009	0.176	0.0163	2.255	16	2
I4-1.4	1.4	0.0045	2.144	0.0045	1.504	–	–	0.0135	1.863	13	3

The reaction solution is then precipitated and treated in the same way as the previous ionomers.

*Annex 9. Polymerization of the monomer **4**: ionomers **I5***

*a) random copolymers **r-I5***

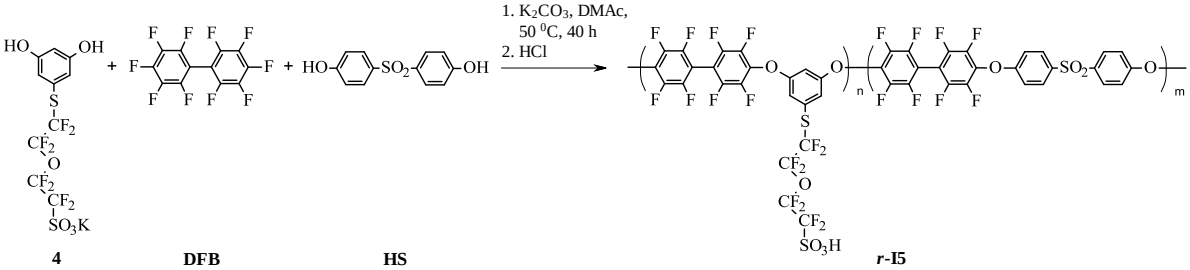

4 **DFB** **HS** ***r*-I5**

1.905 g (0.0040 mol) of **4**, 2.273 g (0.0068 mol) of DFB, 0.701 g (0.0028 mol) of HS, 2.816 g (0.0204 mol) of K_2CO_3 and 19 mL of DMAc are introduced to a RB flask, equipped with an air condenser, a mechanical stirrer and slow argon flow. The reaction is left to proceed at 50 °C for 40 h. Then it is precipitated and treated, as described previously.

b) *block-copolymers* ***b-I5***

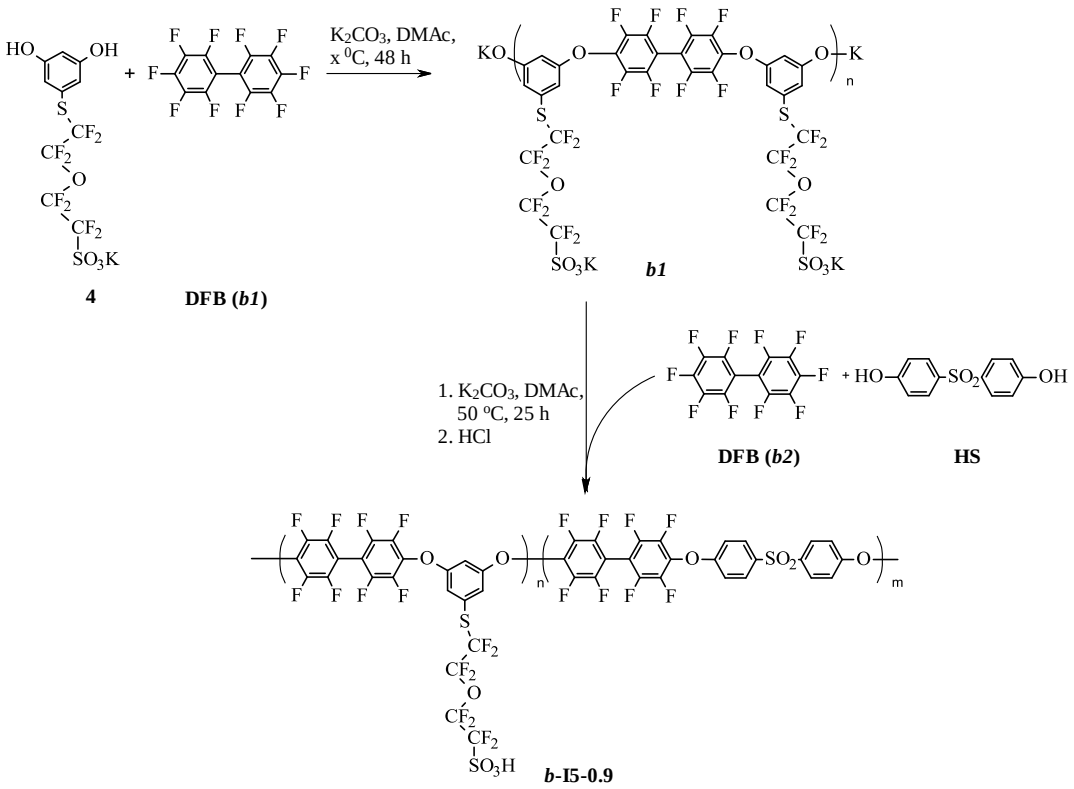

The synthesis of a block-copolymer ***b*-I8** proceeds in a one reaction vessel in two main steps. The lengths of blocks are predefined as 18.4 and $10.0 \cdot 10^3$ g/mol for the hydrophilic and hydrophobic blocks, respectively.

Firstly, 1.905 g (0.004 mol) of **4**, 1.283 g (0.0038 mol) of DFB, 1.656 g (0.012 mol) of K_2CO_3 and 12 mL of DMAc are introduced to a RB flask, equipped with an air condenser, a mechanical stirrer and the slow argon flow. The reaction is left to proceed at 50 °C during 20 h. Formation of the hydrophilic block of the required length is verified by ^{19}F NMR.

Then, 0.692 g (0.0028 mol) of HS, 0.977 g (0.0029 mol) of DFB, 2.289 g (0.0166 mol) of K_2CO_3 and 9 mL of DMAc are introduced to the reaction mixture. Formation of the hydrophobic block together with a polymer chain growth continues at 50 °C for 9 h and at RT overnight until the solution becomes viscous enough. The reaction is stopped by the reaction solution precipitation and treatment, as described above.

*Annex 10. Combination of ionic monomers **3** and **5** for a block-copolymer **b-I9** synthesis*

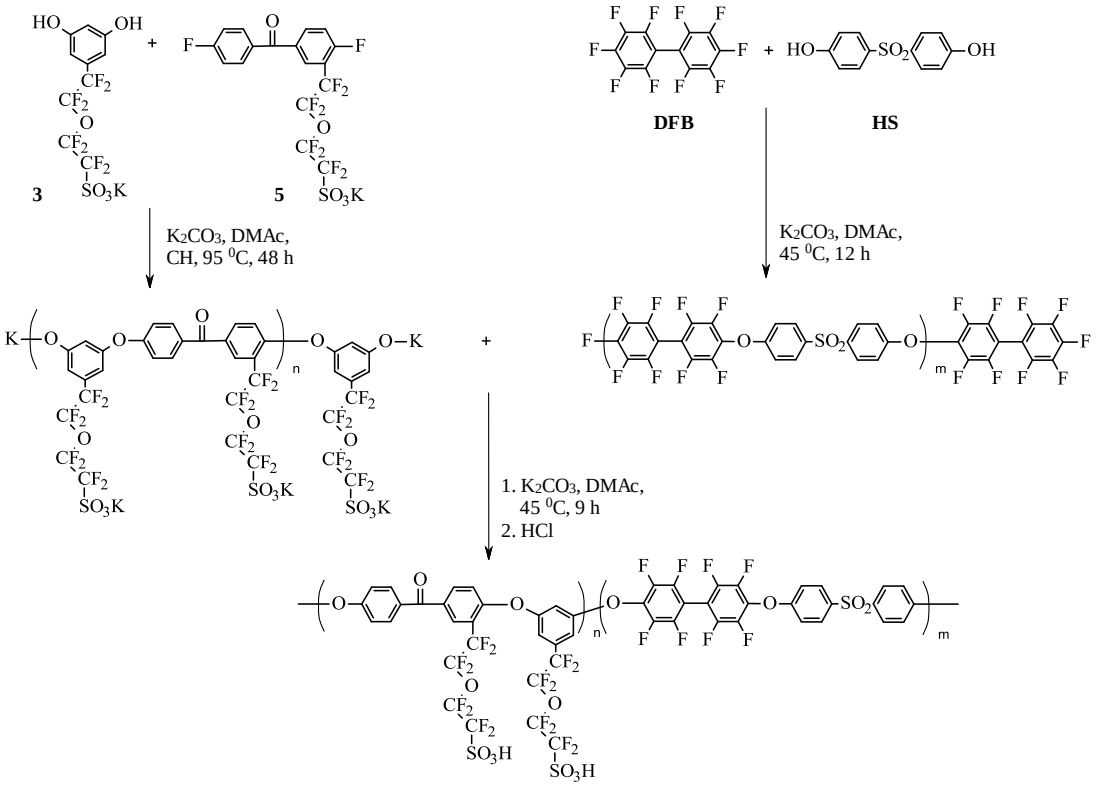

Lengths of blocks are predetermined to be 16.8 and $10.0 \cdot 10^3$ g/mol for a hydrophilic and hydrophobic, respectively. If one calculates molecular weight of the backbone of the hydrophilic block, it is previewed to be $5.0 \cdot 10^3$ g/mol.

Firstly, the hydrophobic block is synthesized by mixing 0.863 g (0.0034 mol) of HS, 1.220 g (0.0037 mol) of DFB, 3.022 g (0.0219 mol) of K_2CO_3 and 7 mL of DMAc. The reaction solution is kept at 40 °C overnight. Formation of the hydrophilic block of the required length is verified by ^{19}F NMR. The reaction solution is then precipitated droplet in a 1 M HCl solution and left overnight. The precipitated hydrophobic block is then washed thoroughly until the solution becomes neutral and it is dried at 70 °C for 48 h.

1.111 g (0.0025 mol) of the monomer **3**, 1.302 g (0.0024 mol) of the monomer **5**, 1.035 g (0.0075 mol) of K_2CO_3, 9 mL of DMAc and 4 mL of cyclohexane (CH) are introduced to a RB flask, equipped with a Dean-Stark trap with a water condenser, and a mechanical agitator, and slow argon flow. The system is left for 5 h for the azeotropic formation of CH/water, then CH is distilled off the system and the polycondensation reaction is left to proceed at 95 °C till the total disappearance of the Fluorine signals at the range of −106 to −108 ppm.

Then 1.200 g of a ready hydrophobic block is solubilized in 7 mL of DMAc. The reaction vessel is cooled down to room temperature, 0.45 g (0.0033 mol) of K_2CO_3 and the solution of the hydrophobic block are introduced there. The reaction is left to complete in 9 h at 45 °C. The precipitation of the polymer solution is made in aqueous acidic solution as described above.

Annex 11. Membrane preparation

All the polymers in their powder or filament form are put to a 1 M aqueous alkaline solution (KOH or LiOH) and left at magnetic stirring for 15 h to assure completeness of cation exchange. The polymers are filtered and washed until the neutral pH, and then dried at 80 °C under the reduced pressure for 48 h.

The membranes are always elaborated out of the polymers in their salt forms to avoid any chain scission during the solvent evaporation in the presence of the protonated superacidic PFSA chains.

The polymer powder or filaments are then solubilized in DMAc to obtain approx. 10 % w/v solution. The solubilization is facilitated by the strong stirring at 40 °C (for 2-3 h).

The polymer solution is then filtered at 0.45 μm Teflon syringe-filter and degased under the reduced pressure until the solution contains no air bubbles. Afterwards, the viscous liquid is cast to a Petri dish and the solvent is evaporated in two ways: i) by a *method A*, when the polymer solutions are kept in an oven at 60 °C for 48 h and then transferred to the DW immediately to detach the membranes from the glass surface; ii) by a *method B*, when evaporation of the solvent proceeds in several steps: first 48 h at 60 °C in the oven, then 12 h at 100 °C, and overnight at 150 °C under the reduced pressure (0.1-0.08 mbar) and only then the membranes are detached from glass surface with help of DW.

The membranes are then kept in the reservoir with DW in an oven at 35 °C for 2 days to ensure the release of the totality of solvent (DMAc).

The membranes in their salt form are analyzed directly (or with preliminary drying, depending on a measurement technique). Acidification of the membranes proceeds in 1 M HCl aqueous solution for 15 h. Then membranes are filtered and washed with DW until the neutral pH of the washing water.

References

References

1. Moore, D. R., Zhou, H., Brunelle, D. J., Hung, J., Liu, H., & Steiger, D. (2006). *U.S. Patent Application 11/598,947*.

2. Hsu, W. Y., & Gierke, T. D. (1983). Ion transport and clustering in Nafion perfluorinated membranes. *Journal of Membrane Science*, *13*(3), 307-326.

3. Hsu, W. Y., & Gierke, T. D. (1982). Elastic theory for ionic clustering in perfluorinated ionomers. *Macromolecules, 15*(1), 101-105.

4. Fujimura, M., Hashimoto, T., & Kawai, H. (1981). Small-angle X-ray scattering study of perfluorinated ionomer membranes. 1. Origin of two scattering maxima. *Macromolecules*, *14*(5), 1309-1315.

5. Fujimura, M., Hashimoto, T., & Kawai, H. (1982). Small-angle X-ray scattering study of perfluorinated ionomer membranes. 2. Models for ionic scattering maximum. *Macromolecules*, *15*(1), 136-144.

6. Roche, E. J., Stein, R. S., Russell, T. P., & MacKnight, W. J. (1980). Small-angle X-ray scattering study of ionomer deformation. *Journal of Polymer Science: Polymer Physics Edition, 18*(7), 1497-1512.

7. Roche, E. J., Stein, R. S., & MacKnight, W. J. (1980). Small-angle X-ray and neutron scattering studies of the morphology of ionomers. *Journal of Polymer Science: Polymer Physics Edition*, *18*(5), 1035-1045.

8. Haubold, H. G., Vad, T., Jungbluth, H., & Hiller, P. (2001). Nano structure of NAFION: a SAXS study. *Electrochimica Acta, 46*(10), 1559-1563.

9. Rubatat, L., Gebel, G., & Diat, O. (2004). Fibrillar structure of Nafion: Matching Fourier and real space studies of corresponding films and solutions. *Macromolecules*, *37*(20), 7772-7783.

10. Gebel, G. (2000). Structural evolution of water swollen perfluorosulfonated ionomers from dry membrane to solution. *Polymer, 41*(15), 5829-5838.

11. Gebel, G., & Diat, O. (2005). Neutron and X-ray Scattering: Suitable Tools for Studying Ionomer Membranes. *Fuel Cells, 5*(2), 261-276.

12. Rubatat, L., Rollet, A. L., Gebel, G., & Diat, O. (2002). Evidence of elongated polymeric aggregates in Nafion. *Macromolecules*, *35*(10), 4050-4055.

13. Mauritz, K. A., & Moore, R. B. (2004). State of understanding of Nafion. *Chemical reviews*, *104*(10), 4535-4586.

14. Gebel, G., Aldebert, P., & Pineri, M. (1987). Structure and related properties of solution-cast perfluorosulfonated ionomer films. *Macromolecules*, *20*(6), 1425-1428.

15. Nolte, R., Ledjeff, K., Bauer, M., & Mülhaupt, R. (1993). Partially sulfonated poly (arylene ether sulfone)-A versatile proton conducting membrane material for modern energy conversion technologies. *Journal of Membrane Science*, *83*(2), 211-220.

16. Genova-Dimitrova, P., Baradie, B., Foscallo, D., Poinsignon, C., & Sanchez, J. Y. (2001). Ionomeric membranes for proton exchange membrane fuel cell (PEMFC): sulfonated polysulfone associated with phosphatoantimonic acid. *Journal of membrane science*, *185*(1), 59-71.

17. Park, C. H., Lee, C. H., Guiver, M. D., & Lee, Y. M. (2011). Sulfonated hydrocarbon membranes for medium-temperature and low-humidity proton exchange membrane fuel cells (PEMFCs). *Progress in Polymer Science*, *36*(11), 1443-1498.

18. Hickner, M. A., Ghassemi, H., Kim, Y. S., Einsla, B. R., & McGrath, J. E. (2004). Alternative polymer systems for proton exchange membranes (PEMs). *Chemical Reviews*, *104*(10), 4587-4612.

19. Chalk, A. J., & Hay, A. S. (1969). Direct metalation of poly (2, 6-dimethyl-1, 4-phenylene ether). *Journal of Polymer Science Part A-1: Polymer Chemistry*, *7*(2), 691-705.

20. Beihoffer, T. W., & Glass, J. E. (1986). Hydrophilic modification of engineering polymers. *Polymer*, *27*(10), 1626-1632.

21. Kerres, J., Cui, W., & Reichle, S. (1996). New sulfonated engineering polymers via the metalation route. I. Sulfonated poly (ethersulfone) PSU Udel® via metalation-sulfination-oxidation. *Journal of Polymer Science Part A: Polymer Chemistry*, *34*(12), 2421-2438.

22. Kerres, J., Ullrich, A., & Hein, M. (2001). Preparation and characterization of novel basic polysulfone polymers. *Journal of Polymer Science Part A: Polymer Chemistry*, *39*(17), 2874-2888.

23. Kerres, J., Ullrich, A., Meier, F., & Häring, T. (1999). Synthesis and characterization of novel acid–base polymer blends for application in membrane fuel cells. *Solid state ionics*, *125*(1), 243-249.

24. Kerres, J., Cui, W., & Junginger, M. (1998). Development and characterization of crosslinked ionomer membranes based upon sulfinated and sulfonated PSU crosslinked PSU blend membranes by alkylation of sulfinate groups with dihalogenoalkanes. *Journal of membrane science*, *139*(2), 227-241.

25. Kerres, J., Zhang, W., & Cui, W. (1998). New sulfonated engineering polymers via the metalation route. II. Sulfinated/sulfonated poly (ether sulfone) PSU Udel and its crosslinking. *Journal of Polymer Science Part A: Polymer Chemistry*, *36*(9), 1441-1448.

26. Jannasch, P. (2005). Fuel Cell Membrane Materials by Chemical Grafting of Aromatic Main-Chain Polymers. *Fuel Cells*, *5*(2), 248-260.

27. Takamuku, S., & Jannasch, P. (2012). Multiblock copolymers containing highly sulfonated poly (arylene sulfone) blocks for proton conducting electrolyte membranes. *Macromolecules*, *45*(16), 6538-6546.

28. Takamuku, S., & Jannasch, P. (2012). Multiblock Copolymers with Highly Sulfonated Blocks Containing Di-and Tetrasulfonated Arylene Sulfone Segments for Proton Exchange Membrane Fuel Cell Applications. *Advanced Energy Materials*, *2*(1), 129-140.

29. Wang, F., Hickner, M., Ji, Q., Harrison, W., Mecham, J., Zawodzinski, T. A., & McGrath, J. E. (2001, October). Synthesis of highly sulfonated poly (arylene ether sulfone) random (statistical) copolymers via direct polymerization. In *Macromolecular Symposia* (Vol. 175, No. 1, pp. 387-396). WILEY-VCH Verlag GmbH.

30. Harrison, W., Ghassemi, H., Zawodzinski Jr, T.A., & McGrath, J.E. (2004). *U.S. Patent Application 10/595,654*.

31. Ueda, M., Toyota, H., Ouchi, T., Sugiyama, J. I., Yonetake, K., Masuko, T., & Teramoto, T. (1993). Synthesis and characterization of aromatic poly (ether sulfone) s containing pendant sodium sulfonate groups. *Journal of Polymer Science Part A: Polymer Chemistry*, *31*(4), 853-858.

32. Harrison, W. L., Wang, F., Mecham, J. B., Bhanu, V. A., Hill, M., Kim, Y. S., & McGrath, J. E. (2003). Influence of the bisphenol structure on the direct synthesis of

sulfonated poly (arylene ether) copolymers. I. *Journal of Polymer Science Part A: Polymer Chemistry*, *41*(14), 2264-2276.

33. Roy, A., Hickner, M. A., Einsla, B. R., Harrison, W. L., & McGrath, J. E. (2009). Synthesis and characterization of partially disulfonated hydroquinone-based poly (arylene ether sulfone) s random copolymers for application as proton exchange membranes. *Journal of Polymer Science Part A: Polymer Chemistry*, *47*(2), 384-391.

34. Badami, A. S., Lane, O., Lee, H. S., Roy, A., & McGrath, J. E. (2009). Fundamental investigations of the effect of the linkage group on the behavior of hydrophilic–hydrophobic poly (arylene ether sulfone) multiblock copolymers for proton exchange membrane fuel cells. *Journal of Membrane Science*, *333*(1), 1-11.

35. Fan, Y., Zhang, M., Moore, R. B., Lee, H. S., McGrath, J. E., & Cornelius, C. J. (2011). Viscoelastic and gas transport properties of a series of multiblock copolymer ionomers. *Polymer*, *52*(18), 3963-3969.

36. Chen, Y., Rowlett, J. R., Lee, C. H., Lane, O. R., VanHouten, D. J., Zhang, Moore, R. B. & McGrath, J. E. (2013). Synthesis and characterization of multiblock partially fluorinated hydrophobic poly (arylene ether sulfone)-hydrophilic disulfonated poly (arylene ether sulfone) copolymers for proton exchange membranes. *Journal of Polymer Science Part A: Polymer Chemistry*, *51*(10), 2301-2310.

37. Yu, X., Roy, A., Dunn, Yang, J., & McGrath, J. E. (2006). Synthesis and characterization of sulfonated-fluorinated, hydrophilic-hydrophobic multiblock copolymers for proton exchange membranes. In *Macromolecular Symposia* (Vol. 245-246, pp. 439-449). WILEY-VCH Verlag GmbH.

38. Yu, X., Roy, A., Dunn, S., Badami, A. S., Yang, J., Good, A. S., & McGrath, J. E. (2009). Synthesis and characterization of sulfonated-fluorinated, hydrophilic-hydrophobic multiblock copolymers for proton exchange membranes. *Journal of Polymer Science Part A: Polymer Chemistry*, *47*(4), 1038-1051.

39. Roy, A., Yu, X., Dunn, S., & McGrath, J. E. (2009). Influence of microstructure and chemical composition on proton exchange membrane properties of sulfonated–fluorinated, hydrophilic–hydrophobic multiblock copolymers. *Journal of membrane Science*, *327*(1), 118-124.

40. Chen, Y., Lee, C. H., Rowlett, J. R., & McGrath, J. E. (2012). Synthesis and characterization of multiblock semi-crystalline hydrophobic poly (ether ether ketone)–

hydrophilic disulfonated poly (arylene ether sulfone) copolymers for proton exchange membranes. *Polymer*, *53*(15), 3143-3153.

41. Roy, A., Lee, H. S., & McGrath, J. E. (2008). Hydrocarbon based BPSH-BPS multiblock copolymers as novel proton exchange membranes. *ECS Transactions*, *6*(26), 1-7.

42. Takimoto, N., Takamuku, S., Abe, M., Ohira, A., Lee, H. S., & McGrath, J. E. (2009). Conductive area ratio of multiblock copolymer electrolyte membranes evaluated by e-AFM and its impact on fuel cell performance. *Journal of Power Sources*, *194*(2), 662-667.

43. Lee, H. S., Roy, A., Lane, O., Dunn, S., & McGrath, J. E. (2008). Hydrophilic–hydrophobic multiblock copolymers based on poly (arylene ether sulfone) via low-temperature coupling reactions for proton exchange membrane fuel cells. *Polymer*, *49*(3), 715-723.

44. Badami, A. S., Roy, A., Lee, H. S., Li, Y., & McGrath, J. E. (2009). Morphological investigations of disulfonated poly (arylene ether sulfone)-b-naphthalene dianhydride-based polyimide multiblock copolymers as potential high temperature proton exchange membranes. *Journal of Membrane Science*, *328*(1), 156-164.

45. Lee, H. S., Badami, A. S., Roy, A., & McGrath, J. E. (2007). Segmented sulfonated poly (arylene ether sulfone)-b-polyimide copolymers for proton exchange membrane fuel cells. I. Copolymer synthesis and fundamental properties. *Journal of Polymer Science Part A: Polymer Chemistry*, *45*(21), 4879-4890.

46. Guo, R., Lane, O., VanHouten, D., & McGrath, J. E. (2010). Synthesis and characterization of phenolphthalein-based poly (arylene ether sulfone) hydrophilic− hydrophobic multiblock copolymers for proton exchange membranes. *Industrial & Engineering Chemistry Research*, *49*(23), 12125-12134.

47. Bae, B., Miyatake, K., & Watanabe, M. (2008). Sulfonated poly (arylene ether sulfone) ionomers containing fluorenyl groups for fuel cell applications. *Journal of Membrane Science*, *310*(1), 110-118.

48. Chen, Y., Guo, R., Lee, C. H., Lee, M., & McGrath, J. E. (2012). Partly fluorinated poly (arylene ether ketone sulfone) hydrophilic–hydrophobic multiblock copolymers for fuel cell membranes. *international journal of hydrogen energy*, *37*(7), 6132-6139.

49. Li, Y., Roy, A., Badami, A. S., Hill, M., Yang, J., Dunn, S., & McGrath, J. E. (2007). Synthesis and characterization of partially fluorinated hydrophobic–hydrophilic multiblock copolymers containing sulfonate groups for proton exchange membrane. *Journal of Power Sources*, *172*(1), 30-38.

50. Wang, S. J., Luo, J. J., Xiao, M., Han, D. M., Shen, P. K., & Meng, Y. Z. (2012). Design, synthesis and properties of polyaromatics with hydrophobic and hydrophilic long blocks as proton exchange membrane for PEM fuel cell application. *international journal of hydrogen energy*, *37*(5), 4545-4552.

51. Zhao, Y., & Yin, J. (2010). Synthesis and evaluation of all-block-sulfonated copolymers as proton exchange membranes for fuel cell application. *Journal of Membrane Science*, *351*(1), 28-35.

52. Miyahara, T., Hayano, T., Matsuno, S., Watanabe, M., & Miyatake, K. (2012). Sulfonated polybenzophenone/poly (arylene ether) block copolymer membranes for fuel cell applications. *ACS applied materials & interfaces*, *4*(6), 2881-2884.

53. Liu, C., Li, L., Liu, Z., Guo, M., Jing, L., Liu, B., ... & Guiver, M. D. (2011). Sulfonated naphthalenic polyimides containing ether and ketone linkages as polymer electrolyte membranes. *Journal of Membrane Science*, *366*(1), 73-81.

54. Einsla, B. R., Kim, Y. S., Hickner, M. A., Hong, Y. T., Hill, M. L., Pivovar, B. S., & McGrath, J. E. (2005). Sulfonated naphthalene dianhydride based polyimide copolymers for proton-exchange-membrane fuel cells: II. Membrane properties and fuel cell performance. *Journal of Membrane Science*, *255*(1), 141-148.

55. Guo, X., Zhai, F., Fang, J., Laguna, M. F., López-González, M., & Riande, E. (2007). Permselectivity and conductivity of membranes based on sulfonated naphthalenic copolyimides. *The Journal of Physical Chemistry B*, *111*(49), 13694-13702.

56. Akbarian-Feizi, L., Mehdipour-Ataei, S., & Yeganeh, H. (2012). Synthesis of new sulfonated copolyimides in organic and ionic liquid media for fuel cell application. *Journal of Applied Polymer Science*, *124*(3), 1981-1992.

57. Akbarian-Feizi, L., Mehdipour-Ataei, S., & Yeganeh, H. (2014). Investigation on the preparation of new sulfonated polyimide fuel cell membranes in organic and ionic liquid media. *International Journal of Polymeric Materials and Polymeric Biomaterials*, *63*(3), 149-160.

58. Miyatake, K., Zhou, H., & Watanabe, M. (2004). Proton conductive polyimide electrolytes containing fluorenyl groups: synthesis, properties, and branching effect. *Macromolecules*, *37*(13), 4956-4960.

59. Schuster, M., Kreuer, K. D., Andersen, H. T., & Maier, J. (2007). Sulfonated poly (phenylene sulfone) polymers as hydrolytically and thermooxidatively stable proton conducting ionomers. *Macromolecules*, *40*(3), 598-607.

60. Gao, Y., Robertson, G. P., Guiver, M. D., Mikhailenko, S. D., Li, X., & Kaliaguine, S. (2006). Low-swelling proton-conducting copoly (aryl ether nitrile) s containing naphthalene structure with sulfonic acid groups meta to the ether linkage. *Polymer*, *47*(3), 808-816.

61. Schuster, M., de Araujo, C. C., Atanasov, V., Andersen, H. T., Kreuer, K. D., & Maier, J. (2009). Highly sulfonated poly (phenylene sulfone): preparation and stability issues. *Macromolecules*, *42*(8), 3129-3137.

62. Titvinidze, G., Kreuer, K. D., Schuster, M., de Araujo, C. C., Melchior, J. P., & Meyer, W. H. (2012). Proton Conducting Phase-Separated Multiblock Copolymers with Sulfonated Poly (phenylene sulfone) Blocks for Electrochemical Applications: Preparation, Morphology, Hydration Behavior, and Transport. *Advanced Functional Materials*, *22*(21), 4456-4470.

63. Kim, D. S., Robertson, G. P., Guiver, M. D., & Lee, Y. M. (2006). Synthesis of highly fluorinated poly (arylene ether) s copolymers for proton exchange membrane materials. *Journal of membrane science*, *281*(1), 111-120.

64. Sakaguchi, Y., Kitamura, K., & Takase, S. (2012). Isomeric effect of sulfonated poly (arylene ether) s comprising dihydroxynaphthalene on properties for polymer electrolyte membranes. *Journal of Polymer Science Part A: Polymer Chemistry*, *50*(22), 4749-4755.

65. Bae, B., Miyatake, K., & Watanabe, M. (2009). Effect of the hydrophobic component on the properties of sulfonated poly (arylene ether sulfone) s. *Macromolecules*, *42*(6), 1873-1880.

66. Li, X. F., Paoloni, F. P., Weiber, E. A., Jiang, Z. H., & Jannasch, P. (2012). Fully aromatic ionomers with precisely sequenced sulfonated moieties for enhanced proton conductivity. *Macromolecules*, *45*(3), 1447-1459.

67. Zhu, Z., Walsby, N. M., Colquhoun, H. M., Thompsett, D., & Petrucco, E. (2009). Microblock Ionomers: A New Concept in High Temperature, Swelling-Resistant Membranes for PEM Fuel Cells. *Fuel Cells*, *9*(4), 305-317.

68. Miyatake, K., Chikashige, Y., Higuchi, E., & Watanabe, M. (2007). Tuned polymer electrolyte membranes based on aromatic polyethers for fuel cell applications. *Journal of the American Chemical Society*, *129*(13), 3879-3887.

69. Ding, J., Chuy, C., & Holdcroft, S. (2002). Enhanced conductivity in morphologically controlled proton exchange membranes: synthesis of macromonomers by SFRP and their incorporation into graft polymers. *Macromolecules*, *35*(4), 1348-1355.

70. Chuy, C., Ding, J., Swanson, E., Holdcroft, S., Horsfall, J., & Lovell, K. V. (2003). Conductivity and electrochemical ORR mass transport properties of solid polymer electrolytes containing poly (styrene sulfonic acid) graft chains. *Journal of the Electrochemical Society*, *150*(5), E271-E279.

71. Ding, J., Chuy, C., & Holdcroft, S. (2002). Solid Polymer Electrolytes Based on Ionic Graft Polymers: Effect of Graft Chain Length on Nano-Structured, Ionic Networks. *Advanced Functional Materials*, *12*(5), 389-394.

72. Ding, J., Chuy, C., & Holdcroft, S. (2001). A self-organized network of nanochannels enhances ion conductivity through polymer films. *Chemistry of materials*, *13*(7), 2231-2233.

73. Chuy, C., Basura, V. I., Simon, E., Holdcroft, S., Horsfall, J., & Lovell, K. V. (2000). Electrochemical Characterization of Ethylenetetrafluoroethylene-g-polystyrenesulfonic Acid Solid Polymer Electrolytes. *Journal of The Electrochemical Society*, *147*(12), 4453-4458.

74. Tsang, E. M. W., Shi, Z., & Holdcroft, S. (2011). Ionic purity and connectivity of proton-conducting channels in fluorous-ionic diblock copolymers. *Macromolecules*, *44*(22), 8845-8857.

75. Yang, A. C., Narimani, R., Zhang, Z., Frisken, B. J., & Holdcroft, S. (2013). Controlling Crystallinity in Graft Ionomers, and Its Effect on Morphology, Water Sorption, and Proton Conductivity of Graft Ionomer Membranes. *Chemistry of Materials*, *25*(9), 1935-1946.

76. Carretta, N., Tricoli, V., & Picchioni, F. (2000). Ionomeric membranes based on partially sulfonated poly (styrene): synthesis, proton conduction and methanol permeation. *Journal of Membrane Science*, *166*(2), 189-197.

77. Serpico, J. M., Ehrenberg, S. G., Fontanella, J. J., Jiao, X., Perahia, D., McGrady, K. A., ... & Wnek, G. E. (2002). Transport and structural studies of sulfonated styrene-ethylene copolymer membranes. *Macromolecules*, *35*(15), 5916-5921.

78. Saito, T., Moore, H. D., & Hickner, M. A. (2009). Synthesis of midblock-sulfonated triblock copolymers. *Macromolecules*, *43*(2), 599-601.

79. Matsumoto, K., Ozaki, F., & Matsuoka, H. (2008). Synthesis of proton-conducting block copolymer membranes composed of a fluorinated segment and a sulfonic acid segment. *Journal of Polymer Science Part A: Polymer Chemistry*, *46*(13), 4479-4485.

80. Mokrini, A., & Acosta, J. L. (2001). Studies of sulfonated block copolymer and its blends. *Polymer*, *42*(1), 9-15.

81. Oh, D. Y., Lee, J. U., Jo, W. H. (2012). Synthesis of fluorinated amphiphilic triblock copolymer ad its application in high temperature PEM fuel cells. *Journal of Materials Chemistry*, *22*, 7187-7193.

82. Li, N., Wang, C., Lee, S. Y., Park, C. H., Lee, Y. M., & Guiver, M. D. (2011). Enhancement of proton transport by nanochannels in comb-shaped copoly (arylene ether sulfone) s. *Angewandte Chemie*, *123*(39), 9324-9327.

83. Liu, B., Robertson, G. P., Kim, D.-S., Guiver, M. D., Hu, W., Jiang, Z. (2007). Aromatic poly(ether ketone)s with pendant sulfonic acid phenyl groups prepared by a mild sulfonation method for proton exchange membranes. *Macromolecules*, *40*, 1934-1944.

84. Liu, B., Hu, W., Kim, Y. S., Zou, H., Robertson, G. P., Jiang, Z., & Guiver, M. D. (2010). Preparation and DMFC performance of a sulfophenylated poly (arylene ether ketone) polymer electrolyte membrane. *Electrochimica Acta*, *55*(11), 3817-3823.

85. Liu, B., Robertson, G. P., Kim, D. S., Sun, X., Jiang, Z., & Guiver, M. D. (2010). Enhanced thermo-oxidative stability of sulfophenylated poly (ether sulfone) s. *Polymer*, *51*(2), 403-413.

86. Li, N., Shin, D. W., Hwang, D. S., Lee, Y. M., & Guiver, M. D. (2010). Polymer Electrolyte Membranes Derived from New Sulfone Monomers with Pendent Sulfonic Acid Groups†. *Macromolecules*, *43*(23), 9810-9820.

87. Li, N., Lee, S. Y., Liu, Y. L., Lee, Y. M., & Guiver, M. D. (2012). A new class of highly-conducting polymer electrolyte membranes: Aromatic ABA triblock copolymers. *Energy & Environmental Science*, *5*(1), 5346-5355.

88. Li, N., Hwang, D. S., Lee, S. Y., Liu, Y. L., Lee, Y. M., & Guiver, M. D. (2011). Densely sulfophenylated segmented copoly (arylene ether sulfone) proton exchange membranes. *Macromolecules*, *44*(12), 4901-4910.

89. Vogel, C., Komber, H., Quetschke, A., Butwilowski, W., Pötschke, A., Schlenstedt, K., & Meier-Haack, J. (2011). Side-chain sulfonated random and multiblock poly (ether sulfone) s for PEM applications. *Reactive and Functional Polymers*, *71*(8), 828-842.

90. Miyatake, K., Chikashige, Y., & Watanabe, M. (2003). Novel sulfonated poly (arylene ether): a proton conductive polymer electrolyte designed for fuel cells. *Macromolecules*, *36*(26), 9691-9693.

91. Kim, D. J., Chang, B. J., Kim, J. H., Lee, S. B., & Joo, H. J. (2008). Sulfonated poly (fluorenyl ether) membranes containing perfluorocyclobutane groups for fuel cell applications. *Journal of Membrane Science*, *325*(1), 217-222.

92. Chikashige, Y., Chikyu, Y., Miyatake, K., & Watanabe, M. (2005). Poly (arylene ether) ionomers containing sulfofluorenyl groups for fuel cell applications. *Macromolecules*, *38*(16), 7121-7126.

93. Shimura, T., Miyatake, K., & Watanabe, M. (2008). Poly (arylene ether) ionomers containing sulfofluorenyl groups: Effect of electron-withdrawing groups on the properties. *European Polymer Journal*, *44*(12), 4054-4062.

94. Bae, B., Miyatake, K., & Watanabe, M. (2009). Synthesis and properties of sulfonated block copolymers having fluorenyl groups for fuel-cell applications. *ACS applied materials & interfaces*, *1*(6), 1279-1286.

95. Hoshi, T., Bae, B., Watanabe, M., & Miyatake, K. (2012). Synthesis and properties of sulfonated poly (arylene ether) block copolymers as proton conductive membranes. *Bulletin of the Chemical Society of Japan*, *85*(3), 389-396.

96. Bae, B., Yoda, T., Miyatake, K., Uchida, H., & Watanabe, M. (2010). Proton-Conductive Aromatic Ionomers Containing Highly Sulfonated Blocks for High-Temperature-Operable Fuel Cells. *Angewandte Chemie*, *122*(2), 327-330.

97. Bae, B., Miyatake, K., & Watanabe, M. (2010). Sulfonated poly (arylene ether sulfone ketone) multiblock copolymers with highly sulfonated block. Synthesis and properties. *Macromolecules*, *43*(6), 2684-2691.

98. Bae, B., Hoshi, T., Miyatake, K., & Watanabe, M. (2011). Sulfonated block poly (arylene ether sulfone) membranes for fuel cell applications via oligomeric sulfonation. *Macromolecules*, *44*(10), 3884-3892.

99. Lee, H. F., Wang, P. H., Huang, Y. C., Su, W. H., Gopal, R., Lee, C. C., ... & Huang, W. Y. (2014). Synthesis and proton conductivity of sulfonated, multi-phenylated poly (arylene ether) s. *Journal of Polymer Science Part A: Polymer Chemistry*, *52*(18), 2579-2587.

100. Miyatake, K., Oyaizu, K., Tsuchida, E., & Hay, A. S. (2001). Synthesis and properties of novel sulfonated arylene ether/fluorinated alkane copolymers. *Macromolecules*, *34*(7), 2065-2071.

101. Miyatake, K., & Hay, A. S. (2001). Synthesis and properties of poly (arylene ether) s bearing sulfonic acid groups on pendant phenyl rings. *Journal of Polymer Science Part A: Polymer Chemistry*, *39*(19), 3211-3217.

102. Matsumoto, K., Higashihara, T., & Ueda, M. (2009). Locally and densely sulfonated poly (ether sulfone) s as proton exchange membrane. *Macromolecules*, *42*(4), 1161-1166.

103. Tian, S., Meng, Y., & Hay, A. S. (2009). Membranes from poly (aryl ether)-based ionomers containing multiblock segments of randomly distributed nanoclusters of 18 sulfonic acid groups. *Journal of Polymer Science Part A: Polymer Chemistry*, *47*(18), 4762-4773.

104. Tian, S., Meng, Y., & Hay, A. S. (2009). Membranes from poly (aryl ether)-based ionomers containing randomly distributed nanoclusters of 6 or 12 sulfonic acid groups. *Macromolecules*, *42*(4), 1153-1160.

105. Matsumura, S., Hlil, A. R., Du, N., Lepiller, C., Gaudet, J., Guay, D., & Hay, A. S. (2008). Ionomers for proton exchange membrane fuel cells with sulfonic acid groups on the end-groups: Novel branched poly (ether-ketone) s with 3, 6-ditrityl-9H-carbazole end-groups. *Journal of Polymer Science Part A: Polymer Chemistry*, *46*(11), 3860-3868.

106. Matsumura, S., Hlil, A. R., Lepiller, C., Gaudet, J., Guay, D., Shi, Z., & Hay, A. S. (2008). Ionomers for proton exchange membrane fuel cells with sulfonic acid groups on the end groups: novel branched poly (ether-ketone) s. *Macromolecules*, *41*(2), 281-284.

107. Matsumura, S., Hlil, A. R., Lepiller, C., Gaudet, J., Guay, D., & Hay, A. S. (2008). Ionomers for proton exchange membrane fuel cells with sulfonic acid groups on the end groups: novel linear aromatic poly (sulfide-ketone) s. *Macromolecules*, *41*(2), 277-280.

108. Lim, Y. D., Seo, D. W., Lee, S. H., Hossain, M. A., Kang, K., Ju, H., & Kim, W. G. (2013). Synthesis and characterization of sulfonated poly (arylene ether ketone sulfone) block copolymers containing multi-phenyl for PEMFC. *International Journal of Hydrogen Energy*, *38*(1), 631-639.

109. Miyatake, K., Shimura, T., Mikami, T., & Watanabe, M. (2009). Aromatic ionomers with superacid groups. *Chem. Commun.*, (42), 6403-6405.

110. Jutemar, E. P., & Jannasch, P. (2010). Locating sulfonic acid groups on various side chains to poly (arylene ether sulfone) s: Effects on the ionic clustering and properties of proton-exchange membranes. *Journal of Membrane Science*, *351*(1), 87-95.

111. Lafitte, B., Karlsson, L. E., & Jannasch, P. (2002). Sulfophenylation of Polysulfones for Proton-Conducting Fuel Cell Membranes. *Macromolecular rapid communications*, *23*(15), 896-900.

112. Karlsson, L. E., & Jannasch, P. (2005). Polysulfone ionomers for proton-conducting fuel cell membranes: 2. Sulfophenylated polysulfones and polyphenylsulfones. *Electrochimica acta*, *50*(9), 1939-1946.

113. Qiu, Z., Wu, S., Li, Z., Zhang, S., Xing, W., & Liu, C. (2006). Sulfonated poly (arylene-co-naphthalimide) s synthesized by copolymerization of primarily sulfonated monomer and fluorinated naphthalimide dichlorides as novel polymers for proton exchange membranes. *Macromolecules*, *39*(19), 6425-6432.

114. Ghassemi, H., & McGrath, J. E. (2004). Synthesis and properties of new sulfonated poly (p-phenylene) derivatives for proton exchange membranes. I. *Polymer*, *45*(17), 5847-5854.

115. Goto, K., Rozhanskii, I., Yamakawa, Y., Otsuki, T., & Naito, Y. (2009). Development of aromatic polymer electrolyte membrane with high conductivity and durability for fuel cell. *Polymer journal*, *41*(2), 95-104.

116. Wu, S., Qiu, Z., Zhang, S., Yang, X., Yang, F., & Li, Z. (2006). The direct synthesis of wholly aromatic poly (p-phenylene) s bearing sulfobenzoyl side groups as proton exchange membranes. *Polymer*, *47*(20), 6993-7000.

117. Chen, S., Chen, K., Zhang, X., Hara, R., Endo, N., Higa, M., ... & Wang, L. (2013). Poly (sulfonated phenylene)-block-poly (arylene ether sulfone) copolymer for polymer electrolyte fuel cell application. *Polymer*, *54*(1), 236-245.

118. Lafitte, B., & Jannasch, P. (2007). Proton-Conducting Aromatic Polymers Carrying Hypersulfonated Side Chains for Fuel Cell Applications. *Advanced Functional Materials*, *17*(15), 2823-2834.

119. Yasuda, T., Miyatake, K., Hirai, M., Nanasawa, M., & Watanabe, M. (2005). Synthesis and properties of polyimide ionomers containing sulfoalkoxy and fluorenyl groups. *Journal of Polymer Science Part A: Polymer Chemistry*, *43*(19), 4439-4445.

120. Asano, N., Aoki, M., Suzuki, S., Miyatake, K., Uchida, H., & Watanabe, M. (2006). Aliphatic/aromatic polyimide ionomers as a proton conductive membrane for fuel cell applications. *Journal of the American Chemical Society*, *128*(5), 1762-1769.

121. Wang, C., Shin, D. W., Lee, S. Y., Kang, N. R., Lee, Y. M., & Guiver, M. D. (2012). Poly (arylene ether sulfone) proton exchange membranes with flexible acid side chains. *Journal of Membrane Science*, *405*, 68-78.

122. Yoshimura, K., & Iwasaki, K. (2009). Aromatic polymer with pendant perfluoroalkyl sulfonic acid for fuel cell applications. *Macromolecules*, *42*(23), 9302-9306.

123. Kreuer, K. D. (2001). On the development of proton conducting polymer membranes for hydrogen and methanol fuel cells. *Journal of membrane science*, *185*(1), 29-39.

124. Li, H., Jackson, A. B., Kirk, N. J., Mauritz, K. A., & Storey, R. F. (2011). Poly (arylene ether sulfone) statistical copolymers bearing perfluoroalkylsulfonic acid moieties. *Macromolecules*, *44*(4), 694-702.

125. Chang, Y., Brunello, G. F., Fuller, J., Hawley, M., Kim, Y. S., Disabb-Miller, M., Hickner, M. A., Jang, S. S., & Bae, C. (2011). Aromatic ionomers with highly acidic sulfonate groups: acidity, hydration, and proton conductivity. *Macromolecules*, *44*(21), 8458-8469.

126. Mikami, T., Miyatake, K., & Watanabe, M. (2010). Poly (arylene ether) s containing superacid groups as proton exchange membranes. *ACS applied materials & interfaces*, *2*(6), 1714-1721.

127. Mikami, T., Miyatake, K., & Watanabe, M. (2011). Synthesis and properties of multiblock copoly (arylene ether) s containing superacid groups for fuel cell membranes. *Journal of Polymer Science Part A: Polymer Chemistry*, *49*(2), 452-464.

128. Assumma, L., Iojoiu, C., Mercier, R., Lyonnard, S., Nguyen, H. D., & Planes, E. (2015). Synthesis of partially fluorinated poly(arylene ether sulfone) multiblock copolymers bearing perfluorosulfonic functions. *Journal of Polymer Science Part A: Polymer Chemistry*.

129. Thomas, B. H., & DesMarteau, D. D. (2005). Self-emulsifying polymerization (SEP) of 3, 6-dioxa-Δ 7-4-trifluoromethyl perfluorooctyl trifluoromethyl sulfonimide with tetrafluoroethylene. *Journal of fluorine chemistry*, *126*(7), 1057-1064.

130. DesMarteau, D. D. (1995). Novel perfluorinated ionomers and ionenes. *Journal of fluorine chemistry*, *72*(2), 203-208.

131. Ford, L. A., DesMarteau, D. D., & Smith, D. W. (2005). Perfluorocyclobutyl (PFCB) aromatic polyethers: Synthesis and characterization of new sulfonimide containing monomers and fluoropolymers. *Journal of fluorine chemistry*, *126*(4), 651-658.

132. Thomas, B. H., Shafer, G., Ma, J. J., Tu, M. H., & DesMarteau, D. D. (2004). Synthesis of 3, 6-dioxa-Δ 7-4-trifluoromethyl perfluorooctyl trifluoromethyl sulfonimide: bis [(perfluoroalkyl) sulfonyl] superacid monomer and polymer. *Journal of fluorine chemistry*, *125*(8), 1231-1240.

133. Desmarteau, D. D., & Witz, M. (1991). N-fluoro-bis (trifluoromethanesulfonyl) imide. An improved synthesis. *Journal of fluorine chemistry*, *52*(1), 7-12.

134. Zhang, J., DesMarteau, D. D., Zuberi, S., Ma, J. J., Xue, L., Gillette, S. M., ... & Gerhardt, R. (2002). Synthesis of the first difunctional N-fluoro perfluoroalkylsulfonylimides, CF 3 SO 2 NFSO 2 (CF 2) n SO 2 NFSO 2 CF 3. *Journal of fluorine chemistry*, *116*(1), 45-48.

135. Hickman, T., & DesMarteau, D. D. (2012). Synthesis of 1, 3-dialkyl imidazolium ionic liquids containing difunctional and tetrafunctional perfluoroalkylsulfonyl imide anions. *Journal of Fluorine Chemistry*, *133*, 11-15.

136. Sumner, J. J., Creager, S. E., Ma, J. J., & DesMarteau, D. D. (1998). Proton conductivity in Nafion® 117 and in a novel bis [(perfluoroalkyl) sulfonyl] imide ionomer membrane. *Journal of the Electrochemical Society*, *145*(1), 107-110.

137. Assumma, L., Iojoiu, C., Ari, G. A., Cointeaux, L., & Sanchez, J. Y. (2014). Polyethersulfone containing sulfonimide groups as proton exchange membrane fuel cells. *International Journal of Hydrogen Energy*, *39*(6), 2740-2750.

138. Oishi, A., Matsuoka, H., Yasuda, T., & Watanabe, M. (2009). Novel styrene/N-phenylmaleimide alternating copolymers with pendant sulfonimide acid groups for polymer electrolyte fuel cell applications. *Journal of Materials Chemistry*, *19*(4), 514-521.

139. Cho, C. G., Kim, Y. S., Yu, X., Hill, M., & McGrath, J. E. (2006). Synthesis and characterization of poly (arylene ether sulfone) copolymers with sulfonimide side groups for a proton-exchange membrane. *Journal of Polymer Science Part A: Polymer Chemistry*, *44*(20), 6007-6014.

140. Assumma, L., Iojoiu, C., Judeinstein, P., Mercier, R., Porcar, L., & Lyonnard, S. (2015) Structure-transport interplay in highly phase-separated proton-conducting aromatic block ionomers. *Publication under submission*.

141. Huang, W. Y., Huang, B. N., & Hu, C. M. (1983). Studies on deiodo-sulfination. Part I. Studies on the deiodo-sulfination of perfluoroalkyl iodides. *Journal of Fluorine Chemistry*, *23*(2), 193-204.

142. Durual, P. (1992). *European Patent Application 92400330.4.*

143. Zhang, C. P., Chen, Q. Y., Xiao, J. C., & Gu, Y. C. (2009). A mild hydrodehalogenation of fluoroalkyl halides. *Journal of Fluorine Chemistry*, *130*(7), 671-673.

144. Meinert, H., Knoblich, A., Mader, J., & Brune, H. A. (1992). On the reaction of perfluoroalkyl halides in the presence of alcohols and bases. *Journal of fluorine chemistry*, *59*(3), 379-385.

145. Wakselman, C. (1992). Single electron-transfer processes in perfluoroalkyl halides reactions. *Journal of fluorine chemistry*, *59*(3), 367-378.

146. Howell, J. L., Muzzi, B. J., Rider, N. L., Aly, E. M., & Abouelmagd, M. K. (1995). On the preparation of 1H-perfluoroalkanes and a mechanism for the reduction of perfluoroalkyl iodides. *Journal of fluorine chemistry*, *72*(1), 61-68.

147. McLoughlin, V. C. R., & Thrower, J. (1969). A route to fluoroalkyl-substituted aromatic compounds involving fluoroalkylcopper intermediates. *Tetrahedron*, *25*(24), 5921-5940.

148. Fanta, P. E. (1946). The Ullmann synthesis of biaryls. *Chemical reviews*, *38*(1), 139-196.

149. Kash, P. W., Sun, D. H., Xi, M., Flynn, G. W., & Bent, B. E. (1996). Cross Coupling of Phenyl Groups with Alkyl Iodides on Copper Surfaces: A Radical Mechanism?. *The Journal of Physical Chemistry*, *100*(41), 16621-16628.

150. Han, X. (2010). Cross coupling of 3-bromopyridine and sulfonamides ($R^1NHSO_2R^2 \cdot R^1$ = H, Me, alkyl; R^2 = alkyl and aryl) catalyzed by CuI/1,3-di(pyridin-2-yl)propane-1,3-dione. *Tetrahedron Letters*, *51*(2), 360-362.

151. Ley, S. V., & Thomas, A. W. (2003). Modern Synthetic Methods for Copper-Mediated C(aryl)-O, C(aryl)-N, and C(aryl)-S Bond Formation. *Angewandte Chemie International Edition*, *42*(44), 5400-5449.

152. Yao, S., Zhang, X., Zhou, J., Qian, R., Xu, Z., Fang, F., Wei, Y., Wang, C., Yuan, S. & Guo, Y. (2009). Electrophilic aromatic substitution and single-electron transfer (SET) by the phenylium ion in the gas phase: characterization of a long-lived SET intermediate. *Journal of Mass Spectrometry*, *44*(1), 32-39.

153. Sharghi, H., & Tamaddon, F. (1996). $BeCl_2$ as a new highly selective reagent for dealkylation of aryl-methyl ethers. *Tetrahedron*, *52*(43), 13623-13640.

154. Weissman, S. A., & Zewge, D. (2005). Recent advances in ether dealkylation. *Tetrahedron*, *61*(33), 7833-7863.

155. Zuo, L., Yao, S., Wang, W., & Duan, W. (2008). An efficient method for demethylation of aryl methyl ethers. *Tetrahedron Letters*, *49*(25), 4054-4056.

156. Babau, R. J. & Bhatt, V. M. (1984). New reagents 41. Reduction of sulphonyl chlorides and sulphoxides with aluminum iodide. *Tetrahedron Letters*, 25, 3497.

157. Vass, A., Dudas, J., Borbely, L., Haasz, F., & Jekkel, P. (2006). *International Application Published under the Patent Cooperation Treaty (PCT) PCT/HU2005/000128*.

158. Paillard

159. van Beek, D., & Fossum, E. (2009). Linear Poly (arylene ether) s with Pendant Benzoyl Groups: Geometric Isomers of PEEK or Substituted Poly (phenylene oxide)?. *Macromolecules*, *42*(12), 4016-4022.

160. Kaiti, S., Himmelberg, P., Williams, J., Abdellatif, M., Fossum, E. (2006). Linear poly(arylene ether)s with pendant benzoyl groups: nucleophilic aromatic substitution activated from the meta position. *Macromolecules*, 39, 7909-7914.

161. Tatli, M., Selhorst, R., & Fossum, E. (2013). Poly (arylene ether) s with pendent 3-iodophenyl sulfonyl groups: synthesis, characterization, and modification. *Macromolecules*, *46*(11), 4388-4394.

162. Tienda, K., Yu, Z., Constandinidis, F., Fortney, A., Feld, W. A., & Fossum, E. (2011). Poly (arylene ether) s with pendant diphenyl phosphoryl groups: Synthesis, characterization, and thermal properties. *Journal of Polymer Science Part A: Polymer Chemistry*, *49*(13), 2908-2915.

163. Selhorst, R., & Fossum, E. (2013). Utilization of N, N-diethyl-3, 5-difluorobenzene sulfonamide to prepare functionalized poly (arylene ether) s. *Polymer*, *54*(2), 530-535.

164. Osborn, S. J., Hassan, M. K., Divoux, G. M., Rhoades, D. W., Mauritz, K. A., & Moore, R. B. (2007). Glass transition temperature of perfluorosulfonic acid ionomers. *Macromolecules*, *40*(10), 3886-3890.